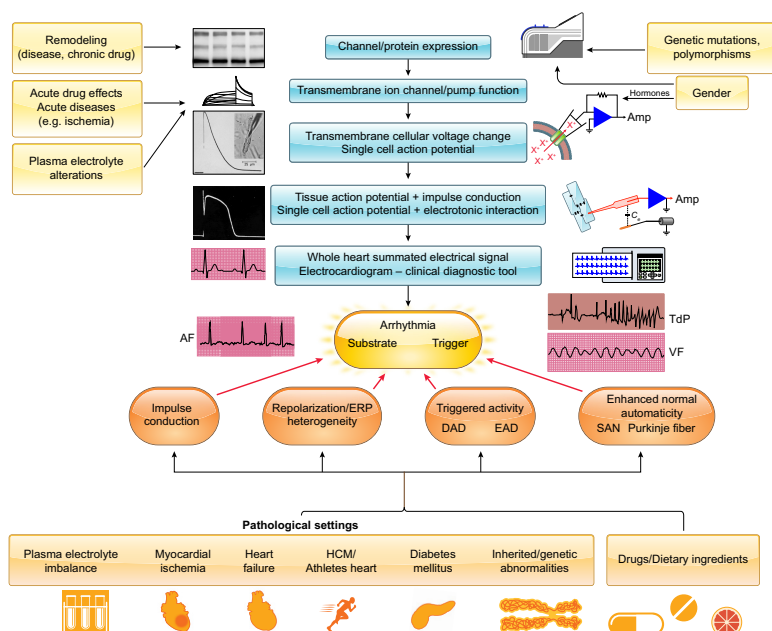


CARDIAC TRANSMEMBRANE ION CHANNELS AND ACTION POTENTIALS: CELLULAR PHYSIOLOGY AND ARRHYTHMOGENIC BEHAVIOR



AUTHORS

András Varró, Jakub Tomek, Norbert Nagy, László Virág, Elisa Passini, Blanca Rodriguez, István Baczkó

CORRESPONDENCE

varro.andras@med.u-szeged.hu

KEY WORDS

action potential; arrhythmia; heart; ion channels; remodeling

CLINICAL HIGHLIGHTS

1. Cardiac arrhythmias are major causes of mortality. They most often arise from pathological changes in the electrophysiological properties of myocardial cells. First, this review summarizes the physiology of cardiac action potentials, their regional and species differences, the underlying transmembrane ionic currents, and transporters, with special focus on their human relevance.
2. Progress in computer modeling and vast quantities of experimental data made computerized replication of the action potential, impulse conduction, and simulation of cardiac electrophysiology possible. Current computer models offer improved observability and controllability via utilization of different modeling scales and can assist future individualized anti-arrhythmic therapy as well as drug electrophysiological safety assessment.
3. A number of diseases evoke changes in the configuration of the action potential caused by altered function and/or densities of transmembrane ion channels and transporters, collectively termed electrical remodeling. Initially, these alterations are often compensatory; however, remodeling significantly contributes to increased arrhythmia susceptibility by impairing impulse generation, conduction, and myocardial refractoriness in these clinical settings. Electrical remodeling in atrial fibrillation, heart failure, hypertrophic cardiomyopathy, myocardial infarction, and advanced age are discussed. Better understanding of the cellular basis of cardiac electrophysiology, electrical remodeling, and mechanisms of arrhythmias has important implications for future clinical therapeutic strategies.

CARDIAC TRANSMEMBRANE ION CHANNELS AND ACTION POTENTIALS: CELLULAR PHYSIOLOGY AND ARRHYTHMOGENIC BEHAVIOR

András Varró,^{1,2} Jakub Tomek,³ Norbert Nagy,^{1,2} László Virág,¹ Elisa Passini,³ Blanca Rodriguez³, and István Baczkó¹

¹Department of Pharmacology and Pharmacotherapy, Faculty of Medicine, University of Szeged, Szeged, Hungary; ²MTA-SZTE Cardiovascular Pharmacology Research Group, Hungarian Academy of Sciences, Szeged, Hungary; and ³Department of Computer Science, British Heart Foundation Centre of Research Excellence, University of Oxford, Oxford, United Kingdom

Abstract

Cardiac arrhythmias are among the leading causes of mortality. They often arise from alterations in the electrophysiological properties of cardiac cells and their underlying ionic mechanisms. It is therefore critical to further unravel the pathophysiology of the ionic basis of human cardiac electrophysiology in health and disease. In the first part of this review, current knowledge on the differences in ion channel expression and properties of the ionic processes that determine the morphology and properties of cardiac action potentials and calcium dynamics from cardiomyocytes in different regions of the heart are described. Then the cellular mechanisms promoting arrhythmias in congenital or acquired conditions of ion channel function (electrical remodeling) are discussed. The focus is on human-relevant findings obtained with clinical, experimental, and computational studies, given that interspecies differences make the extrapolation from animal experiments to human clinical settings difficult. Deepening the understanding of the diverse pathophysiology of human cellular electrophysiology will help in developing novel and effective antiarrhythmic strategies for specific subpopulations and disease conditions.

action potential; arrhythmia; heart; ion channels; remodeling

1.	INTRODUCTION	1083
2.	CARDIAC ACTION POTENTIAL	1086
3.	TRANSMEMBRANE ION CHANNELS AND...	1087
4.	TISSUE-SPECIFIC ACTION POTENTIALS	1107
5.	COMPUTER SIMULATIONS OF ACTION...	1117
6.	CELLULAR ARRHYTHMIA MECHANISMS	1120
7.	ION CHANNEL AND ACTION POTENTIAL...	1126
8.	INHERITED CONDITIONS ASSOCIATED...	1132
9.	OTHER FACTORS INFLUENCING...	1134
10.	CONCLUSIONS	1136

CLINICAL HIGHLIGHTS

- Cardiac arrhythmias are major causes of mortality. They most often arise from pathological changes in the electrophysiological properties of myocardial cells. First, this review summarizes the physiology of cardiac action potentials, their regional and species differences, the underlying transmembrane ionic currents, and transporters, with special focus on their human relevance.
- Progress in computer modeling and vast quantities of experimental data made computerized replication of the action potential, impulse conduction, and simulation of cardiac electrophysiology possible. Current computer models offer improved observability and controllability via utilization of different modeling scales and can assist future individualized anti-arrhythmic therapy as well as drug electrophysiological safety assessment.
- A number of diseases evoke changes in the configuration of the action potential caused by altered function and/or densities of transmembrane ion channels and transporters, collectively termed electrical remodeling. Initially, these alterations are often compensatory; however, remodeling significantly contributes to increased arrhythmia susceptibility by impairing impulse generation, conduction, and myocardial refractoriness in these clinical settings. Electrical remodeling in atrial fibrillation, heart failure, hypertrophic cardiomyopathy, myocardial infarction, and advanced age are discussed. Better understanding of the cellular basis of cardiac electrophysiology, electrical remodeling, and mechanisms of arrhythmias has important implications for future clinical therapeutic strategies.

1. INTRODUCTION

The heart is a mechanical pump with the vital role of supplying blood to other organs. In humans, it contracts and relaxes in a regular fashion ~60 times per minute. If the regular heartbeat is interrupted for more than a couple of minutes, the lack of oxygen supply causes irreversible damage to vital organs, including the heart itself, potentially causing sudden cardiac death (SCD). Cardiac contractions, the most important function of the heart, are initiated by a bioelectrical signal, the action

potential (AP) (1), via a process called excitation-contraction coupling (2). The action potential originates in the sinus node cells, propagates through the whole heart via an active electrophysiological process called impulse conduction, and can be measured as the electrical potential difference between the intra- and extracellular space. The stimulus spreads through both atria, causing their contraction. The next stage of propagation is the atrioventricular (AV) node, which passes the signal to the ventricles with a slight delay to provide enough time for the atria to contract. From the AV node, the bundle of His conducts the stimulus along the septal wall to the subendocardial Purkinje fibers, which then stimulate the ventricles, allowing their synchronized contraction. The action potential is determined by the opening and closing of various complex transmembrane proteins, which consist of ion channels and transporters, i.e., pumps or exchangers (3–5). Disturbances of action potential generation and/or conduction can lead to changes in the regular heart rhythm called arrhythmias (6, 7). These disturbances can impair contraction to such a degree that thromboembolic stroke of atrial origin or sudden cardiac death may eventually occur. Therefore, understanding the function and regulation of transmembrane ion channels and transporters, as well as their impact on the cardiac action potential, is essential to understand arrhythmia mechanisms and treat life-threatening cardiac arrhythmias. Arrhythmias are usually diagnosed based on the analysis of electrocardiogram (ECG) recordings, which represent the electrical activity of the

heart as measured on the body surface. The ECG is determined by many variables, including the function of transmembrane ion channels and transporters in the different heart cells and the consequent changes in the membrane potential (FIGURE 1).

The P wave corresponds to the activation (depolarization) and early repolarization of the atrial cells. The QRS complex reflects the time course of the depolarization of the ventricles caused mainly by the activation of the fast sodium channels. The PQ segment mainly indicates the impulse conduction from the atria to the ventricles. The PQ segment also contains the HQ interval, which reflects fast propagation due to the function of the fast sodium current (I_{Na}). In addition, cell-to-cell coupling is low in the AV node (8), which makes impulse propagation through the AV node relatively unsafe. The isoelectric ST segment reflects the plateau phase of the ventricular action potentials. In this phase, membrane potential hardly changes at the cellular level because of the fine balance of opening/closing of different ion channels. The configuration of the T wave shows the repolarization time course of the ventricles, and it reflects the balance between the slowly activating repolarizing potassium and chloride currents and the depolarizing steady-state, so-called “window” sodium (9) and “window” calcium (10) and the slowly decaying, often called “late,” sodium (I_{NaLate}) and slowly inactivating calcium currents (11–15). Analysis of the PP intervals yields important information regarding heart rate and its regularity.

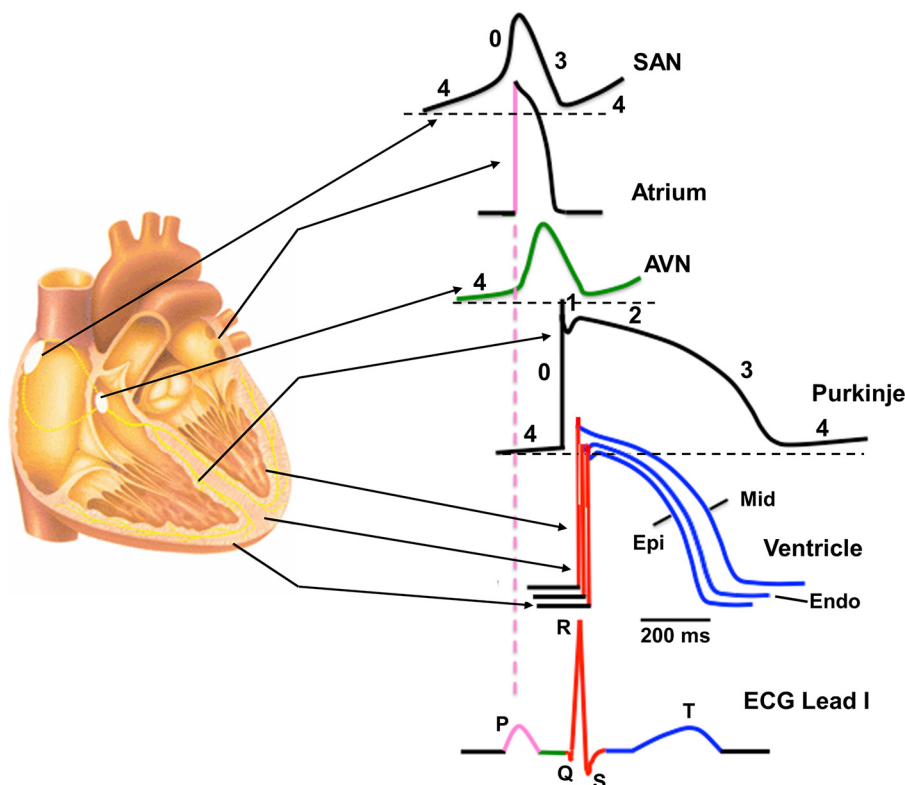


FIGURE 1. Regional differences in cardiac action potential configurations. Schematic cross section of the heart depicting the corresponding action potential configuration from different regions of the heart indicated by arrows. Color-coded sections on the action potentials refer to the corresponding sections on the schematic electrocardiogram (ECG). AVN, atrioventricular node; Endo, endocardial; Epi, epicardial; Mid, midmyocardial; SAN, sinoatrial node.

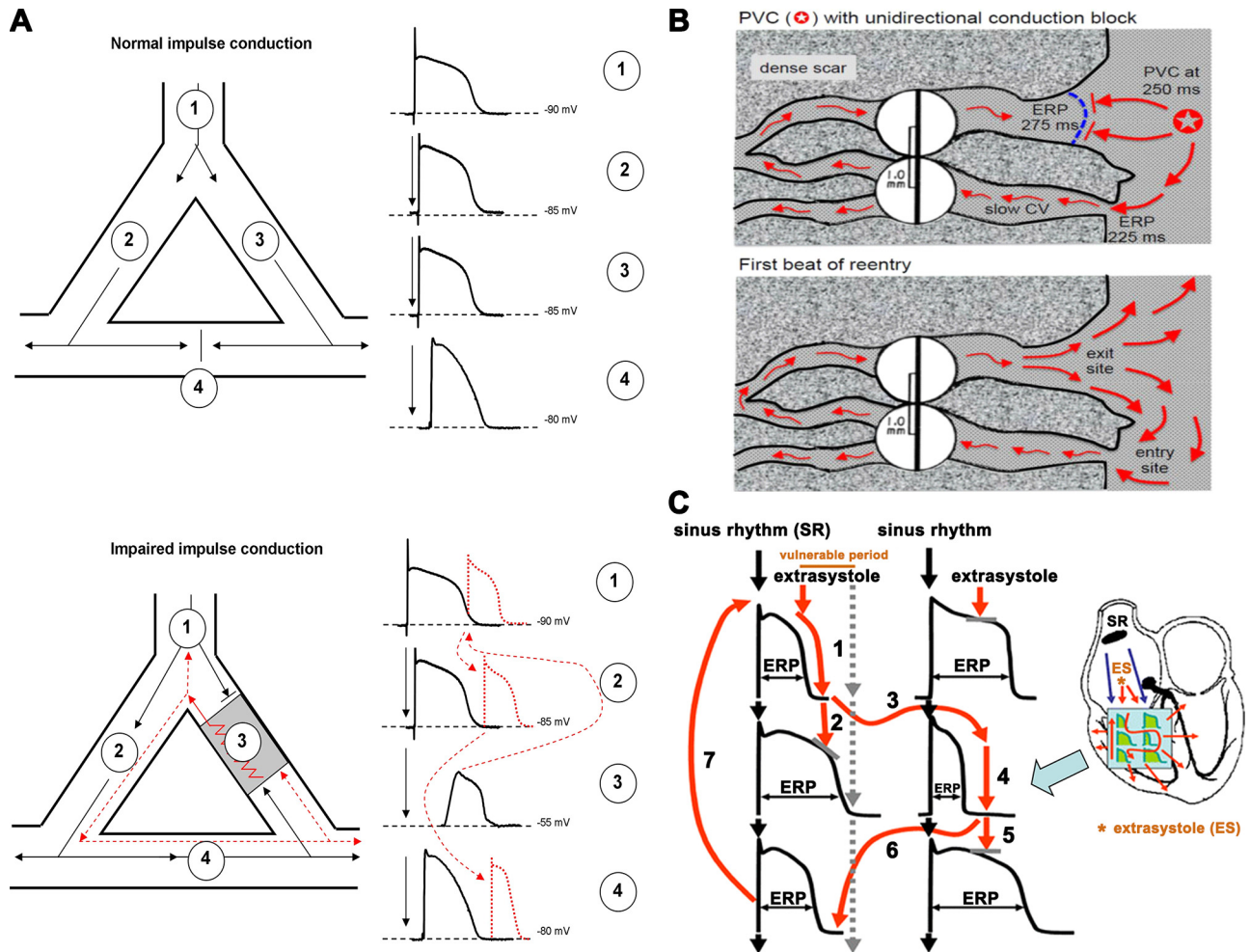


FIGURE 2. *A, top:* an area of branching cardiac tissue, providing separate paths for impulse propagation from proximal (1) to distal (2–4) directions. The separate paths for impulse conduction can be variable, as branching Purkinje fiber-ventricular junctions, ventricular muscle segments with nonconducting fibrosis, scar, or infarcted tissue in the core. If the tissues in these paths are healthy, the impulse conduction is fast and, because of the relatively long effective refractory period (ERP) in cardiac cells, impulses would collide at site 4 and would propagate only into the distal directions. *Bottom:* an area of depolarized myocardium at site 3, due to asymmetric severe local myocardial damage, imposing conduction block from the anterograde direction. However, in the case that the impulse travels from site 4 in the retrograde direction, it can propagate back very slowly into this damaged area, and if its propagation is slow enough to outlast the ERP in front the impulse can reexcite the proximal tissue. Then, this impulse would propagate toward both sites 1 and 2, establishing a circus movement and reentry arrhythmia. *B:* example of a classic mechanism by which a premature ventricular complex (PVC) initiates reentry in the fibrotic border zone of an infarct, due to slow conduction and dispersion of refractoriness. *Top:* a PVC occurring 250 ms after the previous beat arrives too early to propagate through the upper myocyte strand with a long ERP of 275 ms, but it propagates successfully (red arrows) through the lower strand with a shorter ERP of 225 ms (entry site). The impulse propagates slowly (slow CV), eventually reaching the upper strand from the opposite direction. *Bottom:* if the total conduction time is >275 ms, the interface of the upper strand with normal tissue (exit site) has recovered excitability, and the impulse can then propagate through the region of prior conduction block, thus initiating reentry. Dispersion of refractoriness is caused by electrical remodeling. The slow propagation is due to zig-zag conduction through the myocyte strands as well as gap junction remodeling. (Reproduced from Ref. 17 with permission.) *C:* schematic illustration of functional reentry mechanism without a well-defined anatomical obstacle. The arrhythmia substrate is represented by artificially enhanced action potential differences. In normal circumstances, impulses originating from the sinus node (black arrows) use physiological pathways to propagate through atrial and ventricular tissue and the conduction system. An early ectopic impulse (trigger, red arrow) can only propagate via pathways where the tissue is not depolarized, and consequently its refractoriness is over, whereas the conduction is blocked in directions where the tissue is not fully repolarized and cells are still in the refractory state. Thus the abnormal impulse can travel in a zig-zag direction through reentry paths created by heterogeneous repolarization and conduction. The dispersion of repolarization creates a time window called the vulnerable period, where extra stimuli could elicit the reentry arrhythmia. However, outside this window extra stimuli would only cause a single or multiple relatively harmless extrasystoles. CV, conduction velocity; ES, extrasystole; SR, sinus rhythm. Reproduced from Ref. 18 with permission.

Cardiac arrhythmia mechanisms are still the subject of intensive research. Because of the large variability in appearances, types (e.g., bradycardia and different types of tachycardia), locations (supraventricular or ventricular), and underlying diseases, it is

widely accepted that there is not a single mechanism to explain how arrhythmias originate. Therefore, patients are often treated with little knowledge regarding the mechanisms and/or causes of the arrhythmia.

The majority of cardiac arrhythmias are the result of an enhanced proarrhythmic substrate combined with a trigger (16). Enhanced heterogeneity of repolarization and impaired impulse conduction represent typical arrhythmia substrates (conditions that are prerequisites for arrhythmia development) for severe tachyarrhythmia. Impairment of impulse conduction can be caused by anatomical (FIGURE 2, A and B) (17) or functional (FIGURE 2C) (18) alterations. The process was described long ago, first in the early twentieth century (19). Impulse conduction critically depends on the density and kinetics of inward transmembrane ionic currents. Depolarization of the resting membrane potential (RMP), for example, reduces sodium and calcium inward currents and strongly influences their kinetic properties. This can thus slow impulse conduction and cause unidirectional or bidirectional conduction block, and potentially reentry, underpinning a wide range of cardiac arrhythmias.

As mentioned above, reentrant arrhythmias can be caused by functional causes too, without an anatomically well-defined myocardial damage (FIGURE 2C). This form of reentry is more complex and could involve both impulse conduction and repolarization heterogeneities (arrhythmia substrate) as well as enhanced normal or abnormal automaticity (trigger).

Reentrant arrhythmias are often initiated by an extrasystole formed anywhere in the heart, acting as an arrhythmia trigger (20, 21). Both arrhythmia substrate and trigger, like an extrasystole [premature ventricular complex (PVC)], can be promoted by pathological cardiac conditions (FIGURE 2), e.g., myocardial ischemia, heart failure (7), and genetic diseases (22), or by adverse drug reactions (23). General arrhythmia mechanisms include various cellular aspects, e.g., transmembrane ionic currents, transporters, action potential properties, and automaticity, which are the subjects of this review. However, arrhythmia mechanisms at the whole heart level are more complex, since they are also determined by anatomical and structural properties, impulse conduction, and intercellular communication between myocardial and nonmyocardial cells, like fibroblasts. These factors are beyond the scope of the present work, and the interested reader is referred to other reviews (22, 24–34).

2. CARDIAC ACTION POTENTIAL

The cardiac action potential is a transmembrane potential change, with an amplitude ranging between 60 and 120 mV. It starts from a negative value, i.e., the resting membrane potential (RMP) in working myocardial cells or maximal diastolic potential in spontaneously beating cells (1), ranging from –95 to –40 mV. As in other excitable cells, the RMP is mainly defined by the conductance

of inwardly rectifying K^+ currents and can be roughly estimated by the Nernst equation from the uneven distribution of mainly K^+ ions across the cell membrane. The electrogenic ATP-dependent Na^+-K^+ pump also contributes to the RMP, by exporting 3 Na^+ and importing 2 K^+ (35–38). In healthy conditions, the duration of the action potential (APD) determines the effective refractory period (ERP), defined as the shortest time interval needed before a new stimulus, or an early extrasystole, can elicit another action potential. The relationship between APD and ERP can be disrupted in pathological conditions, for example, in hyperkalemia, resulting in postrepolarization refractoriness (39).

In the context of the cardiac action potential, two aspects should be emphasized. First, there is no such uniform entity as “the cardiac action potential,” since its shape, i.e., the time course of the transmembrane potential changes, differs in the various regions of the heart (FIGURE 1), and therefore different action potentials should be considered and discussed separately. Second, there are significant interspecies differences (40), even when action potentials are recorded from similar regions of the heart. This is an important, and often overlooked, issue, since many experimental results have been obtained in small rodents, recently particularly in transgenic mice.

In general, the cardiac action potential is divided into five distinct phases (FIGURE 1). Phase 0 is the fast depolarization due to an abrupt increase in sodium influx, and it is characterized by the upstroke velocity and can result in an overshoot, i.e., the rapid change of potential from the negative RMP to positive voltage values, reaching a peak of up to +30 to +40 mV. The overshoot is followed by a return to negative values, in a process called repolarization, which includes phases 1, 2, and 3. Phase 1 is characterized by a transient and relatively fast repolarization brought about by a decrease in sodium influx and a transient increase in potassium efflux and chloride influx. Phase 2 consists of a long-lasting plateau, still at depolarized voltage, during which the membrane potential remains almost constant or decreases slowly, caused by a small net transmembrane current carried by simultaneous calcium (and some sodium) influx and potassium efflux. Phase 3 represents the large repolarization toward the diastolic potential, mostly due to increased potassium efflux and decreased calcium and sodium influx. Phase 4 represents the resting membrane potential in diastole in working myocytes and the spontaneous depolarization in pacemaker cells. In cardiac myocytes that do not beat spontaneously the voltage remains stable at the RMP, whereas in cells exhibiting automaticity the potential gradually changes toward the positive values, in a process called spontaneous diastolic depolarization. When the threshold potential is

reached, a new spontaneous action potential is generated, with a certain cycle length.

There are four common methods to record cardiac action potentials:

- 1) Weidmann and Coraboeuf were the first to record cardiac action potentials in dog ventricular muscle (41) and later in dog Purkinje fibers, using the sharp glass capillary-based microelectrode technique (42). The classical cardiac cellular electrophysiological knowledge gained by using this technique was elegantly summarized in an early monograph entitled *Electrophysiology of the Heart* by Hoffman and Cranefield (1), published in 1960, which is still useful today. This technique is still considered one of the best for accurate cardiac action potential recordings and can be used for both single-cell and tissue recordings. Its major advantages include 1) the ability to accurately record very fast voltage changes and 2) because of the very fine tip of the pipette, very little diffusion takes place out of the pipette solution, having negligible effects on the intracellular milieu. However, since this technique has some limitations (e.g., difficulties in maintaining a stable impalement for extended periods of time), other methods have also been developed and used widely.
- 2) In intact hearts, in in vivo animal experiments, or in clinical studies, where the microelectrode technique is difficult to apply, monophasic action potential recording can also be used, with either a suction electrode (43, 44) or a Franz catheter (45). With this technique, recordings can be easily performed from multiple sites simultaneously, and impalements/attachments are not lost because of vigorous contractions, even in in vivo or ex vivo conditions. However, rapid voltage changes or action potential amplitudes and shapes cannot be determined accurately.
- 3) Since the introduction of the patch clamp by Neher and Sakmann (46–48), the whole cell configuration of this technique has been widely used. In the current-clamp mode, it can record action potentials from isolated myocytes. Despite its widespread use, this technique has important limitations that should be emphasized. First, measurements are performed in single isolated myocytes or, occasionally, cell pairs, and it is uncertain how, and to what degree, different ion channels are influenced by individual enzymatic digestion during the isolation procedure (49). Therefore, even if the recordings show single-cell action potentials with a normal shape, the function of the finely regulated ion channels can be drastically altered from their original condition. Also, the cell is dialyzed with the pipette contents, and its intracellular composition will change. When carefully and deliberately applied, however, this point can also be considered an advantage, as it allows control of the intracellular milieu. It should also be emphasized that single isolated myocytes are devoid of electrotonic interactions from neighboring cells. Therefore, the stochastic

opening/closing behavior of ion channels has a more profound effect on membrane potential than in well-coupled tissue preparations (50). In addition, in multicellular preparations part of the ionic currents are utilized to depolarize neighboring cells during impulse propagation, and this can considerably reduce the action potential peak compared with single cells (51). Hence, action potential measurements in single isolated myocytes obtained with the patch-clamp technique should be interpreted with caution and not directly extrapolated to intact tissue.

- 4) The latest approach to recording cardiac action potentials is the optical mapping technique, which uses voltage-sensitive dyes and allows simultaneous recordings from multiple sites (52, 53). This technique is also excellent for dynamic studies and for investigations of arrhythmia mechanisms (54, 55). Disadvantages of this method include the difficulty of calibration to millivolts, phototoxicity, photodegradation, and photon scattering effects (56). Also, the application of excitation-contraction uncoupling compounds, e.g., blebbistatin, is necessary to avoid motion artifacts (57). These compounds may interfere with the experiments, since, e.g., blebbistatin was reported to elicit anomalous electrical activities (58) and prolongation of action potential duration (59), and inhibition of contraction will also decrease metabolic rate at the concentrations needed for motion artifact reduction.

3. TRANSMEMBRANE ION CHANNELS AND TRANSPORTERS IN THE HEART

The cardiac action potential is the voltage change caused by ions flowing through transmembrane ion channels, via their dynamic and simultaneous opening and closing (11, 60). Therefore, before addressing different regional action potential patterns, we describe the various transmembrane ion channels that have been reported to operate in the heart cells.

Transmembrane ionic currents in the heart are usually measured with the patch-clamp technique in enzymatically isolated myocytes. This allows recording and analysis of unitary currents through single ion channels or all channels on the sarcolemma. Before the introduction of the patch clamp, transmembrane current recordings were less accurate, because of the lack of proper voltage control of the preparation, and fast current changes and gating kinetics were impossible to determine accurately (61). Therefore, much of the knowledge gained before the introduction of the patch-clamp technique has had to be reevaluated, and some currents have been renamed. To the interested reader, we recommend an excellent monograph by Denis Noble, *The*

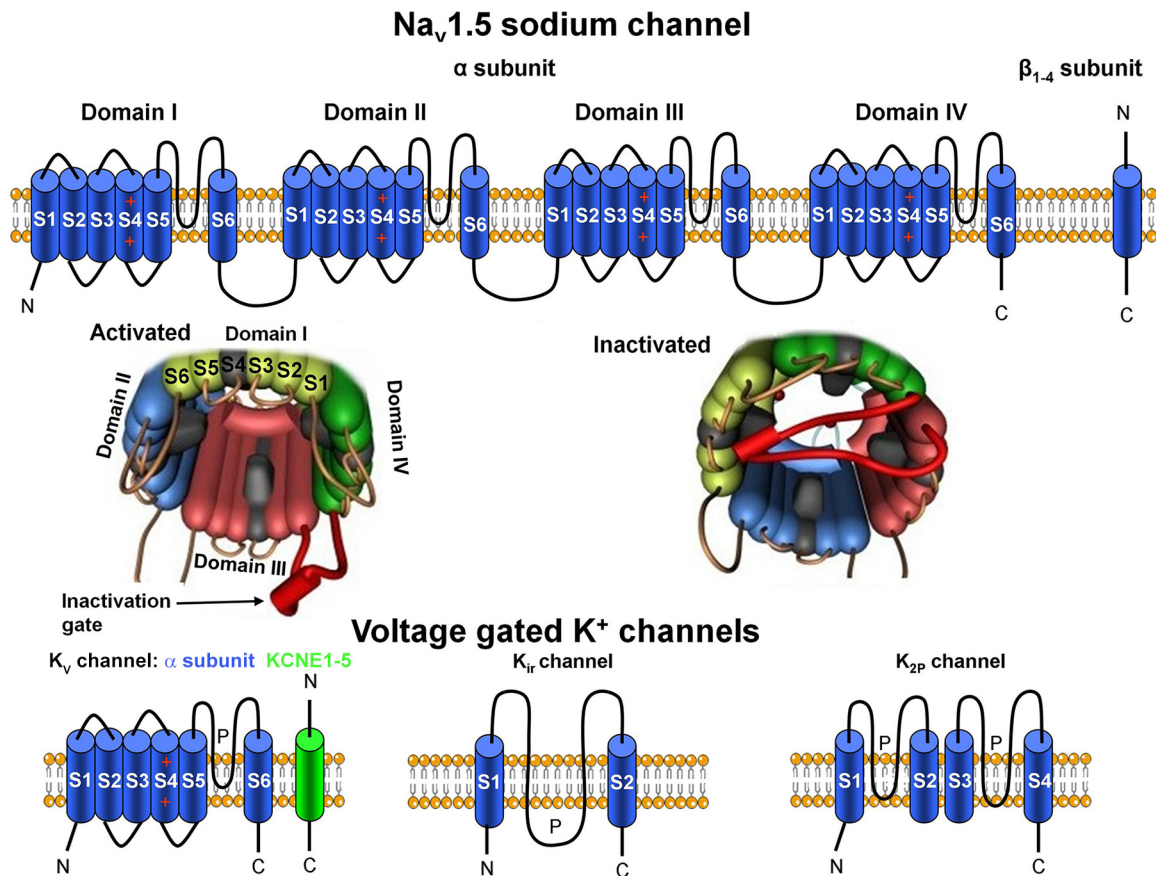


FIGURE 3. Schematic illustration of voltage-gated sodium (Na_v) and potassium (K_v) channels. *Top*: topological models of $\text{Na}_v1.5$ channel subunits and their molecular assembly. Four domains (I–IV) of Na_v α -subunits contribute to individual Na_v channel formation. *Middle*: the activated and inactivated Na_v channel configurations. *Bottom*: the transmembrane topologies of K_v , inward rectifier (K_{ir}), and two-pore domain (K_{2p}) potassium channel subunits.

Initiation of the Heartbeat (62), which deductively and briefly summarizes our knowledge before the use of the patch-clamp technique.

It is important to note that a given ionic current, measured with the patch clamp, does not correspond to a unique ion channel. Certain transmembrane ionic currents can be conducted by several different ionic channels (3, 5), e.g., inward rectifier potassium current (I_{K1}) is carried by inward rectifier potassium (K_{ir})2.1, K_{ir} 2.2, K_{ir} 2.3, and K_{ir} 2.4 channels (5, 63) and tandem of pore domains in a weak inward rectifying potassium channel (TWIK)-related acid-sensitive potassium (TASK) channels (64), whereas transient outward current (I_{to}) is carried by voltage-gated potassium (K_v)4.3, K_v 4.2, and K_v 1.4 channels. In addition, certain channels like human ether-à-go-go-related gene (hERG) have multiple isoforms (hERG 1a and 1b) (65) with different gating kinetics and drug sensitivities (66). This offers the possibility of pharmacologically modulating specific channel isoforms without interfering with others, and thus avoiding undesirable side effects.

Recent advances in genetics and molecular biology have made it possible to further elucidate the structure of ion channels (FIGURE 3). It is widely known that

most transmembrane ion channels consist of multiple subunits: a pore-forming α and modulatory accessory subunits, which can modify channel gating and serve as possible drug binding or phosphorylation sites (3, 5, 67, 68).

3.1. The Fast Inward Sodium Current

The fast inward sodium current (I_{Na}) is the most important current for impulse conduction in cardiomyocytes, with a diastolic potential more negative than -60 mV (69), and is therefore particularly important in atrial, ventricular, and Purkinje fiber myocytes. This current is responsible for the influx of Na^+ during phase 0 of the action potential (FIGURE 1 and FIGURE 4), and it is conducted by voltage-gated sodium (Na_v)1.5 channels, encoded by the gene *SCN5A* coassembled with β_{1-4} (*SCN1–4B*)-subunits (70). The high-molecular-weight pore-forming α -subunit contains four repeat domains (labeled I–IV); each domain consists of six transmembrane segments (S1–S6), and the S4 segment is responsible for voltage sensing (FIGURE 3). Special extracellular regions (P loops) between the S5 and S6 segments of the four domains form the structure that is responsible

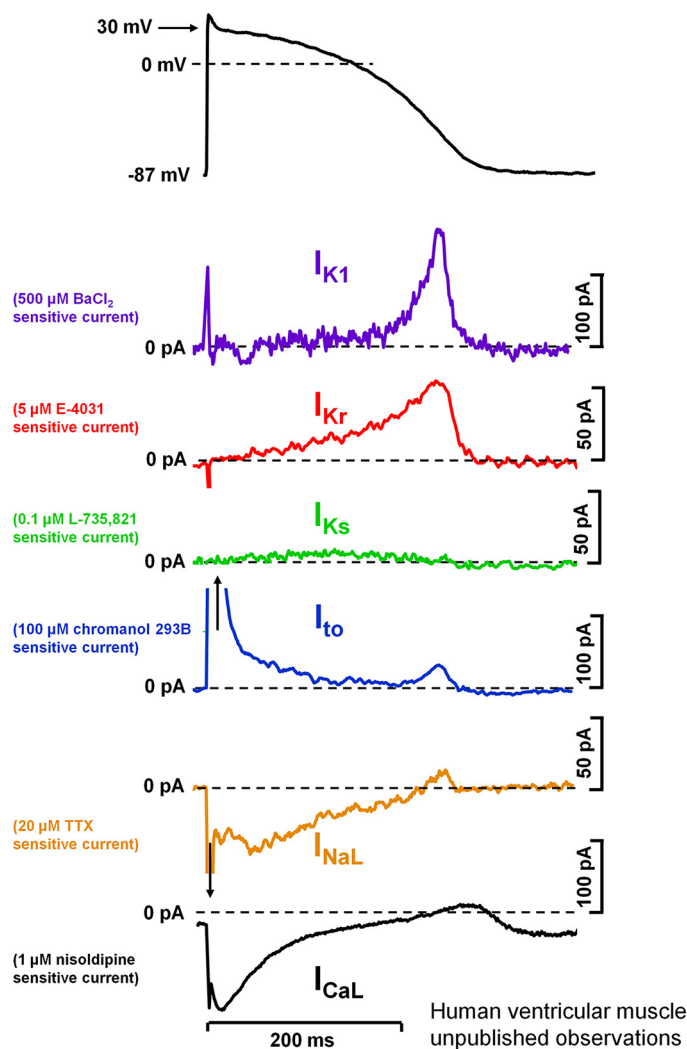


FIGURE 4. Action potential and underlying ionic currents recorded from human ventricular myocytes with the patch-clamp technique applying human ventricular action potential as command pulses at 1 Hz stimulation frequency, in the absence of any sympathetic effects. Inward rectifier potassium current (I_{K1}), rapid (I_{Kr}) and slow (I_{Ks}) components of delayed rectifier potassium current, transient outward current (I_{to}), and L-type calcium current (I_{CaL}) were measured as difference current following application of selective channel inhibitors. I_{NaL} , late sodium current. Unpublished data from our laboratory at the Department of Pharmacology and Pharmacotherapy, University of Szeged.

for the ion selectivity of the channel. The region that links domains III and IV contains the inactivation gate that “plugs” the channel pore after prolonged activation (FIGURE 3). A detailed, comprehensive review on the cardiac sodium channel structure has been published recently (71). $Na_v1.5$ channels open, within a fraction of a millisecond, at potentials more positive than -60 mV, with strong voltage dependence. Since channel density is high, they carry a large inward current, with an amplitude of >100 pA/pF. They also inactivate very rapidly at voltages more positive than -80 mV (at -10 mV with time constant τ_1 of 0.6 ms and τ_2 of 4 ms) (72), with a half-inactivation between -60 and -70 mV. $Na_v1.5$

channels can recover from inactivation with a time constant of 2–20 ms at negative voltages (69, 73, 74). The exact kinetics of their inactivation and recovery are complex and still not fully understood. So far, multiple inactivation kinetics and recovery kinetics from inactivation have been described (12, 69, 75–77).

In addition to this fast component, slow inactivation, occurring over hundreds of milliseconds, has been described (12, 13, 78) and attributed to late openings of $Na_v1.5$ channels (79). Recently, a new term, “late sodium current” (I_{NaLate}), has been used to refer to this current, which, although small in amplitude ($<0.5\%$ of the peak I_{Na}) (79, 80), nonetheless represents an important sustained depolarizing current during phase 2, thus playing a role in maintaining the relatively long plateau of the cardiac action potential (FIGURE 4) (78). This I_{NaLate} is more sensitive to tetrodotoxin (TTX) and other sodium channel inhibitors (81) than the peak I_{Na} (82).

As a steady-state component of I_{Na} , a so-called “window sodium current” in the voltage range from -65 to -15 mV based on a different mechanism than the slow inactivation was also suggested earlier by Attwell et al. (9). This window current was considered to be caused by the overlap between the steady-state activation and inactivation curves. At present, it is still not clear whether such a window current exists, or if the measured overlap is due to an ultraslow inactivation or ultraslow recovery from inactivation when this window current is determined. To better understand the nature of the sodium current during the plateau phase of the action potential, the possible involvement of sodium channels other than the $Na_v1.5$ channel, which is considered to be the major cardiac sodium channel, was also suggested in several studies (83–88). As an example, $Na_v2.1$ α -, β_1 - and β_2 -subunits are highly expressed in human atrial and ventricular cells and Purkinje fibers (84, 85) even if their function has not been explored yet. The expression of various neuronal sodium channel subtypes, e.g., $Na_v1.1$, $Na_v1.2$, $Na_v1.3$, $Na_v1.4$, $Na_v1.6$, and $Na_v1.8$ (encoded by *SCN1A*, *SCN2A*, *SCN3A*, *SCN4A*, and *SCN10A* genes, respectively), has been described in different cardiac preparations (89), but again their functional roles are not fully understood (3, 5, 85, 86, 90). Mishra et al. (86) reported that in failing dog and human hearts neuronal $Na_v1.1$ channels were upregulated and provided significant I_{NaLate} , whereas another recent study (91) showed significant upregulation of $Na_v1.8$ channels in failing human hearts. In addition, selective inhibition of this $Na_v1.8$ current by A-803467 (92) abolished arrhythmogenic Ca^{2+} sparks that were attributed to enhanced intracellular Ca^{2+} load due to increased I_{NaLate} . Mutations in the $Na_v1.8$ encoding gene, *SCN10A*, were reported in patients with atrial fibrillation (AF) (88) and also predisposed to sudden cardiac death (83). Therefore, it is

SCN5A expression in the heart

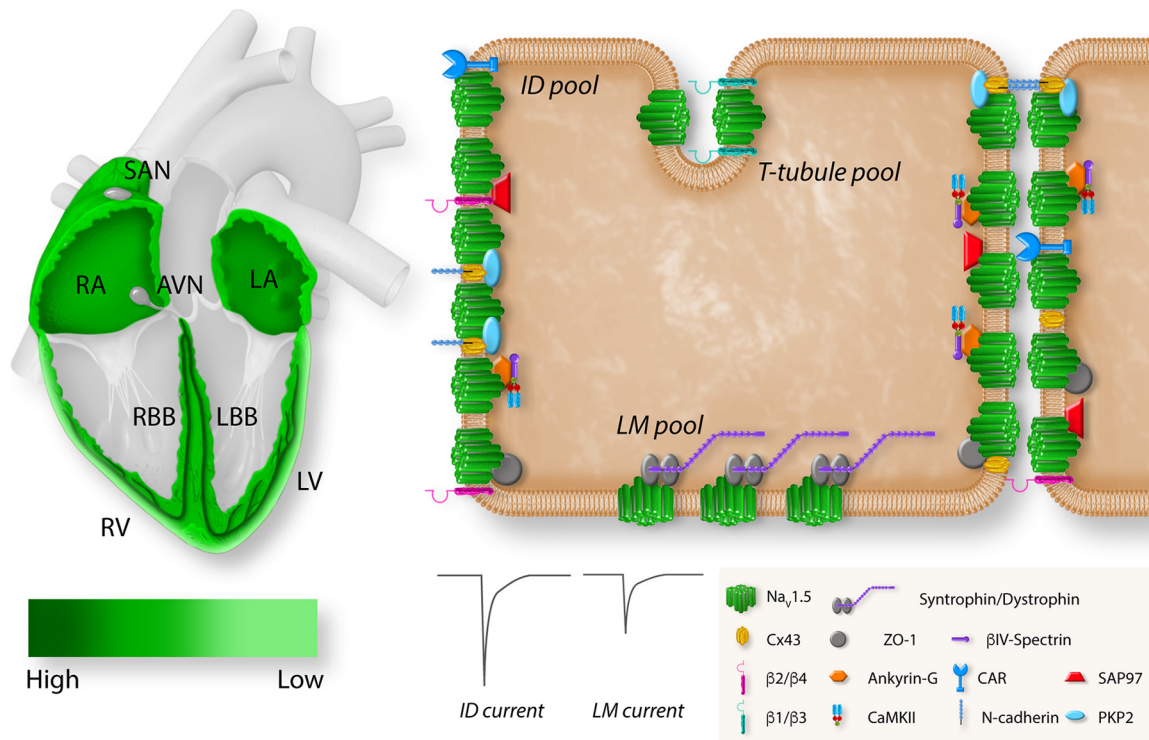
Na_v1.5 localization in the cardiomyocyte

FIGURE 5. Regional and subcellular distribution of *SCN5A*/voltage-gated sodium channel ($\text{Na}_v1.5$) in the heart and cardiomyocytes. *Left:* the expression levels of *SCN5A* in different regions of the heart. Expression of *SCN5A* is highest in the atrioventricular (AV) bundle, His bundle, and right (RBB) and left (LBB) bundle branch (dark green). *SCN5A* is broadly expressed in right (RA) and left (LA) atria and right (RV) and left (LV) ventricle with an epi/endo gradient in the ventricles. *SCN5A* is absent from the central sinoatrial node (SAN) and atrioventricular node (AVN). *Right:* the localization of $\text{Na}_v1.5$ with specific regional partner proteins in the microdomains of a cardiomyocyte: intercalated disk (ID), lateral membrane (LM), and T tubules. The sodium current at the ID is larger than the sodium current at the LM. Reproduced from Ref. 94 with permission.

clear that further studies are needed to elucidate the role of neuronal Na^+ channels in normal and diseased heart (93).

It is known that $\text{Na}_v1.5$ channel expression varies in the different regions of the heart, showing a high level of expression in the specialized conduction system, atria and ventricles, while being absent in the central sinus and atrioventricular nodal tissues (FIGURE 5). Also, $\text{Na}_v1.5$ channels gather in clusters and associate with accessory subunits and partner proteins, forming region-specific macromolecular complexes (95). They are not evenly distributed within the myocyte (96). The current densities are large in the intercalated disk area and smaller in the lateral membrane (96, 97). The complex nature and the observed regional differences in sodium channel expression, as well as the functional significance of $\text{Na}_v1.5$ interactions with partner proteins, justify further studies to better understand the pathophysiology of diseases associated with $\text{Na}_v1.5$ dysfunction, including inherited sodium channelopathies (94, 98).

The function of I_{Na} is regulated by intracellular calcium homeostasis in a complex way that involves multiple

accessory proteins (99). Calmodulin (CaM), the ubiquitous Ca^{2+} -sensing protein, plays a central role in intracellular Ca^{2+} concentration ($[\text{Ca}^{2+}]_i$)-dependent I_{Na} function alterations by modulating fast inactivation of I_{Na} (100). Recent data suggest that CaM facilitates the recovery of the sodium channel from inactivation by interacting with its inactivation gate in a Ca^{2+} -dependent fashion (101). The different binding sites of CaM on the sodium channel are important to understand the mechanisms linked to disease-associated sodium channel mutations (102–104). In addition to CaM, Ca^{2+} /calmodulin-dependent kinase II (CaMKII) has been shown to modify I_{Na} function in a Ca^{2+} -dependent manner. CaMKII phosphorylation regulates cardiac Na^+ channels by slowing their recovery from inactivation (105, 106). This results in reduced availability of fast I_{Na} at a high rate with enhanced late I_{Na} (106). The latter contributes to prolonged repolarization and enhanced arrhythmia susceptibility (106, 107) often seen in heart failure, where CaMKII activity is enhanced (107).

In addition to TTX, I_{Na} is blocked, although not selectively, by a wide range of antiarrhythmic drugs, e.g., lidocaine, mexiletine, quinidine, disopyramide, and

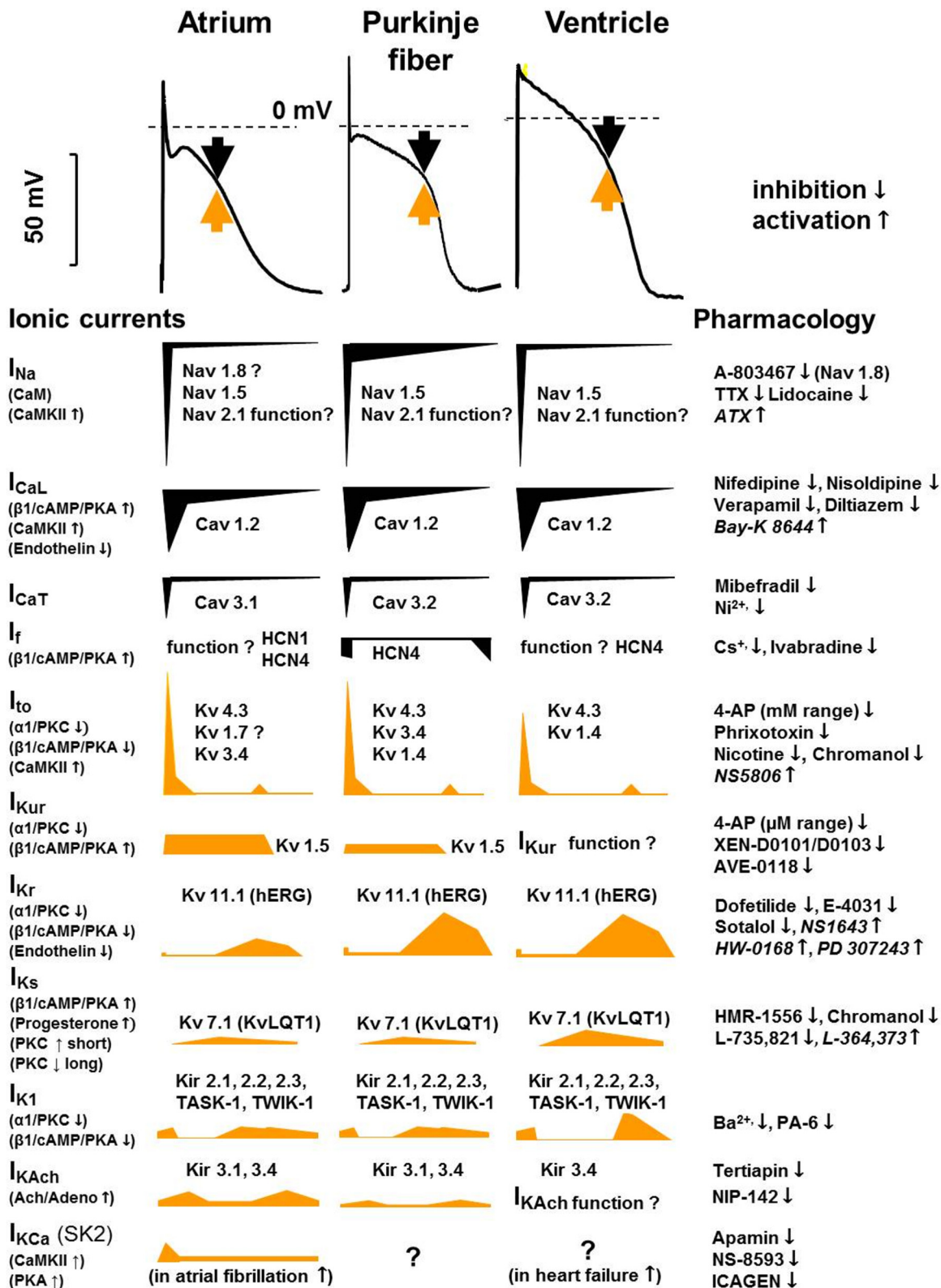


FIGURE 6. Tissue-specific (human) cardiac atrial, Purkinje fiber, and ventricular action potentials and the underlying ionic currents in different action potential phases, indicating their pharmacology and modulation. Black arrows indicate inward and yellow arrows indicate outward current. The contributions of different currents to the action potentials are indicated below, with a time course adjusted to the action potential. CaM, calmodulin; CaMKII, Ca²⁺-calmodulin kinase II; hERG, human ether-à-go-go-related gene; I_{K1}, inward rectifier potassium current; I_{KACh}, acetylcholine-activated potassium current; I_{Na}, sodium current; I_{CaL}, L-type calcium current; I_{CaT}, T-type calcium current; I_f, funny/pacemaker current; I_{to}, transient outward current; I_{KCa}, calcium-activated potassium current; I_{Kr}, I_{Ks}, and I_{Kur}, rapid, slow, and ultrarapid components of delayed rectifier potassium current; Kir, inward rectifier potassium channel; Kv, voltage-gated potassium channel; Nav, voltage-gated sodium channel; TASK, Tandem of pore domains in a weak inward rectifying potassium channel (TWIK)-related acid-sensitive potassium channel; TTX, tetrodotoxin.

flecainide (FIGURE 6) (108, 109) in a frequency-dependent manner. It has recently been reported that certain drugs like ranolazine and GS967 selectively inhibit I_{NaLate} (110, 111). Therefore, these compounds would be particularly effective for long QT (LQT) syndromes, heart failure (HF), or hypertrophic cardiomyopathy (HCM) (110). On the other hand, late I_{Na} can be pharmacologically augmented by veratrine (112), veratridine, and ATX (113).

Genetic mutations that alter I_{Na} function can lead to severe, potentially lethal, conditions and have been shown to play a significant role in a wide array of inherited channelopathies (for recent reviews see Refs. 94, 114–117). As an example, loss-of-function *SCN5A* mutations lead to a reduced I_{Na} peak, thus slowing impulse conduction and possibly causing conduction block. These mutations have been identified in ~20% of patients with Brugada syndrome (BrS) (118) as well as in patients with sick sinus syndrome and progressive cardiac conduction defect (119–121). On the other hand, gain-of-function *SCN5A* mutations have been shown to play key roles in congenital LQT3 syndrome (122). In some cases of familial AF, both loss-of-function and gain-of-function *SCN5A* mutations have been identified (123, 124).

The late sodium or window current, irrespective of its basic mechanism or molecular background, is particularly important in arrhythmogenesis (125). As an example, in HF and in HCM, I_{NaLate} is augmented (126, 127). Since this current is an important contributor to the action potential plateau phase, its enhancement prolongs repolarization and increases repolarization heterogeneity (110, 128). In addition, by increasing intracellular sodium concentration, it also increases intracellular calcium concentration, via the Na^+/Ca^{2+} exchanger (NCX). This can evoke arrhythmogenic triggered activity such as early and delayed afterdepolarizations (EADs and DADs, respectively) (129–131), discussed below in this review. Both triggered automaticity and enhanced dispersion of repolarization are considered major mechanisms in arrhythmogenesis, and their reduction is a major aim in antiarrhythmic drug development.

3.2. The Transient Outward Current

The main channels providing the transient outward potassium current (I_{to}) in human and dog ventricular muscle are $K_v4.3$ and $K_v4.2$ pore-forming α -subunits coassembled with KChIP2 and DPP auxiliary subunits (85) encoded by *KCND3*, *KCND2*, and *KCNIP2* and *DPP6/10* genes, respectively (132–134). $K_v1.4$ α channel subunits (encoded by *KCNA4*) are also expressed with marked regional and interspecies dependence, making up ~10–20% of I_{to} density in humans (135, 136). Accordingly, in humans (unlike in dogs), in addition to the rapid

component (τ_{fast} ~50–100 ms), the I_{to} recovery from inactivation also has a component with a slow recovery time constant (on the order of seconds) that is characteristic of the $K_v1.4$ channels (137). It is interesting that in rabbit ventricle the I_{to} current is primarily conducted by $K_v1.4$ channels (138). However, the functional role of this channel in rabbits is still unclear, as it is inactivated most of the time at their physiological heart rate, which is quite high. In humans, both $K_v4.3$ and $K_v1.4$ channels can have functional roles, particularly in the frequency-dependent modulation of the APD during both different constant or following abrupt changes in cycle lengths during electrical restitution (i.e., following extrasystoles with different coupling intervals). In addition, there are mRNA expression studies (85, 139) supporting the possibility that the $K_v1.7$ channels also have a functional role for I_{to} in human atria and ventricles. However, because of the relative paucity of data regarding $K_v1.7$ channels in the heart, further research is needed to properly elucidate these issues.

Human and dog I_{to} start activating at membrane potentials more positive than –30 mV, rapidly reaching peak values (within 1–2 ms) and then inactivating with a double-exponential time course (τ_{fast} ~5 ms, τ_{slow} ~25 ms) (140). The $K_v4.3$ channel-mediated I_{to} , unlike $K_v1.4$, recovers rapidly from inactivation in the membrane voltage range of –60 to –80 mV, with a time constant of ~50 ms (137). In dog and human Purkinje fibers, $K_v3.4$ channels were also described to contribute to I_{to} , with different kinetic properties compared with $K_v4.3$ channels (141). This raises the possibility for fine-tuning of frequency-dependent modulation of repolarization dispersion between Purkinje fibers and ventricular muscle (142).

The transient outward potassium current and the fast inactivation of I_{Na} are important contributors to the early/fast repolarization of the action potential (phase 1) (137, 143) (FIGURE 4). Phase 1 repolarization and I_{to} are more prominent in Purkinje fibers and atrial, mid-myocardial, and subepicardial ventricular muscle (137), but they are small, or nonexistent, in subendocardial ventricular cells and sinoatrial (SA) and atrioventricular (AV) nodal cells (137). Interestingly, phase 1 repolarization and I_{to} are not present in guinea pig ventricular myocytes (144, 145). Also, it has been reported that in mouse ventricle I_{to} is small and action potential is long after birth and later the action potential shortens as I_{to} develops in adult mice (146, 147). The impact of I_{to} on the shape of the action potential waveform is complex. In addition to its role in phase 1, I_{to} also modulates the voltage level of the plateau, and consequently it has an indirect influence on activation, inactivation, and deactivation of several other transmembrane ionic currents that operate during the plateau phase. Since I_{to} ,

similarly to I_{Na} , has activation, deactivation, and inactivation properties, it was also suggested that a window I_{to} current may be generated, in the membrane potential range from -35 to -10 mV. This window current would also contribute to the final repolarization (140). It was also reported that interaction of DPP10a with $K_v4.3$ channels results in a sustained current component of human atrial I_{to} that can participate in the late repolarization phase (148). However, despite its potential importance, it is difficult to validate or disprove the existence of such current, since selective inhibitors are lacking. This suggests the need for further research to clarify this issue. I_{to} is a typical transmembrane ionic current that can be attributed to the function of a wide variety of distinctly different potassium and also chloride ion channels (137). Although the role of I_{to} in arrhythmias is not well defined, it definitely plays a role in Brugada syndrome (117, 149), where a reduced expression level of the auxiliary I_{to} subunit, KChIP2, in females most likely underlies the male phenotypic predominance (150, 151). The stronger epicardial I_{to} in males could further aggravate the consequence of impaired I_{Na} in Brugada patients; in this case, inhibition of I_{to} would be beneficial. Multiple nonselective I_{to} inhibitors have been reported (FIGURE 6): 4-aminopyridine (4-AP), in millimolar concentrations (152); quinidine, flecainide, and chromanol 293B, in micromolar concentrations (140, 152); and phrixotoxin, in nanomolar concentrations (153). However, a selective I_{to} inhibitor is still lacking. This could constitute a potential treatment in atrial fibrillation, by increasing APD and consequently ERP, in atrial but not or less in ventricular tissue (154). An activator for I_{to} was also reported having effect on canine ventricular but not atrial myocytes (155).

I_{to} is downregulated in HF (156–159), HCM (160), and diabetes mellitus (161, 162), possibly contributing to repolarization prolongation in these pathological settings. Recently, it was shown that $K_v4.3$ (fast I_{to}) and $K_v1.4$ (slow I_{to}) were expressed differently in normal and failing hearts, thus contributing to arrhythmogenic regional heterogeneity in action potential waveforms (101). It was also demonstrated that a slowing of phase 1 repolarization, which can be due to the decreased I_{to} often observed in failing hearts (163–165), decreases the driving force of Ca^{2+} through L-type calcium channels, and it can result in potentially arrhythmogenic asynchronous Ca^{2+} release from the sarcoplasmic reticulum (SR) (166). I_{to} is subject to α - and β -adrenergic regulation, both decreasing I_{to} via the PKA and PKC pathways (167), whereas CaMKII has been shown to increase I_{to} (167).

Thyroid-stimulating hormone and thyroid hormones have been shown to modulate I_{to} (168, 169), thus making

I_{to} an important contributor to repolarization abnormalities in altered thyroid status.

3.3. Inward Calcium Current

The inward calcium current (I_{Ca}) in the heart was first described by Reuter (170), and it has two major types (171, 172). The most abundant type is the L-type calcium channel ($Ca_v1.2$), which conducts current through the pore-forming α -subunit (α_1) encoded by the *CACNA1C* gene (85). The α_1 -subunit consists of $\sim 2,000$ amino acids, organized into four repeat domains (I–IV), each containing six transmembrane segments (S1–S6) (173). The S4 transmembrane helix from each domain collectively constitute the voltage sensor of the channel (173). A region called the “P loop” connecting the S5 and S6 segments is responsible for the Ca^{2+} selectivity of the pore region (174). The pore-forming subunit coassembles with the extracellular $\alpha_2\delta$ and intracellular β auxiliary (predominantly β_2 in cardiac tissue) subunits that modulate kinetics, gating, and trafficking properties of the channel (175–177). Inward L-type Ca^{2+} current ($I_{Ca,L}$) has a very rapid activation (14) and is particularly important for excitation-contraction coupling (178), since it serves as a trigger for the calcium-induced calcium release (CICR) (179) from the SR and as a source of extracellular calcium when needed. In addition, $I_{Ca,L}$ plays a fundamental electrophysiological role in maintaining the plateau phase of the action potential (FIGURE 4) and in the depolarization of SA and AV nodal cells (180). In these cell types, $I_{Ca,L}$ is the main contributor to impulse conduction; therefore its impairment prolongs the PQ interval and can result in AV node conduction block. In addition, since $I_{Ca,L}$ provides depolarizing current, its decrease would reduce the spontaneous frequency of these cells. In AV nodal cells, this shift in threshold potential also contributes to the slowing of AV impulse conduction. The inactivation kinetics of L-type I_{Ca} ($\tau_{fast} \sim 2$ –8 ms, $\tau_{slow} \sim 30$ –100 ms) depend not only on membrane voltage but also on the intracellular Ca^{2+} concentration (14, 15, 181–184), which is dynamically changing during the action potential. The recovery from inactivation is complex and strongly depends on voltage. At -40 mV it can be characterized by an exponential time course ranging between 30 and 60 ms with $\tau_{fast} = \tau_{slow}$ (14, 185). Importantly, the recovery kinetics can be faster in ventricular and Purkinje fibers, which have a resting potential around -80 mV. The $I_{Ca,L}$ was originally called slow inward current (I_{si}), since with the old experimental methods, before the introduction of single-cell voltage clamp, a relatively slow I_{Ca} activation was measured (170, 186). Later, with more advanced voltage-clamp techniques, the proper fast activation kinetics could be determined (187).

Table 1. Changes of genes, channel/transporter proteins, and ionic currents in various genetic disorders

Genetic Disorder	Gene	Protein	Ionic Current/Function
<i>Trigger</i>			
CPVT 1	<i>RYR2</i>	Ryanodine receptor	SR Ca ²⁺ release
CPVT2	<i>CASQ2</i>	Calsequestrin	↑ SR Ca ²⁺ release
Inherited sinus bradycardia	<i>SCN5A</i>	Na _v 1.5	↓ I _{Na}
Sick sinus syndrome	<i>HCN4/SCN5A</i>	HCN4/Na _v 1.5	↓ I _f /I _{Na}
Familial inappropriate tachycardia	<i>HCN4/SCN5A</i>	HCN4/Na _v 1.5	↑ I _f /I _{Na}
<i>Substrate</i>			
Brugada syndrome	<i>SCN5A</i>	Na _v 1.5	↓ Impulse conduction
ARVC (Naxos disease)		Desmosome protein	↓ Impulse conduction
LQT1	<i>KCNQ1</i>	KCNQ1 (Kv7.1)	↓ I _{Ks}
LQT2	<i>KCNH2</i>	hERG (Kv11.1)	↓ I _{Kr}
LQT3	<i>SCN5A</i>	Na _v 1.5	↑ I _{Na}
LQT4 (ankyrin-B syndrome)	<i>ANK2</i>	Ankyrin-B	Multichannel interactions
LQT5	<i>KCNE1</i>	KCNE1 (minK)	↓ I _{Ks}
LQT6	<i>KCNE2</i>	KCNE2 (MiRP1)	↓ I _{Kr}
LQT7 (Andersen–Tawil syndrome type 1)	<i>KCNJ2</i>	K _{ir} 2.1	↓ I _{K1}
LQT8 (Timothy syndrome)	<i>CACNA1C</i>	Ca _v 1.2	↑ I _{Ca}
LQT9	<i>CAV3</i>	Caveolin 3	↑ I _{Na}
LQT10	<i>SCN4B</i>	Na _v 1.5 β4	↑ I _{Na}
LQT11	<i>AKAP9</i>	AKAP-9 (yotiao)	↓ I _{Ks}
LQT12	<i>SNTA1</i>	α1-Syntrophin	↑ I _{Na}
LQT13	<i>KCNJ5</i>	K _{ir} 3.4 (GIRK4)	↓ I _{KACH}
LQT14	<i>CALM1</i>	Calmodulin	Multichannel interactions
LQT15	<i>CALM2</i>	Calmodulin	Multichannel interactions
LQT16	<i>CALM3</i>	Calmodulin	Multichannel interactions
SQT1	<i>KCNH2</i>	HERG	↑ I _{Kr}
SQT2	<i>KCNQ1</i>	KVQT1	↑ I _{Ks}
SQT3	<i>KCNJ2</i>	K _{ir} 2.1	↑ I _{K1}
SQT4	<i>CACNA1C</i>	Ca _v α1	↓ I _{Ca,L}

Continued

Table 1.—Continued

Genetic Disorder	Gene	Protein	Ionic Current/Function
SQT5	<i>CACNB2b</i>	Ca _v β2b	↓ <i>I</i> _{Ca,L}
SQT6	<i>CACNA2D1</i>	Ca _v α(2) δ-1	↓ <i>I</i> _{Ca,L}
SQT7	<i>SLC22A5</i>	OCTN2	Carnitine deficiency
SQT8	<i>SLC4A3</i>	AE3	↓ Cl [−] /HCO ₃ [−] exchanger function
Familial AF	<i>KCNQ1</i>	K _v LQT1	↓ <i>I</i> _{Ks}
	<i>KCNE2</i>	MIRP1	↓ ?
	<i>KCNJ8</i>	K _{ir} 6.1	↑ <i>I</i> _{K,ATP}

AF, atrial fibrillation; ARVC, arrhythmogenic right ventricular cardiomyopathy; CPVT, catecholaminergic polymorphic ventricular tachycardia; *I*_{Ca}, calcium current; *I*_{Ca,L}, L-type Ca²⁺ current; *I*_f, funny/pacemaker current; *I*_{K,ACH}, acetylcholine-activated potassium current; *I*_{K,ATP}, ATP-sensitive potassium current; *I*_{Kr}, rapid component of delayed rectifier potassium current; *I*_{Ks}, slow component of delayed rectifier potassium current; *I*_{K1}, inward rectifier potassium current; *I*_{Na}, sodium current; LQT, long QT syndrome; SQT, short QT syndrome; SR, sarcoplasmic reticulum.

*I*_{Ca,L} is modulated (FIGURE 6) by cAMP-dependent phosphorylation and other factors, including intracellular Ca²⁺ levels (15). It has been shown that CaM supports both inactivation and facilitation of *I*_{Ca} (188). The intracellular Ca²⁺ enhances *I*_{Ca} via CaMKII, involving direct phosphorylation of L-type Ca²⁺ channels (189, 190) independently of cAMP via PKA (191) involving Rad, a monomeric G protein that closely interacts with Ca_v1.2 (192). *I*_{Ca,L} can be effectively blocked (FIGURE 6) by Cd²⁺, verapamil, and diltiazem, but the inhibition with these drugs is not selective (193–195). Dihydropyridines, e.g., nifedipine (196) and nisoldipine (197), are more selective *I*_{Ca,L} blockers, but they may be sensitive to light (198). Pharmacological activation of *I*_{Ca,L} is also possible by Bay K8644 (FIGURE 6) (199).

The *I*_{Ca,L} has key roles in several diseases like HF (200), HCM (27), AF (201), and myocardial ischemia and in other pathophysiological conditions, such as the development of EADs, DADs, (202–204) and cardiac ischemia-reperfusion (205), discussed in more detail in other parts of this review.

A gain-of-function G406R mutation of the Ca_v1.2 channel causes type 8 of congenital LQT syndrome, also called Timothy syndrome (TABLE 1). This disease is characterized by slower inactivation of *I*_{Ca,L} (206–208) and by the fact that small clusters of Ca_v1.2 channels have a larger probability for coordinated opening and closing (“coupled gating”) (209), thus leading to tachyarrhythmia and congenital heart defects (ductus arteriosus, ventricular septal defect, Fallot tetralogy, HCM) (210).

The second type is the T-type calcium current (*I*_{Ca,T}), for which significantly less data are available. Its functional role in atrial and ventricular cells and Purkinje

fibers is still unclear. However, it plays an important role in the SA and AV nodal cells (211), where it makes a significant contribution to the pacemaker function. This current is conducted by Ca_v3.1 and Ca_v3.2 channels, encoded by *CACNA1G* and *CACNA1H* genes, respectively (212). *I*_{Ca,T} activates at more negative membrane potentials than *I*_{Ca,L}, and its overlap with *I*_{Na} makes it difficult to study (172). *I*_{Ca,T} can be inhibited by low concentrations (100–200 μM) of Ni²⁺ (172) and by the organic compound mibefradil, which was developed with the aim of decreasing elevated heart rate (213).

3.4. Delayed Rectifier Potassium Currents

Before the introduction of the patch-clamp technique, a slowly activating current carried by K⁺ was recorded during the plateau phase. This current was named the delayed rectifier potassium current (*I*_{x/2}). Later, by applying single-cell patch-clamp technique, Sanguinetti and Jurkiewicz (214) showed that this delayed rectifier outward potassium current can be separated into a rapid (*I*_{Kr}) and a slow (*I*_{Ks}) component. Molecular biological studies also confirmed that these two *I*_K components are conducted by distinctly different ion channels.

3.4.1. The rapid delayed-rectifying potassium current.

The rapid delayed rectifier outward potassium current (*I*_{Kr}) is conducted by the K_v11.1 pore-forming α-subunit, also called hERG in humans (human ether-à-go-go related gene), which is associated with various accessory β and possibly other subunits (85, 215, 216).

Similarly to other K_v channel pore-forming α -subunits, $K_v11.1$ consists of six transmembrane segments (S1–S6) and the functional channel contains four α -subunits (FIGURE 3) (217). The $K_v11.1$ hERG α -subunit has two isoforms (a and b), which are different in terms of gating and drug sensitivity (65, 66). The wide variety of interacting accessory β -subunits include MinK (human minimal potassium ion channel), MiRP1 (mink-related peptide 1), and MiRP2, MiRP3, and MiRP4 proteins encoded by *KCNE1*, *KCNE2*, *KCNE3*, *KCNE4*, and *KCNE5* genes, respectively (85, 215). Initially, it was suggested that MiRP1 interacted with hERG ($K_v10.1$) to form I_{Kr} channels (218). This is due to the fact that when hERG ($K_v11.1$) α channel subunits were expressed alone in HEK cells, a very rapidly activating steady-state-like current was observed, and only coexpression with MiRP1 resulted in currents that resembled native I_{Kr} . On the basis of this observation MiRP1 was considered the most important accessory subunit to form the native I_{Kr} channel. However, later studies indicated very low levels of *KCNE2* expression in human heart, whereas genes of

other β -subunits like MinK, MiRP2, MiRP3, and MiRP4 were abundantly expressed in human atrial and ventricular tissue and Purkinje fibers (85). Coexpression of the β - and hERG α -subunits produced currents with kinetics similar to those native currents that can be recorded in different species including human (219, 220). However, the exact role of these β and other possible accessory subunits, how they regulate I_{Kr} , and whether they are responsible for the observed species-dependent differences and drug sensitivities are unclear at present and need to be elucidated in the future. I_{Kr} activates in a voltage-dependent manner, with an activation τ of 31 ms at +30 mV in human ventricular myocyte (221). It also slowly deactivates (222) in a voltage-dependent manner; its deactivation can be fitted by a double exponential with τ_{fast} of 600 ms and τ_{slow} of 6,800 ms at –40 mV. The ratio of the amplitudes of the fast and slow components increases at more negative potentials. I_{Kr} exhibits a peculiar, very rapid, inactivation (223–225), which starts even before it activates.

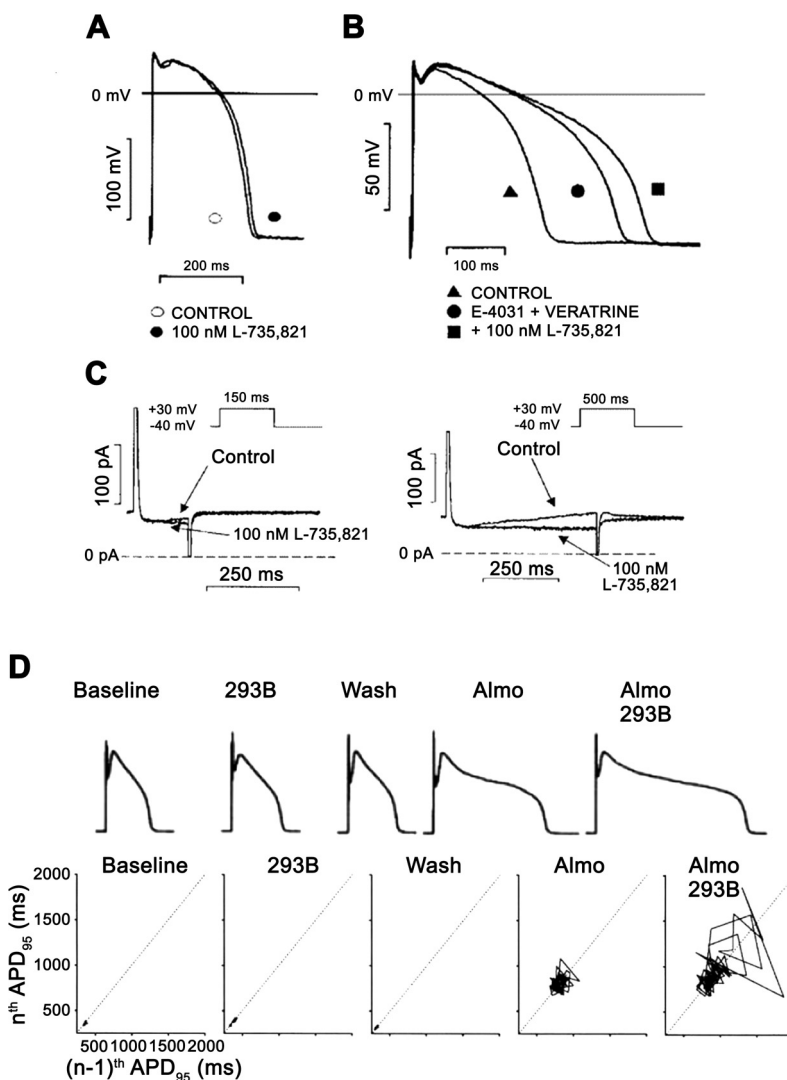


FIGURE 7. The role of the slow component of the delayed rectifier potassium current (I_{Ks}) in the repolarization in dog ventricular papillary muscle (A–C) and in dog single ventricular myocyte (D). In A, action potential duration (APD) is not, or minimally, changed after full I_{Ks} inhibition by 100 nM L-735,821 without external sympathetic stimulation. In B, in the same preparation full I_{Ks} inhibition elicited significant prolongation of repolarization in a preparation where the rapid component of the delayed rectifier potassium current (I_{Kr}) was inhibited by E-4031 and late sodium current (I_{NaLate}) was augmented by veratrine. In C, transmembrane current recordings show that during a short (150 ms) voltage pulse very little I_{Ks} develops, but when pulse duration was increased to 500 ms significant I_{Ks} developed, explaining the lack and significant changes of APD after I_{Ks} inhibition in A and B. (Reproduced from Ref. 228 with permission.) In D, the result of a representative experiment is shown in dog ventricular myocytes. In the baseline (control) situation, small short-term APD variability and normal APD were recorded that did not change significantly after I_{Ks} inhibition by chromanol 293B. Additional application of I_{Kr} block by almokalant increased both APD and short-term APD variability illustrated by the Poincaré plot, which was substantially further lengthened and increased by additional I_{Ks} inhibition, respectively. (Reproduced from Ref. 255 with permission.)

During the action potential in early plateau and in phase 3, I_{Kr} channels rapidly recover from inactivation and they reopen as voltage changes toward more negative values, and deactivation progresses. Accordingly, despite the rapid activation of the current during the plateau phase, a relatively tiny current develops that gradually increases and decreases during phase 3 repolarization (FIGURE 4); therefore it is a crucially important current to secure repolarization.

Since I_{Kr} deactivates slowly, it does not have time to fully deactivate during an action potential. Therefore, a residual and gradually decreasing outward current can still flow through this channel, thus shortening the next action potential when diastolic interval is relatively short, i.e., during fast heart rate or during an early extrasystole (222). Consequently, I_{Kr} is considered a key player in frequency-dependent APD regulation, and it can influence the pacemaker function as well (226).

I_{Kr} can be blocked by specific compounds in the sub-micromolar or micromolar range (e.g., dofetilide and E-4031) (FIGURE 13 and FIGURE 7), causing a marked prolongation of the action potential (227, 228). It was reported that this current can be modulated (FIGURE 6) by endogenous substances like endothelin, which suppresses I_{Kr} (229). Decreased I_{Kr} was also observed after α_1 - and β_1 -receptor activation, linked to the PKC and PKA pathways, respectively (230–232). There are also some compounds known to enhance I_{Kr} (FIGURE 6).

In pathophysiological conditions, I_{Kr} can change. In hypokalemia, the magnitude of the current decreases (233–235), thus making the heart vulnerable to torsades de pointes (TdP) arrhythmia, especially in the presence

of I_{Kr} -blocking drugs (236). The effect of ischemia on I_{Kr} is complex, since acidosis was reported to decrease I_{Kr} (237, 238), particularly by inhibition of the hERG1b isoform of the channel (239), but hyperkalemia can increase (234, 235) the current—and both are present in ischemia. Reduced I_{Kr} was also reported in the infarcted zone in dog myocytes (240). In HF, I_{Kr} is generally considered downregulated (241), even if different studies report sometimes contradictory results.

Loss-of-function mutations in hERG channel can cause congenital long QT syndromes (237, 242, 243), whereas gain-of-function mutations lead to short QT syndromes (244–246) (TABLE 1).

3.4.2. The slow delayed-rectifying potassium current.

The slow component (I_{Ks}) of I_K is carried by the $K_v7.1$ channel, consisting of a pore-forming α -subunit (FIGURE 3) (217), encoded by the *KCNQ1* gene, that coassembles with various MinK, MiRP1, MiRP2, MiRP3, MiRP4, and other accessory subunits, encoded by *KCNE1*, *KCNE2*, *KCNE3*, *KCNE4*, and *KCNE5* genes, respectively (85, 215). MinK was the first β accessory protein (247, 248) that was identified for the $K_v7.1$ channel, but later the importance of other β -subunits (e.g., MiRP1, MiRP2, MiRP3, MiRP4) was recognized, suggesting that this variability in β -subunits may serve as the basis for the marked inter-species variability in native I_{Ks} properties (67, 68). In guinea pig, the amplitude of I_{Ks} is large [(3, 214, 249), and its kinetics differs from those measured in rabbit (250, 251), dog (228) or human (252, 253) ventricular muscle. In

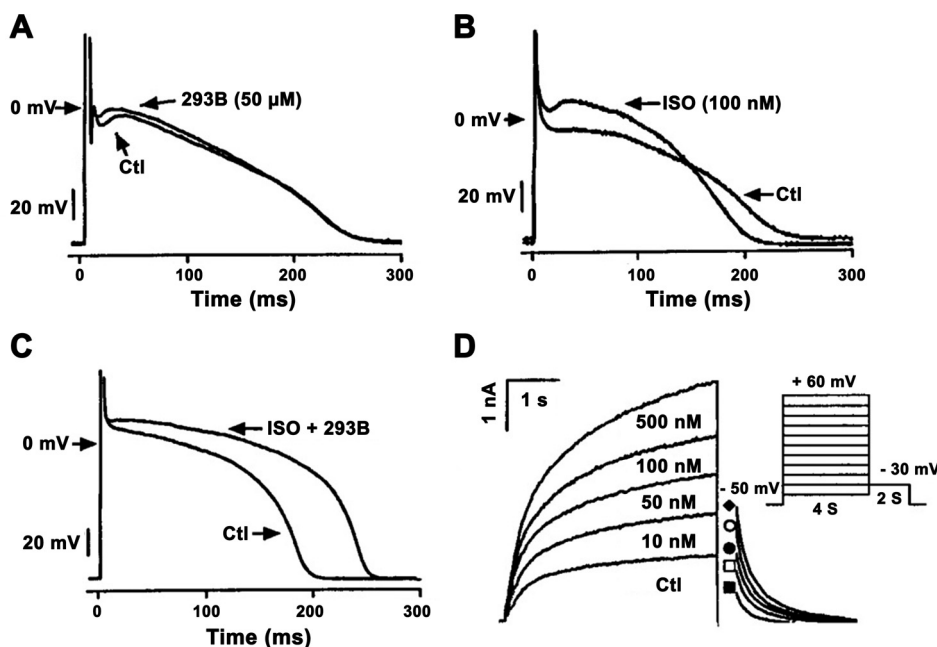


FIGURE 8. A–C: influence of slow component of delayed rectifier potassium current (I_{Ks}) inhibition by chromanol 293B (A), sympathetic stimulation by isoproterenol (ISO, B), and combination of I_{Ks} block and sympathetic stimulation (C) in isolated dog cardiac Purkinje cells. Note that in control (Ctl) condition plateau phases of the Purkinje cells are at more negative voltage than the activation threshold of I_{Ks} , and accordingly I_{Ks} inhibition did not change repolarization. In B, isoproterenol shifted the action potential plateau voltage to more positive values because of substantially increased I_{Ks} . D: in this situation, I_{Ks} inhibition substantially lengthened repolarization as shown in C. (Reproduced from Ref. 157 with permission.)

most species, I_{Ks} activates slowly and in a voltage-dependent manner, at potentials more positive than -30 mV, with τ of several hundred milliseconds to seconds (254). The current deactivates rapidly, except in guinea pigs, in a voltage-dependent manner, with τ of <200 ms at -40 mV (253). The density of I_{Ks} during the plateau of a normal action potential is small (FIGURE 4), because of its slow activation. Therefore, its contribution to repolarization without β -adrenergic stimulation is minimal, except in guinea pig (FIGURE 7A). However, normal physiological conditions always involve some level of sympathetic tone that increases basal I_{Ks} density (255). In addition, when plateau voltage is enhanced by the elevated sympathetic tone, more I_{Ks} develops and contributes more to repolarization (256) (FIGURE 8). I_{Ks} is a critical contributor to the repolarization reserve (257, 258). According to this concept, cardiac repolarization is provided by multiple redundant ionic currents that can compensate for each other's loss of function. Therefore, a dysfunction of a single repolarizing current does not necessarily cause a measurable effect on repolarization. However, congenital or acquired defects in the function of multiple currents can be additive. As shown in FIGURE 7, A and D, I_{Ks} block at baseline does not prolong ventricular repolarization and does not increase short-term variability of APD, which is a recently suggested predictive parameter of proarrhythmic risk (259). However, after I_{Kr} block (by E-4031 or almokalant), I_{Ks} inhibition significantly prolongs repolarization (FIGURE 7B) and increases short-term variability of repolarization. At longer repolarization duration, induced either by I_{Kr} block or by longer voltage pulses (FIGURE 7, B and C), more I_{Ks} develops and, as a negative feedback mechanism, it can limit excessive APD lengthening (221, 228, 260). Although some studies have reported I_{Ks} in atrial tissue (261, 262), and both KCNQ1 and its accessory subunits are expressed in the atria at levels similar to those in the ventricle (263), the presence and role of I_{Ks} in human and canine atrial including sinoatrial node (SAN) cells are still unclear. Assuming similar I_{Ks} kinetics in atria and ventricles, less I_{Ks} activation can be expected in atrial myocytes, since the plateau phase is shorter and it develops at more negative voltages than in ventricular myocytes. One may speculate that at very rapid rates (e.g., during atrial fibrillation or flutter) the continuous presence of a very tiny I_{Ks} current during the action potential, due to frequent channel opening and slow recovery compared with the diastolic interval, may produce a steady-state-like sustained outward current, which may have a role in modulating the resting membrane potential, the pacemaker activity, or even the APD. To resolve these controversies, further research is needed.

I_{Ks} is regulated by endogenous substances (FIGURE 6). Progesterone, and cAMP/PKA-dependent phosphorylation via the Yotiao accessory subunit protein (264), increases I_{Ks}

(255, 265). PKC has a biphasic influence, increasing I_{Ks} after short-term application and decreasing I_{Ks} after long-term application (266). It was also reported that the PKC-mediated I_{Ks} augmentation was PKC isoform dependent (267, 268). Drugs are available to inhibit (228) and to activate (269) I_{Ks} (FIGURE 6). Hypokalemia and elevated intracellular Ca^{2+} enhance and hyperkalemia decreases I_{Ks} (235, 270).

Diseases like heart failure (7) and diabetes mellitus (271) and genetic mutations (LQT1) (114, 149) or drugs (228) can reduce I_{Ks} channel expression, and, as a consequence, the reserve repolarizing current provided by I_{Ks} would be diminished.

This scenario can be further aggravated when intracellular cAMP is elevated, and cAMP-dependent phosphorylation enhances L-type I_{Ca} . Since $I_{Ca,L}$ is an inward current, which prolongs repolarization, the negative feedback function of impaired I_{Ks} cannot sufficiently limit excessive APD prolongation. Therefore, dispersion of repolarization and propensity for life-threatening arrhythmia can increase (272). Genetic mutations can also lead to gain of function of I_{Ks} , resulting in increased current. The mutations have been shown to have concomitant effects in sinoatrial, ventricular, and atrial cardiomyocytes and lead to complex clinical phenotypes (273–281).

3.5. Inward Rectifier Potassium Current

Inward rectifier potassium current (I_{K1}), similarly to I_{to} , is a current that is carried by several channels (282), even if this fact is sometimes overlooked when its behavior is discussed (283). Therefore, the definition of I_{K1} needs

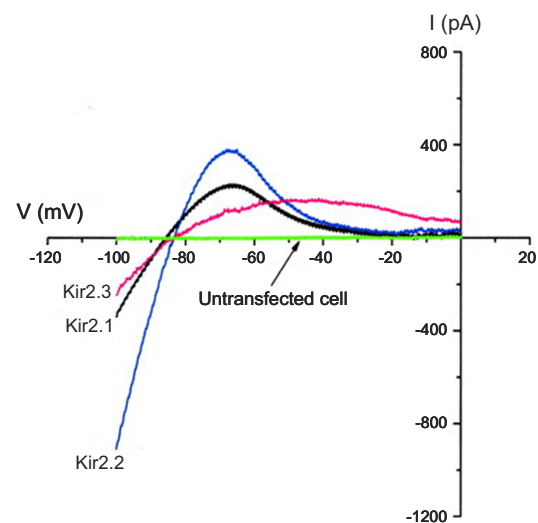


FIGURE 9. Distinct current (I)-voltage (V) relations of inward rectifier potassium (K_{ir})2.x channels expressed in HEK293 cells. Different colors depict ramp (-100 to 0 mV)-generated, barium-sensitive currents in cells expressing Kir2.x channels. The current in an untransfected cell is shown in green. (Reproduced from Ref. 63 with permission.)

particular care. Here we define I_{K1} as a current conducted by channels consisting of $K_{ir}2.1$, $K_{ir}2.2$, $K_{ir}2.3$, and $K_{ir}2.4$ pore-forming α -subunits, encoded by *KCNJ2*, *KCNJ12*, *KCNJ4*, and *KCNJ14* genes, respectively (215, 282). Four α -subunits (each containing 2 transmembrane segments, S1 and S2) combine to form the tetrameric, functional K_{ir} channel (FIGURE 3) (217). I_{K1} channels may also have other, as yet undefined, accessory subunits. Remarkable differences have been observed between currents flowing through the different K_{ir} channel isoforms (63) expressed in mammalian cell lines (FIGURE 9), thus raising the possibility that different species and cardiac tissue types express different channel isoforms, with various phenotypes. Further research will elucidate the exact roles of different K_{ir} channel isoforms.

I_{K1} is considered one of the most important currents securing the resting membrane potential and shaping terminal repolarization in phase 3 of the action potential (FIGURE 4). According to classical electrophysiological principles, one would expect potassium channels to conduct current more easily in the outward direction, as the intracellular K^+ concentration is much greater than the extracellular. Instead, inward rectification means that the steady-state current decreases at potentials positive to about -50 mV. This inward rectification was attributed to channel inactivation caused by intracellular Mg^{2+} and polyamines (284, 285). At potentials more negative than the K^+ reversal potential, I_{K1} is an inward current that has a rapidly inactivating component (286) negative to -120 mV, but the physiological importance of this inactivation has not been established. This current is regularly measured as a Ba^{2+} -sensitive steady-state current at the end of voltage pulses (287). However, Ba^{2+} is not fully selective for any of the K^+ channels described so far, and the steady-state current-voltage relation measured can also include other, not well-characterized, currents, described as “leak” or “plateau” currents (I_{leak} or I_p , respectively) (4, 283, 288).

There are reports suggesting that intracellular $[Ca^{2+}]$ changes can modulate I_{K1} (287, 289, 290), possibly relevant to frequency-dependent APD regulation or in certain pathological settings (291). I_{K1} is also increased by elevated extracellular K^+ concentration ($[K^+]$) (292, 293). Hyperkalemia increases I_{K1} by electrostatically destabilizing Mg^{2+} - and polyamine-induced I_{K1} block by displacing these cations from their binding sites (294).

Activation of both the $\alpha_1/$ PKC and $\beta_1/$ PKA pathways have been shown to reduce I_{K1} in human isolated cardiomyocytes (295, 296). A similar effect of neurokinin-3 was observed on I_{K1} in rabbit and human atria (297). These results further emphasize the importance of autonomic control of atrial APD and electrical function. I_{K1} can be inhibited (FIGURE 6) by Ba^{2+} in the micromolar range (140) and

by the organic compound PA-6 in the nanomolar range (298).

The autosomal dominant mutation of *KCNJ2* causes Andersen–Tawil syndrome (LQT7), having a characteristic triad of episodic flaccid muscle weakness, ventricular arrhythmias, and prolonged QT interval (299) (TABLE 1). Pharmacological approaches to investigate *KCNJ2* loss-of-function mutation revealed that the I_{K1} blocker $BaCl_2$ prolonged the QT interval without causing a major increase in transmural depolarization. EADs and spontaneous torsades de pointes arrhythmias were not observed, nor could they be induced by electrical stimulation. These observations may explain why QT prolongation of the Andersen–Tawil syndrome was found to be relatively benign in clinical settings (300).

The upregulation of $K_{ir}2.1$ was observed in atrial fibrillation, where it may contribute to APD shortening (205). In contrast, $K_{ir}2.1$ downregulation was reported in HF, leading to APD prolongation and facilitating delayed afterdepolarization (DAD) formation (157). Sections 7.1, 7.2, 7.3, and 7.5 provide more detailed information regarding the relevance of altered I_{K1} function and expression in several diseases.

3.6. Ultrarapid Delayed Rectifier Current

The channel carrying the ultrarapid delayed-rectifying potassium current (I_{Kur}) was first cloned from human ventricles (301) but is markedly more expressed in atria (302). At first, it was considered to be a sustained component of I_{to} (303)—“ $I_{to,sus}$.” However, this current is carried by a distinct channel consisting of one $K_v1.5$ α -subunit, encoded by the *KCNA5* gene, and $K_v\beta1.2$ and 1.3 accessory subunits (304, 305).

I_{Kur} is activated rapidly upon depolarization at membrane potentials more positive than 0 mV, with an activation τ of 13 ms at 0 mV potential (302). I_{Kur} inactivates slowly at depolarized potentials, with a double-exponential τ (609 ms and 5,563 ms, respectively, at +40 mV voltage) (306), and its inactivation can be enhanced by sympathetic stimulation (307). This current is thought to operate during phases 1–3 of the action potential of atrial cardiomyocytes and Purkinje fibers but not in ventricular muscle. However, this was challenged by the group of Carnes (308), who measured I_{Kur} as a 4-AP-sensitive current in dog ventricular myocytes. In these dog ventricular myocytes, 50 μ M 4-AP also lengthened APD. These findings, however, need to be confirmed by other investigations. In connection with this, similar mRNA expression levels were measured in ventricles and in Purkinje fibers, but one order of magnitude smaller than in atria (85). Since mRNA measurements from cardiac samples may be contaminated by coronary vessel neuronal tissue and also mRNA from fibroblasts, whether

I_{Kur} exists and/or operates in ventricular muscle is still not fully clarified (252). This question is particularly important because the impact of I_{Kur} on the cardiac repolarization seems complex (309). After the discovery of I_{Kur} , it was thought that selective I_{Kur} inhibitors would have a particular advantage in the treatment of atrial fibrillation, by lengthening APD and ERP in the atria but not in the ventricles. Despite promising animal experiments, these expectations have not been fulfilled, since clinical studies did not result in convincing outcomes with newly developed I_{Kur} blockers (FIGURE 6), e.g., XEN-D0101 and XEN-D0103 (310, 311). Inhibition of I_{Kur} by XEN-D0101 and XEN-D0103 (310) moderately but significantly increased APD in atrial preparations from patients with atrial fibrillation and remodeling, whereas no significant changes were observed in preparations from patients with sinus rhythm (309). These experiments also showed that I_{Kur} inhibition shifts the atrial plateau phase toward the positive direction, thus potentially affecting activation, inactivation, or deactivation of other plateau currents, most notably I_{Kr} . Thereby, I_{Kur} inhibition may produce variable effects of APD and repolarization depending on tissue and experimental conditions (154). This could have important implications if I_{Kur} is actually present in the ventricles, where repolarization reserve would be decreased by I_{Kur} inhibition, with a consequent increase in proarrhythmic risk. I_{Kur} is under adrenergic control: α_1 -receptor stimulation reduces and β_1 -receptor stimulation increases this current in atrial myocytes (306).

3.7. Calcium-Activated K^+ Current

This current is conducted by small-conductance calcium-activated potassium channels (SK2 or $K_{Ca2.1-2}$ and 3), which constitutively bind calmodulin and are encoded by *KCNN1*, *KCNN2*, and *KCNN3* genes (5). The question of whether a calcium-activated K^+ current exists in cardiac tissue and what impact it could have on the action potential was raised long ago (312). Although >35 yr have passed since then, and its existence is now well established in various species and tissues (313), its physiological and pathophysiological roles in cardiac muscle are still not fully elucidated. Most evidence suggests that this current plays a role in the atria (5, 314), and it is also implicated in diseases such as atrial fibrillation and heart failure (5, 315–317). A recent study in rat ventricle showed that SK2 channels are upregulated in HF and also enhanced by PKA phosphorylation (318). In atrial myocytes isolated from patients with AF, SK2 current was increased by enhanced activation of CaMKII (319). The calcium-activated K^+ current is activated in a voltage-independent manner or in response to intracellular Ca^{2+} concentration increase, with a half-maximal activation of 300 nM $[Ca^{2+}]_i$ (320). Despite SK2 channel

expression, this current was not detected, nor was APD lengthened by apamin, the most established inhibitor of this channel, in rat, dog, rabbit, and human undiseased ventricular muscle, thus bringing into question its role in physiological conditions (321). However, other studies have reported an important role for SK2 channels in the human atria.

Most of the evidence regarding the highly apamin-sensitive SK2 current originates from experiments carried out in mice, rats, or rabbits (313, 315, 322, 323). In these species, atrial cellular electrophysiology is not well explored and may differ from dogs or humans. In addition, a marked chloride current was described in rabbit atria that was not found in dog or human atria (324). Furthermore, some of the evidence comes from drug studies performed with NS8593, a putative selective inhibitor of SK2 channels (5), whose effects on all important ionic currents in native cardiac cells have not been tested. Therefore, further investigations are needed for a better understanding of the exact role of SK2 current in cardiac physiology and pathophysiology, which is currently a very interesting and important issue.

3.8. Ligand-Gated Ion Channels

3.8.1. ATP-sensitive potassium channels.

ATP-sensitive potassium channels, carrying the $I_{K_{ATP}}$ current, were first identified in cardiac sarcolemmal membrane by Noma in 1983 (325). K_{ATP} channels were first cloned by Aguilar-Bryan and colleagues (92) and comprise heterooctamers consisting of four inward-rectifying potassium channel pore-forming subunits ($K_{ir6.1}$ or $K_{ir6.2}$, encoded by *KCNJ8* and *KCNJ11* genes, respectively) and four ATP-binding cassette protein sulfonylurea receptors (SUR1 or SUR2, encoded by *ABCC8* and *ABCC9* genes, respectively) (326). The SUR2 has two alternative RNA splice variants, SUR2A and SUR2B; the two polypeptides differ in their COOH terminals (327). Different tissues express K_{ATP} channels with distinctly different subunit composition, thus leading to distinct pharmacological properties of these channels; the myocardial plasma membrane K_{ATP} channel consists of $K_{ir6.2}$ /SUR2A (327). At first glance, their nomenclature might be misleading: these channels are kept closed by physiological intracellular ATP levels in normoxic cardiac tissue, and they activate during metabolic stress, when the ratio of ATP to ADP is decreased, e.g., in myocardial ischemia (328). This makes these channels unique, directly connecting cellular metabolism to membrane excitability. K_{ATP} channels are not regulated by membrane voltage or calcium levels. Indeed, they belong to the inward rectifier (K_{ir}) potassium channel group, with

$I_{K_{ATP}}$ exhibiting weak inward rectification properties on the current-voltage relationship that is regulated by intracellular Mg^{2+} and polyamines (329–331). Activation of sarcolemmal $I_{K_{ATP}}$ during myocardial ischemia heterogeneously shortens the action potential, and may promote reentry (31). Accordingly, several investigations found K_{ATP} activation to be proarrhythmic (332), thus suggesting sarcolemmal $I_{K_{ATP}}$ inhibition for the prevention of myocardial ischemia and ischemia-reperfusion-induced arrhythmias (333–335). In contrast, some studies found no antiarrhythmic effects of K_{ATP} blockers in this setting (336, 337). Furthermore, pharmacological K_{ATP} channel activation was also found to exert antiarrhythmic effects (200, 338, 339) that could be, at least in part, be explained by reduction of monophasic action potential duration heterogeneity (340) and decreased triggered activity in Purkinje fibers upon K_{ATP} opener administration after myocardial infarction (341, 342). It should be also emphasized that K_{ATP} channel activation is very important for prolongation of cell survival during ischemia, since, according to the classical hypothesis, the consequent action potential shortening would reduce contractility by reducing calcium entry into the cardiomyocytes and enhancing Ca^{2+} extrusion via forward-mode NCX activity (343–345). However, cardioprotection following sarcolemmal $I_{K_{ATP}}$ activation in quiescent myocardial cells subjected to hypoxia was also observed (346), suggesting that decreased Ca^{2+} overload via reduced reverse-mode NCX activity during resting membrane hyperpolarization (347) can also contribute to sarcolemmal K_{ATP} -mediated cardioprotection. Therefore, the effects of K_{ATP} channel modulation on ischemia and ischemia-reperfusion-associated cardiac arrhythmias remains controversial.

In addition to the K_{ATP} channels found in the sarcolemma, K_{ATP} channels are also present in mitochondria (348, 349). Evidence suggests that both sarcolemmal and mitochondrial K_{ATP} play cardioprotective roles, albeit via different mechanisms (350). However, because of the lack of truly specific modulators for sarcolemmal and mitochondrial K_{ATP} channels, this remains controversial and further research is needed.

3.8.2. Acetylcholine- and adenosine-activated potassium channels.

It has been known for a long time that acetylcholine shortens APD and has been implicated in atrial fibrillation (351). The ion channel that is directly affected by acetylcholine is called GIRK1/4 or $K_{ir3.1/K_{ir3.4}}$ channel (352, 353), encoded by *KCNJ3* and *KCNJ5* genes, whose α -subunits are closely coupled to muscarinic M_2 - and adenosine A_1 -receptor proteins (354). These channels carry an inwardly

rectifying current, the acetylcholine-activated potassium current ($I_{K_{ACh}}$), and are largely expressed in atrial, SA, and AV nodal cells (355, 356). $I_{K_{ACh}}$ (355, 356) is particularly important in atrial, sinus, and AV nodal cells where they are abundantly expressed. Genes for $K_{ir3.1}$ and $K_{ir3.4}$ are also present in significant amounts in human cardiac Purkinje fibers (85), consistent with the observation that acetylcholine and carbachol shorten APD via $I_{K_{ACh}}$ in atria, SA, and Purkinje fibers (357). However, its influence on repolarization in the ventricles is uncertain (205), and its expression level is relatively low (85). It must be emphasized that increased parasympathetic tone and adenosine can also indirectly decrease $I_{Ca,L}$ amplitude, through the G inhibitory protein decreasing cAMP, thus contributing to shortening of repolarization and shifting the plateau potential toward the negative direction. The $I_{K_{ACh}}$ -induced repolarization shortening is generally considered an important factor in the development of atrial fibrillation (358), and this initiated intensive efforts in the drug industry to develop specific $I_{K_{ACh}}$ inhibitors (359). Cholesterol was also reported to enhance $I_{K_{ACh}}$ (360). The $I_{K_{ACh}}$ current has an important role in modulating the resting or maximal diastolic potential as well, thus hyperpolarizing atrial, SA, and AV nodal tissues and Purkinje fibers. This effect interferes with the pacemaker function, slowing the rate of spontaneous automaticity (361), and it could also slow conduction in the SA and AV nodes, since hyperpolarization can increase the potential difference between the maximum diastolic potential and threshold of activation of $I_{Ca,L}$, which is responsible for depolarization in these tissues.

It has been reported that $I_{K_{ACh}}$ is constitutively active (362) in atrial cells isolated from patients with chronic atrial fibrillation (358) and therefore plays a pivotal role in the shortening of APD or ERP and in the development of atrial fibrillation. Interestingly, however, downregulation of *KCNJ3* gene coded mRNA, $K_{ir3.1}$ channel protein, and $I_{K_{ACh}}$ and upregulation of microRNA (miR)-30d were also observed in atrial tissue obtained from patients with atrial fibrillation (363). In this study, downregulation of $K_{ir3.4}$ protein was also reported (363), thus suggesting a complex, microRNA-regulated ion channel expression in atrial fibrillation that needs further investigation. In addition, after adenosine-induced atrial fibrillation, APD shortened, more so in the right than in the left atrium, and this effect was prevented by inhibition of $I_{K_{ACh}}$ with the selective blocker tertiapin (364). Accordingly, the expressions of both adenosine receptor and $K_{ir3.4}$ GIRK4 channel protein were different between the right and the left atrium (365), thus suggesting a possible role of $I_{K_{ACh}}$ effect heterogeneity in evoking atrial fibrillation.

Recently, it has been reported that an inherited gain-of-function mutation of *KCNJ5* caused familial human sinus node disease. The enhanced activity of GIRK

channels was associated with maintained hyperpolarization of the pacemaker cells that resulted in reduced heart rate (366).

3.9. Chloride Channels

Chloride or anion currents in cardiac muscle were described long ago (367). However, despite intensive and valuable research by some laboratories, relatively little attention has been paid to their possible role in cardiac electrophysiology and arrhythmogenesis (368). One possible explanation is that the functions of chloride channels are diverse (369, 370) and complex and their activation usually needs external triggers like enhanced intracellular cAMP, Ca^{2+} , and swelling or stretch (371). Also the research on Cl^- currents is hindered by the lack of specific blockers, since the established inhibitors of these currents, e.g., DIDS, 9-anthracene (9-AC), tamoxifen, and Cd^{2+} , are not specific. For these reasons, there are uncertainties regarding the degree to which Cl^- channels affect different types of cardiac action potentials. In the basal condition, they carry less current than other well-established transmembrane ion channels. However, in pathological conditions they may play a more important role on arrhythmogenesis than previously thought. Therefore, Cl^- channels deserve more attention, ideally in large-animal or human hearts.

So far, at least four Cl^- channels have been identified convincingly in the heart (369, 370).

3.9.1. Calcium-activated Cl^- channels.

It has been suggested that a current with properties similar to I_{to} may be carried by Ca^{2+} -dependent chloride and potassium currents (372, 373). In this context, it is important to note that the first report of I_{to} in calf Purkinje fiber by Dudel et al. (372) attributed the current to a Cl^- conductance. The kinetics of this Ca^{2+} -dependent I_{to} reflects the kinetics of the calcium transient or rather the changes of intracellular Ca^{2+} in the vicinity of the sarcolemma. This current was also defined earlier as I_{to2} or $I_{\text{to,slow}}$ and could be abolished by depleting the intracellular Ca^{2+} store with caffeine (374) or directly inhibited by DIDS or SITS (375) or by 9-anthracene (9-AC). To avoid confusion, it must be emphasized that this current should be distinguished from the $\text{K}_v1.4$ current, which has also been referred to recently as slow I_{to} because of its slow recovery from inactivation. The physiological and pathophysiological roles of the Ca^{2+} -dependent I_{to} are not well defined but were suggested to play some role in frequency-dependent APD regulation and to secure or shorten repolarization, possibly preventing or diminishing calcium overload in pathological settings

(376). It has been also demonstrated that TMEM16 and Bestrophin-3 are colocalized with $\text{Ca}_v1.2$ in canine and human left ventricular myocytes. In line with this, it was found that activation of calcium-activated Cl^- current ($I_{\text{Cl,Ca}}$) requires Ca^{2+} entry through sarcolemmal $I_{\text{Ca,L}}$, and it is activated by Ca^{2+} release from the SR. Furthermore, $I_{\text{Cl,Ca}}$ exerts an early repolarizing and a late depolarizing component during the action potential, determined by 9-anthracene current in canine ventricular myocytes (377).

Despite the fact that $I_{\text{Cl,Ca}}$ had been discovered a long time ago in the heart, its genetic background was not known for some time and was first attributed to the bestrophin channel protein encoded by the *VMD* gene (378–380), even if later *TMEM16* was reported as an alternative (381–383). The impact of this current on the action potential is different from the other Cl^- currents since it is strongly and dynamically dependent on the intracellular Ca^{2+} concentration (375, 384, 385). It has an important contribution to phase 1, early plateau repolarization, and it also contributes to the repolarization reserve. During Ca^{2+} overload, when spontaneous Ca^{2+} release can happen during diastole, $I_{\text{Cl,Ca}}$ can contribute to the development of DADs by carrying inward current at voltages more negative than the Cl^- equilibrium potential (386). Recently, an anoctamin 1 (*ANO1*)-encoded Ca^{2+} -activated Cl^- channel was identified in the ischemic heart, and its increased density was attributed, at least in part, to the genesis of ischemia-induced arrhythmias (387).

In contrast, in 5-day infarcted canine heart, the I_{to2} current measured from myocytes of the epicardial border zone exerted a significantly smaller peak amplitude, which may contribute to the development of an abnormal action potential (388).

3.9.2. cAMP-dependent cystic fibrosis transmembrane conductance regulator Cl^- channels.

These channels are mostly closed under basal condition, and they carry outwardly rectifying Cl^- current only when intracellular PKA- and PKC-dependent phosphorylation is enhanced. Since the equilibrium potential for Cl^- in normal conditions is between -65 and -40 mV (389–391), they can carry both inward and outward current during the action potential. However, because of its outward rectification, the main effect of the cystic fibrosis transmembrane conductance regulator (CFTR) Cl^- current is to shorten APD and consequently ERP, which in turn may facilitate reentry arrhythmias. Interestingly, it was found that the CFTR Cl^- current abolishes early and late preconditioning and also plays a role in

postconditioning-related cardioprotection (392). It was also reported that intracellular Na^+ modulated the cAMP-dependent regulation of this channel (391).

3.9.3. Swelling- and acidosis-activated Cl^- channels.

In cardiac myocytes, another Cl^- channel was also described, encoded by the *CIC-2* gene and carrying a current that is activated by hyperpolarization more negative than -40 mV, with a relatively slow biexponential time course (393). The current is increased by swelling and acidosis, and it is blocked by 9-AC and Ca^{2+} but not by tamoxifen or DIDS (394). *CIC-2* current, also called $I_{\text{Cl,ir}}$, is strongly rectifying in the inward direction (370, 394, 395), and therefore it plays no or little role in cardiac repolarization. However, it seems to be important in the SA node (396), where it is abundantly expressed, and may contribute to enhanced automaticity during ischemic cell swelling and acidosis.

There are some data regarding a strongly outwardly rectifying acidosis-induced Cl^- current ($I_{\text{Cl,acid}}$), but its molecular entity is unknown. It can be assumed that this current can contribute to the APD shortening in ischemia (397).

Protein tyrosine kinase is one of the initial factors responding to cell swelling, providing the possibility that tyrosine kinase is an important upstream regulator of the swelling-activated Cl^- current ($I_{\text{Cl,swell}}$) (398, 399). Furthermore, angiotensin II is released during stretch, and it is implicated in cardiac remodeling and development of HF, where $I_{\text{Cl,swell}}$ is chronically activated (400, 401). Block of AT_1 receptors prevented activation of $I_{\text{Cl,swell}}$, thus suggesting a potential role of angiotensin II in the activation of the current (402).

3.9.4. Volume-regulated *CIC-3* Cl^- channels.

The channel encoded by the *CIC-3* gene carries a time-independent and robust outwardly rectifying Cl^- current ($I_{\text{Cl,swell}}$) that is small in basal isotonic conditions but is increased by swelling or stretching (369, 370). During ischemia and reperfusion, when swelling of myocytes can occur, $I_{\text{Cl,swell}}$ shortens APD and may enhance dispersion of repolarization between ischemic and nonischemic zones, thus facilitating both atrial and ventricular fibrillation (371, 393). Since the *CIC-3* channels are expressed in atria, ventricles, Purkinje fibers, and SA node cells, they could also play a role in mechanotransduction and in normal pacemaker function, and they may contribute to the development of extrasystoles by promoting membrane depolarization in both the atria and ventricles during stretch (403, 404). *CIC-3* chloride

channels are constitutively active in cardiac hypertrophy and heart failure (370, 371). This may limit APD prolongation, but it may facilitate DADs at elevated diastolic $[\text{Ca}^{2+}]$. In addition, since I_{to} and I_{K1} are downregulated in the failing heart (7), this persistent $I_{\text{Cl,swell}}$ may further change the balance of inward and outward currents toward the inward direction, thus favoring membrane depolarization (405). It was also reported that targeted inactivation of the *CIC-3* gene prevents the cardioprotective effect of the late but not the early phase of preconditioning in mice (405).

3.10. Two-Pore Domain Channels

Two-pore domain K^+ channels ($\text{K}_{2\text{P}}$) are widely expressed in different organs, including the heart, but relatively little is known regarding their function in the myocardium. Except for a few studies, the physiology of these channels has been studied only in mice or rats, but they are abundantly expressed in the human heart as well (406, 407). In general, two-pore domain K^+ channels represent a superfamily of large-conductance K^+ channels, which lack voltage dependence or may exhibit outward rectification (64, 408). They are composed of two α -subunits, each containing four transmembrane segments that form two ion-conducting large-conductance pores (FIGURE 3), and may be associated with several types of accessory subunits (5, 64). These channels are considered important determinants of background K^+ conductance (408). They contribute to the resting or maximal diastolic potential and to the repolarization phase and are regulated by stretch, pH, temperature, and lipids or various signaling messengers (408). In general, the exact roles of the two-pore channels in cardiac electrophysiology and arrhythmogenesis are not well explored and offer challenging targets for further research. Therefore, future intensive research seems worthwhile to clarify the function of these channels in larger mammals and humans, including their potential role in arrhythmogenesis.

3.10.1. TWIK-1 channels.

The “two-pore” or “Tandem of pore domains in a weak inward-rectifying K^+ channel 1” (TWIK-1) channel, encoded by the *KCNK1* gene, was first described in 1996 (407). They are expressed in the heart, are activated by mechanical stretch, intracellular acidification (409), and polyunsaturated fatty acids, and facilitate repolarization and membrane hyperpolarization (5). Recently, it has been reported that TWIK-1 channels can change selectivity from K^+ to Na^+ under extracellular acidic conditions and low K^+ concentration

(410), and this phenomenon is responsible for the paradoxical depolarization contributing to enhanced arrhythmic activity in hypokalemia (411).

3.10.2. TASK-1 ($K_{2P3.1}$) and TASK-3 (K_{2P9}) channels.

The “TWIK-related acid-sensitive K^+ ” (TASK) channels, encoded by the *KCNK3* and *KCNK9* genes, respectively, are voltage-independent channels highly sensitive to extracellular pH, and TASK-1 channels can be selectively inhibited by A293 (5, 64, 412). TASK-1 channels can contribute to APD shortening in ischemia because of their inhibition by extracellular acidosis (412). In addition, they were shown to be upregulated in the atria of patients with chronic atrial fibrillation and preserved cardiac function (413), whereas a downregulation was recently observed in the atria of patients with atrial fibrillation and reduced cardiac function (414, 415), associated with atrial APD shortening (412) and prolongation, respectively. In human atria, TASK-1 channels can form heterodimers with TASK-3 channels (*KCNK9*) that can be regulated by stress and thus contribute to the pathogenesis of chronic atrial fibrillation (416, 417). Interestingly, a gain-of-function mutation in the TASK-4 (*KCNK17*) channel, which is sensitive to pH in the alkaline direction, was reported recently (418), linked to a severe conduction disorder and suggesting the role of the TASK-4 channel in both repolarization and membrane hyperpolarization-related conduction changes.

3.10.3. TREK-1 ($K_{2P2.1}$) channels.

The “TWIK-related K^+ -channel” (TREK-1) represents another two-pore K^+ channel entity that is widely and abundantly expressed in various cardiac tissues (5, 419, 420). TREK-1 channels are particularly important since they carry the outwardly rectifying K^+ current activated by stretch (420), the so-called stretch-activated cation current (SAC), temperature, or polyunsaturated fatty acids, the latter also called arachidonic acid-sensitive current (I_{KAA}). TREK-1-mediated SAC can shorten repolarization, by carrying outward current during the whole duration of the action potential, and hyperpolarize the membrane, thus in turn affecting spontaneous frequency and impulse conduction. This current seems to play a larger role in the atria and SA node than in the ventricles. However, a pathophysiological effect known as “commotio cordis,” describing the accidental chest hit that can cause sudden cardiac death, is presumably due to the function of TREK-1 channels in the ventricles (420). Interestingly, mutations in the selectivity filter can make the TREK-1 channels permeable to Na^+ , thus causing ventricular tachycardia (421). TREK-1 channels are downregulated in atrial fibrillation and heart failure (422–425). They also mediate cardiac fibrosis and diastolic dysfunction, via activation of c-Jun NH₂-terminal kinase (JNK) in myocytes and fibroblasts (426, 427), thus enhancing the propensity of arrhythmias. Genes (*Popdc 1–3*) were identified encoding the cAMP-binding Popeye protein, which associates with TREK-1 channels,

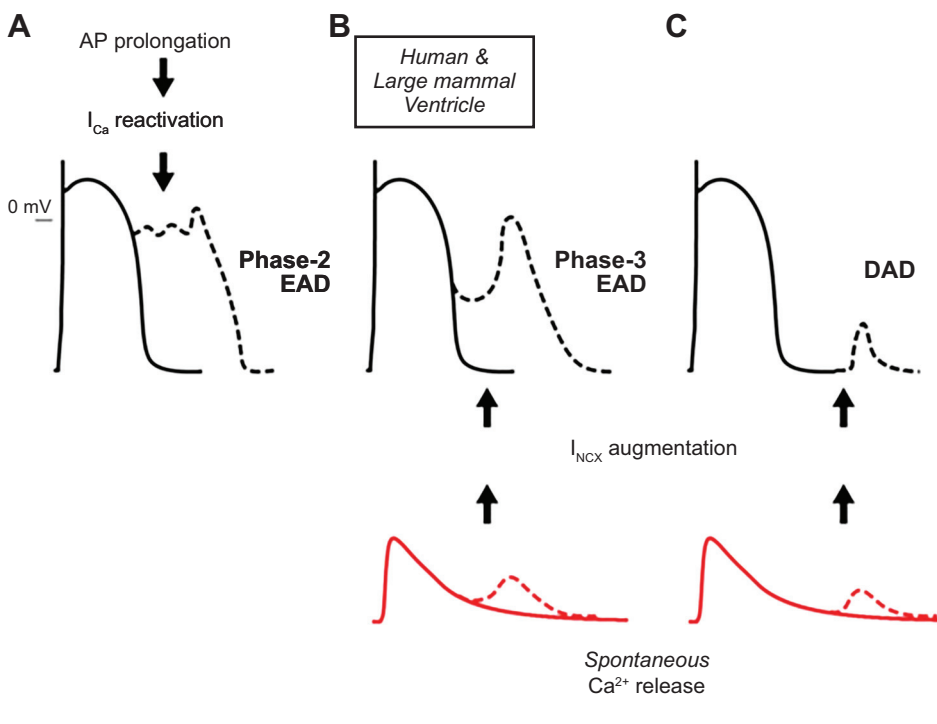


FIGURE 10. Mechanisms of afterdepolarization formation in cardiomyocytes. In ventricular myocytes from large mammals, phase 2 early afterdepolarizations (EADs) are associated with L-type Ca^{2+} current ($I_{Ca,L}$) recovery from inactivation and reactivation during prolonged action potentials (APs) (A). Spontaneous sarcoplasmic reticulum Ca^{2+} release, which increases Ca^{2+} extrusion via Na^+/Ca^{2+} exchange (inward current) (I_{NCX}), can lead to phase 3 EADs (B) or delayed afterdepolarizations (DADs) (C) when occurring during or after the termination of repolarization, respectively. (Reproduced from Ref. 434 with permission.)

modifying their function. Accordingly, the absence of *Popdc 1–2* genes should reduce TREK-1 current, increasing sinus node activity; however, the opposite has been observed experimentally in mouse mutants (242, 428), suggesting the presence of yet unidentified interaction partners for Popeye proteins. Recently, it was proposed that TREK-1 channels could also play a role in establishing the two levels of resting potential (429), a phenomenon that had been described long ago in ventricular and Purkinje fibers (430, 431).

3.10.4. Two levels of resting potential.

Because of the N-shaped steady-state current-voltage relationship of the Purkinje (431, 432) and ventricular (433) cells, two stable levels of resting membrane potentials can develop in these cells. The conductance of potassium channels at 4 mM extracellular $[K^+]$ near the equilibrium potential for K^+ is ~ 100 times greater than that of the Na^+ and Ca^{2+} background channels; therefore it determines the resting potential to be around -90 mV. When the conductance of potassium channels decreases because of I_{K1} inward rectification (FIGURE 9) and/or hypokalemia, the conductance ratio of K^+ and Na^+/Ca^{2+} channels can dramatically decrease, which results in a second stable, albeit lower, potential in the range of -50 to -25 mV depending on extracellular $[K^+]$ or the actual strength of the background Na^+ and Ca^{2+} currents (431–433). This second stable potential has an important role in the genesis of the arrhythmogenic triggered spontaneous automaticity like phase 2 or 3 early afterdepolarizations (FIGURE 10).

3.11. Transmembrane Ion Transporters

Transmembrane ion transporters, which exchange cations across the sarcolemma, are essential to maintain the uneven ion distribution between the extra- and intracellular space. These ion pumps influence cardiac cellular electrophysiology indirectly, by changing various intracellular concentrations (282), most importantly Ca^{2+} , which activates and regulates several other transmembrane ionic currents. In addition, some transmembrane ion transporters are electrogenic, i.e., they exchange charges unevenly, thereby carrying inward or outward transmembrane ion currents, which can influence the action potential repolarization and maximal diastolic or resting potential.

3.11.1. The Na^+-K^+ ATPase/pump.

The primary role of the Na^+-K^+ pump (NKA) is to remove from the intracellular space the Na^+ that

enters during the action potential (36). The pump exchanges 3 Na^+ for 2 K^+ and thereby carries an outward current ($I_{Na/K\text{pump}}$) (282). The size of the generated current ranges between 0.34 and 0.68 pA/pF (37), which can result in RMP changes of 8–9 mV at near-physiological conditions (35, 38), even though its effect is often overlooked. It plays an important role in ionic homeostasis and also in cardiac repolarization (435). The $I_{Na/K\text{pump}}$ shortens repolarization in simulations (436), contributes to the resting potential, and, if its activity is enhanced by elevated extracellular $[K^+]$, intracellular Na^+ concentration ($[Na^+]$), cAMP, or high firing rate (437), can even hyperpolarize the cell (438). The Na^+-K^+ pump needs energy to work, since it pumps out Na^+ against its electrochemical gradient. The source of this energy comes from intracellular ATP, through the function of the Na^+-K^+ -ATPase, which is part of the pump (438). So far, two α -subunits have been identified for NKA: α_1 and α_2 (439, 440). The α_1 is evenly distributed in the sarcolemma (441), and it regulates intracellular Na^+ in the bulk of the cytoplasm. The α_2 is mostly expressed in the dyadic cleft (440, 442, 443) and therefore may have a special role in controlling, via interaction with the NCX, the Ca^{2+} released from the sarcoplasmic reticulum (440). The fact that the α_1 -subunits of the Na^+-K^+ pump are evenly distributed in the sarcolemma and carry $>80\%$ of the $I_{Na/K\text{pump}}$ (440, 444) raises the possibility to develop drugs that selectively modulate the Na^+-K^+ pump α_1 - and α_2 -subunits (440). As well as being regulated by intracellular Na^+ concentration (445), Na^+-K^+ pump activity is controlled by the phosphorylation of FXYP protein phospholemman (PLM) (446). Dephosphorylated PLM exerts a tonic inhibition of Na^+-K^+ pump, and its phosphorylation would relieve this inhibition. Stimulation of the β -receptor increased the pump activity (447), and α -receptor activation enhanced the Na^+-K^+ pump in canine Purkinje fibers (448). It was further reported that insulin flattened the pump current (I_p)-voltage (V) curve of the pump, depending on the patch pipette $[Na^+]$ and voltage (449). The β -subunit is also essential for pump function, providing a stabilization role for the α -subunit. The γ -subunit seems to contribute in regulation of the sodium pump activity (450, 451).

The cardiac glycosides (such as ouabain) are specific inhibitors of the Na^+-K^+ pump (452). Application of 1 μM ouabain increases the AP duration at 90% repolarization (APD_{90}) by 17% and 10 μM by 21%, also increasing the AP plateau (453).

The Na^+-K^+ pump is a key player in the cellular mechanism of ischemia-reperfusion injury. In myocardial ischemia, reduced ATP levels cause a decline in activity

for the $\text{Na}^+\text{-K}^+$ pump. The suppressed function of the pump leads to elevated intracellular Na^+ level, which activates reverse mode of the $\text{Na}^+/\text{Ca}^{2+}$ exchanger (NCX), thus providing enhanced Ca^{2+} entry and Ca^{2+} overload (4).

3.11.2. The $\text{Na}^+/\text{Ca}^{2+}$ exchanger.

The NCX is a member of a large Ca^{2+} /cation antiporter superfamily (454). The mammalian tissues express three NCX isoforms, NCX1–NCX3, encoded by the genes *SLC8A1*–*SLC8A3*, respectively (455–457). Alternative splicing of the primary nuclear *SLC8A1* transcript generates at least 17 NCX1 proteins (454), and the NCX1.1 splice variant represents the cardiac isoform of the NCX (458). The NCX1.1 comprises 10 transmembrane segments, where two groups of five transmembrane segments are separated by an intracellular loop (459). This loop contains the exchanger inhibitory peptide (XIP) region that plays a key role in NCX inactivation by increased intracellular $[\text{Na}^+]$ (460, 461). The cytoplasmic loop also contains two calcium-binding domains that are responsible for Ca^{2+} regulation of the NCX (462). The main function of the NCX is to control calcium flux through the plasma membrane, and it transports 3 Na^+ for 1 Ca^{2+} , using the driving force of the Na^+ gradient provided by the NKA as discussed previously (458, 463–465). The stoichiometry makes NCX electrogenic (466), with one net positive charge moving either into the cell (“forward mode”) or out of the cell (“reverse mode”), eliciting inward or outward transmembrane current (I_{NCX}), accordingly. The magnitude and direction of ion transport and generated transmembrane current therefore depend on the membrane potential as well as the transmembrane concentration gradients of Na^+ and Ca^{2+} , thereby dynamically changing during the action potential (467). During the early phases of the action potential when transmembrane voltage is positive and intracellular Ca^{2+} is low, Ca^{2+} enters the cell by reverse NCX, generating outward current. Later on, when $[\text{Ca}^{2+}]_i$ is increased, Na^+ enters and Ca^{2+} leaves the cell, generating an inward current (468). This function results in complex changes on the cardiac action potential (467) and arrhythmogenicity depending on heart rate, possible Ca^{2+} overload, or NCX expression levels. It was reported that a substantial degree of selective NCX inhibition did not change the shape of the action potential waveform in normal physiological settings in dog ventricular papillary muscle (469, 470) and in human right atrial preparations (471). However, when NCX forward mode was experimentally enhanced in dogs, selective NCX inhibition by 1 μM ORM-10962 shifted the plateau voltage toward negative values (469). On the contrary, when reverse NCX mode was experimentally

augmented, 1 μM ORM-10962 moderately lengthened the action potential (469). It is generally considered that NCX is the major, but not the only (472, 473), source of Ca^{2+} removal from the cell during the later phase of the action potential and diastole, carrying an inward current that can contribute to both EADs and DADs (FIGURE 10). Indeed, it was demonstrated that inhibition of NCX abolishes both EAD and DAD development (470, 474–476) and also arrhythmias caused by enhanced dispersion of repolarization (477) or by ouabain application (469).

Some studies suggest that NCX proteins are relatively concentrated in the dyadic clefts, where the SR-ryanodine Ca^{2+} release site faces the sarcolemma (478–480), but another study (481) provided different results, and thus this issue is still unresolved (440, 463). Na^+ entering the cell can increase the intracellular Na^+ concentration in the small volume of the dyadic clefts, thereby increasing Ca^{2+} entry into the cell on reverse-mode NCX (470, 482). This may increase Ca^{2+} -induced Ca^{2+} release from the SR. It is important to note that Ca^{2+} concentration changes in the clefts and close to the sarcolemma can be orders of magnitude higher than in the bulk of the cytosol (483), which is what is measured routinely with fluorescent Ca^{2+} indicators. Therefore, experiments can severely underestimate the electrophysiological role of NCX in cardiac myocytes. Further methodological improvements are necessary to determine Ca^{2+} concentrations most accurately in the dyads and clefts in order to better define and understand the electrophysiological role of NCX in arrhythmogenesis.

Sorcin is a penta EF-hand protein that interacts with intracellular target proteins after Ca^{2+} binding. It has been reported that NCX1 could be an important target of sorcin: downregulation of sorcin decreases NCX activity, but a higher level of sorcin increases it (484). It was also described that insulin is able to increase the NCX activity via interaction with the 562–670 f-loop domain (485). Furthermore, the wild-type NCX1.1 associates with the F-actin cytoskeleton, probably through interactions involving the central hydrophilic domain of the NCX, and this association interferes with allosteric Ca^{2+} activation (486). Phosphatidylinositol 4,5-bisphosphate (PIP_2) plays an essential role in NCX regulation, since PIP_2 increases reverse-mode NCX1 activity, causing a net increase in Ca^{2+} influx (1133, 1134). Long-chain acyl-CoA esters, found to be elevated in cardiac ischemia (487), hypertrophy (488), and failure (489), have been shown to be endogenous activators of reverse-mode NCX activity by interacting directly with the XIP sequence, and thus linking altered fat metabolism to NCX function and NCX-mediated calcium overload in the myocardium, in

pathological conditions (490). Importantly, protons are powerful inhibitors of NCX1.1 forward-mode activity, further emphasizing the role of NCX1.1 as a key contributor to pathologically altered Ca^{2+} homeostasis and arrhythmia generation during cardiac intracellular acidosis, including myocardial ischemia (491, 492).

The effects of genetic mutations influencing NCX function are poorly understood. However, a genetic mutation in NCX1 was demonstrated to cause cardiac fibrillation in a zebrafish model (493).

3.11.3. The Na^+/H^+ exchanger.

The Na^+/H^+ exchanger (NHE) was first described in rat intestinal and kidney tissue (494). Since then, nine NHE isoforms have been identified (NHE1 to NHE9, encoded by the genes *SLC9A1* to *SLC9A9*, respectively) (495, 496), and in the plasma membrane of mammalian myocardial cells NHE1 is the primary isoform (497). The NHE1 consists of 12 trans-membrane segments, with the NH_2 terminal (~500 residues) catalyzing ion transport and interacting with pharmacological NHE inhibitors and the COOH terminal (~300 residues) responsible for regulation of the exchanger by calmodulin, PIP_2 , and calcineurin B homologous proteins (498–504). The NHE1 can be found as a homodimer in the plasma membrane (505). The NHE1 dimer exchanges 2 extracellular Na^+ for 2 intracellular H^+ in one cycle (506), and it is an important regulator of intracellular pH

(507) and cell volume (508). The function of NHE is electrically neutral; therefore, it does not directly affect the AP and arrhythmogenesis in normal conditions. However, it has been shown to play important pathophysiological roles by indirectly changing intracellular Na^+ concentration and pH (509, 510), both affecting several ion channels and transporters. The role of NHE is considered significant in arrhythmogenesis in pathological settings, including myocardial ischemia-reperfusion, heart failure, or diabetes, when intracellular pH or Na^+ deviates from physiological levels (496, 511–514).

4. TISSUE-SPECIFIC ACTION POTENTIALS

4.1. Sinoatrial Node and Pacemaker Function

The sinoatrial node (SAN) is located in the upper part of the right atrium, and it has a special role in the heart, serving as the natural pacemaker. SAN cells have a relatively low maximal diastolic potential (less than -60 mV), that, after the termination of repolarization, gradually becomes less negative during the so-called spontaneous diastolic depolarization—until it reaches the potential range of L-type Ca^{2+} channel activation, thereby generating a new action potential. The exact nature of the pacemaker function in the SAN is still under debate (515–519). Originally, it was thought that the slow diastolic depolarization was

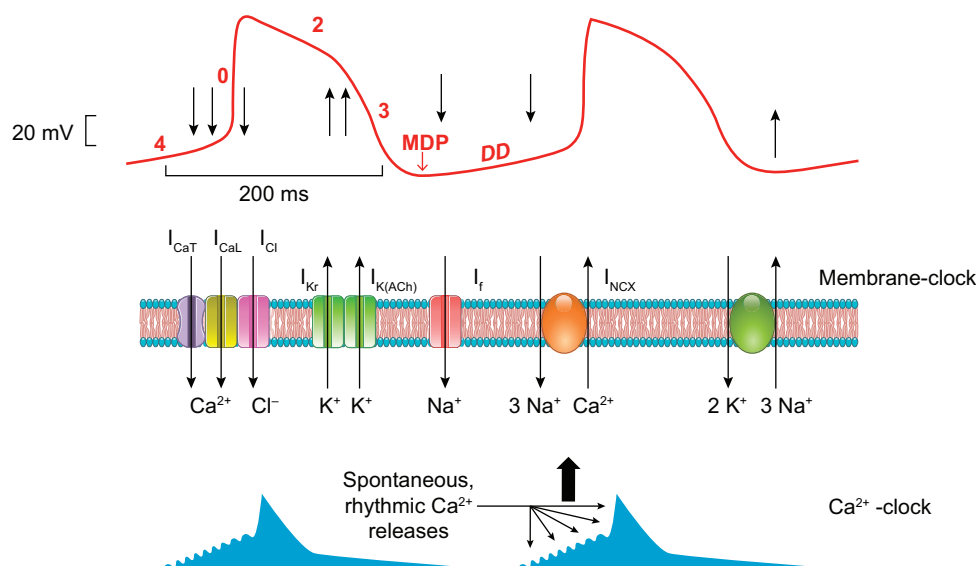


FIGURE 11. Hypothetical mechanism for sinus node pacemaking. The figure illustrates a typical sinus node action potential (red trace) and the timing of the membrane and Ca^{2+} clock components. Upon phase 0, the T (I_{CaT})- and L (I_{CaL})-type Ca^{2+} channels (and presumably the Cl^- channels, I_{Cl}) open, providing inward current (downward arrows), and depolarize the membrane. During repolarization (phase 3) the opening of the delayed rectifier (I_{Kr}) and the acetylcholine-dependent ($I_{\text{K(ACh)}}$) K^+ currents (upward arrows) repolarizes the membrane to reach the maximal diastolic potential (MDP). Upon diastolic depolarization (DD), the cAMP-dependent “funny current” (I_f) slowly depolarizes the membrane in close cooperation with the sodium-calcium exchanger (I_{NCX}) that is governed by spontaneous, rhythmic Ca^{2+} oscillations from the sarcoplasmic reticulum.

due to a hyperpolarization-activated inward current. This current was first described in cardiac Purkinje fibers and was thought to be carried by Na^+ , based on its dependence on extracellular $[\text{Na}^+]$ (520). Later on, other studies suggested that the slow diastolic depolarization was the result of a decaying K^+ current called I_{K2} (521, 522). These data were subsequently reinterpreted in terms of ionic currents resulting from extracellular accumulation of K^+ , and a hyperpolarization-activated inward current, called “funny current” (I_f), carried by both Na^+ and K^+ , was described by Di Francesco (524) and others (523, 525). Despite the fact that other currents, such as I_{Kr} , T-type I_{Ca} and NCX, were also suggested to play a role in the SAN pacemaker activity (526–529), for more than two decades since its discovery the major mechanism underlying the pacemaker function was generally considered to be I_f . However, in an early study of Noma, Morad, and Irisawa (530), the significance of I_f in the SAN pacemaker function was questioned. These authors showed that cesium, an inhibitor of I_f , did not influence the SAN spontaneous frequency and did not eliminate the epinephrine-induced increase in SAN frequency. The dominant role of I_f in SAN pacemaker function was later also challenged by studies showing that a cycling spontaneous release of Ca^{2+} happens during diastole, and this can cause spontaneous depolarization by activating forward NCX as an alternative mechanism for the pacemaker function (“calcium clock hypothesis”) (203, 531–534). This controversy seems to be settled by the “coupled clock hypothesis” (FIGURE 11), suggesting an important role for both the “calcium clock” and the “membrane clock” (I_f) (528, 535). Also, in a recent study, Morad and Zhang (517) demonstrated and pointed out that I_f was very small and very slowly activating at the range of maximal diastolic potential of the SAN cells (–60 mV), therefore not enough to generate a significant amount of pacemaker current. These authors suggested that expression and function of inward I_f in SAN cells can counterbalance the electrotonic interaction of the more negative resting potential of the surrounding atrial cells. According to this suggested function, I_f is important since it insulates SAN cells from the hyperpolarizing influence of the atria, thus allowing a proper SAN function. Consistent with this speculation, Boyett et al. (536) found higher HCN (I_f) expression in peripheral rabbit SAN tissue than in the central core.

A recent study in human induced pluripotent stem cell (hiPSC)-derived myocytes suggested that mitochondria could also play a role in the spontaneous activity, setting the rhythm of the “calcium clock” by taking up and releasing Ca^{2+} from and to the cytosol (517). However, other

studies suggested that mitochondrial Ca^{2+} transient decay is slow, and that their Ca^{2+} efflux is relatively small during one cardiac cycle (463), thus raising questions about a significant role of mitochondrial Ca^{2+} release on SAN frequency. Further studies in adult SAN cells are necessary to confirm the possible role of mitochondria in pacemaking.

In general, SAN frequency can be slowed down by inhibiting I_f , NCX, $I_{Ca,L}$, or I_{Kr} in feline, rabbit, and porcine SAN myocytes (537–540). Inhibition of I_f and NCX decreases the slope of diastolic depolarization, while inhibition of $I_{Ca,L}$ would shift the threshold potential toward more positive values, and thereby the cycle length is increased in all cases. Inhibiting I_{Kr} prolongs repolarization of SAN cells and lengthens their spontaneous cycle lengths. It has to be considered, however, that loss-of-function mutation of I_f results in sinus bradycardia, arguing for some role of I_f in SAN pacemaking (541).

SAN frequency can also be affected by intracellular cAMP levels. Elevation of intracellular cAMP increases I_f and shifts its activation to more negative potentials (542), which in turn enhances I_{Ca} and intracellular Ca^{2+} , further favoring the increase of SAN frequency. Vagal stimulation has an opposite effect on intracellular cAMP and SAN frequency. Data from SAN cells isolated from Girk4 ($\text{K}_{ir3.4}$)-knockout mice lacking $I_{K,ACh}$ suggest that it may also activate $I_{K,ACh}$, which can cause hyperpolarization and may also contribute to SAN bradycardia (543).

SAN cells lack cardiac type $\text{Na}_v1.5$ fast Na^+ channels, and therefore their depolarization is caused by $I_{Ca,L}$ (544). Recently, neuronal $\text{Na}_v1.6$ Na^+ channels were reported in SAN cells (90, 545), but their role in SAN function is not well understood (529). The SAN action potential does not show a distinct plateau phase with relatively weak I_{K1} current.

Experimental evidence obtained in spontaneously beating guinea pig sinoatrial cells suggests that I_f function decreases SAN frequency variability, which is the intrinsic behavior of the calcium clock function (546).

Elucidating the exact mechanisms underlying pacemaker function and its regulation still remains an important task for the future, since it provides the regular heartbeat but it can also act as a possible trigger for serious atrial and ventricular arrhythmias (547, 548).

4.2. Atrial Action Potential

Large species-dependent variations make it difficult to describe the general shape of cardiac action potentials, including atrial action potentials (FIGURE 12 and FIGURE 13). There is also significant diversity within the same heart (549), at least in humans (3, 550), and this results in a relatively large dispersion of repolarization, which favors the development of atrial fibrillation.

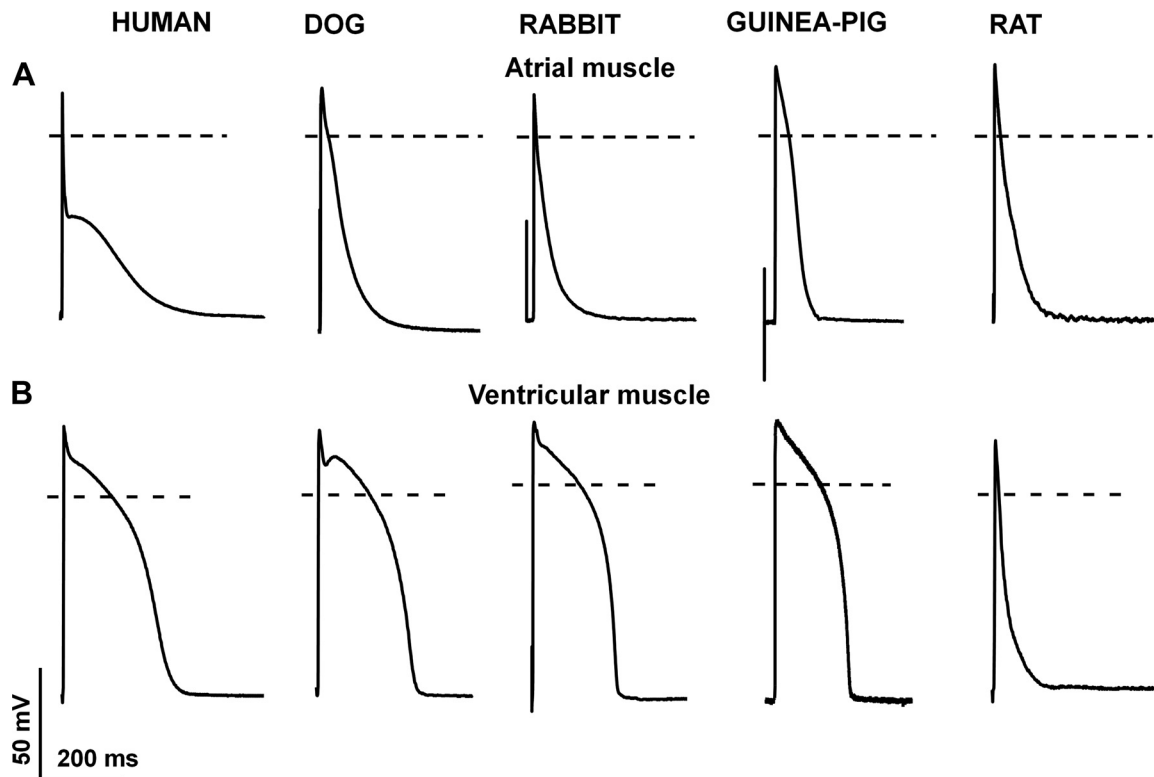


FIGURE 12. Species-dependent differences in atrial (A) and ventricular (B) action potential configuration. Original action potential recordings at 1 Hz stimulating frequency from human, dog, rabbit, guinea pig, and rat ventricular muscle preparations recorded by the conventional microelectrode technique. Unpublished data from our laboratory at the Department of Pharmacology and Pharmacotherapy, University of Szeged.

In most species, the atrial action potential lacks a long and stable plateau phase. In human atria, most of the atrial action potential recordings show a plateau phase, but at a more negative voltage range (−10 to −30 mV) than observed in the ventricle. This is due to the function of the abundantly expressed I_{to} and I_{Kur} potassium currents (FIGURE 6). I_{to} in the atria has slower inactivation kinetics than in the ventricles, having a robust slowly deactivating component ($\tau = 91$ ms at −20 mV), with slower recovery (551) from inactivation ($\tau = 125$ ms) than the ventricular one. Therefore, frequency-dependent changes of APD and restitution are different in atrium and ventricle. In the atria I_{Kur} is large (85) and contributes to repolarization, in contrast with the ventricle, where it is absent or very weakly expressed (85). Therefore, I_{Kur} inhibition would be expected to prolong the AP. However, inhibition of I_{Kur} shortens repolarization by shifting the plateau voltage to the positive voltage range (309), thus changing the activation and deactivation/inactivation of other plateau currents, such as I_{Kr} , I_{Ks} , I_{Ca} , and I_{NaLate} . I_{Kur} inhibition has also been shown to slightly prolong human atrial APD in tissue obtained from chronic AF patients (309, 552). However, in this case, phase 1 and 2 repolarization were delayed and shifted to positive potentials, because of electrophysiological remodeling, thus allowing for a larger I_{Kur} contribution

compared with normal conditions. It is interesting that, in rabbit (unlike in human) atrial muscle, sustained Cl^- current was reported after I_{to} inactivation (324, 553). This should be taken into consideration when drugs are studied in rabbit atrial preparations, and it highlights the importance of species-dependent electrophysiological differences. A distinct, cellular swelling-induced Cl^- current has also been described in human atrial myocytes (554), which is also modulated by PKA-independent, cAMP-mediated β -adrenoceptor signaling (555). The existence and potential role of $Na_v1.8$ channels in I_{NaLate} in the atria represents an interesting issue; however, it is still the subject of debate (556) and requires further studies. L-type and T-type I_{Ca} have similar properties in atria and ventricle (557). I_{K1} current density is relatively small in the atria, especially in the voltage range between −80 and 0 mV. This is consistent with the finding of lower $K_{ir2.1}$ mRNA expression in right atrial compared with right ventricular human tissues (85). Recently, it has also been reported that neurokinin-3 receptor activation induced prolongation of atrial refractoriness, which was attributed to the inhibition of a nonspecific K^+ background current (297). It is difficult to measure I_{Kr} and I_{Ks} in atrial myocytes, most likely because of the cell isolation techniques (252). Regardless of that, I_{Kr} block significantly lengthens atrial repolarization, in both

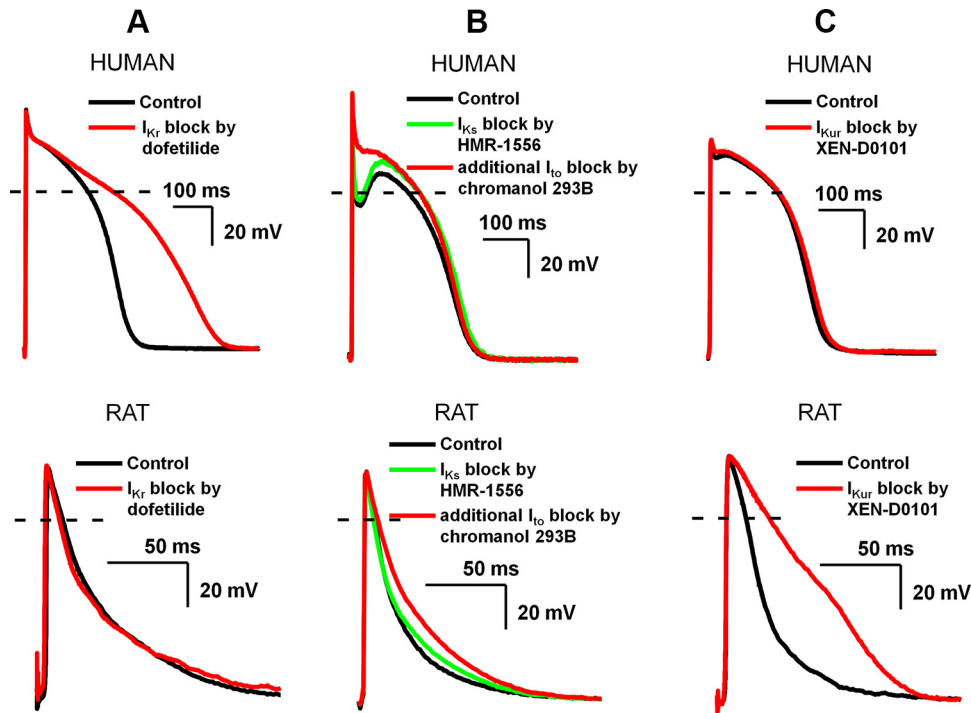


FIGURE 13. Distinctly different effects of slow component of delayed rectifier potassium current (I_{Ks}), transient outward current (I_{to}), and ultrarapid component of delayed rectifier potassium current (I_{Kur}) inhibition on ventricular repolarization in human (top) and rat (bottom). In these experiments, action potentials were recorded in ventricular papillary muscle with the conventional microelectrode technique at 1 Hz stimulation frequency. Note the extended timescale of the recordings in rat papillary muscle. **A:** rapid component of delayed rectifier potassium current (I_{Kr}) inhibition by 50 nM dofetilide markedly prolonged action potential duration (APD) in human but not rat papillary muscle. **B:** I_{to} block by 100 μ M chromanol 293B in human eliminated the notch and elevated the plateau potential to positive direction without changing the APD; however, the APD was significantly prolonged in rat. Since chromanol 293B fully blocks I_{Ks} in addition to inhibition of I_{to} at 100 μ M, prior I_{Ks} block was elicited by 500 nM HMR-1556 to dissect these effects (140). **C:** I_{Kur} inhibition by 3 μ M XEN-D0101 (310) does not affect APD in human but markedly prolongs APD in rat ventricular papillary muscle (unpublished experiments from the Department of Pharmacology and Pharmacotherapy, University of Szeged).

animal and human studies (558, 559). On the other hand, the role of I_{Ks} in atria is not well explored. Experiments with chromanol 293B on atrial action potential are not conclusive, since this drug inhibits both I_{Ks} and I_{to} (560). It must be emphasized that, in physiological conditions, the atrial plateau voltage is more negative than the activation threshold of I_{Ks} . Therefore, I_{Ks} is not expected to contribute to atrial repolarization. However, it has been reported that in atrial tissue LQT1, MinK, and MiRP levels are similar to those in ventricular tissues (85). On the basis of these results, it can be speculated that, at fast heart rate (enhanced sympathetic tone) and in situations where the atrial plateau is shifted to positive voltage, I_{Ks} may have a role in atrial repolarization. Therefore, its modulation could influence arrhythmogenesis. Indeed, it has been shown that two gain-of-function mutations in *KCNQ1* (S140G and V141M), detected in patients with AF (275, 277), markedly slowed deactivation of I_{Ks} and contributed to the development of AF (561). Unlike in the ventricles, most studies showed the existence and function of small-conductance, apamin-sensitive and calcium-dependent potassium current (SK2) in normal atria, but its significance seems to be far more pronounced in diseased tissue (5, 314, 316, 317,

562). The increased apamin-sensitive SK current was found along with decreased mRNA and protein levels of SK1, SK2, and SK3 channels in human atrial cardiomyocytes isolated from patients with AF (319). However, in the same experiments CaMKII was increased and its inhibition by KN-93 reduced the apamin-sensitive SK currents to a higher degree in myocytes isolated from patients with AF compared with those in sinus rhythm (319), suggesting that SK channels are more sensitive to Ca^{2+} in AF patients and CaMKII modulation may represent a pharmacological target in the management of AF. Neurohormonal modulation of the atria is particularly important. Acetylcholine (358, 563), catecholamines (555, 563), substance P (297), adenosine (564, 565), and serotonin (566) have been reported to influence atrial action potential and its underlying currents. In the atria, $I_{K_{ACH}}$ is robust and even has a small but persistent constitutively active component, which operates without parasympathetic stimulation and seems greatly augmented during chronic AF (358). Accordingly, atrial tissue expresses mRNAs for $K_{ir}3.1$ and GIRK channels abundantly. Of note, TWIK TASK channels are also relatively abundantly expressed in the atria (85), but their roles in atrial electrophysiology are not well explored yet.

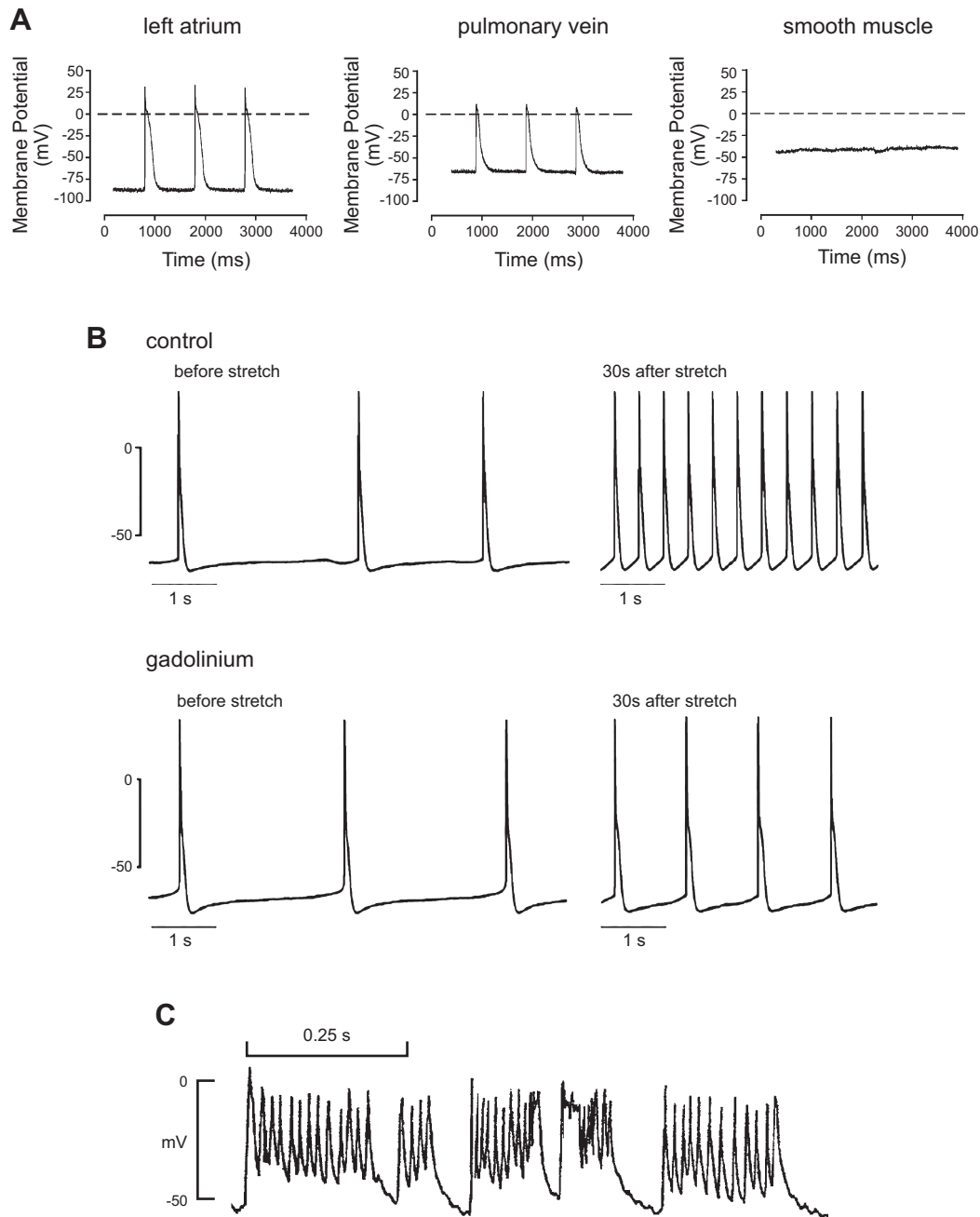


FIGURE 14. Properties of action potentials from left atrial and pulmonary vein myocytes. *A*: recordings of action potentials from the left atrium and pulmonary vein and a transmembrane potential in the smooth muscle cell layer. (Reproduced from Ref. 576 with permission.) *B*: effects of mechanical stretch on the spontaneous electrical activity of the pulmonary vein myocardium. Expanded traces obtained before (*left*) and 30 s after (*right*) the application of mechanical stretch (100 mg) in the absence (*top*) and presence (*bottom*) of gadolinium. (Reproduced from Ref. 577 with permission.) *C*: spontaneous action potential with early after-depolarizations in canine pulmonary veins from dogs subjected to chronic atrial tachypacing. (Reproduced from Ref. 578 with permission.)

4.3. Pulmonary Veins

The spontaneous activity of the pulmonary vein (PV) was described long ago by several investigators (567, 568). Later, Haïssaguerre and colleagues (569, 570) demonstrated that electrical activity in the pulmonary vein sleeves (PVs) in patients has an important role in atrial fibrillation. In the following years, intensive research was carried out both in the clinical and experimental fields

(571, 572), to understand their role (573, 574), the mechanisms, and possible treatment of arrhythmias initiated and maintained by the PVs. It was demonstrated that tissue with myocardial origin is present in the PVs of dogs and guinea pigs, with electrophysiological properties that are similar to but also distinct from the neighboring atrial tissue (568, 575) (FIGURE 14). PVs cells have less negative resting potential and shorter APD than atrial myocytes and also lack a prominent plateau phase

(FIGURE 14). Work on canine PVs found that these cells either do not show spontaneous diastolic depolarization or, if they do, their rate is normally lower than that of SAN cells (576, 579). Stretch can also increase automaticity and induce high-frequency firing in guinea pig PV cells (577) (FIGURE 14). Sympathetic stimulation or diseases like hyperthyroidism (580) increase intracellular $[Ca^{2+}]$, causing PVs cells to develop triggered activity (FIGURE 14), and both early (EAD) and delayed (DAD) afterdepolarizations can occur (578) (FIGURE 14). Compared with atrial myocytes, PVs cells have similar I_{CaL} , I_{CaT} , I_{to} , and NCX but lower current density of I_{K1} , I_{Kr} , and I_{Ks} , with inconsistent results available regarding I_{Na} (576, 581). Interestingly, a hyperpolarization-activated inward K^+ current was reported in canine PVs cells, which was highly sensitive to low submicromolar concentration of Ba^{2+} (579). Based on this finding, K_{ir3} subunits were speculated to be involved as the channel background of this current, and it was suggested that it may play a significant role in atrial pathophysiology (579). This current, $I_{K_{ACH}}$, was enhanced in a conscious tachypaced dog AF model, and its inhibition by tertiapin-Q resulted in a marked reduction in the incidence of AF episodes (558).

In rat PV, a voltage-dependent Cl^- current was also reported and suggested to contribute to norepinephrine-induced automaticity in the PVs. (582). PVs electrophysiology is also modulated by a wide variety of drugs that are used in clinical practice including celecoxib, amiodarone, ranolazine, losartan, and enalapril (583–587). Several factors and diseases, e.g., stretch (585), electrolyte disturbances, sex differences, air pollutants (H_2S) (588), thyroid hormone (580), ischemia-reperfusion (589), uremic substances, renal and heart failure, and aging, have been reported to influence the electrophysiology of PVs.

Recently, it was shown that factor Xa inhibitor anticoagulants, which reduce the incidence of AF-related stroke, also decrease the activity of rabbit PV cells, by inhibiting PAR1 and also diminish I_{NaLate} . Based on this, it was speculated that they can modulate the occurrence of atrial fibrillation (590).

Although it is generally accepted that PVs represents an important trigger for arrhythmias, further research in this field is still necessary to fully elucidate the role of PVs in arrhythmogenesis and to develop new effective therapies involving PVs in general (586, 587). Nevertheless, PV isolation by catheter ablation has become an established therapeutic intervention in the management of paroxysmal and persistent AF (591, 592).

4.4. AV Nodal Action Potential and Conduction

Although they have similarities, AV node cells differ from the SAN cells (593–595), with a lower spontaneous

frequency and a more negative maximal diastolic potential (596, 597). The structure of the AV node, like the SAN, includes a large variety of different cell types (598, 599), with different channel expression (600–603). In the rat AV node, high expression levels of HCN4, $Ca_v3.1$, $Ca_v3.2$, $K_v1.5$, $K_{ir3.1}$, and $K_{ir3.4}$ and low expression of $Na_v1.5$ and $K_{ir2.1}$ mRNA were measured compared with those observed in the ventricle (600). In rabbit AV node, no or low expression of $Na_v1.5$, $Ca_v1.2$, $K_v1.4$, KChIP2, and RYR3 and high expression of $Ca_v1.3$ and HCN4 mRNA were reported (601). Like SAN cells, AV nodal cells do not have functioning fast $Na_v1.5$ I_{Na} channels, and therefore their depolarization and impulse conduction depend on the function of I_{CaL} (565, 603). In AV nodal cells, the expression and function of $I_{K_{ACH}}$ is particularly important (604, 605), since their activation via the adenosine 1 or muscarinic receptors (606) hyperpolarizes the AV nodal cells, which slows or blocks impulse conduction in the AV node (607, 608). In addition, adenosine and acetylcholine decrease I_{CaL} via G_i protein signaling pathway, further decreasing the safety of impulse propagation through the AV node. These are the principal cellular mechanisms that make intravenous adenosine so useful in stopping AV nodal reentry tachycardia (604). The T-type Ca^{2+} channel is expressed and is functional in the AV node as in the SAN (607). Indeed, mibefradil, a potent I_{CaT} inhibitor, increased AV nodal conduction time and even elicited second- or third-degree AV block in isolated, blood-perfused dog hearts (607). The slow conduction through the AV node is physiological and provides a time lag for contraction between the atria and the ventricles. AV nodal tissue has diverse and different connexin 40, 43, and 45 distribution compared with other parts of the heart (8), with a complex and diverse structure, containing a dual faster and slower impulse conduction pathway (594, 603, 609). This latter can provide the basis of fixed-rate supraventricular reentry tachycardia as was elegantly demonstrated in an early study in rabbits by Janse et al. (610), and this tachycardia can be terminated by blocking I_{CaL} and $I_{K_{ACH}}$ and by adenosine (604, 611, 612).

AVN cells lack I_{to} and have background sodium inward current flowing through a nonselective cation channel (605, 613). These cells express functioning I_{Kr} , I_{Ks} , and I_f , but I_f is not required for their pacemaking (614).

4.5. Purkinje Fiber Action Potential

Purkinje fibers play a pivotal role in impulse conduction and propagation in the ventricles (615, 616). Purkinje cells can also act as subsidiary pacemakers, and they display a spontaneous diastolic depolarization, although their frequency is normally inhibited by the higher-frequency discharges of the SAN, causing overdrive

suppression. Purkinje fibers have a longer APD than do ventricular cells, and this may have a protective function against retrogradely propagating stimuli (615) but it can also represent a source of arrhythmogenic repolarization inhomogeneity, even in the normal heart, which can increase in diseased conditions or after drug exposure. In certain pathophysiological situations, Purkinje fibers can show triggered activities (617), such as EADs, DADs, and cellwide ectopic Ca^{2+} waves, in surviving tissue in the border zone of an infarct (618). It was recognized long ago that Purkinje strand fibers, which run close to or on the surface of the endocardium, are less affected by ischemia-induced tissue damage compared with ventricular cells (118, 619). Purkinje fibers have been extensively studied with the conventional microelectrode (620) and the two-electrode voltage-clamp (621) techniques. However, since cell isolation from cardiac Purkinje tissue is particularly difficult, research in Purkinje fibers has benefited less from the introduction of the patch-clamp technique, despite its importance (622).

Purkinje fibers have a special role in impulse conduction, with their depolarization being about two to three times faster (300–750 V/s) than in atrial or ventricular (100–250 V/s) muscle preparations (623). The fast depolarization is thought to be due to the abundant expression of the TTX-sensitive $\text{Na}_v1.5$ channel isoform (85), but low density of TTX-sensitive neuronal $\text{Na}_v1.1$ and 1.2 Na^+ channel isoforms may also significantly contribute to I_{Na} in Purkinje fibers (624, 625). Importantly, the relation between impulse conduction, upstroke velocity (V_{max}), and ionic currents is not linear (626–628), and V_{max} is not a direct measure of ionic currents. I_{Na} in Purkinje fiber also seems to have a particular impact on repolarization, due to its relatively large slowly inactivating component (12, 13, 82). Some authors suggested that the skeletal muscle Na^+ channel isoform $\text{Na}_v1.4$ (78) while others suggested that $\text{Na}_v1.7$ subunits (85) were responsible for this slowly inactivating component in Purkinje fibers; however, this issue is not clarified and needs further investigations. In canine Purkinje fibers, connexin 40 is more abundantly whereas connexin 43 is similarly expressed compared with ventricular myocardium (629): this can play a role in differences between their conduction properties. The large phase 1 repolarization in Purkinje fibers (FIGURE 6) is caused by the fast inactivation of I_{Na} and activation of I_{to} . Not only is I_{to} larger than in ventricular muscle, but it inactivates somewhat slower and recovers from inactivation >10 times slower than that in the ventricular muscle cells (630). This behavior of I_{to} is attributed to the different expression of I_{to} α - and β -subunits in dog ventricular muscle and Purkinje fibers (141, 157). In human ventricular myocytes $\text{K}_v4.3$ channel subunits dominate,

whereas in human Purkinje fibers abundant $\text{K}_v3.4$ and $\text{K}_v4.3$ expressions were reported, with marked differences also in β -subunit (KChIP2, KChAP, KCNE2) expression patterns (158). The slow Ca^{2+} -dependent I_{to2} Cl^- current was also described in rabbit Purkinje fibers (631) and implicated in phase 1 repolarization and DAD formation in sheep Purkinje cells (632), since at potentials more negative than the chloride equilibrium potential chloride channels conduct depolarizing current. The L-type I_{Ca} is well expressed in Purkinje fibers and, unlike in ventricular myocytes, it is carried not only by $\text{Ca}_v1.2$ but also by $\text{Ca}_v1.3$ channels (633), and this may result in some differences in the properties of $I_{\text{Ca,L}}$ between ventricular and Purkinje myocytes. In the canine Purkinje fiber, there is larger T-type I_{Ca} , with a higher $\text{Ca}_v3.2$ expression than in ventricular and atrial myocytes (633). Based on this, it was speculated that T-type I_{Ca} has an important role in Purkinje fibers, by contributing to both depolarization and pacemaker function (634). I_{Kr} , I_{Ks} , calcium-activated K^+ currents, as well as I_{K1} have been described in Purkinje fiber (323, 635, 636). Accordingly, inhibition of I_{Kr} and I_{K1} significantly lengthens repolarization, even more so than in the ventricular muscle (615). However, the inhibition of I_{Ks} does not change repolarization of Purkinje fibers in the normal situation (256). This is not surprising, since Purkinje fibers have a plateau voltage less positive than 0 mV, which is below the activation threshold of I_{Ks} . However, at high frequencies and a high level of sympathetic activation, the plateau level is shifted toward more positive values, increasing both I_{Ks} amplitude and speed to such a level to influence both repolarization and pacemaker function (256).

Unlike ventricular but similarly to atrial muscles, Purkinje fibers express $I_{\text{K,ACh}}$ and $\text{K}_{\text{ir}3.1}$ GIRK channel subunits, thus responding with an APD shortening upon acetylcholine administration (637). The pacemaker I_f current is robust in Purkinje fibers (638–640), where it was first discovered (524), and it plays an important role in the pacemaker function. Later, a K^+ current, I_{Kdd} , was also described in Purkinje fibers (640), deactivating at more positive potentials than I_f and thus having an additional role in the pacemaker function in Purkinje fibers. In addition, spontaneous Ca^{2+} release-induced intracellular Ca^{2+} waves can also modulate normal Purkinje fiber pacemaker activity (641). This may have particular importance in ectopic automaticity of Purkinje fibers surviving myocardial infarction (618). Recently, significant SK2 current and channel expression were described in rabbit Purkinje fibers, and an important role for SK2 current in Purkinje fiber repolarization was suggested (323).

Free-running Purkinje strands emerging distally into ventricular muscle constitute a relatively large-

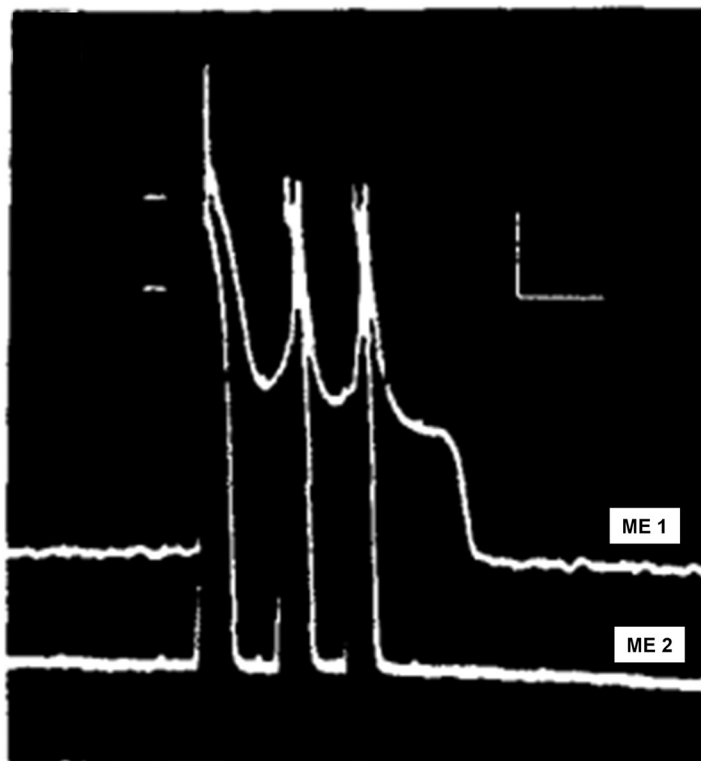
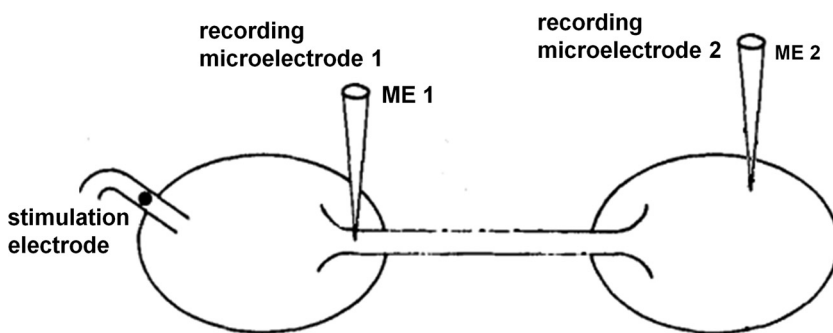


FIGURE 15. Quinidine-induced early afterdepolarizations (EADs) in canine Purkinje fibers propagate to the ventricular myocardium. *Top:* multiple EADs originating from Purkinje fiber (ME1) and propagating to the ventricular myocardium, recorded at position ME2. *Bottom:* experimental setup and the positions of the 2 microelectrodes (ME). (Modified from Ref. 643 with permission.)



resistance connection (642), and a high degree of sink for current flow, and a more favorable site of conduction block than other parts of the healthy myocardium. Also, because of the weaker electrotonic coupling, the dispersion of repolarization here can be far greater than in other places (201). Indeed, it was experimentally proven that EADs in free-running Purkinje strands could elicit extrasystoles in ventricular muscle (643) by electrotonic interaction (FIGURE 15), which is unlikely to happen in healthy and well-coupled regions within the ventricular wall.

Since Purkinje fibers are considered particularly important in arrhythmogenesis (644), further research studying Purkinje fiber ventricular muscle junctions or subendocardial layer containing a mixture of Purkinje fibers and ventricular muscle would offer promising results.

4.6. Ventricular Action Potentials: Transmural and Regional Differences

Ventricular action potentials (FIGURE 6) in humans and in most mammals have a positive (+20 to +30 mV) and relatively long plateau phase, with a small or pronounced phase 1 repolarization and notch afterwards, depending on their transmural site of origin (subendocardial, midmyocardial, or subepicardial) (143, 645, 646). Regardless of their origin, they express large I_{Na} and $I_{Ca,L}$ and relatively weak but persistent I_{NaLate} (80). These currents provide robust depolarization and thereby secure impulse conduction. In addition, by counterbalancing outward potassium currents, e.g., I_{to} , I_{Kr} , I_{Ks} , and I_{K1} , they participate in the maintenance of the plateau phase (FIGURE 6). As mentioned above, I_{Kur} and $I_{K,Ach}$ are expressed weakly or not at all in the ventricles.

There are several reports indicating electrophysiological differences between the right and left ventricle. In dog hearts, it was found that left ventricular myocytes had longer APD than those in the right ventricle (647, 648). Also, right ventricular myocytes exhibited more pronounced phase 1 repolarization and larger I_{to} (648, 649) and increased I_{Ks} (648). It was also reported that canine subepicardial and subendocardial myocytes in the left ventricle possessed larger I_{Na} with higher V_{max} compared with those in the right ventricle (650). The authors suggested that these differences provided a mechanism for the right ventricular manifestation of Brugada syndrome (650).

Almokalant, a drug with APD-prolonging effects, increased interventricular dispersion of repolarization that was associated with the occurrence of EADs and torsade de pointes arrhythmia in dogs with chronic AV block (647). In these dogs, the APD prolongation was larger in the left ventricle than in the right ventricle (647). The opposite was observed in guinea pigs, i.e., the APD-prolonging drugs dofetilide and quinidine lengthened APD more in the right ventricle (651). These findings highlight important differences among species in their responses to drugs with repolarization-prolonging effects. In humans, similarly to dogs, the APD is longer in the left ventricle with slower adaptation to increased heart rate than in the right ventricle (652). These interventricular differences in repolarization are not sufficient to cause arrhythmias in the normal heart; however, in the presence of an ischemic region at the left ventricle (LV)-right ventricle (RV) junction, the interventricular APD heterogeneity and different AP rate adaptation promote reentry arrhythmias (652).

Important regional electrophysiological differences were described in the dog ventricle long ago (653), transmurally (654), regionally (655), and in the basoapical direction (143). These differences are due to substantial differences in the density of expression of various transmembrane ion channels, shaping the action potentials accordingly in the different regions of the ventricles (645). Transmural differences in repolarization have been extensively studied and are well explored (656). It has been found that subepicardial cardiomyocytes exhibit a large phase 1 repolarization and I_{to} compared with those in the subepicardium (657). Myocytes isolated from the midmyocardium, called M cells (654), are variable in this respect, but they are still characterized by a distinct phase 1 repolarization and a relatively large I_{to} (654), I_{NaLate} (658), and NCX (659) and small I_{Ks} (660). All these ion current characteristics contribute to the longer APD of M cells compared with subepicardial and subendocardial myocytes leading to a substantial transmural dispersion of repolarization (656). Augmented transmural dispersion of repolarization has been

considered a contributor to ventricular tachycardia and fibrillation development in patients with Brugada syndrome, acquired and congenital LQT syndromes, short QT syndrome, and catecholaminergic polymorphic ventricular tachycardia (CPVT) (656). However, these differences in transmural repolarization are relatively small in the intact, undiseased ventricles (642, 661), since the neighboring myocytes are well coupled. Accordingly, experimental evidence suggests that in the intact heart the transmural dispersion of repolarization is considerably less (642, 661, 662) than that reported in tissue slices and perfused wedge preparations (663, 664). Therefore, it was argued that it is unlikely that a large, significant repolarization gradient between the subendocardium, M cells, and subepicardium existed, contributing to EADs or arrhythmias (665). However, in pathological settings and/or drug treatment and at Purkinje fiber ventricular junctions (FIGURE 15), APDs can lengthen in a nonuniform manner and cellular coupling can deteriorate, thus resulting in a substrate for serious ventricular arrhythmias.

Apico-basal electrophysiological differences have also been described: the APD was shorter and phase 1 repolarization was markedly larger in canine cardiomyocytes isolated from the apical region than in those from the basal region (655). In the same study, larger I_{to} and I_{Ks} were observed in apical than in basal cardiomyocytes (655). In this context, the apico-basal and the antero-posterior, and not the transmural, repolarization gradients have been considered to contribute to the generation of the T wave (665, 666).

Since idiopathic ventricular arrhythmias often originate from the right and left ventricular outflow tracts (RVOT and LVOT), the electrophysiological properties of these regions have also been investigated (667–670). It was found that rabbit right ventricular myocytes from the apex had longer APD, larger Ca^{2+} transients, higher Ca^{2+} stores, increased I_{NaLate} and I_{to} , but smaller I_{Kr} , L-type Ca^{2+} current, and NCX than RVOT myocytes (671). These differences were associated with increased incidence of DADs induced by pacing (671). Myocytes from the LVOT exhibited longer APD, larger I_{NaLate} and NCX, and smaller I_{to} and I_{Kr} than those from the RVOT (669).

4.7. Species-Dependent Differences in Action Potentials

Arrhythmia research is often performed in different animal models, but its ultimate goal is to understand the mechanisms in humans and to prevent, or successfully treat, arrhythmias in patients. Therefore, it should always be kept in mind how experimental results can be extrapolated to humans. It is often overlooked that rodents (rats and mice) have ion channel expression profiles

distinctly different from humans (40, 672). This also results in different cardiac electrophysiology properties (672, 673), especially during repolarization (FIGURE 12). Mice and rats have a high heart rate (600 and 400 beats/min, corresponding to cycle lengths of 100 and 150 ms), ~10-fold faster than in humans. As a consequence, mice and rats have very short ventricular and atrial action potentials, to provide enough time for diastole. These short action potentials result from the presence of transmembrane currents like I_{to} and I_{Kur} (144). In the ventricles of larger mammals (guinea pig, rabbit, dog, etc.) or humans, these channels are expressed less or not at all and also have a different molecular background and functional role. Action potentials in mice or rats lack a plateau phase (144); therefore I_{Kr} and I_{Ks} are not likely to operate despite the fact that expression of mRNA for these channels has been reported (674). Notably, both I_{Kr} and I_{Ks} were observed in neonatal mouse ventricle, but after further development neither I_{Kr} nor I_{Ks} was detected in adult mouse ventricular myocytes (675). Also, inward currents like I_{Ca} and I_{Na} have different impact on ventricular repolarization than in other mammals. Consequently, drugs can have marked species-dependent effects on action potentials as demonstrated with an example of I_{Kr} inhibition in FIGURE 13. These fundamental differences mean that mice and rats can only be properly used in arrhythmia and related pharmacological research if the limitations of the models are described. As FIGURE 13 illustrates, pharmacological inhibition of specific potassium channels, such as I_{Kr} , I_{to} , and I_{Kur} , elicits strikingly different effects on ventricular repolarization in the rat, a commonly used laboratory experimental animal, compared with humans. Despite this, hundreds or thousands of papers using mice or rats have been published on this topic, because these animals are relatively cheap and easy to house. In addition, transgenic manipulations of transmembrane ion channels are almost entirely applied in mice (674), with very few exceptions (676–678). This makes the mouse a favorable target, despite the fact that the mouse can be useful to study sodium and calcium channels and connexins but not potassium channels.

There are far less consistent data on characteristic species-dependent differences in atrial action potentials and the underlying specific transmembrane currents. As FIGURE 10 shows and several papers indicate (297, 645, 679, 680), most of the species commonly used in experimental laboratories exhibit similar action potentials and underlying currents, with the atrial action potentials lacking a plateau phase, except in humans (556, 681). Human atrial tissue samples, unlike ventricular samples, can be obtained from cardiac surgery departments (from patients undergoing open heart surgery for coronary artery bypass grafting,

heart valve repair or replacement); therefore, human atrial cellular electrophysiological data are abundant, somewhat limiting the need for such studies in experimental animals.

Although the species differences in the shape of ventricular action potentials are most striking between small rodents and humans, important species differences also exist in the action potentials between humans and other mammals. Guinea pig ventricular muscle, unlike human, does not express I_{to} and does not exhibit a prominent phase 1 repolarization (144, 145); however, it expresses large I_{Ks} with distinct gating properties compared with human (3, 214, 249). Rabbit I_{to} , unlike human, is conducted mainly by $K_v1.4$ channels, and as a consequence cycle length-dependent APD is markedly different from that observed in human ventricle (682). Pig ventricular muscle exhibits Ca^{2+} -activated I_{to} chloride current that shapes phase 1 repolarization (683) but lacks 4-AP-sensitive I_{to} despite abundant expression of $K_v4.2$ and $KChIP2$ mRNA and proteins (684). The dog ventricular muscle was found to express a considerably higher density of I_{K1} compared with human (685). This results in a stronger repolarization reserve and consequently less APD prolongation upon I_{Kr} inhibition in the dog ventricle compared with human. All of these differences have a particular significance when drug effects and pathophysiological electrophysiological alterations are extrapolated from animal models to humans.

Human induced pluripotent stem cell-derived cardiac myocytes (HiPSCs) are increasingly used in cellular arrhythmia research (686, 687). This new approach is promising and expanding rapidly (688). At the present stage, however, it seems that HiPSCs have some important limitations (689). Although in HiPSCs experiments can be performed relatively fast, at present they cannot provide a substitute for carefully applied animal preparations. The so-far unresolved problems with HiPSCs are the following: data include cardiomyocytes that have not fully differentiated, still showing an immature phenotype (690, 691), and the cells spontaneously beat and often have a relatively low resting potential because they lack I_{K1} and also have low upstroke velocity (692–694). However, an interesting study suggests that the low resting potential and reduced I_{K1} are not necessarily inherent characteristics of HiPSC-derived cardiomyocytes; rather, these observations might be due to technical issues related to performing patch clamp on the relatively smaller cells (692). Also, HiPSC sarcomeres are disorganized, and their shapes are different from those of the adult cells (691). So far, atrial and ventricular-like HiPSC cells have been successfully generated, whereas SAN, AV node, or Purkinje-like stem cell generation has been unsuccessful (691). However, HiPSC-derived myocytes from patients with defined mutations using

CRISPR/Cas9-edited cells can mimic diseases (688, 695–698) that are often hard or impossible to recreate properly in animal experiments. Recent efforts to culture and continuously pace HiPSC-derived cardiomyocytes cultured in collagen gels as “engineered heart tissue” represent a new two-dimensional (2-D) and three-dimensional (3-D) approach (699–701), since it resembles more the mature myocardium. Future research in this area, however, may revolutionize the field, opening new horizons for arrhythmia research.

5. COMPUTER SIMULATIONS OF ACTION POTENTIAL

The vast quantity of experimental data describing structure and function of myocytes has enabled the development of computer electrophysiology models capable of replicating action potential and conduction properties in a variety of species including human. Thus, the last 60 yr have seen huge progress in our ability to model and simulate the electrophysiology of the heart. Cellular

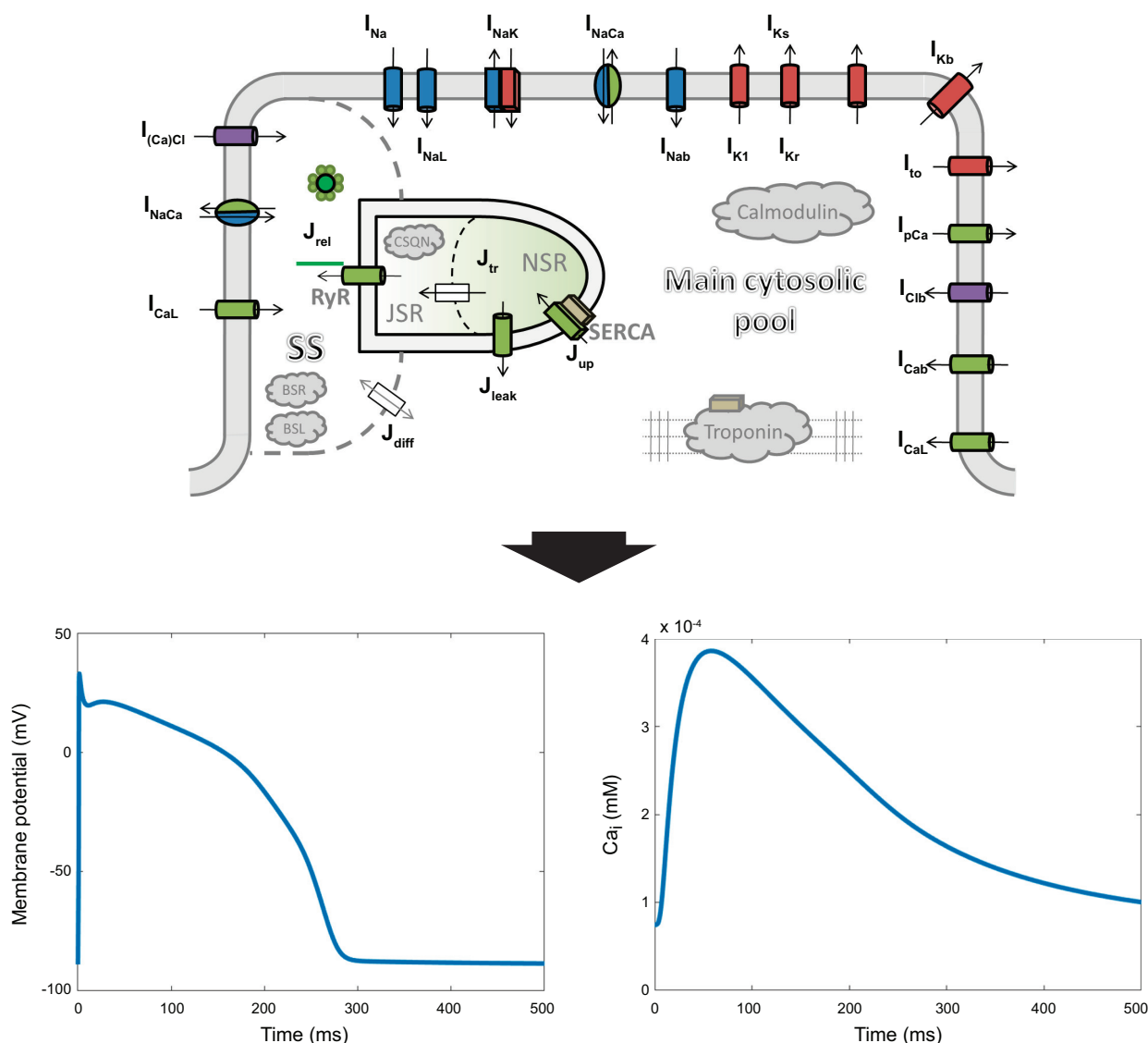


FIGURE 16. Structure of the Tomek, Rodriguez—following O'Hara–Rudy dynamic (ToR-ORd) ventricular myocyte model. The cell consists of 4 compartments: main cytosolic pool of ions, SS [junctional subspace along T tubules, where Ca^{2+} influx via L-type Ca^{2+} current (I_{CaL}) and Ca^{2+} release from the sarcoplasmic reticulum (SR) interact, and where local calcium concentrations may reach much higher values than in the main cytosolic compartment], and 2 subcompartments of the SR [network (NSR) and junctional (JSR)]. I , ionic currents; J , ionic fluxes. Clouds correspond to calcium buffers. Key effects of Ca^{2+} -calmodulin kinase-II on ionic currents and fluxes (such as I_{CaL} or SR release and reuptake) are also represented (717). Below the model diagram the simulated membrane potential and calcium transient are shown, in agreement with experimental data. RyR, ryanodine receptor; SERCA, sarcoplasmic reticulum CaATPase; CSQN, calsequestrin; I_{Cab} , background calcium current; $I_{\text{(Ca)Cl}}$, calcium-sensitive chloride current; I_{Clb} , background chloride current; I_{K1} , inward rectifier potassium current; I_{Kb} , background potassium current; I_{Kr} , rapid delayed-rectifying potassium current; I_{Ks} , slow delayed-rectifying potassium current; I_{Na} , sodium current; I_{Nab} , background sodium current; I_{NaK} , sodium-potassium pump current; I_{NaL} , late sodium current; I_{NaCa} , sodium-calcium exchange current; I_{to} , transient outward potassium current. Reproduced from Ref. 717 with permission.

computational models of different species and cell types are now available, through data and knowledge integration in an iterative process between experimental and computational work (702). The first models of a cardiac cell were the Noble model of the Purkinje cell (703) and the Beeler and Reuter model of ventricular muscle fiber (704), following the pioneering work of Hodgkin and Huxley in giant squid axon (705). Since those times, computer models have developed tremendously in their capabilities, robustness, and applications, ranging from understanding of arrhythmogenesis (706–712) to drug safety testing in industrial and regulatory settings (713–715).

Simulations with computational models offer perfect observability and controllability, which help to overcome limitations in experimental models. They can be viewed as an organized and formalized literature review that can be probed through simulation studies. They provide mechanistically informed and tractable predictions, which can then inform additional experiments and be linked back to existing knowledge of physiological mechanisms. At the same time, when simulations with a computational model fail to reproduce a particular phenomenon, gaps in knowledge or inconsistencies in the state of the art can be identified. This may be an opportunity for discovery of key factors or processes not included in the model, which may be critical for specific phenomena in living cells (716).

A computational model of cardiac cellular electrophysiology typically consists of a set of differential equations describing the mechanisms of transmembrane ionic transport and excitation-contraction coupling. Today's models are commonly separated into multiple subcellular compartments to allow localized calcium signaling and diffusion [an example of the structure of the recent human ventricular myocyte model [Tomek, Rodriguez—following O'Hara–Rudy dynamic (ORd) (ToR-ORd)] (717) is reproduced in **FIGURE 16**].

The most broadly used framework of modeling distinct ionic currents is the Hodgkin–Huxley equations (705), where several independent “gates” (activation, inactivation, etc.) of the respective current are formulated based on experimental data; a combination of the gates then determines the fraction of open channels. This is subsequently combined with open channel conductance and ionic driving force through the open channel to produce total current. Traditionally, single-pulse square voltage clamp was used to collect data used to create ionic current models. However, in some cases it was shown that predictions based on such data do not match behavior of the current under AP clamp, such as in the late sodium current (693). Consequently, more complex protocols such as two-pulse voltage clamp, AP

clamp, or sine-wave protocols are also used to construct models with complex gating properties (718, 719). Similarly to the necessity of collecting more complex data, a mathematical model of a current sometimes requires more complex structure. There are data that cannot be represented accurately with the Hodgkin–Huxley equations, and a more sophisticated modeling method is needed. In such cases, Markov models are typically used instead, where distinct states of a channel are represented (e.g., open, closed, inactivated by voltage, inactivated by drug, etc.) along with probabilities of transitions between these states (719–721). Recently, electrophysiological measurements were combined with molecular dynamics simulation (<0.25 Å) of the channel behavior to simulate ionic currents, which may allow simulations of mutations and drug effects representing the actual molecular processes (722, 723).

5.1. Ventricular Models

Given the relevance of ventricular fibrillation, the field of computational cardiac electrophysiology has focused predominantly on ventricular cardiomyocytes. A milestone in the development of ventricular models was the Luo–Rudy model of a guinea pig cell (707, 708), setting standards in how models are constructed and evaluated based on experimental data and how such models are used to study physiological behaviors. These models include the key ionic currents, such as fast sodium current, L-type calcium current, delayed repolarization current, sodium-calcium exchanger, and the inward rectifier potassium current. The main features of calcium handling, including sarcoplasmic reticulum release and reuptake, are also incorporated. The model was subsequently used to study the interplay of ionic currents and ion concentrations in formation of early and delayed afterdepolarizations (707, 708). The Hund–Rudy canine model (724) separated the delayed rectifier currents into rapid (I_{Kr}) and slow (I_{Ks}) components (as in Ref. 725), added two components of transient outward current ($I_{to,1}$ and $I_{to,2}$), and included a model of CaMKII activation and signaling, studying the impact on rate-dependent behaviors. In addition, it introduced an intracellular subcompartment: the junctional subspace (where L-type calcium channels and ryanodine receptors colocalize and where calcium concentration reaches a much higher value than in the bulk cytosol), which is also a standard in today's models. The model was subsequently updated (726) and used to study the effect of disease (727) and of β -adrenergic stimulation (728).

Another very influential model, created in 2004, is the Shannon rabbit model (729), which also separated different components of delayed rectifier current and included the junctional subspace and which focused

predominantly on an accurate representation of calcium handling. The model was subsequently modified to improve its rate-dependent behavior (721) and was used to study alternans. Interestingly, even though a large proportion of experimental cardiac research is carried out in rodents, there are very few detailed rodent models. Relatively recent models by Bondarenko et al. (730) and Morotti et al. (731) thus provide an important tool in complementing rodent-based experimental research, and they may be used to gain insight into species differences (40).

5.2. Human-Specific Ventricular Models

Modeling and simulation of human ventricular electrophysiology are crucial subcategories of computational cardiac electrophysiology. The central species difference between human and other mammals is the high reliance of human cardiomyocytes on I_{Kr} for repolarization, unlike in other species, where the also relatively highly expressed I_{Ks} provides an additional repolarization reserve. This is of utmost importance, e.g., in the study of drug safety, where hERG/ I_{Kr} blockers may cause a much greater APD prolongation in humans than in animals (685). The specifics of human repolarization thus warrant the development of specifically human-driven computer models. The first of these that gained wide popularity was the pair of models by ten Tusscher et al. (732, 733). A second family of widely used human ventricular myocytes is the model by Grandi et al. (734) and the Carro-Rodríguez-Laguna-Pueyo (CRLP) model that followed it, focusing on rate dependence and behavior in hyperkalemic conditions (735). Possibly the currently most popular human ventricular model is the one by O'Hara et al. (ORd) (736), created and evaluated with a wide range of experimental data, many of which were collected specifically for the purpose of the model development. The ORd model incorporates CaMKII signaling and is capable of manifesting early afterdepolarizations among other features. Together with its humanlike mixture of repolarization currents, it has become, with various modifications, a dominant model in the assessment of drug safety (713, 715) and is a prime example of how computer modeling and simulation may be used for regulatory purposes (737). Recently, a new human ventricular myocyte model, ToR-ORd, was published (717), improving on its predecessor ORd in multiple aspects, such as similarity of the action potential morphology to experimental data or the response to sodium channel blockers. The model also brought biophysical insight into properties of $I_{Ca,L}$ and I_{Kr} , which are important for the understanding of sodium and calcium dynamics in ventricular myocytes.

5.3. Other Tissue-Specific Modeling

As discussed in sect. 4 of this review, different tissues manifest markedly different action potentials, achieved by differential function of ionic currents. Cardiac models reflect this, allowing tissue-specific simulations representing specific features of atrial, Purkinje, or sinoatrial cells.

5.3.1. Atrial models.

Human atrial electrophysiology modeling and simulations are active topics of research. Two prominent models of human atrial electrophysiology are by Courtemanche et al. (738) and Nygren et al. (739), both recapitulating specific AP morphology of atrial myocytes. The Courtemanche model used the Luo–Rudy94 model as a starting point (708) but reformulated the ionic currents according to human and canine data from atrial myocytes. The model was used to understand the importance of L-type current inactivation in APD shortening in the S1S2 protocol and to gain insight into the role of I_{to} in variability of atrial AP morphology. The Nygren model (739) was mostly based on a similar set of data, but it used a different model as the starting point (740). Its analysis provided insight into differences between human and rabbit repolarization, focusing on the role of the sustained outward potassium current. More recent models, adding and studying ionic homeostasis, additional currents, and signaling, are described in Refs. 741–743. We refer the reader to more comprehensive reviews (744–746) on atrial modeling and simulation.

5.3.2. Purkinje cell models.

Even though Purkinje fiber cells were the focus of the first cardiac electrophysiology models (703), progress in this area has been irregular. In 1985 an updated model was published, describing both electrophysiology and changes in ionic concentrations (639), but the focus subsequently shifted toward other cell types discussed above (747). In recent years, the interest in Purkinje fibers has been reinvigorated, producing models focusing on their role and changes in heart failure (748), the electrophysiological basis of rabbit Purkinje electrophysiology (749), and the importance of Purkinje fibers in arrhythmogenesis (750, 751). The very recent Purkinje model by Trovato et al. (752) introduced a comprehensive calibration to human data in a wide range of conditions, bringing insights into Purkinje cell EADs and abnormal automaticity such as following I_{K1} reduction or I_f increase.

5.3.3. Sinoatrial cell models.

Sinoatrial cell modeling and simulation has also made significant progress in recent years in both rabbit (753, 754) and human (755), enabling investigations into the ionic basis of the cardiac pacemaker in normal and disease conditions including the effect of mutations (281, 755, 756).

5.3.4. HiPSC models.

An additional cell type that is gaining increasing popularity is human-induced pluripotent stem cells (HiPSCs), which offer a new human-based paradigm in experimental research. Computer modeling and simulation of HiPSC is an important tool complementing the experimental system. This was pioneered by Paci et al. (757) and is now an active research field (758, 759).

5.4. Different Modeling Scales

In sect. 5.3, we focused predominantly on cell-level modeling, where one set of equations describes the cellwide current. This usually provides a good trade-off of relatively high biological detail but still affordable computational time (<1 s per 1 action potential). For specific purposes, it may be necessary, however, to either increase or decrease the level of detail. In particular, detailed phenomena driven by cellular calcium handling (such as calcium waves and resulting delayed afterdepolarization as well as some mechanisms of calcium-driven alternans) usually require a high degree of detail (760–762). In such models, a single cell is subdivided into small (microscale or even nanoscale) cuboids that may represent membrane, calcium release units from the SR, cytosol, etc. and are coupled together to represent the cell. Such a level of detail, however, considerably increases computational time, such as hours (microscale models) or more than a day (nanoscale) for several beats on a personal computer. On the other side of the spectrum of model complexity are models such as the Fenton–Karma (763) and minimal ventricular (MV) (764) models, which are more than an order of magnitude faster to simulate compared with biologically detailed cellular level models. This makes such models an attractive tool, for example, model personalization using clinical electrophysiological recordings (765) or when tissue properties (rather than ionic properties) are the target of the investigations (766, 767).

5.5. Variability in Computer Models

In recent years, representing variability in cardiac models has emerged as a key new concept (50, 768–773). There

are multiple sources of variability in experimental and clinical data, caused by both intra- and interheart differences as well as differences in experimental settings and/or measurement techniques (50). One of the techniques to investigate potential causes and modulators of biological variability is the use of populations of models rather than a single generic computational model (768, 774, 775). Populations of models are ensembles of models sharing the same structure based on a particular cardiomyocyte model (such as the O'Hara–Rudy model) but with variations in model parameters, such as the conductances of ionic currents. To achieve plausible populations, a calibration to experimental or clinical data can be carried out (768): e.g., a model is accepted in a population only if its action potential morphology and calcium transient properties fall within an experimentally observed range. Such calibrated populations have proven to be useful in the study of hypertrophic cardiomyopathy (776) and atrial fibrillation (775, 777) and for drug safety assessment (715, 775). An intrinsic limitation is that a plausible phenotype may be produced by an unplausible mechanism and/or by a biologically unrealistic combination of conductances of ionic currents. More comprehensive data collection, reporting, and understanding of biological variability is thus an important future step for the fields of both experimental and computational cardiac electrophysiology.

6. CELLULAR ARRHYTHMIA MECHANISMS

6.1. Depolarization Abnormalities

Impaired depolarization capability in cardiomyocytes can reduce conduction safety, providing proarrhythmic substrate and potentially contributing to conduction block and reentry arrhythmia. One example of depolarization abnormality leading to reentry arrhythmia is the Brugada syndrome, caused by the loss of function of *SCN5A* (778, 779). It should be noted, however, that in patients with Brugada syndrome the mechanisms of arrhythmia are more complex, since decreased function of L-type I_{Ca} and enhanced function of I_{to} also contribute to the development of phase 2 reentry (780), due to enhancement of dispersion of repolarization across the ventricular wall (779).

Ischemia can cause regional membrane depolarizations, which indirectly decrease the strength of I_{Na} by eliciting partial or full channel inactivation and result in slowing of impulse conduction or unidirectional or bidirectional conduction block. All of these factors are considered important in arrhythmogenesis. However, their detailed discussion is beyond the scope of this review, since they are described by others in great detail (31, 781–785). Drugs that inhibit I_{Na} can have similar effects and can also cause reentry arrhythmias (202, 786, 787).

Upregulation of the I_f current (788) and HCN channels (789) in the ventricles and atria (790) was reported in HF (789) and HCM (791, 792). These changes can cause abnormal myocardial depolarizations, and they can relate to increased incidence of ectopic beats, providing possible triggers for arrhythmias in an environment where dispersion of repolarization (arrhythmia substrate) is already augmented by structural heart disease.

6.2. Triggered Automaticity

Abnormal myocardial automaticity (formation of propagating spontaneous action potential) is an established trigger contributing to arrhythmia onset (26). One particular type of such automaticity closely linked to disturbance of normal cellular electrophysiology is the so-called “triggered automaticity,” which requires preceding action potentials that are essential for the subsequent spontaneous firing (793). Depending on the temporal relationship between such depolarization and the preceding action potential, triggered automaticity is typically separated into early and delayed afterdepolarizations.

6.2.1. Early afterdepolarizations.

Early afterdepolarization (EAD; **FIGURE 10, A** and **B**) is characterized by depolarizing potential changes occurring before the termination of the preceding action potential during phase 2 or phase 3 repolarization. EADs are usually generated when action potential duration is excessively prolonged, e.g., when I_{Kr} is impaired. As a consequence of the lengthened action potential, those L-type calcium channels that have already recovered from inactivation can reopen, and some of the calcium channels carry a Ca^{2+} window current (707, 708), causing positive voltage oscillations during the plateau (phase 2 EAD) or terminal repolarization (phase 3 EAD). The Luo–Rudy studies (707, 708) also proposed a second type of EADs, phase 3, resulting from spontaneous calcium release during repolarization, which then translates into depolarization via NCX. The relevance of this mechanism was subsequently demonstrated experimentally in Purkinje fibers (131). This type of EAD strongly resembles delayed afterdepolarizations in its mechanism but differs in the timing (during AP vs. after AP). Both types of EADs are rate dependent, with the reactivation-driven mechanism appearing predominantly at slow pacing, whereas the release-driven EADs occur at fast pacing (794).

In general, both the L-type calcium current and NCX are known to act synergistically in EAD formation (795, 796), and the controllability of computational models has been used to understand their interplay. For

example, Kurata et al. (797) demonstrated how NCX contributes to EADs in the popular O’Hara–Rudy model (736) via two distinct mechanisms. First, the influx of calcium via the L-type calcium current upon its reactivation translates into calcium efflux via NCX and thus additional inward current (which can, in turn, promote further activation of L-type calcium current). Second, NCX expressed adjacent to L-type calcium channels acts as a “sanitizer” of calcium in the cellular region, removing calcium ions from the junctional subspace during repolarization. This may subsequently reduce the calcium-dependent inactivation of L-type calcium current, facilitating earlier reactivation. The insight into EAD origins is not limited to L-type calcium current and NCX; nonequilibrium gating of late sodium current was implicated in EAD formations (798). The increased availability of data on signaling pathways has also enabled computationally driven insights on how EADs are facilitated via CaMKII- or PKA-driven pathways (799). This is particularly important for our understanding of EADs in disease conditions such as heart failure, where these pathways are dysregulated.

One interesting involvement of I_{Kr} in EAD formation beyond the role in APD prolongation lies in its dynamic of activation and reactivation. Lu et al. (719) used a range of electrophysiological protocols to demonstrate an intriguing interplay of I_{Kr} activation, inactivation, and recovery from inactivation, which leads to rapid increase of I_{Kr} during late-plateau reactivation, such as during an EAD. Such an increase in repolarizing current would be expected to counteract and potentially outweigh depolarizing currents, potentially preventing the formation of a larger-amplitude EAD.

6.2.2. Delayed afterdepolarizations.

The delayed afterdepolarization (DAD) is characterized by depolarizing potential changes following the termination of the preceding action potential (129, 130, 632) during diastole (**FIGURE 10C**). DAD is generally attributed to calcium-sensitive depolarizing currents after spontaneous Ca^{2+} release from the SR during Ca^{2+} overload, or CaMKII-dependent phosphorylation (800, 801), which is promoted by diseases like chronic AF, ischemia, heart failure (801–803), and catecholaminergic polymorphic ventricular tachycardia (CPVT) or drugs like digitalis. The most important calcium-sensitive current implicated in DAD formation is the forward-mode NCX, but a role for the calcium-sensitive chloride current has also been suggested (804). The calcium-induced depolarization is opposed primarily by I_{K1} , which tries to maintain resting potential (805). When the depolarization induced by calcium-sensitive currents is of sufficient magnitude, overcoming I_{K1} , it activates I_{Na} , triggering a new action potential. Automaticity occurring in the pulmonary veins

and in the myocytes represents important abnormal impulse formations, and at present it seems that their cellular mechanisms are complex, including the possibility of DAD and EAD generation as well (FIGURE 14).

The spontaneous calcium release is a stochastic phenomenon, represented by calcium sparks (806, 807) and intracellular calcium waves (807–810), and multiple calcium release sites need to synchronize to produce a cellwide calcium release (811, 812). The stochastic nature of such events as well as generally limited controllability and observability of subcellular calcium handling in the experimental setting, complicate detailed understanding of their origins. On the other hand, computer models (736) offer excellent controllability and observability and thus are a popular tool to understand origins of spontaneous calcium release and ultimately DADs. Increasing availability of subcellular experimental data has enabled the construction of spatially detailed models, where the cell is subdivided into up to hundreds of thousands of subdomains with separate clusters of potentially stochastic ryanodine receptors (760, 813, 814). As a result, such models can give very detailed predictions, elucidating how originally random calcium sparks are recruited into calcium waves and ultimately DADs but also giving explanations for DADs that do not rely on calcium waves (814).

6.2.3. From afterdepolarizations to arrhythmic behavior.

One important aspect of triggered automaticity is that the role of EAD and DADs in arrhythmogenesis is most likely overestimated in single-cell experiments versus the intact heart. Even in relatively poorly coupled tissue, electrotonic interactions with neighboring cells will decrease the depolarization produced by an EAD or a DAD. However, moderate uncoupling will decrease the electrotonic interaction between a focus and the surrounding cells and can actually favor action potential propagation (815).

Computer simulations studies have significantly contributed to the understanding of the conditions under which the afterdepolarizations of single cells may translate into propagation throughout myocardium (816). These modeling studies showed that when simulating healthy cells and their afterdepolarizations, ~70 cells manifesting an afterdepolarization are needed to trigger excitation in a fiber, ~7,000 in 2-D tissue, and ~700,000 in 3-D tissue. The specific numbers may very well vary with numerical aspects related to the simulations, such as the mesh discretization, but this nevertheless suggests the unlikelihood of EADs or DADs promoting into tissue reactivation in a healthy tissue. At the same time, however, the study by Xie et al. (816) also

investigated the effect of gap junction uncoupling, fibrosis, and heart failure-like remodeling, showing that the combined effect may reduce the number of cells needed for an afterdepolarization-driven propagation by two orders of magnitude. Specific patterns of uncoupling, such as thin strands of myocytes within postinfarction scars (817), which are similar to a fiber with regard to coupling, may increase the relevance of afterdepolarizations of arrhythmia even further. Another type of weakly coupled tissue that might enable synchronization of afterdepolarizations is the endocardial Purkinje ventricular junctions, as mentioned above (FIGURE 15).

In addition to promotion of extrasystolic reactivation via cell decoupling, other mechanisms of synchronization of afterdepolarizations are via stretch-activated channels (818), current flow in the border zone of acute ischemia (706), and partial chaos synchronization (369). In a modeling study of calcium-driven afterdepolarizations, it was suggested that calcium waves also synchronize by calcium flux through gap junctions (819); however, experimental results argued against this possibility (811). Ultimately, simulation studies have shown that the baseline risk of EADs may be considerably increased in diseased conditions (776, 820), further facilitating translation of a depolarization to tissue activation.

In the case of increase in intracellular calcium during elevated sympathetic drive and/or diseases like heart failure or catecholaminergic polymorphic ventricular tachycardia (CPVT) (821), Ca^{2+} overload may occur and the SR can become leaky and release additional Ca^{2+} (822). Mutations in the gene encoding the cardiac ryanodine receptor-related Ca^{2+} release channels (RyRs) can cause extrasystole and serious tachycardia such as CPVT by abnormally releasing Ca^{2+} from the SR (823) into the cytosol on the response of catecholamines which Ca^{2+} would activate the electrogenic forward NCX depolarizing cells beyond their threshold of activation. In a recent study, in a new model for CPVT in engineered human tissue fabricated from human pluripotent stem cell-derived cardiomyocytes, high-frequency pacing and isoproterenol administration increased Ca^{2+} wave propagation heterogeneity and elevated intracellular $[\text{Ca}^{2+}]$, leading to local depolarizations and conduction block (creating the arrhythmia substrate), and subsequently resulting in reentry (700). Similarly to CPVT, leaky ryanodine receptor-related Ca^{2+} release channels were also reported in heart failure (802, 824).

6.3. Frequency Dependence and Restitution

It was observed long ago that action potential duration and impulse conduction depend on heart rate or on the stimulation frequency. To study frequency-independent repolarization changes caused by disease, drugs, or any

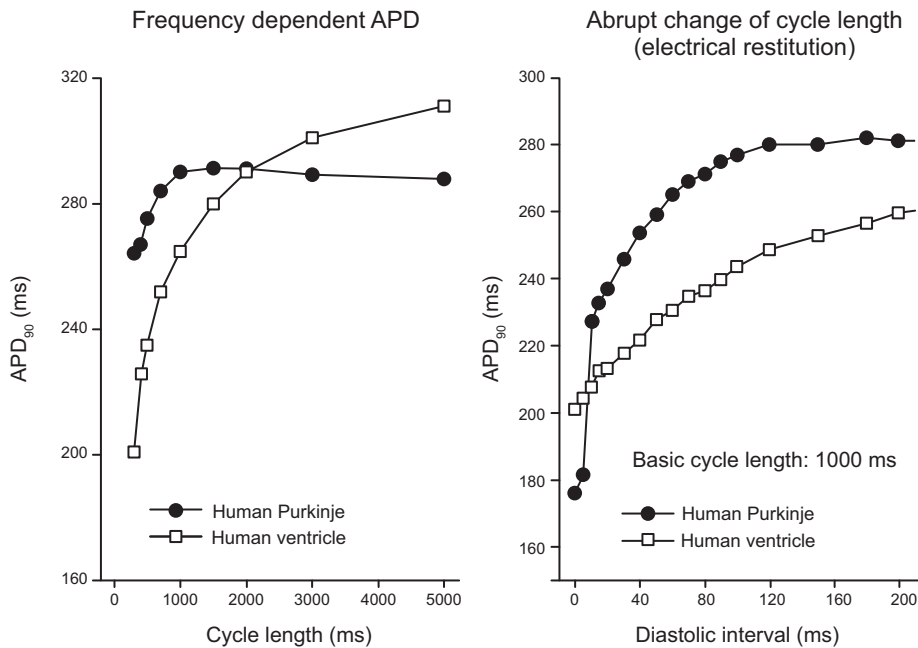


FIGURE 17. Cycle length-dependent action potential duration (APD₉₀) changes (*left*) in undiseased human (donor) ventricular muscle (open symbols) and Purkinje fiber (filled symbols) preparations. *Right*: the relationship between APD₉₀ and the preceding diastolic interval (S1S2 restitution) in human ventricle (open symbols) and Purkinje fibers (filled symbols). Both protocols were measured with the conventional microelectrode technique. APD₉₀, APD at 90% repolarization. Unpublished observations from our laboratory at the Department of Pharmacology and Pharmacotherapy, University of Szeged, Hungary.

other factors, correction formulas have been used to estimate QT intervals corrected for heart rate (QTc) on the ECG. At elevated heart rate, extracellular K⁺ accumulation may occur in the clefts, slightly depolarizing the resting membrane potential that slows impulse conduction and impairs safety of impulse propagation. At extrasystoles early following the end of ERP, repolarization is still not fully terminated and Na⁺ and Ca²⁺ channels are partially inactivated, resulting in less depolarizing current and

decreased safety or slowed impulse propagation. Frequency-dependent APD changes show general patterns (682, 825–830) that APD is short at high and longer at slow constant rates (FIGURE 17). The frequency dependence of APD shows substantial species, tissue, and regional variation and has important implication for arrhythmogenesis. At slower heart rate, APD can be markedly prolonged, favoring triggered arrhythmias via EAD formation, and may also result in enhanced

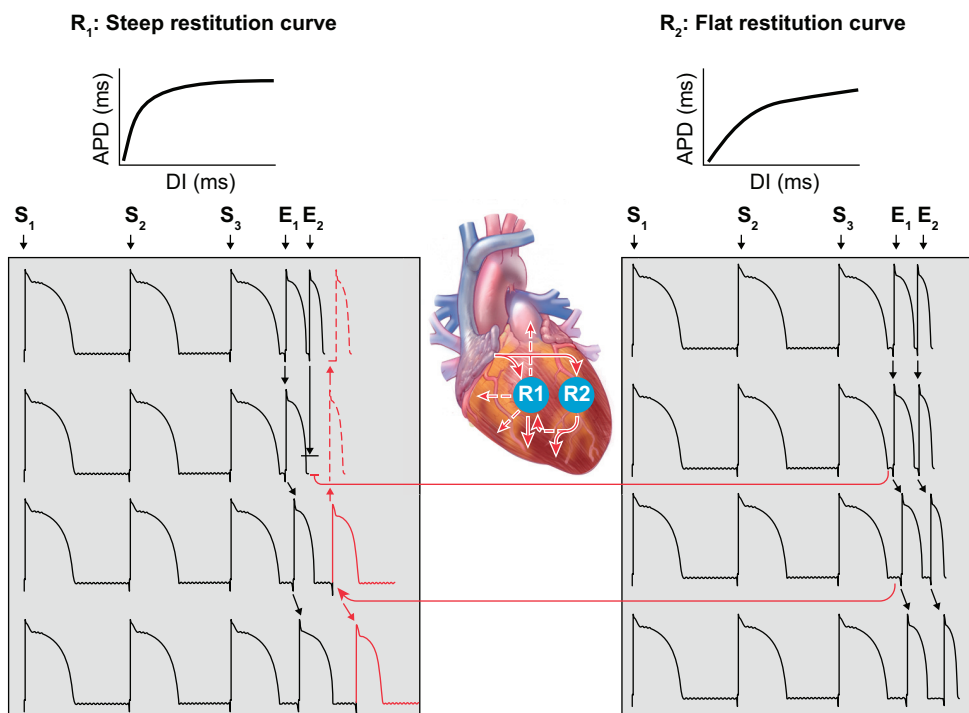


FIGURE 18. Arrhythmia development via regional differences of the action potential (AP) restitution. *Left*: consecutive action potentials from a region with a steep restitution curve (R₁). *Right*: a region with flat action potential duration (APD) restitution (R₂). In both cases, S₁–S₃ indicate 3 consecutive sinus node stimuli followed by 2 extra stimuli (E₁ and E₂). In the case of steep APD restitution, the E₁ is able to propagate while the conduction of E₂ is blocked since the refractory period of the developed extra AP is sufficiently long. In contrast, in the flat restitution region both extra stimuli will propagate, since the APD of the extra beats are not markedly prolonged. Therefore, these APs can reach the R₁ region (red arrow) and evoke extra beats where the refractory period has already been terminated (red curves), establishing a circulating movement of impulse propagation. DI, diastolic interval.

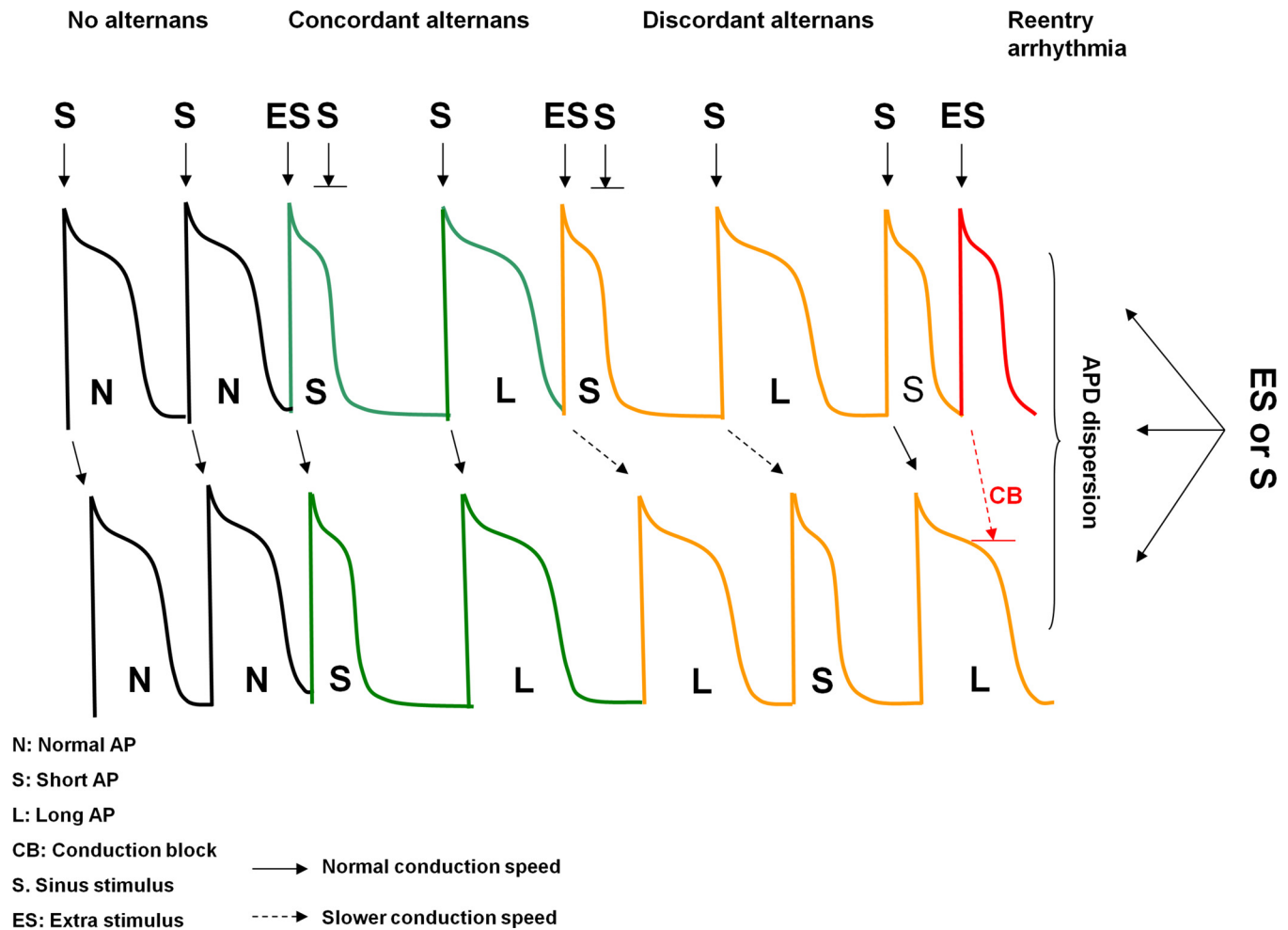


FIGURE 19. Proposed mechanism of action potential (AP) alternans and arrhythmia development. The *top* sequence of the AP illustrates a proximal and the *bottom* sequence a distal area of the left ventricle in respect of impulse propagation. On *left*, 2 consecutive normal (N) action potentials are shown; the depolarization is readily conducted toward the distal area (black arrows), evoking further APs. When an extra stimulus (ES) with short coupling interval reaches the proximal area, the evoked APs will be organized as a short-long-short pattern in both regions, establishing concordant alternans (green curves). Under this condition, a second extra beat will evoke a short AP in the proximal region but a long AP in the distal area, since the refractory period causes slowed impulse propagation (discordant alternans, orange curves). In this case the heterogeneity of the repolarization causes a third extrasystole (red curve) in the proximal region to be blocked in the distal area (red dashed arrow), providing possibility for development of reentry arrhythmia. APD, action potential duration.

substrate for arrhythmias by increasing dispersion of repolarization.

Electrical restitution refers to the recovery of the APD of an interpolated beat as a function of time following the previous beat. This changes in a manner that is somewhat similar to that seen (831) during frequency-dependent steady-state APD changes (FIGURE 17, *left*). Despite the similarities, there are important differences (FIGURE 17, *right*) that warrant the restitution being studied as a separate rate-dependent property (826, 827, 832–835), with importance for arrhythmia research (20, 836). According to the restitution hypothesis, as the diastolic interval increases because of the propagation of an extra beat, the second extrasystole would encounter longer APD/ERP and local conduction block may occur. A steeper restitution curve would favor such an effect and

is considered proarrhythmic (20, 662, 837, 838), whereas flattened electrical restitution curves would have an opposite consequence (FIGURE 18). Local regional differences in the APD restitution curves (839) may also favor arrhythmogenesis (840). The ion channel background of cycle length-dependent APD changes including APD restitution is attributed to the incomplete recovery and/or deactivation of different inward (I_{Na} , $I_{Ca,L}$) or outward (I_{to} , I_{Kr} , I_{Ks} , I_{Cl}) currents based on the gating behavior of these channels (841, 842). In addition, intracellular ion concentration changes for Ca^{2+} and Na^{+} rapidly or slowly would activate electrogenic NCX or Na^{+} - K^{+} pumps. Also, frequency changes can result in significant alterations in extracellular K^{+} concentration in the extra-cellular clefts (843), causing changes not only in depolarizing but also in repolarizing transmembrane ionic currents. Detailed

discussion of these mechanisms is beyond the scope of this review.

6.4. Repolarization Alternans and Temporal Repolarization Variability

Repolarization alternans (**FIGURE 19**) at the cellular level manifests as oscillation of long and short APD at rapid heart rates, typically with concurrent oscillations in calcium transient amplitude (712, 844). It has been demonstrated that alternans can precede the formation of arrhythmia in the heart (845, 846). Multiple studies and reviews explain the mechanisms of arrhythmia induction following alternans, typically linked to increased dispersion of repolarization (712, 847, 848). The spatial pattern of alternans across cardiac tissue is typically “concordant” at submaximal heart rates, i.e., the APD is either simultaneously shortened or prolonged in all sites (**FIGURE 19**) (712). However, further increase in the pacing rate can elicit so-called discordant APD alternans (**FIGURE 19**), when APDs at more distant regions can alternate with opposing phases (712), substantially increasing dispersion of repolarization and thereby the substrate for arrhythmias (849).

The fact that repolarization alternans typically occurs together with underlying oscillation of calcium transient amplitude (850, 851) poses the question of which of these two drives the other.

The first hypothesis suggests that the steep slope of APD restitution is the alternans driver (852), and this mechanism of arrhythmia is replicated by the ten Tusscher–Noble–Noble–Panfilov model of human ventricular myocyte (732, 733). As mentioned above, the ion channel background of APD alternans is attributed to the incomplete recovery and/or deactivation of different inward (I_{Na} , I_{Ca}) or outward (I_{to} , I_{Kr} , I_{Ks} , I_{Cl}) currents based on the gating behavior of these channels (841, 842). In addition, intracellular ion concentration changes for Ca^{2+} and Na^{+} rapidly or slowly would activate electrogenic NCX or Na^{+} - K^{+} pumps. Also, frequency changes can result in significant alterations in extracellular K^{+} concentration in the extracellular clefts (843), causing changes not only in depolarizing but also in repolarizing transmembrane ionic currents.

On the other hand, other studies suggested that oscillations in the calcium transient amplitude are the primary alternans driver (851, 853). Such oscillation of calcium transient can be subsequently translated into APD alternans by NCX and other calcium-sensitive currents. Calcium-driven alternans was first suggested to originate from a Ca^{2+} release-reuptake mismatch due to the steep dependence of Ca^{2+} release on SR loading (851, 854). While in good agreement with a majority of experimental data, the experiments by Picht et al. (855)

suggested that refractoriness of the ryanodine receptor rather than release-reuptake mismatch may underlie at least some of the observed alternans. Such a mechanism is also supported by certain computer models and may be either due to the refractoriness of the channel or due to changes in calsequestrin conformations with subsequent RyR block from within the SR (761). In a recent study utilizing iterated maps as well as a spatially detailed myocyte model, Qu et al. (856) showed that both mechanisms may act synergistically to promote alternans. A third explanation of calcium-driven alternans is the alternans driven by sarcoplasmic reticulum calcium cycling refractoriness (SRCCR) (857, 858). SRCCR alternans arises from a combination of steep load-release relationship (similar to release-reuptake mismatch hypothesis) and refractoriness of the SR release (similar to RyR refractoriness hypothesis). However, the latter does not result from an intrinsic RyR refractoriness but is a result of a limited rate of refilling of releasable calcium in the junctional SR. This mechanism underlies alternans in the Rudy-family models (728, 736, 857).

Alternans typically occurs only at rapid heart rates; however, data from human hearts show that in some cases alternans manifesting at rapid heart rate may cease with a further increase in pacing frequency (“eye-type alternans”) (859). The eye-type pattern was replicated with a populations-of-models approach (859), with the mechanism of the eye closure at rapid pacing being linked to flattening of the SR load-release relationship in certain conditions (858). Using a spatially distributed model of calcium handling, Qu et al. (856) also observed eye-type alternans in simulations where sarcoplasmic reticulum Ca^{2+} -ATPase (SERCA) pumps were downregulated.

One important question pertaining to the spatial pattern of alternans in tissue is what determines whether alternans manifests in the relatively benign spatially concordant pattern or the highly proarrhythmic discordant one. Pastore et al. (849) observed in their experiments that nodal lines (lines in tissue separating areas of opposing alternans phase) were associated with structural abnormalities. However, discordant alternans may arise even in tissue with no obvious structural abnormality. Computer models provide two explanations of this phenomenon. Qu et al. (860) have shown that discordant alternans may emerge as a result of conduction velocity restitution. This explanation is characterized by the radial pattern of nodal lines with regard to pacing site. The second explanation by Sato et al. (762) relies on tissue synchronization of discordant alternans arising at the subcellular level. This explanation does not rely on a particular pattern of nodal lines and can explain experimental observations in Ref. 847.

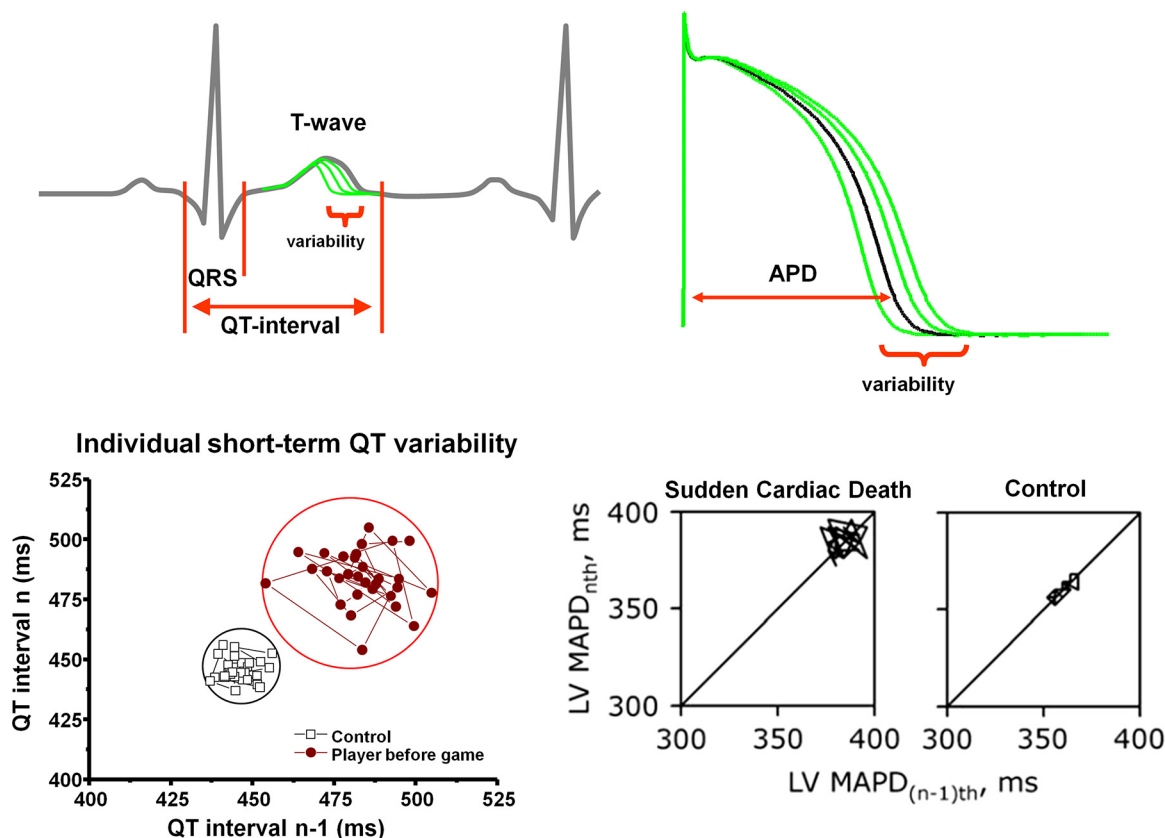


FIGURE 20. Short-term temporal variability of repolarization and the risk of sudden cardiac death (SCD). *Top left:* schematic illustration of QT interval variability on an electrocardiogram trace. *Top right:* schematic illustration of action potential duration (APD) variability. *Bottom left:* increased QT interval short-term variability in a representative professional soccer player compared with a control individual, illustrated on a Poincaré plot, where each QT interval n is plotted against its former value, $n - 1$. *Bottom right:* individual Poincaré plots illustrating increased short-term variability of left ventricular (LV) monophasic action potential duration (MAPD) in chronic atrioventricular block dogs with SCD compared with control dogs without SCD. (Modified from Ref. 861 with permission.)

Spontaneous episodes of ventricular tachyarrhythmia in patients are often preceded by a short-long-short sequence of cardiac cycles or irregular beat-to-beat variation of the QT intervals. This temporal instability of repolarization measured as short-term APD or QT variability similarly to spatial repolarization inhomogeneity is considered as an important marker for proarrhythmia (250, 861) (FIGURE 20). The mechanisms of short-term APD variability are not fully understood; however, they may relate to the stochastic behavior of the ion channels underlying the action potentials or the fluctuation of the intracellular Ca^{2+} movements and its electrophysiological consequences (822).

7. ION CHANNEL AND ACTION POTENTIAL REMODELING IN ACQUIRED CONDITIONS

Certain diseases and alterations in physiological functions evoke changes in the heart that are collectively termed remodeling (7). Remodeling can also affect the

densities or functions of transmembrane ion channels and/or pumps, so-called electrical remodeling (TABLE 2) (7). Thus, electrophysiological remodeling is the result of changes in the expression of ion channels and pumps, and it can affect both repolarization and impulse conduction. In parallel, remodeling often affects the structure of cardiac tissue, which can be detected by microscopy (880). Structural remodeling includes fibrosis and wound healing, resulting mainly from the activity of fibroblasts and myofibroblasts (681, 881, 882). Fibrosis and scars impair impulse conduction, eliciting conduction blocks, changing the directions of normal impulse propagation, and enhancing the heterogeneity of impulse conduction. Finally, remodeling of the postinfarction border zone includes alterations to the pattern and function of gap junctions, further increasing heterogeneity of conduction (883). The combined effects of electrical and structural remodeling increase the propensity of reentry-based arrhythmias.

In this section, electrical remodeling following from the best-explored and probably most important

Table 2. Remodeling of transmembrane currents/transporters in disease

Current	AF-Atrial Muscle		HF-Ventricular Muscle		DM-Ventricular Muscle	
		Reference		Reference		Reference
I_{Na}	↓	7	↓	7, 862	↓	863,864
I_{NaL}			↑	126,127		
$I_{Ca,L}$	↓	7	∅		∅ slow inactiv.	865
I_{to}	↓	7, 549	↓	7, 156, 159, 866	↓	271, 867,868
I_{K1}	↑	205	↓	7, 157		
I_{Kr}			↓	7	↓ ∅	271, 867, 869
I_{Ks}			↓	7	↓	271, 867
I_{Kur}	↓ ∅	549, 870				
$I_{K,ACh}$	↑	358, 584, 871				
I_{KCa} (SK2)	↑	562, 872	↑	315, 873	↓	874
I_f			↑	788,789, 875,876		
NCX			↑	7, 365		
Connexin	↓	7	↓	877–879		

AF, atrial fibrillation; DM, diabetes mellitus; HF, heart failure; $I_{Ca,L}$, L-type Ca^{2+} current; I_f , funny/pacemaker current; $I_{K,ACh}$, acetylcholine-activated potassium current; I_{KCa} , calcium-activated potassium current; I_{Kr} , rapid component of delayed rectifier potassium current; I_{Ks} , slow component of delayed rectifier potassium current; I_{Kur} , ultrarapid component of delayed rectifier potassium current; I_{K1} , inward rectifier potassium current; I_{Na} , sodium current; I_{NaL} , late sodium current; I_{to} , transient outward current; NCX, Na^+/Ca^{2+} exchanger.

diseases is briefly summarized in order to better understand the mechanisms of cardiac arrhythmias.

7.1. Remodeling in Atrial Fibrillation

AF is the most common sustained arrhythmia in the developed world, and its prevalence increases with age, exceeding 10% after the age of 80 yr (6, 884). AF itself is seldom directly life-threatening and usually has few acute hemodynamic consequences, but it represents a high risk for thromboembolism and stroke given an increased risk of thrombus formation in the hypodynamic atria (885). It can furthermore contribute to the development of heart failure; therefore AF has great significance in cardiovascular morbidity and mortality (886).

Studies performed in atrial tissue originating from chronic AF patients or experimental animals show significantly shorter and often triangular-shaped action potentials compared with those obtained from sinus rate patients and animals. It must be emphasized that data regarding electrophysiological remodeling can be controversial. For example, in pacing-induced AF in

dog hearts, atrial APD is abbreviated less (1135) than those observed in human (7, 309). This emphasizes the importance of the substantial species differences mentioned above, in this case between dog and human atrial action potential waveforms (FIGURE 12). Therefore, the interpretation of results based on animal experiments should be considered with care in not only pharmacological but pathophysiological studies as well.

High atrial rate or tachypacing in experimental animals induces atrial remodeling (7, 363, 777, 887, 888) that is characteristic for chronic AF. Atrial extrasystoles or electrical stimulation can easily induce AF in remodeled atria, and the longer and more often AF episodes are present, the more pronounced atrial remodeling and vulnerability for further AF development become (“AF begets AF”) (889).

Remodeling in AF is a complex and still not fully elucidated process (7, 30, 34, 887, 890–892). The most well-established phenomenon in AF is downregulation of L-type I_{Ca} and the corresponding mRNA and proteins. This occurs irrespective of the underlying cause of AF and is observed in AF both with and without heart failure. It is

considered to be the main cause of APD shortening in chronic AF. Also, the upregulation of $K_{ir}2.1$ (the main channel protein of I_{K1}) and TASK-1 channels has been reported to contribute to atrial APD shortening in AF (205). The overall $I_{K,ACH}$ channel ($K_{ir}3.1/3.4 + GIRK$) expression is not significantly changed in chronic AF (871), but a constitutively active component of this current that is very weak in sinus rhythm is greatly enhanced (358) and is assumed to shorten the APD in AF. A very recent study also indicated that cholinergic M_1 receptors were upregulated, further activating $I_{K,ACH}$ and thereby shortening atrial repolarization (871). Both downregulation (549, 870) and no change of I_{Kur} have been observed in chronic AF. A recent study in a tachypaced dog AF model (562) confirmed the expression changes of SK2 or SK3 channels, which supported the results of an earlier study (872) in mice. I_{to} is downregulated in chronic AF (7, 549), which is well reflected in the widening of early atrial repolarization of AF and its increased AP duration at 20% repolarization (APD_{20}). Intracellular Ca^{2+} handling is impaired in chronic AF associated with heart failure (893), as increased open probability of the ryanodine receptor SR channels results in more frequent Ca^{2+} release from the intracellular Ca^{2+} store (681, 824, 887). This may subsequently enhance the frequency of spontaneous depolarization in AF via NCX, possibly contributing to the increased triggered activity in chronic AF (803).

Structural remodeling has been observed in a tachypaced AF goat model (880), which seems even more pronounced in AF associated with heart failure (894). This includes elevated levels of fibrosis (34) and other extracellular matrix components such as myofibroblasts, periostin, matrix metalloproteinases (MMPs), and transforming growth factor $\beta 1$ (TGF- $\beta 1$). Kidney disease (895), inflammation (29), and oxidative stress (896, 897) were also associated with arrhythmogenesis and remodeling in AF. Several reports proved the important role of calmodulin-dependent protein kinase II (CaMKII) in both abnormal Ca^{2+} handling and structural remodeling in AF, suggesting CaMKII inhibition as a promising new strategy to treat AF (573, 898, 899).

7.2. Remodeling in Heart Failure

Sudden cardiac death caused by arrhythmias (900) is responsible for a substantial proportion of the mortality in heart failure. The overwhelming majority of published papers confirmed significant lengthening of repolarization of the ventricular muscle without substantial species differences and regardless of its origin. This is also associated with increased dispersion of repolarization (241), which can be further enhanced by bradycardia-induced AP prolongation often seen in this situation. Enhanced

fibroblast/myofibroblast activity, fibrosis, and altered connexin expression (877, 879) impair impulse conduction (881) and contribute to impulse propagation heterogeneity (901, 902). These changes alone and in combination with heterogeneity of repolarization (25, 903) would result in a favorable substrate for reentry arrhythmias (FIGURE 2). An additional source of proarrhythmic substrate is the high vulnerability of failing hearts to repolarization alternans (846, 904), which appears to result mainly from remodeling of calcium handling. For example, Nivala et al. (905) utilized a detailed model of spatiotemporal calcium handling to investigate the consequences of heart failure remodeling. They have shown complex interactions of disruption of T tubules together with SERCA downregulation to promote increased alternans vulnerability. A different theoretical study also highlighted the importance of SR calcium release dynamics and how their changes in heart failure promote alternans (858).

The ionic mechanisms underlying electrophysiological remodeling in the ventricle include downregulation of $K_v4.3$ channels and I_{to} , $K_{ir}2$ channels and I_{K1} , SK2 channels, K_vLQT1 channels, and I_{Ks} (156–159, 866, 873). Peak I_{Na} can be reduced in failing heart by posttranscriptional reduction and deficient glycosylation of $Na_v1.5$ channel α -subunit (862), and these changes may contribute to slowing of impulse and conduction. In a mouse transverse aortic constriction HF model, $Na_v1.5$ remodeling was observed in subcellular microdomains: $Na_v1.5$ cluster size at the lateral membrane and at the intercalated disk was reduced in failing myocytes, in agreement with reduced peak I_{Na} and impaired transversal and longitudinal conduction in failing myocardium (98). More importantly, late I_{Na} is significantly increased both in an experimental heart failure model (127) and in patients (126); the substantial inward current during the plateau phase causes failure of repolarization and decreases its homogeneity, providing substrate for reentry arrhythmias. In rabbit and human ventricular muscle, downregulation and change of the transmural expression pattern of CFTR Cl^- channels was observed (906) in the hypertrophied heart. Connexin 43 protein downregulation and its lateralization delay impulse conduction and can enhance anisotropic impulse propagation (878), further contributing to substrate generation for arrhythmias.

In addition to remodeling of ionic channels, calcium handling is substantially altered, showing increased SR leak and reduced SR reuptake, resulting in low SR calcium loading and thus diminished calcium transient (802). An additional factor contributing to low SR loading and calcium transient is the increased NCX (907). The alterations of calcium

handling affect the SR-mitochondria cross talk, leading to energy starvation of failing cells, affecting energy-sensitive processes (908). CaMKII signaling is also strongly affected, with relevance for arrhythmia formation (802).

Changes in electrophysiology and calcium handling in heart failure promote ectopic automaticity in the PVs, atria, and ventricle, serving as an important trigger for reentry arrhythmias (788, 790, 875, 909, 910). One type of automaticity may arise from pacemaker-like currents in ventricles. The pacemaker HCN4 and HCN2 channels that carry the I_f inward pacemaker current have been reported to be upregulated in ventricular (788, 789, 875, 876, 911) and atrial (912) tissue of heart failure patients. In contrast, downregulation of I_f in the SAN has also been observed (913). A second type of automaticity may arise from afterdepolarizations resulting from increased calcium leak and subsequent spontaneous SR release, together with the upregulated NCX (907). This increased risk of DADs is further enhanced by the above-mentioned reduction in I_{K1} (291), which makes it easier for the depolarization to reach the threshold of I_{Na} reactivation. More importantly, heart failure alters cellular Ca^{2+} handling (681, 914). Calcium leak from the SR is enhanced, resulting in spontaneous Ca^{2+} release from the SR (802, 824, 915). This transient intracellular Ca^{2+} concentration increase activates the already upregulated (907) forward NCX, leading to arrhythmogenic depolarizations serving as triggers in an environment where the substrate also favors the development of arrhythmias due to heterogeneity of impulse conduction and repolarization. In this process, CaMKII seems to have an important role since its inhibition can have beneficial antiarrhythmic consequences (802).

7.3. Remodeling in Hypertrophic Cardiomyopathy and in Athlete's Heart

Hypertrophic cardiomyopathy (HCM) was first described in 1958 after autopsies on individuals who suffered unexpected sudden cardiac death (916). Since then, HCM has been identified as the most common inherited heart disease, with a prevalence of 1:500 (917), caused by >1,400 known mutations in at least 11 genes (most commonly in β -myosin heavy chain, *MYH7* and myosin binding protein C, *MYBPC3* genes) encoding different sarcomeric and Z-disk proteins (243). The disease is characterized by variable left ventricular hypertrophy and fibrosis (918) and increased incidence of serious ventricular arrhythmias (919, 920). Moreover, HCM is the most common cause of SCD in young persons and competitive athletes under the age of 35 yr (919, 921). The increased propensity for ventricular arrhythmia development in patients with HCM is mainly attributed to

structural left ventricular remodeling (922). Indeed, disorganized myocyte architecture (923), intramyocardial and replacement fibrosis, and collagen deposition in regions with chronic microvascular ischemia (924) can serve as substrates for sustained arrhythmias (925). In addition, the surrounding ischemic myocardium manifests impaired conduction and heterogeneous repolarization dispersion in advanced stages of HCM (926). Alternans is another source of proarrhythmic substrate in HCM (927). However, most SCD events occur in HCM patients at early disease progression stages, when left ventricular hypertrophy is the only major structural abnormality (928). Accordingly, several key elements and consequences of electrical remodeling have been identified in cardiomyocytes from HCM patients, including more frequent EAD and DAD formation (160), increased diastolic Ca^{2+} concentration and elevated NCX expression (160), and increased left ventricular *HCN4* expression (792), all capable of providing arrhythmia triggers in HCM (27, 929, 930). In addition, prolongation of the APD (160) and, consequently, QTc lengthening were observed in patients with HCM, which can be caused by the reduced densities of I_{to} and I_{K1} , decreased expressions of *hERG1b* and *KCNQ1*, and increased I_{NaLate} and slower I_{CaL} inactivation kinetics (160, 931) in myocytes from HCM patients. These elements of ionic current remodeling were sufficient to recapitulate increased vulnerability to EADs when incorporated into a ventricular myocyte model (776).

In competitive athletes, chronic endurance training leads to the development of the so-called athlete's heart, characterized by lower resting heart rate due to increased vagal tone (932), I_f downregulation (933), and symmetric cardiac hypertrophy (934). The incidence of sudden cardiac death in top competitive athletes is two to four times higher compared with the age-matched population (935). Interestingly, hypertrophic cardiomyopathy is found in almost 40% of the cases of SCD in athletes (919). The electrophysiological mechanisms underlying SCD in athletes are not known (for a review see Ref. 18); nevertheless, a significantly larger short-term variability of the QT interval was found in professional soccer players, indicating increased repolarization temporal instability (936) that can refer to increased arrhythmia susceptibility in this population (259, 937).

7.4. Remodeling in Diabetes Mellitus

Diabetes mellitus represents a significant burden on health care systems all over the world since its prevalence is continuously increasing. Diabetes mellitus, an endocrine disorder, is characterized by reduced insulin production (type 1) or increased insulin resistance (type 2), with the latter belonging to cardiometabolic disorders

and being responsible for ~90% of diabetes mellitus cases. Cardiac repolarization disturbances like QTc lengthening or increased QT dispersion are associated with the disease, and cardiovascular complications including arrhythmias and sudden death are major causes of mortality and morbidity in diabetes. These complications usually develop slowly over several decades and are associated with cardiomyopathy, ischemia, vascular sclerosis, and neuropathy with complex and not fully understood mechanisms. Here, we briefly summarize those electrophysiological and structural changes that can be attributed directly to diabetes-induced remodeling (938). The majority of the available data regarding electrical remodeling are derived from type 1 diabetes animal models. There, diabetes is induced acutely by alloxan or streptozotocin (raising the question of how well the model corresponds to chronic changes developing slowly over decades in humans). Results in type 1 diabetes animal models include lengthening of ventricular repolarization, attributed to downregulation of I_{to} (868) and I_{Ks} currents. At the level of mRNA and protein, $K_v4.2$, $K_v4.3$, and $minK$ were reduced but $K_v1.4$ and K_vLQT1 did not change or were upregulated. Zhang et al. (869, 939) reported significant lengthening of QTc and downregulation of cardiac HERG channels and I_{Kr} in alloxan-induced type 1 rabbit diabetes; however, the latter results regarding I_{Kr} were not confirmed by other studies in rabbits and dogs (271, 867). In Goto–Kakizaki type 2 diabetic rats, $I_{Ca,L}$ and Ca^{2+} transient did not change compared with those in the control animals but decreased atrial KCNN2 mRNA, $K_{Ca2.2}$ protein levels, and corresponding SK2 current densities were observed (874, 940), with concomitantly enhanced myocardial hypertrophy and extracellular matrix deposition with fibrosis (941). In Zucker rats, another type 2 diabetic model, enhanced fibrosis, Cx43 lateralization, and significant APD prolongation with delayed $I_{Ca,L}$ inactivation (942) were observed (865). Another observation in type 1 and 2 rat diabetes models is the reduced impulse conduction reserve (863, 943). In a recent paper, O-GlcNAcylation and impaired function of $Na_v1.5$ channel (864) and I_{Na} were described, which together with the fibrotic structural changes (944) can also contribute to the arrhythmogenic impulse conduction defects (945).

In addition to changes in ionic channels, calcium handling is also altered. Several experimental studies in both type 1 and 2 diabetes models in rat established increased SR Ca^{2+} leak due to enhanced RyR2 channel activity (946, 947), which, as mentioned above, would be expected to result in DADs and extrasystoles. Accordingly, Yaras et al. (948) showed increases in Ca^{2+} spark frequency in cardiomyocytes from RYR2 and decrease in FKBP12.6 (calstabin) association. Also,

enhanced CaMKII-mediated phosphorylation of RyR2 has been linked to aberrant Ca^{2+} handling in the same animal model (949, 950). Although it is less well established, similar pathophysiological alterations have been observed in type 2 diabetic rats (951, 952). Results obtained from experimental diabetes suggest that the diabetic heart provides favorable substrate and increased propensity of trigger for arrhythmias due to enhanced ectopic activity and both impaired impulse conduction and repolarization, but results are not conclusive. Therefore, further studies with more appropriate experimental diabetes models are needed to better understand the mechanisms of arrhythmias in diabetes mellitus.

7.5. Myocardial Ischemia, Infarction, and Arrhythmias

Myocardial ischemia mostly develops on the basis of coronary artery disease following critical decreases in blood flow in obstructed coronary arteries. Occlusion of coronary arteries induces a chain of events within minutes of the onset of ischemia, leading to altered function of ion channels and concomitant ischemia- and infarction-induced cardiac arrhythmias. The majority of cases where ventricular tachyarrhythmias including ventricular fibrillation lead to sudden cardiac death are clearly associated with coronary artery disease and myocardial infarction (953, 954). Reperfusion of the myocardium is necessary for tissue survival; however, it can also lead to reperfusion-induced arrhythmias (955, 956). When timely revascularization is not performed, coronary obstruction leads to irreversible cell damage termed myocardial infarction, and the dead cardiomyocytes are replaced by scar tissue. The remodeling in surviving epicardial and border zone myocytes mostly leads to conduction abnormalities, while surviving endocardial Purkinje fibers can be important sources of triggered activity (618). In addition, over the course of days and weeks, the noninfarcted myocardium, including the peri-infarct border zone, also undergoes significant remodeling that favors arrhythmia development due to changes in conduction, refractoriness, and triggered activity (31). An additional source of increased dispersion of refractoriness is the vulnerability of the infarct border zone to alternans, shown both computationally (847) and experimentally (847). Such spatially localized alternans is proarrhythmic in a fashion similar to spatially discordant alternans, forming steep gradients of repolarization. Multiple other studies have investigated arrhythmia mechanisms associated with myocardial ischemia and infarction; for comprehensive detailed reviews, the reader is referred to works by Janse and Wit (31) and Pinto and Boyden (784).

In the acute phase of myocardial ischemia (within minutes to 2–4 h after coronary blood flow reduction), ventricular arrhythmias including fibrillation occur in humans (957) and also in experimental animals subjected to complete coronary artery occlusion (958, 959).

Acute ischemia promotes the formation of arrhythmia substrate, which allows reentry via several mechanisms. The resting membrane potential of ischemic cardiomyocytes is significantly depolarized (960), partly due to marked K^+ loss and intracellular acidosis (783), leading to extracellular K^+ accumulation in ischemic tissue (961). The depolarization of the resting membrane potential depresses action potential upstroke and amplitude by reducing I_{Na} and results in the prolongation of the refractory period via slow recovery from inactivation of the sodium gates (39). Activation of ATP-dependent potassium channels shortens the action potential duration (962). Within 15 min of the onset of ischemia, gap junction channel phosphorylation status is changed and they get translocated into intracellular pools in ischemic cells (963), severely reducing cell-to-cell coupling (815, 964, 965). These changes result in impaired impulse conduction in acute ischemia (966). Increased spatial dispersion of repolarization and refractoriness between different regions of the myocardium is also an important arrhythmia substrate (128). Nonuniform shortening of the action potential due to heterogeneous sarcolemmal $I_{K,ATP}$ activation in myocytes from the ischemic and border zone (reviewed in Ref. 967) and no shortening of AP in the normoxic myocardium increases dispersion of repolarization and effective refractory period within minutes after ischemia onset (340). The first phase of ventricular arrhythmias (“phase 1a”) peaking between 5 and 6 min after the onset of ischemia in experimental models is usually, but not exclusively, attributed to the mechanisms described above (31, 968), which have been further investigated in computer simulation studies using human biventricular models (969).

Multiple mechanisms underlie the formation of arrhythmia triggers in acute ischemia. The increased release of catecholamines occurs 15–20 min after the onset of myocardial ischemia (970), possibly increasing ectopic activity. Early and delayed afterdepolarizations can supply the triggers for arrhythmia initiation in acute myocardial ischemia. Early afterdepolarizations can develop in Purkinje fibers in acute ischemia because of intracellular acidosis and exposure to ischemia-induced release of lysophosphatidylcholine (971). Delayed afterdepolarizations can occur in ischemic cells because of acidosis, hypoxia, and calcium overload (617). A so-called “injury current” flowing from ischemic myocardium to normal myocardium can cause increased abnormal automaticity in acute myocardial ischemia. The basis for this current is the difference in membrane

potentials between neighboring ischemic (depolarized) and normoxic (hyperpolarized) myocardium and has been shown to contribute to ectopic activity in experimental conditions (972–974) and computer simulations (706). In general, the initiation of so-called “phase 1b” arrhythmias in experimental models of myocardial ischemia is mostly attributed to increased automaticity (31).

In the subacute and chronic phases of myocardial infarction, reentry and triggered activity caused by early and delayed afterdepolarizations are major mechanisms of infarction-induced ventricular arrhythmias (28, 975), where surviving Purkinje fibers (976) and epicardial border zone myocytes (977) play a critical role in arrhythmia development. A series of papers by the Boyden group describe the morphological and electrophysiological changes occurring over 24–48 h after an infarction in surviving left ventricular Purkinje cells that underlie subacute spontaneous arrhythmias (for a detailed review, see Ref. 784). In general, surviving Purkinje fibers exhibit depolarized resting potentials associated with reduced I_{K1} (978), decreased $I_{Ca,L}$ and $I_{Ca,T}$ densities (979), prolonged repolarization with up to 51% smaller I_{to} density, and delayed I_{to} reactivation kinetics (980). Also observed were nonuniform calcium transients and abnormal calcium waves leading to spontaneous action potentials and triggered activity in the infarcted heart (619). The surviving epicardial myocytes of the border zone next to the infarcted area exhibit decreased excitability and resting potential, reduced upstroke velocity and amplitude of the action potential (977), and, importantly, marked postrepolarization refractoriness (32, 981) due to decreased I_{Na} density and altered I_{Na} kinetics (982). A pathological redistribution of connexin 43 gap junction protein and reduced gap junctional conductance was observed in border zone surviving cardiomyocytes (983). These changes lead to abnormal, slow, and anisotropic impulse conduction (28, 984, 985). Interestingly, in these surviving epicardial myocytes, a gradual shortening and triangularization of the action potential was observed over 2 wk, followed by a return of action potential parameters to normal by 2 mo after myocardial infarction (986). The reduced $I_{Ca,L}$ density (987) may be partly responsible for the triangularization of the action potentials on these cells. Several important repolarizing K^+ currents are downregulated in surviving epicardial cells, including I_{to} (977) and I_{Kr} and I_{Ks} (240), leading to prolonged action potentials. These changes described above in epicardial border zone myocytes strongly favor the development of reentry and, of particular interest, anisotropic reentry (7).

In addition to the changes described above, the remote noninfarcted regions of the myocardium also

exhibit structural and electrical remodeling as the remaining myocardium in the infarcted heart adapts to increased workload (988). The developing regional left ventricular hypertrophy is an important risk factor for the generation of severe ventricular arrhythmias (989) and probably relates to enhanced dispersion of repolarization associated with myocardial hypertrophy.

7.6. Aging-Associated Cardiac Remodeling

There is a dramatic increase in the incidence and prevalence of cardiovascular disease and mortality with age, and aging is now identified as a major risk factor for cardiovascular morbidity (990). Evidence suggests that cardiovascular aging is associated with remodeling of the heart, setting the stage for arrhythmia development (especially atrial fibrillation and ventricular tachycardia) and reduced cardiac function. The incidence of sudden cardiac death increases with age (991); however, our understanding of the mechanisms responsible for increased incidence of arrhythmias in the elderly remains limited (992). Many of the aging-associated alterations are, at least in part, inevitably due to the observed coronary artery dysfunction, increased artery stiffness, decreased responsiveness to β -adrenergic stimulation, and cardiac extracellular matrix remodeling found in the elderly (993–995).

The pacemaker function of the sinus node significantly decreases in older patients, probably because of replacement of pacemaker cells within the sinoatrial node (SAN) by extracellular matrix (996). Animal studies suggest that decreased expression of HCN2, $I_{Ca,L}$, $I_{Ca,T}$, and $K_{v1.5}$ channels can also contribute (548, 997, 998). Consequently, the rate of spontaneous diastolic depolarization falls and action potential duration is prolonged in pacemaker cells (523, 999). The intrinsic heart rate decreases (997), with concomitant fatigue, bradycardia, and increased incidence of supraventricular arrhythmias including atrial fibrillation in the elderly (1000).

The observed delayed and impaired cardiac impulse conduction, with concomitant QRS complex widening, is the result of decreased Cx43 expression and degenerative changes in the cardiac connective tissue (992, 1001–1003).

In aged ventricles, even without the presence of structural heart disease, loss of cardiomyocytes, reactive hypertrophy in the left ventricle, fibrosis, and changes in repolarization occur (161, 1004–1006). The prolongation of the ventricular action potential was observed in senescent sheep (1007), and consequent QT interval lengthening was shown in old dogs (1007, 1008). In an attempt to maintain cardiac function, ion channel remodeling involving $I_{Ca,L}$, I_{to} , K_{ATP} expression changes, delayed $I_{Ca,L}$ inactivation, and increased $I_{Na,late}$ are probably

responsible for repolarization prolongation in aged hearts (1009, 1010). These elements of ventricular remodeling in the aged heart increase susceptibility toward arrhythmias by altering cellular coupling, increasing anisotropic conduction, and enhancing heterogeneity of refractoriness in the myocardium, which are changes that all together favor reentry initiation and stabilization. The increased expression of NCX, the delayed inactivation of $I_{Ca,L}$, together with reduced expression of SERCA and other proteins related to calcium handling all contribute to impaired calcium homeostasis and provide the mechanisms for increased triggered activity in the aging myocardium (1011–1015).

The ability of the heart to properly respond to autonomic stimuli also decreases with aging (1016). Reduced β -adrenoceptor responses and receptor densities were identified in the aging myocardium (1017, 1018), exacerbated by decreased cAMP production (995). It is not clear how impaired cAMP-dependent regulation of I_{Ks} (1019) and $I_{Ca,L}$ (1020) translates into alterations of repolarization reserve in the elderly. In addition, decreased vagal component of heart rate variability and heart rate responses were observed after muscarinic acetylcholine receptor blockade (1021, 1022). The impaired autonomic regulation of the heart and the electrical and structural remodeling described above in the elderly contribute to reduced cardiac adaptive responses and increased supraventricular and ventricular arrhythmia susceptibility (1023).

8. INHERITED CONDITIONS ASSOCIATED WITH ION CHANNEL DYSFUNCTION

Cardiac arrhythmias are usually symptoms or consequences of other underlying diseases such as myocardial ischemia or infarction, heart failure, hypertension, diabetes, etc. However, cardiac ion channel mutations or polymorphisms (1024) can represent the primary cause of arrhythmias, collectively called “ion channelopathies” (1025). This field is particularly rapidly expanding, and detailed discussion is far beyond the scope of this review; some excellent recent reviews are suggested for further reading (114–117, 149, 246, 1026–1029).

In general, mutation of a certain ion channel can cause gain or loss of function (1029–1032) resulting in increased or decreased current through the affected ion channel, which may alter arrhythmia trigger and/or substrate (TABLE 1) (245, 1033, 1034).

Congenital LQT syndrome is characterized by prolongation of myocardial AP and QT interval caused by the reduction of repolarizing current due to either loss-of-function mutations in repolarizing current-conducting potassium channels or gain-of-function mutations in

depolarizing current-conducting sodium or calcium channels (114, 115) (TABLE 1). Congenital LQT syndrome is commonly associated with the development of TdP and sudden cardiac death (1035), and most LQT syndrome subtypes show an autosomal dominant inheritance (115). In >90% of patients with congenital LQT, genetic variants of *KCNQ1* encoding the α -subunit $K_v7.1$ of I_{Ks} (LQT1; 30–35% of cases), *KCNH2* encoding the α -subunit $K_v1.1$ of I_{Kr} (LQT2; 25–40% of cases), and *SCN5A* encoding the α -subunit $Na_v1.5$ for I_{Na} (LQT3; 5–10% of cases) underlie the disorder (122, 1036, 1037) (TABLE 1). A number of other genes encoding ion channel proteins or their regulators have been implicated as causes of congenital LQT syndrome (TABLE 1). For details on the causative roles of the genetic variants involved in the different congenital LQT syndrome subtypes, the reader is referred to other comprehensive reviews (115, 246). In LQT syndrome, prolongation of repolarization and refractoriness, accompanied with increased dispersion of repolarization (1038, 1039), enhance the substrate for typical ventricular arrhythmias in patients with LQT syndrome such as TdP polymorphic tachycardia and ventricular fibrillation. Enhanced triggered activity due to early afterdepolarizations, elicited by reactivation of $I_{Ca,L}$ during the prolonged AP, provides the trigger for the development of TdP in LQT syndrome (796, 1038). LQT syndrome is characterized by incomplete penetrance and can be “silent,” i.e., no significant prolongation of repolarization and QT interval is observed. However, congenital LQT syndrome greatly enhances the effect of any other factor which delays repolarization by other mechanisms. This can be explained by the concept of “repolarization reserve,” as introduced in sect. 3.4.2 (228, 257, 1040, 1041). Accordingly, impaired function of different types of potassium channels (caused by genetic mutation, disease-induced downregulation, or drug effects) can add together, further enhancing the substrate for ventricular arrhythmias. Of note, ion channel polymorphisms can also play a role in arrhythmia development, thus emphasizing the importance of pharmacogenetics during the evaluation of proarrhythmic drug-induced adverse effects (798, 1024). Which current is affected by such polymorphisms (usually potassium currents, $I_{Ca,L}$, or I_{NaLate}), may largely determine the individual’s response to antiarrhythmic channel-blocking drugs, emphasizing the concept of personalized medicine.

SQT syndrome (1042, 1043) is a rare, albeit severe, channelopathy that is characterized by abnormally short frequency-corrected QT intervals (<360 ms), due to accelerated ventricular repolarization (1044), with a high risk of sudden cardiac death and AF (1045). SQT syndrome shows autosomal dominant inheritance, and gain-of-function mutations in genes encoding different potassium

channels, i.e., *KCNH2* (SQT1), *KCNQ1* (SQT2), and *KCNJ2* (SQT3), have been associated with the disorder (1046–1048) (TABLE 1). In addition, loss-of-function mutations in genes encoding voltage-gated calcium channel subunits *CACNA1C*, *CACNB2b*, and *CACNA2D1* were designated as SQT4, SQT5, and SQT6, respectively (1049) (TABLE 1). Patients with SQT syndrome involving calcium channel mutations exhibit an overlapping phenotype combining short QT and a Brugada syndrome phenotype (1050). Loss-of-function mutations in the gene (*SLC22A5*) encoding a sodium-dependent carnitine transporter have been termed SQT7 (1051) (TABLE 1). In SQT7, the mechanistic link between short QT and carnitine concentrations remains elusive; however, increased I_{Kr} due to the lack of long-chain acylcarnitines may play a role (1052). SQT8 syndrome involves a mutation in the gene (*SLC4A3*) encoding a Cl^-/HCO_3^- exchanger (AE3) leading to a trafficking defect of the mutated AE3 to the cell membrane (1053) (TABLE 1). The shortening of APD and ERP in the myocardium, as well as the increased spatial dispersion of repolarization, due to more enhanced APD shortening in the epicardium, all favor reentry tachycardia development both in the ventricles and in the atria in SQT syndrome (1054, 1055).

Brugada syndrome (BrS) (1056) and arrhythmogenic right ventricular cardiomyopathy (ARVC) (1057) are inherited cardiac diseases with a complex genetic background. Brugada syndrome is characterized by ST segment elevation in right precordial leads and has been considered as the cause of SCD in up to 20% of patients with a structurally normal heart (778). Approximately 20–30% of patients with BrS exhibit pathogenic mutations in the *SCN5A* gene encoding the α pore-forming subunit of the cardiac $Na_v1.5$ sodium channel (1058), leading to loss of function in fast I_{Na} and, consequently, conduction slowing and delayed right ventricular activation (1059, 1060). In BrS, because of decreased I_{Na} the balance of outward and inward currents changes and the repolarizing effect of I_{to} is amplified in epicardial but not in endocardial cells, resulting in enhanced transmural dispersion of repolarization. This increased dispersion can create a vulnerable window for extrasystoles to induce phase 2 reentry arrhythmias (1061, 1062). In a genome-wide association study, genetic variants of *SCN10A*-encoded $Na_v1.8$ sodium channels, playing a key role in cardiac neurons (1063) but also expressed in the working myocardium (1064), have been identified as strong modulators for BrS (1065). In addition, in ~2–5% of BrS patients pathogenic variants have been identified in a number of genes encoding other ion channel proteins, and up to 70% of patients with BrS have an unidentified genetic cause (778, 1058). Interestingly, the expression of $K_v4.3$, a key subunit of I_{to} (135), was markedly reduced in the endocardium but not in the epicardium in patients with BrS (1066). This enhanced transmural difference in

I_{to} can lead to increased transmural dispersion of repolarization in BrS patients, favoring the development of reentry arrhythmias (24, 1062).

In patients with ARVC, a significant number of cardiomyocytes in patches of the right ventricular free wall are replaced by fibroadipose tissue, with marked pathophysiological consequences for myocardial depolarization and repolarization of the right ventricle (1057). The causative role of mutations in at least 16 genes, mostly encoding different desmosomal proteins, has been identified in ARVC (1067), whereas in 40–50% of patients the genetic cause is unknown (1068). The exact molecular mechanisms for how desmosome assembly impairment and dysfunction lead to cardiomyocyte apoptosis and their fibroadipose replacement are not fully understood (1069, 1070). ARVC is associated with frequent ventricular extrasystoles, ventricular tachycardia with left bundle branch block morphology, syncope, and SCD (1071). On autopsy, ARVC is found to be responsible for SCD in 5% of young competitive athletes in the United States, whereas this number is around 27% in northern Italy (1072, 1073). The fibroadipose tissue patches correspond to electroanatomical scars that promote the establishment of scar-related macro reentry circuits (1074, 1075).

Catecholaminergic polymorphic ventricular tachycardia (CPVT) is characterized by a normal resting ECG; however, malignant ventricular arrhythmias and SCD are induced by adrenergic stimulation (821, 1076). Mutations in *RYR2*, encoding the ryanodine receptor 2, the Ca^{2+} release channel located on the SR (autosomal dominant CPVT type 1), and in *CASQ2*, encoding calsequestrin 2, the calcium binding protein inside the SR (autosomal recessive CPVT type 2), makes these channels and calcium storage sites more sensitive to catecholamine-induced Ca^{2+} release (1077). Consequently, spontaneous triggered automaticity is induced by depolarizations due to increased transient inward current elicited by forward NCX activity during diastole. Iyer et al. (1078) used computer simulations to characterize the impact of *RYR2* and calsequestrin mutations in the CPVT phenotype. Their study shows how impaired SR calcium sensing and increased spontaneous SR calcium release promote DADs and how these events are aggravated by β -adrenergic stimulation.

Mutations in I_f pacemaker channels can cause both brady- and tachycardias (1034) by altering sinus automaticity. Sinus bradycardia was also reported in patients with loss-of-function mutation of the *SCN5A* sodium channels resulting in failure of pacemaker capture (1079). Some familial AF cases are also linked to different ion channel mutations in the atria, influencing repolarization, depolarization, connexin function, and consequently impulse conduction properties (1080).

9. OTHER FACTORS INFLUENCING ARRHYTHMOGENESIS

9.1. Sex Differences in Cardiac Electrophysiology and Arrhythmias

Sex differences in cardiac electrophysiology carry marked clinical significance because they translate into distinct arrhythmia risks and outcome in men and women. Although women have a somewhat smaller risk of AF or ventricular fibrillation (VF) compared with men (1081), this does not hold for all causes of arrhythmia. For example, women have a longer frequency-corrected QT interval and are more susceptible to development of drug-induced polymorphic ventricular tachycardia (1082–1085), whereas men are more likely to exhibit early repolarization (150). Here we briefly discuss the underlying mechanisms for sex differences in cardiac electrophysiology; for more detailed discussions the reader is directed to recent comprehensive reviews (265, 1081).

Sex hormones exert their effects via both transcriptional regulation (1086, 1087) and acute, nongenomic modulation of intracellular signaling (1088). Women exhibit greater sinoatrial node automaticity (1089), and pregnancy increases pacemaker I_f current density along with HCN2 expression in mice (1090). A larger I_{NaLate} was observed in male rabbit left atrial posterior wall myocytes (1091). Since these cells are major sources of non-pulmonary vein triggered activity (204, 1092), and I_{NaLate} is an important contributor in atrial arrhythmogenesis (1093), the larger I_{NaLate} may contribute to higher triggered activity in males, leading to the initiation of AF.

The prolonged ventricular repolarization in women is partly due to decreased expression of pore-forming and/or auxiliary subunits of ion channels carrying repolarizing currents, including I_{to} , I_{K1} , I_{Kr} , I_{Ks} , and K_{ATP} in humans (151), and these results are generally in agreement with animal studies showing lower densities for these currents (263, 1094–1096). In addition, 17β -estradiol (E_2) directly (nongenomic effect) reduces I_{Kr} and enhances I_{Kr} block and QTc prolongation by HERG blocker drugs (1085, 1097), whereas testosterone increases I_{Kr} and I_{Ks} (1094, 1098) and progesterone enhances I_{Ks} (1099). Indeed, the normalization of the QTc interval in a woman with long QT syndrome was observed during pregnancy due to increased progesterone levels (1100). A greater transmural I_{Ks} density gradient was found in female dogs compared with males (1101), possibly contributing to larger transmural APD heterogeneity in females. Opposite effects of β -adrenergic stimulation by isoproterenol on Purkinje fiber APD were observed in male dogs (APD shortening) compared with female dogs (APD prolongation), highlighting sex- and age-related differences in the autonomic regulation of

the cAMP-dependent I_{Ks} current (1102, 1103). Since I_{Ks} is a key current for repolarization reserve (228, 250, 260), these changes may lead to reduced repolarization reserve and an increased arrhythmia substrate in women.

A more heterogeneous transmural I_{Na} distribution was found in female canine left ventricle (1104), and testosterone increased epicardial I_{Na} amplitude in female dogs to levels similar to those measured in male epicardium (1104). As I_{Na} and I_{to} have opposing effects on repolarization, increased transmural heterogeneity in ion channel expression creates transmural dispersion of repolarization that serves as an arrhythmogenic substrate (128). Sex-dependent differences in $I_{Ca,L}$ densities and Ca^{2+} homeostasis protein expression and regulation (162) lead to sex differences in triggered activity, since the reactivation of the L-type calcium current during the plateau of the action potential and Ca^{2+} cycling protein dysfunction importantly contribute to EAD formation (10). Larger $I_{Ca,L}$ densities were found in all transmural layers of the left ventricle in female dogs (1101), possibly contributing to a bigger transmural heterogeneity of APD in females, since I_{Ks} (similar in male and female midmyocardium) could not offset the increased $I_{Ca,L}$. In addition, estradiol increased $I_{Ca,L}$ (1105) and promoted EAD formation and sudden cardiac death in rabbits with LQT2 syndrome (1106), whereas testosterone and progesterone exerted opposite effects (1088, 1106, 1107). In female rabbit left ventricle, NCX expression and current were higher, resulting in increased EAD development following the administration of the HERG blocker dofetilide (1108). Testosterone, however, increased SERCA function, causing rapid removal of excess intracellular Ca^{2+} (1109). Testosterone increased RyR2 activity (1109), whereas estradiol increased RyR2 leakiness and contributed to the formation of proarrhythmic afterdepolarizations (1110). A significantly lower expression of Cx43 was found in left ventricular myocardium in women compared with men (151) that can make women more susceptible to ventricular conduction impairment.

In summary, sex hormones significantly modulate both the arrhythmia substrate and triggered activity leading to sex differences in ECG morphology and susceptibility to supraventricular and ventricular arrhythmias. Estradiol lengthens repolarization, promotes EAD formation, and exacerbates the QT-prolonging effect of HERG blocker drugs, leading to higher incidence of cardiac arrhythmias in females, whereas testosterone and progesterone exert mostly opposite effects.

9.2. Serum Ion Concentration Changes

Potassium is by far the most important ion in blood that affects arrhythmogenesis (233, 1111–1113). As mentioned

above, extracellular K^+ concentration significantly modulates several K^+ currents (225, 233–235, 294, 1114) in the range of blood K^+ concentrations (2–10 mM) observed frequently in clinical practice. Hyperkalemia depolarizes the cell, as expected from the Nernst equation. The depolarization caused by elevated extracellular $[K^+]$ can also slow impulse conduction indirectly, by decreasing I_{K1} and partially inactivating inward currents. This happens during ischemia and when K^+ accumulation occurs in the intercellular clefts, not immediately handled by the Na^+-K^+ pump. This latter mechanism may contribute to frequency-dependent regulation of APD and conduction as well (4). I_{Kr} is increased by elevation of extracellular K^+ concentration and decreased in hypokalemia (235, 294, 1115), which is not what would be expected from its transmembrane concentration gradient and is explained by hypokalemia-induced acceleration of rapid I_{Kr} inactivation (225). This may have a role in frequency-dependent APD regulation, and it helps in understanding why hypokalemia enhances the risk of arrhythmias by causing prolongation of repolarization at slow heart rate. I_{Ks} , unlike I_{Kr} , is reduced by elevated $[K^+]_o$ and increased by hypokalemia (235, 294). Therefore, I_{Ks} may serve as part of the repolarization reserve in hypokalemic patients. Hypokalemia and diminished I_{K1} can decrease background K^+ currents, which may favor ectopic automaticity not counterbalancing existing inward currents such as I_f or NCX and may act as enhanced triggers for arrhythmia development. Hypokalemia was shown to decrease Na^+-K^+ pump activity, thereby elevating intracellular $[Na^+]$ and leading to increased DAD formation via enhanced NCX function (1116). Hypokalemia also decreases I_{Kr} and consequently prolongs repolarization (225, 235, 1117), decreases repolarization reserve, and often leads to torsade de pointes tachycardia, especially when K^+ channels are already inhibited by concomitant drug therapy. Hypomagnesemia has a similar effect but with a different mechanism. The Mg^{2+} ion acts as endogenous Ca^{2+} antagonist, and in the case where its serum level is low it cannot fine-tune the influence of $I_{Ca,L}$ in sinus node function, repolarization, and possible EAD and DAD formation (1118).

9.3. Proarrhythmic Drug Effects

Not only can diseases, remodeling, serum electrolyte disturbances, and genetic disorders contribute to arrhythmogenesis, but so can drugs, i.e., they may possess proarrhythmic actions. Positive inotropic drugs like digitalis, which inhibits the Na^+-K^+ pump and enhances Ca^{2+} release of SR, can cause DADs, whereas phosphodiesterase inhibitors like milrinone or sympathetic stimulators (1119) like amphetamine, epinephrine, and norepinephrine increase intracellular cAMP levels (1120,

1121), and they consequently increase I_f -related and Ca^{2+} overload-induced automaticity; all of these represent enhanced triggers for arrhythmias. A large number of drugs inhibit I_{Na} and impulse conduction including class I antiarrhythmic drugs like quinidine, flecainide, propafenone, and tricyclic antidepressants (202, 1122, 1123). These drugs, despite the fact that some of them are used to abolish arrhythmias, can also elicit ventricular tachyarrhythmia (1124, 1125), presumably by converting areas in damaged tissue into areas with unidirectional impulse conduction block, which is one prerequisite of reentry arrhythmias, i.e., enhancing the substrate for arrhythmogenesis.

Another proarrhythmic drug effect is prolongation of ventricular repolarization (1126). This proarrhythmic mechanism, which was discussed above, can enhance both the arrhythmic triggers by inducing EADs and the substrate by enhancing dispersion of repolarization. A constantly growing number of drugs have such effects, such as class III antiarrhythmics like sotalol and ibutilide, antibiotics like erythromycin, antihistamines like terfenadine and astemizole, antidepressants like sertindole, and antimalarial drugs like dihydroartemisinin and piperazine (1127). Most of these drugs had been identified to inhibit I_{Kr} or HERG current; therefore, the assessment of HERG current-blocking properties of drug candidates became mandatory in cardiac safety testing in drug development (1128). It must be emphasized that some drugs can induce repolarization abnormality-related arrhythmias without apparent repolarization prolongation by impairing repolarization reserve (260). Therefore, drug effects on other repolarizing currents such as I_{Ks} , I_{K1} , and I_{to} should also be considered to avoid possible proarrhythmic complications of novel compounds in development. Computer simulation studies have recently demonstrated the importance of evaluating multichannel effects for the prediction of drug-induced arrhythmic risk (715).

For a more detailed overview of proarrhythmic adverse effects of drugs, we refer the reader to Refs. 108, 597, 1129–1132.

10. CONCLUSIONS

Cardiac arrhythmias such as VF, TdP, and AF still threaten the lives of millions of patients worldwide. Although the underlying causes of arrhythmia development are variable, including ischemia, heart failure, HCM, diabetes, extreme endurance training, or genetic causes, the direct mechanisms leading to these arrhythmias depend on changes of cellular electrophysiological properties or function of the heart. Therefore, to prevent or treat cardiac arrhythmias, and their most serious consequences, sudden cardiac death and stroke, improved

management and prevention of underlying diseases are needed. This requires a better understanding of the cardiac electrophysiological function and how it may be modulated. The latter includes the improved understanding of the nature of cardiac action potentials in various regions of the heart and the function of the underlying transmembrane ionic currents, pumps, and the development of novel techniques and tools like in silico modeling. Pathophysiological changes in the expression and function of transmembrane currents and pumps lead to disturbances of impulse formation, conduction, and refractoriness of cardiac muscle. These would favor the onset of “triggers” and providing the “substrate” for these arrhythmias to develop. Therefore, further intensive research is required to improve our understanding of the physiology, pathophysiology, and genetic and hormonal modulation of these ion channels and pumps in order to develop more efficacious treatment modalities, thereby saving millions of lives in the future.

CORRESPONDENCE

A. Varró (varro.andras@med.u-szeged.hu).

ACKNOWLEDGMENTS

We sincerely thank Gabriella Baczkó and Dr. Noémi Tóth for administrative work on the manuscript.

GRANTS

This work was supported by the National Research, Development and Innovation Office [NKFIH-K-119992, and GINOP-2.3.2-15-2016-00006 (MOLMEDEX) to A.V., NKFIH-K-128851 to I.B., PD-125402, FK-129117 to N.N.], the János Bolyai Research Scholarship of the Hungarian Academy of Sciences to N.N., and the Hungarian Academy of Sciences, as well as a Wellcome Trust Fellowship in Basic Biomedical Sciences (214290/Z/18/Z) and an NC3Rs Infrastructure for Impact Award (NC/P001076/1) to B.R.

DISCLOSURES

No conflicts of interest, financial or otherwise, are declared by the authors.

AUTHOR CONTRIBUTIONS

A.V., N.N., L.V., B.R., and I.B. prepared figures; A.V., J.T., N.N., E.P., B.R., and I.B. drafted manuscript; A.V., J.T., N.N., L.V., E.P.,

B.R., and I.B. edited and revised manuscript; A.V., J.T., N.N., L.V., E.P., B.R., and I.B. approved final version of manuscript;

REFERENCES

- Hoffman BF, Cranefield PF. **Electrophysiology of the Heart**. New York: McGraw-Hill, 1960, p. 323.
- Bers DM. Cardiac excitation-contraction coupling. **Nature** 415: 198–205, 2002. doi:10.1038/415198a.
- Bartos DC, Grandi E, Ripplinger CM. Ion channels in the heart. **Compr Physiol** 5: 1423–1464, 2015. doi:10.1002/cphy.c140069.
- Carmeliet E. Cardiac ionic currents and acute ischemia: from channels to arrhythmias. **Physiol Rev** 79: 917–1017, 1999. doi:10.1152/physrev.1999.79.3.917.
- Schmitt N, Grunnet M, Olesen SP. Cardiac potassium channel subtypes: new roles in repolarization and arrhythmia. **Physiol Rev** 94: 609–653, 2014. doi:10.1152/physrev.00022.2013.
- Benjamin EJ, Wolf PA, D'Agostino RB, Silbershatz H, Kannel WB, Levy D. Impact of atrial fibrillation on the risk of death: the Framingham Heart Study. **Circulation** 98: 946–952, 1998. doi:10.1161/01.cir.98.10.946.
- Nattel S, Maguy A, Le Bouter S, Yeh YH. Arrhythmogenic ion-channel remodeling in the heart: heart failure, myocardial infarction, and atrial fibrillation. **Physiol Rev** 87: 425–456, 2007. doi:10.1152/physrev.00014.2006.
- Temple IP, Inada S, Dobrzynski H, Boyett MR. Connexins and the atrioventricular node. **Heart Rhythm** 10: 297–304, 2013. doi:10.1016/j.hrthm.2012.10.020.
- Attwell D, Cohen I, Eisner D, Ohba M, Ojeda C. The steady state TTX-sensitive (“window”) sodium current in cardiac Purkinje fibres. **Pflügers Arch** 379: 137–142, 1979. doi:10.1007/BF00586939.
- January CT, Riddle JM. Early afterdepolarizations: mechanism of induction and block. A role for L-type Ca^{2+} current. **Circ Res** 64: 977–990, 1989. doi:10.1161/01.res.64.5.977.
- Banyasz T, Horvath B, Jian Z, Izu LT, Chen-Izu Y. Profile of L-type Ca^{2+} current and $\text{Na}^{+}/\text{Ca}^{2+}$ exchange current during cardiac action potential in ventricular myocytes. **Heart Rhythm** 9: 134–142, 2012. doi:10.1016/j.hrthm.2011.08.029.
- Carmeliet E. Slow inactivation of the sodium current in rabbit cardiac Purkinje fibres. **Pflügers Arch** 408: 18–26, 1987. doi:10.1007/BF00581835.
- Gintant GA, Dwyer NB, Cohen IS. Slow inactivation of a tetrodotoxin-sensitive current in canine cardiac Purkinje fibers. **Biophys J** 45: 509–512, 1984. doi:10.1016/S0006-3495(84)84187-9.
- Isenberg G, Klöckner U. Calcium currents of isolated bovine ventricular myocytes are fast and of large amplitude. **Pflügers Arch** 395: 30–41, 1982. doi:10.1007/BF00584965.
- Kokubun S, Irisawa H. Effects of various intracellular Ca ion concentrations on the calcium current of guinea-pig single ventricular cells. **Jpn J Physiol** 34: 599–611, 1984. doi:10.2170/jjphysiol.34.599.
- Liu MB, de Lange E, Garfinkel A, Weiss JN, Qu Z. Delayed afterdepolarizations generate both triggers and a vulnerable substrate promoting reentry in cardiac tissue. **Heart Rhythm** 12: 2115–2124, 2015. doi:10.1016/j.hrthm.2015.06.019.
- Nguyen TP, Qu Z, Weiss JN. Cardiac fibrosis and arrhythmogenesis: the road to repair is paved with perils. **J Mol Cell Cardiol** 70: 83–91, 2014. doi:10.1016/j.jmcc.2013.10.018.
- Varro A, Baczkó I. Possible mechanisms of sudden cardiac death in top athletes: a basic cardiac electrophysiological point of view. **Pflügers Arch** 460: 31–40, 2010. doi:10.1007/s00424-010-0798-0.
- Mines GR. Further experiments on the action of the vagus on the electrogram of the frog's heart. **J Physiol** 47: 419–430, 1914. doi:10.1113/jphysiol.1914.sp001634.
- Coronel R, Wilms-Schopman FJ, Opthof T, Janse MJ. Dispersion of repolarization and arrhythmogenesis. **Heart Rhythm** 6: 537–543, 2009. doi:10.1016/j.hrthm.2009.01.013.
- Opthof T, Janse MJ, Meijborg VM, Cinca J, Rosen MR, Coronel R. Dispersion in ventricular repolarization in the human, canine and porcine heart. **Prog Biophys Mol Biol** 120: 222–235, 2016. doi:10.1016/j.pbiomolbio.2016.01.007.
- Kline J, Costantini O. Inherited cardiac arrhythmias and channelopathies. **Med Clin North Am** 103: 809–820, 2019. doi:10.1016/j.mcna.2019.05.001.
- Skibbye L, Ravens U. Mechanism of proarrhythmic effects of potassium channel blockers. **Card Electrophysiol Clin** 8: 395–410, 2016. doi:10.1016/j.ccep.2016.02.004.
- Aiba T, Shimizu W, Hidaka I, Uemura K, Noda T, Zheng C, Kamiya A, Inagaki M, Sugimachi M, Sunagawa K. Cellular basis for trigger and maintenance of ventricular fibrillation in the Brugada syndrome model: high-resolution optical mapping study. **J Am Coll Cardiol** 47: 2074–2085, 2006. doi:10.1016/j.jacc.2005.12.064.
- Akar FG, Rosenbaum DS. Transmural electrophysiological heterogeneities underlying arrhythmogenesis in heart failure. **Circ Res** 93: 638–645, 2003. doi:10.1161/01.RES.0000092248.59479.AE.
- Antzelevitch C, Burashnikov A. Overview of basic mechanisms of cardiac arrhythmia. **Card Electrophysiol Clin** 3: 23–45, 2011. doi:10.1016/j.ccep.2010.10.012.
- Coppini R, Ferrantini C, Mugelli A, Poggesi C, Cerbai E. Altered Ca^{2+} and Na^{+} homeostasis in human hypertrophic cardiomyopathy: implications for arrhythmogenesis. **Front Physiol** 9: 1391, 2018. doi:10.3389/fphys.2018.01391.
- de Bakker JM, van Capelle FJ, Janse MJ, Wilde AA, Coronel R, Becker AE, Dingemans KP, van Hemel NM, Hauer RN. Reentry as a cause of ventricular tachycardia in patients with chronic ischemic heart disease: electrophysiologic and anatomic correlation. **Circulation** 77: 589–606, 1988. doi:10.1161/01.cir.77.3.589.
- Harada M, Van Wagoner DR, Nattel S. Role of inflammation in atrial fibrillation pathophysiology and management. **Circ J** 79: 495–502, 2015. doi:10.1253/circj.CJ-15-0138.
- Heijman J, Voigt N, Nattel S, Dobrev D. Cellular and molecular electrophysiology of atrial fibrillation initiation, maintenance, and progression. **Circ Res** 114: 1483–1499, 2014. doi:10.1161/CIRCRESAHA.114.302226.
- Janse MJ, Wit AL. Electrophysiological mechanisms of ventricular arrhythmias resulting from myocardial ischemia and infarction. **Physiol Rev** 69: 1049–1169, 1989. doi:10.1152/physrev.1989.69.4.1049.
- Lazzara R, Scherlag BJ. Electrophysiologic basis for arrhythmias in ischemic heart disease. **Am J Cardiol** 53: 1B–7B, 1984. doi:10.1016/0002-9149(84)90493-4.

33. Park S, Nguyen NB, Pezhouman A, Ardehali R. Cardiac fibrosis: potential therapeutic targets. **Transl Res** 209: 121–137, 2019. doi:[10.1016/j.trsl.2019.03.001](https://doi.org/10.1016/j.trsl.2019.03.001).
34. Schotten U, Verheule S, Kirchhof P, Goette A. Pathophysiological mechanisms of atrial fibrillation: a translational appraisal. **Physiol Rev** 91: 265–325, 2011. doi:[10.1152/physrev.00031.2009](https://doi.org/10.1152/physrev.00031.2009).
35. Attwell D, Cohen I, Eisner DA. The effects of heart rate on the action potential of guinea-pig and human ventricular muscle. **J Physiol** 313: 439–461, 1981. doi:[10.1113/jphysiol.1981.sp013675](https://doi.org/10.1113/jphysiol.1981.sp013675).
36. Gadsby DC. Influence of Na/K pump current on action potentials in Purkinje fibers. **Adv Myocardiol** 5: 279–294, 1985. doi:[10.1007/978-1-4757-1287-2_22](https://doi.org/10.1007/978-1-4757-1287-2_22).
37. Gao J, Wang W, Cohen IS, Mathias RT. Transmural gradients in Na/K pump activity and $[Na^+]_i$ in canine ventricle. **Biophys J** 89: 1700–1709, 2005. doi:[10.1529/biophysj.105.062406](https://doi.org/10.1529/biophysj.105.062406).
38. Lee JH. The Na/K pump, resting potential and selective permeability in canine Purkinje fibres at physiologic and room temperatures. **Experientia** 52: 657–660, 1996. doi:[10.1007/BF01925568](https://doi.org/10.1007/BF01925568).
39. Shaw RM, Rudy Y. Electrophysiologic effects of acute myocardial ischemia: a theoretical study of altered cell excitability and action potential duration. **Cardiovasc Res** 35: 256–272, 1997. doi:[10.1016/s0008-6363\(97\)00093-x](https://doi.org/10.1016/s0008-6363(97)00093-x).
40. Clauss S, Bleyer C, Schüttler D, Tomsits P, Renner S, Klymiuk N, Wakili R, Massberg S, Wolf E, Käb S. Animal models of arrhythmia: classic electrophysiology to genetically modified large animals. **Nat Rev Cardiol** 16: 457–475, 2019. doi:[10.1038/s41569-019-0179-0](https://doi.org/10.1038/s41569-019-0179-0).
41. Coraboeuf E, Weidmann S. Potentiels d'action du muscle cardiaque obtenus a l'aide de microélectrodes intracellulaires. Présence d'une inversion de potentiel. **C R Soc Biol Paris** 143: 1360–1361, 1949.
42. Coraboeuf E, Boistel J. [Study with the aid of intracellular micro-electrodes of the action of a cardiotonic: 2-methyl-6-amino-2-heptanol on nodal tissue of dog heart]. **C R Seances Soc Biol Fil** 147: 774–779, 1953.
43. Franz MR. Method and theory of monophasic action potential recording. **Prog Cardiovasc Dis** 33: 347–368, 1991. doi:[10.1016/0033-0620\(91\)90002-4](https://doi.org/10.1016/0033-0620(91)90002-4).
44. Harper RW, Olsson SB, Varnauskas E. Effect of mexiletine on monophasic action potentials recorded from the right ventricle in man. **Cardiovasc Res** 13: 303–310, 1979. doi:[10.1093/cvr/13.6.303](https://doi.org/10.1093/cvr/13.6.303).
45. Franz MR. Long-term recording of monophasic action potentials from human endocardium. **Am J Cardiol** 51: 1629–1634, 1983. doi:[10.1016/0002-9149\(83\)90199-6](https://doi.org/10.1016/0002-9149(83)90199-6).
46. Carmeliet E. From Bernstein's rheotome to Neher-Sakmann's patch electrode. The action potential. **Physiol Rep** 7: e13861, 2019. doi:[10.14814/phy2.13861](https://doi.org/10.14814/phy2.13861).
47. Hamill OP, Marty A, Neher E, Sakmann B, Sigworth FJ. Improved patch-clamp techniques for high-resolution current recording from cells and cell-free membrane patches. **Pflugers Arch** 391: 85–100, 1981. doi:[10.1007/BF00656997](https://doi.org/10.1007/BF00656997).
48. Neher E, Sakmann B. Single-channel currents recorded from membrane of denervated frog muscle fibres. **Nature** 260: 799–802, 1976. doi:[10.1038/260799a0](https://doi.org/10.1038/260799a0).
49. Yue L, Feng J, Li GR, Nattel S. Transient outward and delayed rectifier currents in canine atrium: properties and role of isolation methods. **Am J Heart Circ Physiol** 270: H2157–H2168, 1996. doi:[10.1152/ajpheart.1996.270.6.H2157](https://doi.org/10.1152/ajpheart.1996.270.6.H2157).
50. Pueyo E, Corrias A, Virág L, Jost N, Szél T, Varró A, Szentandrassy N, Nánási PP, Burrage K, Rodríguez B. A multiscale investigation of repolarization variability and its role in cardiac arrhythmogenesis. **Biophys J** 101: 2892–2902, 2011. doi:[10.1016/j.bpj.2011.09.060](https://doi.org/10.1016/j.bpj.2011.09.060).
51. Sharp GH, Joyner RW. Simulated propagation of cardiac action potentials. **Biophys J** 31: 403–423, 1980. doi:[10.1016/S0006-3495\(80\)85068-5](https://doi.org/10.1016/S0006-3495(80)85068-5).
52. Morad M, Salama G. Optical probes of membrane potential in heart muscle. **J Physiol** 292: 267–295, 1979. doi:[10.1113/jphysiol.1979.sp012850](https://doi.org/10.1113/jphysiol.1979.sp012850).
53. Salama G, Lombardi R, Elson J. Maps of optical action potentials and NADH fluorescence in intact working hearts. **Am J Physiol Heart Circ Physiol** 252: H384–H394, 1987. doi:[10.1152/ajpheart.1987.252.2.H384](https://doi.org/10.1152/ajpheart.1987.252.2.H384).
54. Berenfeld O, Efimov I. Optical mapping. **Card Electrophysiol Clin** 11: 495–510, 2019. doi:[10.1016/j.ccep.2019.04.004](https://doi.org/10.1016/j.ccep.2019.04.004).
55. Jaimes R 3rd, Walton RD, Pasdois P, Bernus O, Efimov IR, Kay MW. A technical review of optical mapping of intracellular calcium within myocardial tissue. **Am J Physiol Heart Circ Physiol** 310: H1388–H1401, 2016. doi:[10.1152/ajpheart.00665.2015](https://doi.org/10.1152/ajpheart.00665.2015).
56. Bishop MJ, Gavaghan DJ, Trayanova NA, Rodríguez B. Photon scattering effects in optical mapping of propagation and arrhythmogenesis in the heart. **J Electrocardiol** 40: S75–S80, 2007. doi:[10.1016/j.jelectrocard.2007.06.020](https://doi.org/10.1016/j.jelectrocard.2007.06.020).
57. Fedorov VV, Lozinsky IT, Sosunov EA, Anyukhovskiy EP, Rosen MR, Balke CW, Efimov IR. Application of blebbistatin as an excitation-contraction uncoupler for electrophysiologic study of rat and rabbit hearts. **Heart Rhythm** 4: 619–626, 2007. doi:[10.1016/j.hrthm.2006.12.047](https://doi.org/10.1016/j.hrthm.2006.12.047).
58. Kanlop N, Sakai T. Optical mapping study of blebbistatin-induced chaotic electrical activities in isolated rat atrium preparations. **J Physiol Sci** 60: 109–117, 2010. doi:[10.1007/s12576-009-0074-2](https://doi.org/10.1007/s12576-009-0074-2).
59. Brack KE, Narang R, Winter J, Ng GA. The mechanical uncoupler blebbistatin is associated with significant electrophysiological effects in the isolated rabbit heart. **Exp Physiol** 98: 1009–1027, 2013. doi:[10.1113/expphysiol.2012.069369](https://doi.org/10.1113/expphysiol.2012.069369).
60. Banyasz T, Horvath B, Jian Z, Izu LT, Chen-Izu Y. Sequential dissection of multiple ionic currents in single cardiac myocytes under action potential-clamp. **J Mol Cell Cardiol** 50: 578–581, 2011. doi:[10.1016/j.yjmcc.2010.12.020](https://doi.org/10.1016/j.yjmcc.2010.12.020).
61. Reuter H. Slow inactivation of currents in cardiac Purkinje fibres. **J Physiol** 197: 233–253, 1968. doi:[10.1113/jphysiol.1968.sp008557](https://doi.org/10.1113/jphysiol.1968.sp008557).
62. Noble D. **The Initiation of the Heartbeat**. Oxford: Oxford University Press, 1980.
63. Dhamoon AS, Pandit SV, Sarmast F, Parisian KR, Guha P, Li Y, Bagwe S, Taffet SM, Anumonwo JM. Unique Kir2.x properties determine regional and species differences in the cardiac inward rectifier K⁺ current. **Circ Res** 94: 1332–1339, 2004. doi:[10.1161/01.RES.0000128408.66946.67](https://doi.org/10.1161/01.RES.0000128408.66946.67).
64. Gurney A, Manoury B. Two-pore potassium channels in the cardiovascular system. **Eur Biophys J** 38: 305–318, 2009. doi:[10.1007/s00249-008-0326-8](https://doi.org/10.1007/s00249-008-0326-8).
65. Jones EM, Roti EC, Wang J, Delfosse SA, Robertson GA. Cardiac IKr channels minimally comprise hERG 1a and 1b subunits. **J Biol Chem** 279: 44690–44694, 2004. doi:[10.1074/jbc.M408344200](https://doi.org/10.1074/jbc.M408344200).

66. Robertson GA, Jones EM, Wang J. Gating and assembly of heteromeric hERG1a/1b channels underlying I_{Kr} in the heart. **Novartis Found Symp** 266: 4–15, 2005.
67. Bendahhou S, Marionneau C, Haurogne K, Larroque MM, Derand R, Szuts V, Escande D, Demolombe S, Barhanin J. In vitro molecular interactions and distribution of KCNE family with KCNQ1 in the human heart. **Cardiovasc Res** 67: 529–538, 2005. doi:10.1016/j.cardiores.2005.02.014.
68. Lundquist AL, Manderfield LJ, Vanoye CG, Rogers CS, Donahue BS, Chang PA, Drinkwater DC, Murray KT, George AL Jr. Expression of multiple KCNE genes in human heart may enable variable modulation of I_{Ks} . **J Mol Cell Cardiol** 38: 277–287, 2005. doi:10.1016/j.yjmcc.2004.11.012.
69. Fozzard HA, January CT, Makielski JC. New studies of the excitatory sodium currents in heart muscle. **Circ Res** 56: 475–485, 1985. doi:10.1161/01.res.56.4.475.
70. Rook MB, Evers MM, Vos MA, Bierhuizen MF. Biology of cardiac sodium channel Nav1.5 expression. **Cardiovasc Res** 93: 12–23, 2012. doi:10.1093/cvr/cvr252.
71. Jiang D, Shi H, Tonggu L, Gamal El-Din TM, Lenaeus MJ, Zhao Y, Yoshioka C, Zheng N, Catterall WA. Structure of the cardiac sodium channel. **Cell** 180: 122–134.e10, 2020. doi:10.1016/j.cell.2019.11.041.
72. Antoni H, Böcker D, Eickhorn R. Sodium current kinetics in intact rat papillary muscle: measurements with the loose-patch-clamp technique. **J Physiol** 406: 199–213, 1988. doi:10.1113/jphysiol.1988.sp017376.
73. Brown AM, Lee KS, Powell T. Sodium current in single rat heart muscle cells. **J Physiol** 318: 479–500, 1981. doi:10.1113/jphysiol.1981.sp013879.
74. Fozzard HA, Friedlander IR, Hanck DA, January CT, Makielski JC, Sheets MF. Sodium currents in single cardiac Purkinje cells. **J Am Coll Cardiol** 8: 79A–85A, 1986. doi:10.1016/s0735-1097(86)80033-x.
75. Morad M, Tung L. Ionic events responsible for the cardiac resting and action potential. **Am J Cardiol** 49: 584–594, 1982. doi:10.1016/s0002-9149(82)80016-7.
76. Reuter H. Properties of two inward membrane currents in the heart. **Annu Rev Physiol** 41: 413–424, 1979. doi:10.1146/annurev.ph.41.030179.002213.
77. Ten Eick RE, Baumgarten CM, Singer DH. Ventricular dysrhythmia: membrane basis of currents, channels, gates, and cables. **Prog Cardiovasc Dis** 24: 157–188, 1981. doi:10.1016/0033-0620(81)90003-7.
78. Bocchi L, Vassalle M. Characterization of the slowly inactivating sodium current I_{Na2} in canine cardiac single Purkinje cells. **Exp Physiol** 93: 347–361, 2008. doi:10.1113/expphysiol.2007.040881.
79. Maltsev VA, Undrovinas AI. A multi-modal composition of the late Na^+ current in human ventricular cardiomyocytes. **Cardiovasc Res** 69: 116–127, 2006. doi:10.1016/j.cardiores.2005.08.015.
80. Kiyosue T, Arita M. Late sodium current and its contribution to action potential configuration in guinea pig ventricular myocytes. **Circ Res** 64: 389–397, 1989. doi:10.1161/01.res.64.2.389.
81. Zaza A, Belardinelli L, Shryock JC. Pathophysiology and pharmacology of the cardiac “late sodium current”. **Pharmacol Ther** 119: 326–339, 2008. doi:10.1016/j.pharmthera.2008.06.001.
82. Coraboeuf E, Deroubaix E, Coulombe A. Effect of tetrodotoxin on action potentials of the conducting system in the dog heart. **Am J Physiol Heart Circ Physiol** 236: H561–H567, 1979. doi:10.1152/ajpheart.1979.236.4.H561.
83. Di Stolfo G, Palumbo P, Castellana S, Mastroianno S, Biagini T, Palumbo O, Leone MP, De Luca G, Potenza DR, Mazza T, Russo AA, Carella M. Sudden cardiac death in J wave syndrome with short QT associated to a novel mutation in Nav 1.8 coding gene SCN10A: first case report for a possible pharmacogenomic role. **J Electrocardiol** 51: 809–813, 2018. doi:10.1016/j.jelectrocard.2018.06.005.
84. Felipe A, Knittle TJ, Doyle KL, Tamkun MM. Primary structure and differential expression during development and pregnancy of a novel voltage-gated sodium channel in the mouse. **J Biol Chem** 269: 30125–30131, 1994. doi:10.1016/S0021-9258(18)43786-6.
85. Gaborit N, Le Bouter S, Szuts V, Varro A, Escande D, Nattel S, Demolombe S. Regional and tissue specific transcript signatures of ion channel genes in the non-diseased human heart. **J Physiol** 582: 675–693, 2007. doi:10.1113/jphysiol.2006.126714.
86. Mishra S, Reznikov V, Maltsev VA, Undrovinas NA, Sabbah HN, Undrovinas A. Contribution of sodium channel neuronal isoform Nav1.1 to late sodium current in ventricular myocytes from failing hearts. **J Physiol** 593: 1409–1427, 2015. doi:10.1113/jphysiol.2014.278259.
87. Pabel S, Ahmad S, Tirilomis P, Stehle T, Mustroph J, Knierim M, Dybkova N, Bengel P, Holzamer A, Hilker M, Streckfuss-Bömeke K, Hasenfuss G, Maier LS, Sossalla S. Inhibition of Nav1.8 prevents atrial arrhythmogenesis in human and mice. **Basic Res Cardiol** 115: 20, 2020. doi:10.1007/s00395-020-0780-8.
88. Savio-Galimberti E, Weeke P, Muhammad R, Blair M, Ansari S, Short L, Attack TC, Kor K, Vanoye CG, Olesen MS, LuCamp, Yang T, George AL Jr, Roden DM, Darbar D. SCN10A/Nav1.8 modulation of peak and late sodium currents in patients with early onset atrial fibrillation. **Cardiovasc Res** 104: 355–363, 2014. doi:10.1093/cvr/cvu170.
89. Biet M, Barajas-Martínez H, Ton AT, Delabre JF, Morin N, Dumaine R. About half of the late sodium current in cardiac myocytes from dog ventricle is due to non-cardiac-type Na^+ channels. **J Mol Cell Cardiol** 53: 593–598, 2012. doi:10.1016/j.yjmcc.2012.06.012.
90. Du Y, Huang X, Wang T, Han K, Zhang J, Xi Y, Wu G, Ma A. Downregulation of neuronal sodium channel subunits Nav1.1 and Nav1.6 in the sinoatrial node from volume-overloaded heart failure rat. **Pflugers Arch** 454: 451–459, 2007. doi:10.1007/s00424-007-0216-4.
91. Ahmad S, Tirilomis P, Pabel S, Dybkova N, Hartmann N, Molina CE, Tirilomis T, Kutschka I, Frey N, Maier LS, Hasenfuss G, Streckfuss-Bömeke K, Sossalla S. The functional consequences of sodium channel $Na_v1.8$ in human left ventricular hypertrophy. **ESC Heart Fail** 6: 154–163, 2019. doi:10.1002/ehf2.12378.
92. Aguilar-Bryan L, Nichols CG, Wechsler SW, Clement JP 4th, Boyd AE 3rd, González G, Herrera-Sosa H, Nguy K, Bryan J, Nelson DA. Cloning of the beta cell high-affinity sulfonylurea receptor: a regulator of insulin secretion. **Science** 268: 423–426, 1995. doi:10.1126/science.7716547.
93. Maier SK, Westenbroek RE, Schenkman KA, Feigl EO, Scheuer T, Catterall WA. An unexpected role for brain-type sodium channels in coupling of cell surface depolarization to contraction in the heart. **Proc Natl Acad Sci USA** 99: 4073–4078, 2002. doi:10.1073/pnas.261705699.

94. Rivaud MR, Delmar M, Remme CA. Heritable arrhythmia syndromes associated with abnormal cardiac sodium channel function: ionic and non-ionic mechanisms. **Cardiovasc Res** 116: 1557–1570, 2020. doi:10.1093/cvr/cvaa082.
95. Leo-Macias A, Agullo-Pascual E, Sanchez-Alonso JL, Keegan S, Lin X, Arcos T, Feng-Xia L, Korchev YE, Gorelik J, Fenyő D, Rothenberg E, Rothenberg E, Delmar M. Nanoscale visualization of functional adhesion/excitability nodes at the intercalated disc. **Nat Commun** 7: 10342, 2016. doi:10.1038/ncomms10342.
96. Rougier JS, Essers MC, Gillet L, Guichard S, Sonntag S, Shmerling D, Abriel H. A distinct pool of Nav1.5 channels at the lateral membrane of murine ventricular cardiomyocytes. **Front Physiol** 10: 834, 2019. doi:10.3389/fphys.2019.00834.
97. Lin X, Liu N, Lu J, Zhang J, Anumonwo JM, Isom LL, Fishman GI, Delmar M. Subcellular heterogeneity of sodium current properties in adult cardiac ventricular myocytes. **Heart Rhythm** 8: 1923–1930, 2011. doi:10.1016/j.hrthm.2011.07.016.
98. Rivaud MR, Agullo-Pascual E, Lin X, Leo-Macias A, Zhang M, Rothenberg E, Bezzina CR, Delmar M, Remme CA. Sodium channel remodeling in subcellular microdomains of murine failing cardiomyocytes. **J Am Heart Assoc** 6: e007622, 2017. doi:10.1161/JAHA.117.007622.
99. Johnson CN. Calcium modulation of cardiac sodium channels. **J Physiol** 598: 2835–2846, 2020. doi:10.1113/JP277553.
100. Tan HL, Kupersmidt S, Zhang R, Stepanovic S, Roden DM, Wilde AA, Anderson ME, Balser JR. A calcium sensor in the sodium channel modulates cardiac excitability. **Nature** 415: 442–447, 2002. doi:10.1038/415442a.
101. Johnson EK, Springer SJ, Wang W, Dranoff EJ, Zhang Y, Kanter EM, Yamada KA, Nerbonne JM. Differential expression and remodeling of transient outward potassium currents in human left ventricles. **Circ Arrhythm Electrophysiol** 11: e005914, 2018. doi:10.1161/CIRCEP.117.005914.
102. Gabelli SB, Boto A, Kuhns VH, Bianchet MA, Farinelli F, Aripirala S, Yoder J, Jakoncic J, Tomaselli GF, Amzel LM. Regulation of the Nav1.5 cytoplasmic domain by calmodulin. **Nat Commun** 5: 5126, 2014. doi:10.1038/ncomms6126.
103. Johnson C, Forsythe L, Somauroo J, Papadakis M, George K, Oxborough D. Cardiac structure and function in elite Native Hawaiian and Pacific Islander Rugby Football League athletes: an exploratory study. **Int J Cardiovasc Imaging** 34: 725–734, 2018. doi:10.1007/s10554-017-1285-x.
104. Wang C, Chung BC, Yan H, Wang HG, Lee SY, Pitt GS. Structural analyses of Ca²⁺/CaM interaction with NaV channel C-termini reveal mechanisms of calcium-dependent regulation. **Nat Commun** 5: 4896, 2014. doi:10.1038/ncomms5896.
105. Maltsev VA, Reznikov V, Undrovinas NA, Sabbah HN, Undrovinas A. Modulation of late sodium current by Ca²⁺, calmodulin, and CaMKII in normal and failing dog cardiomyocytes: similarities and differences. **Am J Physiol Heart Circ Physiol** 294: H1597–H1608, 2008. doi:10.1152/ajpheart.00484.2007.
106. Wagner S, Dybkova N, Rasenack EC, Jacobshagen C, Fabritz L, Kirchhof P, Maier SK, Zhang T, Hasenfuss G, Brown JH, Bers DM, Maier LS. Ca²⁺/calmodulin-dependent protein kinase II regulates cardiac Na⁺ channels. **J Clin Invest** 116: 3127–3138, 2006. doi:10.1172/JCI26620.
107. Anderson ME, Brown JH, Bers DM. CaMKII in myocardial hypertrophy and heart failure. **J Mol Cell Cardiol** 51: 468–473, 2011. doi:10.1016/j.jmcc.2011.01.012.
108. Lei M, Wu L, Terrar DA, Huang CL. Modernized classification of cardiac antiarrhythmic drugs. **Circulation** 138: 1879–1896, 2018. doi:10.1161/CIRCULATIONAHA.118.035455.
109. Roden DM. Pharmacology and toxicology of Nav1.5-class 1 antiarrhythmic drugs. **Card Electrophysiol Clin** 6: 695–704, 2014. doi:10.1016/j.ccep.2014.07.003.
110. Coppini R, Santini L, Olivetto I, Ackerman MJ, Cerbai E. Abnormalities in sodium current and calcium homeostasis as drivers of arrhythmogenesis in hypertrophic cardiomyopathy. **Cardiovasc Res** 116: 1585–1599, 2020. doi:10.1093/cvr/cvaa124.
111. Rajamani S, Liu G, El-Bizri N, Guo D, Li C, Chen XL, Kahlig KM, Mollova N, Elzein E, Zablocki J, Belardinelli L. The novel late Na⁺ current inhibitor, GS-6615 (eleclazine) and its anti-arrhythmic effects in rabbit isolated heart preparations. **Br J Pharmacol** 173: 3088–3098, 2016. doi:10.1111/bph.13563.
112. Le Grand B, Coulombe A, John GW. Late sodium current inhibition in human isolated cardiomyocytes by R 56865. **J Cardiovasc Pharmacol** 31: 800–804, 1998. doi:10.1097/00005344-199805000-00021.
113. Wu M, Tran PN, Sheng J, Randolph AL, Wu WW. Drug potency on inhibiting late Na⁺ current is sensitive to gating modifier and current region where drug effects were measured. **J Pharmacol Toxicol Methods** 100: 106605, 2019. doi:10.1016/j.vascn.2019.106605.
114. Bohnen MS, Peng G, Robey SH, Terrenoire C, Iyer V, Sampson KJ, Kass RS. Molecular pathophysiology of congenital long QT syndrome. **Physiol Rev** 97: 89–134, 2017. doi:10.1152/physrev.00008.2016.
115. Giudicessi JR, Wilde AA, Ackerman MJ. The genetic architecture of long QT syndrome: a critical reappraisal. **Trends Cardiovasc Med** 28: 453–464, 2018. doi:10.1016/j.tcm.2018.03.003.
116. Gourraud JB, Barc J, Thollet A, Le Marec H, Probst V. Brugada syndrome: diagnosis, risk stratification and management. **Arch Cardiovasc Dis** 110: 188–195, 2017. doi:10.1016/j.acvd.2016.09.009.
117. Skinner JR, Winbo A, Abrams D, Vohra J, Wilde AA. Channelopathies that lead to sudden cardiac death: clinical and genetic aspects. **Heart Lung Circ** 28: 22–30, 2019. doi:10.1016/j.hlc.2018.09.007.
118. Boyden PA, Dun W, Barbhuiya C, Ter Keurs HE. 2APB- and JTV519 (K201)-sensitive micro Ca²⁺ waves in arrhythmogenic Purkinje cells that survive in infarcted canine heart. **Heart Rhythm** 1: 218–226, 2004. doi:10.1016/j.hrthm.2004.03.068.
119. Benson DW, Wang DW, Dyment M, Knilans TK, Fish FA, Strieper MJ, Rhodes TH, George AL Jr. Congenital sick sinus syndrome caused by recessive mutations in the cardiac sodium channel gene (SCN5A). **J Clin Invest** 112: 1019–1028, 2003. doi:10.1172/JCI18062.
120. Schott JJ, Alshinawi C, Kyndt F, Probst V, Hoortje TM, Hulsbeek M, Wilde AA, Escande D, Mannens MM, Le Marec H. Cardiac conduction defects associate with mutations in SCN5A. **Nat Genet** 23: 20–21, 1999. doi:10.1038/12618.
121. Smits JP, Koopmann TT, Wilders R, Veldkamp MW, Opthof T, Bhuiyan ZA, Mannens MM, Balser JR, Tan HL, Bezzina CR, Wilde AA. A mutation in the human cardiac sodium channel (E161K) contributes to sick sinus syndrome, conduction disease and Brugada syndrome in two families. **J Mol Cell Cardiol** 38: 969–981, 2005. doi:10.1016/j.jmcc.2005.02.024.
122. Wang Q, Shen J, Li Z, Timothy K, Vincent GM, Priori SG, Schwartz PJ, Keating MT. Cardiac sodium channel mutations in patients with

- long QT syndrome, an inherited cardiac arrhythmia. **Hum Mol Genet** 4: 1603–1607, 1995. doi:[10.1093/hmg/4.9.1603](https://doi.org/10.1093/hmg/4.9.1603).
123. Li Q, Huang H, Liu G, Lam K, Rutberg J, Green MS, Birnie DH, Lemery R, Chahine M, Gollob MH. Gain-of-function mutation of Nav1.5 in atrial fibrillation enhances cellular excitability and lowers the threshold for action potential firing. **Biochem Biophys Res Commun** 380: 132–137, 2009. doi:[10.1016/j.bbrc.2009.01.052](https://doi.org/10.1016/j.bbrc.2009.01.052).
124. Makiyama T, Akao M, Shizuta S, Doi T, Nishiyama K, Oka Y, Ohno S, Nishio Y, Tsuji K, Itoh H, Kimura T, Kita T, Horie M. A novel SCN5A gain-of-function mutation M1875T associated with familial atrial fibrillation. **J Am Coll Cardiol** 52: 1326–1334, 2008. doi:[10.1016/j.jacc.2008.07.013](https://doi.org/10.1016/j.jacc.2008.07.013).
125. Remme CA, Wilde AA. Late sodium current inhibition in acquired and inherited ventricular (dys)function and arrhythmias. **Cardiovasc Drugs Ther** 27: 91–101, 2013. doi:[10.1007/s10557-012-6433-x](https://doi.org/10.1007/s10557-012-6433-x).
126. Undrovinas AI, Maltsev VA, Kyle JW, Silverman N, Sabbah HN. Gating of the late Na⁺ channel in normal and failing human myocardium. **J Mol Cell Cardiol** 34: 1477–1489, 2002. doi:[10.1006/jmcc.2002.2100](https://doi.org/10.1006/jmcc.2002.2100).
127. Undrovinas AI, Maltsev VA, Sabbah HN. Repolarization abnormalities in cardiomyocytes of dogs with chronic heart failure: role of sustained inward current. **Cell Mol Life Sci** 55: 494–505, 1999. doi:[10.1007/s000180050306](https://doi.org/10.1007/s000180050306).
128. Antzelevitch C, Fish J. Electrical heterogeneity within the ventricular wall. **Basic Res Cardiol** 96: 517–527, 2001. doi:[10.1007/s003950170002](https://doi.org/10.1007/s003950170002).
129. Ferrier GR. Digitalis arrhythmias: role of oscillatory afterpotentials. **Prog Cardiovasc Dis** 19: 459–474, 1977. [doi:[10.1016/0033-0620\(77\)90010-X](https://doi.org/10.1016/0033-0620(77)90010-X)].
130. Ferrier GR, Moe GK. Effect of calcium on acetylcholine-induced transient depolarizations in canine Purkinje tissue. **Circ Res** 33: 508–515, 1973. doi:[10.1161/01.res.33.5.508](https://doi.org/10.1161/01.res.33.5.508).
131. Szabo B, Kovacs T, Lazzara R. Role of calcium loading in early after-depolarizations generated by Cs⁺ in canine and guinea pig Purkinje fibers. **J Cardiovasc Electrophysiol** 6: 796–812, 1995. doi:[10.1111/j.1540-8167.1995.tb00356.x](https://doi.org/10.1111/j.1540-8167.1995.tb00356.x).
132. Dehghani-Samani A, Madreseh-Ghahfarokhi S, Dehghani-Samani A. Mutations of voltage-gated ionic channels and risk of severe cardiac arrhythmias. **Acta Cardiol Sin** 35: 99–110, 2019. doi:[10.6515/ACS.201903_35\(2\).20181028A](https://doi.org/10.6515/ACS.201903_35(2).20181028A).
133. Foeger NC, Norris AJ, Wren LM, Nerbonne JM. Augmentation of Kv4.2-encoded currents by accessory dipeptidyl peptidase 6 and 10 subunits reflects selective cell surface Kv4.2 protein stabilization. **J Biol Chem** 287: 9640–9650, 2012. doi:[10.1074/jbc.M111.324574](https://doi.org/10.1074/jbc.M111.324574).
134. Jimenez J, Rentschler SL. Transcriptional and epigenetic regulation of cardiac electrophysiology. **Pediatr Cardiol** 40: 1325–1330, 2019. doi:[10.1007/s00246-019-02160-w](https://doi.org/10.1007/s00246-019-02160-w).
135. Kääb S, Dixon J, Duc J, Ashen D, Näbauer M, Beuckelmann DJ, Steinbeck G, McKinnon D, Tomaselli GF. Molecular basis of transient outward potassium current downregulation in human heart failure: a decrease in Kv4.3 mRNA correlates with a reduction in current density. **Circulation** 98: 1383–1393, 1998. doi:[10.1161/01.cir.98.14.1383](https://doi.org/10.1161/01.cir.98.14.1383).
136. Näbauer M, Beuckelmann DJ, Überfuhr P, Steinbeck G. Regional differences in current density and rate-dependent properties of the transient outward current in subepicardial and subendocardial myocytes of human left ventricle. **Circulation** 93: 168–177, 1996. doi:[10.1161/01.cir.93.1.168](https://doi.org/10.1161/01.cir.93.1.168); doi:[10.1161/01.CIR.93.1.168](https://doi.org/10.1161/01.CIR.93.1.168).
137. Patel SP, Campbell DL. Transient outward potassium current, 'I_{to}', phenotypes in the mammalian left ventricle: underlying molecular, cellular and biophysical mechanisms. **J Physiol** 569: 7–39, 2005. doi:[10.1113/jphysiol.2005.086223](https://doi.org/10.1113/jphysiol.2005.086223).
138. Wang Z, Feng J, Shi H, Pond A, Nerbonne JM, Nattel S. Potential molecular basis of different physiological properties of the transient outward K⁺ current in rabbit and human atrial myocytes. **Circ Res** 84: 551–561, 1999. doi:[10.1161/01.res.84.5.551](https://doi.org/10.1161/01.res.84.5.551).
139. Ordög B, Brutyó E, Puskás LG, Papp JG, Varró A, Szabad J, Boldogkoi Z. Gene expression profiling of human cardiac potassium and sodium channels. **Int J Cardiol** 111: 386–393, 2006. doi:[10.1016/j.ijcard.2005.07.063](https://doi.org/10.1016/j.ijcard.2005.07.063).
140. Virág L, Jost N, Papp R, Koncz I, Kristóf A, Kohajda Z, Harmati G, Carbonell-Pascual B, Ferrero JM Jr, Papp JG, Nanási PP, Varró A. Analysis of the contribution of I_{to} to repolarization in canine ventricular myocardium. **Br J Pharmacol** 164: 93–105, 2011. doi:[10.1111/j.1476-5381.2011.01331.x](https://doi.org/10.1111/j.1476-5381.2011.01331.x).
141. Han W, Wang Z, Nattel S. A comparison of transient outward currents in canine cardiac Purkinje cells and ventricular myocytes. **Am J Physiol Heart Circ Physiol** 279: H466–H474, 2000. doi:[10.1152/ajpheart.2000.279.2.H466](https://doi.org/10.1152/ajpheart.2000.279.2.H466).
142. Surawicz B. Role of potassium channels in cycle length dependent regulation of action potential duration in mammalian cardiac Purkinje and ventricular muscle fibres. **Cardiovasc Res** 26: 1021–1029, 1992. doi:[10.1093/cvr/26.11.1021](https://doi.org/10.1093/cvr/26.11.1021).
143. Chiamvimonvat N, Chen-Izu Y, Clancy CE, Deschenes I, Dobrev D, Heijman J, Izu L, Qu Z, Ripplinger CM, Vandenberg JI, Weiss JN, Koren G, Banyasz T, Grandi E, Sanguinetti MC, Bers DM, Nerbonne JM. Potassium currents in the heart: functional roles in repolarization, arrhythmia and therapeutics. **J Physiol** 595: 2229–2252, 2017. doi:[10.1113/JP272883](https://doi.org/10.1113/JP272883).
144. Varró A, Lathrop DA, Hester SB, Nanási PP, Papp JG. Ionic currents and action potentials in rabbit, rat, and guinea pig ventricular myocytes. **Basic Res Cardiol** 88: 93–102, 1993. doi:[10.1007/BF00798257](https://doi.org/10.1007/BF00798257).
145. Zicha S, Moss I, Allen B, Varro A, Papp J, Dumaine R, Antzelevitch C, Nattel S. Molecular basis of species-specific expression of repolarizing K⁺ currents in the heart. **Am J Physiol Heart Circ Physiol** 285: H1641–H1649, 2003. doi:[10.1152/ajpheart.00346.2003](https://doi.org/10.1152/ajpheart.00346.2003).
146. Thomas SP, Bircher-Lehmann L, Thomas SA, Zhuang J, Saffitz JE, Kléber AG. Synthetic strands of neonatal mouse cardiac myocytes: structural and electrophysiological properties. **Circ Res** 87: 467–473, 2000. doi:[10.1161/01.RES.87.6.467](https://doi.org/10.1161/01.RES.87.6.467).
147. Wang L, Duff HJ. Developmental changes in transient outward current in mouse ventricle. **Circ Res** 81: 120–127, 1997. doi:[10.1161/01.RES.81.1.120](https://doi.org/10.1161/01.RES.81.1.120).
148. Turnow K, Metzner K, Cotella D, Morales MJ, Schaefer M, Christ T, Ravens U, Wettwer E, Kammerer S. Interaction of DPP10a with Kv4.3 channel complex results in a sustained current component of human transient outward current I_{to}. **Basic Res Cardiol** 110: 5, 2015. doi:[10.1007/s00395-014-0457-2](https://doi.org/10.1007/s00395-014-0457-2).
149. Wilde AA, Bezzina CR. Genetics of cardiac arrhythmias. **Heart** 91: 1352–1358, 2005. doi:[10.1136/hrt.2004.046334](https://doi.org/10.1136/hrt.2004.046334).
150. Di Diego JM, Cordeiro JM, Goodrow RJ, Fish JM, Zygmunt AC, Pérez GJ, Scornik FS, Antzelevitch C. Ionic and cellular basis for the predominance of the Brugada syndrome phenotype in males.

- Circulation** 106: 2004–2011, 2002. doi:[10.1161/01.CIR.0000032002.22105.7A](https://doi.org/10.1161/01.CIR.0000032002.22105.7A).
151. Gaborit N, Varro A, Le Bouter S, Szuts V, Escande D, Nattel S, Demolombe S. Gender-related differences in ion-channel and transporter subunit expression in non-diseased human hearts. **J Mol Cell Cardiol** 49: 639–646, 2010. doi:[10.1016/j.yjmcc.2010.06.005](https://doi.org/10.1016/j.yjmcc.2010.06.005).
152. Wang Z, Fermini B, Nattel S. Effects of flecainide, quinidine, and 4-aminopyridine on transient outward and ultrarapid delayed rectifier currents in human atrial myocytes. **J Pharmacol Exp Ther** 272: 184–196, 1995.
153. Diochot S, Drici MD, Moinier D, Fink M, Lazdunski M. Effects of phrixotoxins on the Kv4 family of potassium channels and implications for the role of Ito1 in cardiac electrogenesis. **Br J Pharmacol** 126: 251–263, 1999. doi:[10.1038/sj.bjp.0702283](https://doi.org/10.1038/sj.bjp.0702283).
154. Christ T, Wettwer E, Voigt N, Hála O, Radicke S, Matschke K, Varro A, Dobrev D, Ravens U. Pathology-specific effects of the IKur/Ito/IK, ACh blocker AVE0118 on ion channels in human chronic atrial fibrillation. **Br J Pharmacol** 154: 1619–1630, 2008. doi:[10.1038/bjp.2008.209](https://doi.org/10.1038/bjp.2008.209).
155. Calloe K, Nof E, Jespersen T, Di Diego JM, Chlus N, Olesen SP, Antzelevitch C, Cordeiro JM. Comparison of the effects of a transient outward potassium channel activator on currents recorded from atrial and ventricular cardiomyocytes. **J Cardiovasc Electrophysiol** 22: 1057–1066, 2011. doi:[10.1111/j.1540-8167.2011.02053.x](https://doi.org/10.1111/j.1540-8167.2011.02053.x).
156. Beuckelmann DJ, Näbauer M, Erdmann E. Alterations of K⁺ currents in isolated human ventricular myocytes from patients with terminal heart failure. **Circ Res** 73: 379–385, 1993. doi:[10.1161/01.RES.73.2.379](https://doi.org/10.1161/01.RES.73.2.379).
157. Han W, Chartier D, Li D, Nattel S. Ionic remodeling of cardiac Purkinje cells by congestive heart failure. **Circulation** 104: 2095–2100, 2001. doi:[10.1161/hc4201.097134](https://doi.org/10.1161/hc4201.097134).
158. Han W, Zhang L, Schram G, Nattel S. Properties of potassium currents in Purkinje cells of failing human hearts. **Am J Physiol Heart Circ Physiol** 283: H2495–H2503, 2002. doi:[10.1152/ajpheart.00389.2002](https://doi.org/10.1152/ajpheart.00389.2002).
159. Zicha S, Xiao L, Stafford S, Cha TJ, Han W, Varro A, Nattel S. Transmural expression of transient outward potassium current subunits in normal and failing canine and human hearts. **J Physiol** 561: 735–748, 2004. doi:[10.1113/jphysiol.2004.075861](https://doi.org/10.1113/jphysiol.2004.075861).
160. Coppini R, Ferrantini C, Yao L, Fan P, Del Lungo M, Stillitano F, Sartiani L, Tosi B, Suffredini S, Tesi C, Yacoub M, Olivotto I, Belardinelli L, Poggesi C, Cerbai E, Mugelli A. Late sodium current inhibition reverses electromechanical dysfunction in human hypertrophic cardiomyopathy. **Circulation** 127: 575–584, 2013. doi:[10.1161/CIRCULATIONAHA.112.134932](https://doi.org/10.1161/CIRCULATIONAHA.112.134932).
161. Keller KM, Howlett SE. Sex differences in the biology and pathology of the aging heart. **Can J Cardiol** 32: 1065–1073, 2016. doi:[10.1016/j.cjca.2016.03.017](https://doi.org/10.1016/j.cjca.2016.03.017).
162. Regitz-Zagrosek V, Kararigas G. Mechanistic pathways of sex differences in cardiovascular disease. **Physiol Rev** 97: 1–37, 2017. doi:[10.1152/physrev.00021.2015](https://doi.org/10.1152/physrev.00021.2015).
163. Cordeiro JM, Calloe K, Aschar-Sobbi R, Kim KH, Korogyi A, Occhipinti D, Backx PH, Panama BK. Physiological roles of the transient outward current Ito in normal and diseased hearts. **Front Biosci (Schol Ed)** 8: 143–159, 2016. doi:[10.2741/s454](https://doi.org/10.2741/s454).
164. Long VP 3rd, Bonilla IM, Vargas-Pinto P, Nishijima Y, Sridhar A, Li C, Mowrey K, Wright P, Velayutham M, Kumar S, Lee NY, Zweier JL, Mohler PJ, Györke S, Carnes CA. Heart failure duration progressively modulates the arrhythmia substrate through structural and electrical remodeling. **Life Sci** 123: 61–71, 2015. doi:[10.1016/j.lfs.2014.12.024](https://doi.org/10.1016/j.lfs.2014.12.024).
165. Näbauer M, Beuckelmann DJ, Erdmann E. Characteristics of transient outward current in human ventricular myocytes from patients with terminal heart failure. **Circ Res** 73: 386–394, 1993. doi:[10.1161/01.res.73.2.386](https://doi.org/10.1161/01.res.73.2.386).
166. Sah R, Ramirez RJ, Backx PH. Modulation of Ca²⁺ release in cardiac myocytes by changes in repolarization rate: role of phase-1 action potential repolarization in excitation-contraction coupling. **Circ Res** 90: 165–173, 2002. doi:[10.1161/hh0202.103315](https://doi.org/10.1161/hh0202.103315).
167. van der Heyden MA, Wijnhoven TJ, Opthof T. Molecular aspects of adrenergic modulation of the transient outward current. **Cardiovasc Res** 71: 430–442, 2006. doi:[10.1016/j.cardiores.2006.04.012](https://doi.org/10.1016/j.cardiores.2006.04.012).
168. Alonso H, Fernández-Ruocco J, Gallego M, Malagueta-Vieira LL, Rodríguez-de-Yurre A, Medei E, Casis O. Thyroid stimulating hormone directly modulates cardiac electrical activity. **J Mol Cell Cardiol** 89: 280–286, 2015. doi:[10.1016/j.yjmcc.2015.10.019](https://doi.org/10.1016/j.yjmcc.2015.10.019).
169. Nishiyama A, Kambe F, Kamiya K, Seo H, Toyama J. Effects of thyroid status on expression of voltage-gated potassium channels in rat left ventricle. **Cardiovasc Res** 40: 343–351, 1998. doi:[10.1016/S0008-6363\(98\)00135-7](https://doi.org/10.1016/S0008-6363(98)00135-7).
170. Reuter H. The dependence of slow inward current in Purkinje fibres on the extracellular calcium-concentration. **J Physiol** 192: 479–492, 1967. doi:[10.1113/jphysiol.1967.sp008310](https://doi.org/10.1113/jphysiol.1967.sp008310).
171. Hirano Y, Fozzard HA, January CT. Characteristics of L- and T-type Ca²⁺ currents in canine cardiac Purkinje cells. **Am J Physiol Heart Circ Physiol** 256: H1478–H1492, 1989. doi:[10.1152/ajpheart.1989.256.5.H1478](https://doi.org/10.1152/ajpheart.1989.256.5.H1478).
172. Mitra R, Morad M. Two types of calcium channels in guinea pig ventricular myocytes. **Proc Natl Acad Sci USA** 83: 5340–5344, 1986. doi:[10.1073/pnas.83.14.5340](https://doi.org/10.1073/pnas.83.14.5340).
173. Hofmann F, Flockerzi V, Kahl S, Wegener JW. L-type CaV1.2 calcium channels: from in vitro findings to in vivo function. **Physiol Rev** 94: 303–326, 2014. doi:[10.1152/physrev.00016.2013](https://doi.org/10.1152/physrev.00016.2013).
174. Catterall WA. Structure and function of voltage-sensitive ion channels. **Science** 242: 50–61, 1988. doi:[10.1126/science.2459775](https://doi.org/10.1126/science.2459775).
175. Buraei Z, Yang J. The β subunit of voltage-gated Ca²⁺ channels. **Physiol Rev** 90: 1461–1506, 2010. doi:[10.1152/physrev.00057.2009](https://doi.org/10.1152/physrev.00057.2009).
176. Davies A, Hendrich J, Van Minh AT, Wratten J, Douglas L, Dolphin AC. Functional biology of the $\alpha(2)\delta$ subunits of voltage-gated calcium channels. **Trends Pharmacol Sci** 28: 220–228, 2007. doi:[10.1016/j.tips.2007.03.005](https://doi.org/10.1016/j.tips.2007.03.005).
177. Kang MG, Campbell KP. Gamma subunit of voltage-activated calcium channels. **J Biol Chem** 278: 21315–21318, 2003. doi:[10.1074/jbc.R300004200](https://doi.org/10.1074/jbc.R300004200).
178. Bers DM. Calcium cycling and signaling in cardiac myocytes. **Annu Rev Physiol** 70: 23–49, 2008. doi:[10.1146/annurev.physiol.70.113006.100455](https://doi.org/10.1146/annurev.physiol.70.113006.100455).
179. Dibb KM, Eisner DA, Trafford AW. Regulation of systolic [Ca²⁺]_i and cellular Ca²⁺ flux balance in rat ventricular myocytes by SR Ca²⁺, L-type Ca²⁺ current and diastolic [Ca²⁺]_i. **J Physiol** 585: 579–592, 2007. doi:[10.1113/jphysiol.2007.141473](https://doi.org/10.1113/jphysiol.2007.141473).

180. Mesirca P, Torrente AG, Mangoni ME. Functional role of voltage gated Ca^{2+} channels in heart automaticity. **Front Physiol** 6: 19, 2015. doi:[10.3389/fphys.2015.00019](https://doi.org/10.3389/fphys.2015.00019).
181. Adachi-Akahane S, Cleemann L, Morad M. Cross-signaling between L-type Ca^{2+} channels and ryanodine receptors in rat ventricular myocytes. **J Gen Physiol** 108: 435–454, 1996. doi:[10.1085/jgp.108.5.435](https://doi.org/10.1085/jgp.108.5.435).
182. Bechem M, Pott L. Evidence for Ca-mediated inactivation of I_{Ca} in dialysed guinea-pig atrial cardioballs. **Basic Res Cardiol** 80: 101–105, 1985. doi:[10.1007/978-3-662-11041-6_20](https://doi.org/10.1007/978-3-662-11041-6_20).
183. Kass RS, Sanguinetti MC. Inactivation of calcium channel current in the calf cardiac Purkinje fiber. Evidence for voltage- and calcium-mediated mechanisms. **J Gen Physiol** 84: 705–726, 1984. doi:[10.1085/jgp.84.5.705](https://doi.org/10.1085/jgp.84.5.705).
184. Sham JS. Ca^{2+} release-induced inactivation of Ca^{2+} current in rat ventricular myocytes: evidence for local Ca^{2+} signalling. **J Physiol** 500: 285–295, 1997. doi:[10.1113/jphysiol.1997.sp022020](https://doi.org/10.1113/jphysiol.1997.sp022020).
185. Tseng GN, Boyden PA. Multiple types of Ca^{2+} currents in single canine Purkinje cells. **Circ Res** 65: 1735–1750, 1989. doi:[10.1161/01.res.65.6.1735](https://doi.org/10.1161/01.res.65.6.1735).
186. Ochi R, Trautwein W. The dependence of cardiac contraction on depolarization and slow inward current. **Pflugers Arch** 323: 187–203, 1971. doi:[10.1007/BF00586383](https://doi.org/10.1007/BF00586383).
187. Isenberg G. Ca entry and contraction as studied in isolated bovine ventricular myocytes. **Z Naturforsch C Biosci** 37: 502–512, 1982. doi:[10.1515/znc-1982-5-623](https://doi.org/10.1515/znc-1982-5-623).
188. Zühlke RD, Pitt GS, Deisseroth K, Tsien RW, Reuter H. Calmodulin supports both inactivation and facilitation of L-type calcium channels. **Nature** 399: 159–162, 1999. doi:[10.1038/20200](https://doi.org/10.1038/20200).
189. Anderson ME, Braun AP, Schulman H, Premack BA. Multifunctional Ca^{2+} /calmodulin-dependent protein kinase mediates Ca^{2+} -induced enhancement of the L-type Ca^{2+} current in rabbit ventricular myocytes. **Circ Res** 75: 854–861, 1994. doi:[10.1161/01.RES.75.5.854](https://doi.org/10.1161/01.RES.75.5.854).
190. Yuan W, Bers DM. Ca-dependent facilitation of cardiac Ca current is due to Ca-calmodulin-dependent protein kinase. **Am J Physiol Heart Circ Physiol** 267: H982–H993, 1994. doi:[10.1152/ajpheart.1994.267.3.H982](https://doi.org/10.1152/ajpheart.1994.267.3.H982).
191. Bers DM, Morotti S. Ca^{2+} current facilitation is CaMKII-dependent and has arrhythmogenic consequences. **Front Pharmacol** 5: 144, 2014. doi:[10.3389/fphar.2014.00144](https://doi.org/10.3389/fphar.2014.00144).
192. Liu G, Papa A, Katchman AN, Zakharov SI, Roybal D, Hennessey JA, Kushner J, Yang L, Chen BX, Kushnir A, Dangas K, Gygi SP, Pitt GS, Colecraft HM, Ben-Johny M, Kalocsay M, Marx SO. Mechanism of adrenergic CaV1.2 stimulation revealed by proximity proteomics. **Nature** 577: 695–700, 2020. doi:[10.1038/s41586-020-1947-z](https://doi.org/10.1038/s41586-020-1947-z).
193. Rolf S, Haverkamp W, Borggrefe M, Musshoff U, Eckardt L, Mergenthaler J, Snyders DJ, Pongs O, Speckmann EJ, Breithardt G, Madeja M. Effects of antiarrhythmic drugs on cloned cardiac voltage-gated potassium channels expressed in *Xenopus* oocytes. **Naunyn Schmiedeberg Arch Pharmacol** 362: 22–31, 2000. doi:[10.1007/s002100000257](https://doi.org/10.1007/s002100000257).
194. Szentandrássy N, Nagy D, Ruzsnavszky F, Harmati G, Bányász T, Magyar J, Szentmiklósi AJ, Nánási PP. Powerful technique to test selectivity of agents acting on cardiac ion channels: the action potential voltage-clamp. **Curr Med Chem** 18: 3737–3756, 2011. doi:[10.2174/092986711796642418](https://doi.org/10.2174/092986711796642418).
195. Zhang S, Zhou Z, Gong Q, Makielski JC, January CT. Mechanism of block and identification of the verapamil binding domain to HERG potassium channels. **Circ Res** 84: 989–998, 1999. doi:[10.1161/01.res.84.9.989](https://doi.org/10.1161/01.res.84.9.989).
196. Koidl B, Miyawaki N, Tritthart HA. A novel benzothiazine Ca^{2+} channel antagonist, semotiadil, inhibits cardiac L-type Ca^{2+} currents. **Eur J Pharmacol** 322: 243–247, 1997. doi:[10.1016/S0014-2999\(96\)00995-8](https://doi.org/10.1016/S0014-2999(96)00995-8).
197. Hume JR. Comparative interactions of organic Ca^{++} channel antagonists with myocardial Ca^{++} and K^{+} channels. **J Pharmacol Exp Ther** 234: 134–140, 1985.
198. Morad M, Goldman YE, Trentham DR. Rapid photochemical inactivation of Ca^{2+} -antagonists shows that Ca^{2+} entry directly activates contraction in frog heart. **Nature** 304: 635–638, 1983. doi:[10.1038/304635a0](https://doi.org/10.1038/304635a0).
199. Artigas P, Ferreira G, Reyes N, Brum G, Pizarro G. Effects of the enantiomers of BayK 8644 on the charge movement of L-type Ca channels in guinea-pig ventricular myocytes. **J Membr Biol** 193: 215–227, 2003. doi:[10.1007/s00232-003-2020-1](https://doi.org/10.1007/s00232-003-2020-1).
200. Leprán I, Baczkó I, Varró A, Papp JG. ATP-sensitive potassium channel modulators: both pinacidil and glibenclamide produce antiarrhythmic activity during acute myocardial infarction in conscious rats. **J Pharmacol Exp Ther** 277: 1215–1220, 1996.
201. Martinez ME, Walton RD, Bayer JD, Haissaguerre M, Vigmond EJ, Hocini M, Bernus O. Role of the Purkinje-muscle junction on the ventricular repolarization heterogeneity in the healthy and ischemic ovine ventricular myocardium. **Front Physiol** 9: 718, 2018. doi:[10.3389/fphys.2018.00718](https://doi.org/10.3389/fphys.2018.00718).
202. Hondeghem LM, Carlsson L, Duker G. Instability and triangulation of the action potential predict serious proarrhythmia, but action potential duration prolongation is antiarrhythmic. **Circulation** 103: 2004–2013, 2001. doi:[10.1161/01.CIR.103.15.2004](https://doi.org/10.1161/01.CIR.103.15.2004).
203. Rigg L, Terrar DA. Possible role of calcium release from the sarcoplasmic reticulum in pacemaking in guinea-pig sino-atrial node. **Exp Physiol** 81: 877–880, 1996. doi:[10.1113/expphysiol.1996.sp003983](https://doi.org/10.1113/expphysiol.1996.sp003983).
204. Suenari K, Chen YC, Kao YH, Cheng CC, Lin YK, Chen YJ, Chen SA. Discrepant electrophysiological characteristics and calcium homeostasis of left atrial anterior and posterior myocytes. **Basic Res Cardiol** 106: 65–74, 2011. doi:[10.1007/s00395-010-0132-1](https://doi.org/10.1007/s00395-010-0132-1).
205. Liang B, Nissen JD, Laursen M, Wang X, Skibsbjerg L, Hearing MC, Andersen MN, Rasmussen HB, Wickman K, Grunnet M, Olesen SP, Jespersen T. G-protein-coupled inward rectifier potassium current contributes to ventricular repolarization. **Cardiovasc Res** 101: 175–184, 2014. doi:[10.1093/cvr/cvt240](https://doi.org/10.1093/cvr/cvt240).
206. Barrett CF, Tsien RW. The Timothy syndrome mutation differentially affects voltage- and calcium-dependent inactivation of CaV1.2 L-type calcium channels. **Proc Natl Acad Sci USA** 105: 2157–2162, 2008. doi:[10.1073/pnas.0710501105](https://doi.org/10.1073/pnas.0710501105).
207. Splawski I, Timothy KW, Sharpe LM, Decher N, Kumar P, Bloise R, Napolitano C, Schwartz PJ, Joseph RM, Condouris K, Tager-Flusberg H, Priori SG, Sanguinetti MC, Keating MT. $\text{Ca}_v1.2$ calcium channel dysfunction causes a multisystem disorder including arrhythmia and autism. **Cell** 119: 19–31, 2004. doi:[10.1016/j.cell.2004.09.011](https://doi.org/10.1016/j.cell.2004.09.011).
208. Thiel WH, Chen B, Hund TJ, Koval OM, Purohit A, Song LS, Mohler PJ, Anderson ME. Proarrhythmic defects in Timothy syndrome require calmodulin kinase II. **Circulation** 118: 2225–2234, 2008. doi:[10.1161/CIRCULATIONAHA.108.788067](https://doi.org/10.1161/CIRCULATIONAHA.108.788067).

209. Navedo MF, Cheng EP, Yuan C, Votaw S, Molkentin JD, Scott JD, Santana LF. Increased coupled gating of L-type Ca^{2+} channels during hypertension and Timothy syndrome. **Circ Res** 106: 748–756, 2010. doi:10.1161/CIRCRESAHA.109.213363.
210. Napolitano C, Splawski I, Timothy KW, Bloise R, Priori SG. Timothy syndrome. In: **GeneReviews**, edited by Adam MP, Ardinger HH, Pagon RA, Wallace SE, Bean LJ, Stephens K, Amemiya A. Seattle, WA: Univ. of Washington, 1993.
211. Zhou Z, Lipsius SL. T-type calcium current in latent pacemaker cells isolated from cat right atrium. **J Mol Cell Cardiol** 26: 1211–1219, 1994. doi:10.1006/jmcc.1994.1139.
212. Bohn G, Moosmang S, Conrad H, Ludwig A, Hofmann F, Klugbauer N. Expression of T- and L-type calcium channel mRNA in murine sinoatrial node. **FEBS Lett** 481: 73–76, 2000. doi:10.1016/S0014-5793(00)01979-7.
213. Massie BM. Mibefradil, a T-type channel-selective calcium antagonist: clinical trials in chronic stable angina pectoris. **Am J Hypertens** 11: 95S–102S, 1998. doi:10.1016/s0895-7061(98)00006-5.
214. Sanguinetti MC, Jurkiewicz NK. Two components of cardiac delayed rectifier K^{+} current. Differential sensitivity to block by class III antiarrhythmic agents. **J Gen Physiol** 96: 195–215, 1990. doi:10.1085/jgp.96.1.195.
215. Nerbonne JM. Molecular basis of functional myocardial potassium channel diversity. **Card Electrophysiol Clin** 8: 257–273, 2016. doi:10.1016/j.ccep.2016.01.001.
216. Vandenberg JI, Perry MD, Perrin MJ, Mann SA, Ke Y, Hill AP. hERG K^{+} channels: structure, function, and clinical significance. **Physiol Rev** 92: 1393–1478, 2012. doi:10.1152/physrev.00036.2011.
217. Nerbonne JM, Kass RS. Molecular physiology of cardiac repolarization. **Physiol Rev** 85: 1205–1253, 2005. doi:10.1152/physrev.00002.2005.
218. Abbott GW, Sesti F, Splawski I, Buck ME, Lehmann MH, Timothy KW, Keating MT, Goldstein SA. MiRP1 forms IKr potassium channels with HERG and is associated with cardiac arrhythmia. **Cell** 97: 175–187, 1999. doi:10.1016/s0092-8674(00)80728-x.
219. Jones DK, Liu F, Vaidyanathan R, Eckhardt LL, Trudeau MC, Robertson GA. hERG1b is critical for human cardiac repolarization. **Proc Natl Acad Sci USA** 111: 18073–18077, 2014. doi:10.1073/pnas.1414945111.
220. Trudeau MC, Leung LM, Roti ER, Robertson GA. hERG1a N-terminal eag domain-containing polypeptides regulate homomeric hERG1b and heteromeric hERG1a/hERG1b channels: a possible mechanism for long QT syndrome. **J Gen Physiol** 138: 581–592, 2011. doi:10.1085/jgp.20110683.
221. Jost N, Virág L, Bitay M, Takács J, Lengyel C, Biliczki P, Nagy Z, Boga'ts G, Lathrop DA, Papp JG, Varró A. Restricting excessive cardiac action potential and QT prolongation: a vital role for IKs in human ventricular muscle. **Circulation** 112: 1392–1399, 2005. doi:10.1161/CIRCULATIONAHA.105.550111.
222. Jost N, Virág L, Opincariu M, Szécsi J, Varró A, Papp JG. Delayed rectifier potassium current in undiseased human ventricular myocytes. **Cardiovasc Res** 40: 508–515, 1998. doi:10.1016/s0008-6363(98)00204-1.
223. Smith PL, Baukowitz T, Yellen G. The inward rectification mechanism of the HERG cardiac potassium channel. **Nature** 379: 833–836, 1996. doi:10.1038/379833a0.
224. Spector PS, Curran ME, Zou A, Keating MT, Sanguinetti MC. Fast inactivation causes rectification of the IKr channel. **J Gen Physiol** 107: 611–619, 1996. doi:10.1085/jgp.107.5.611.
225. Yang T, Snyders DJ, Roden DM. Rapid inactivation determines the rectification and $[\text{K}^{+}]_o$ dependence of the rapid component of the delayed rectifier K^{+} current in cardiac cells. **Circ Res** 80: 782–789, 1997. doi:10.1161/01.res.80.6.782.
226. Clark RB, Mangoni ME, Lueger A, Couette B, Nargeot J, Giles WR. A rapidly activating delayed rectifier K^{+} current regulates pacemaker activity in adult mouse sinoatrial node cells. **Am J Physiol Heart Circ Physiol** 286: H1757–H1766, 2004. doi:10.1152/ajpheart.00753.2003.
227. Jurkiewicz NK, Sanguinetti MC. Rate-dependent prolongation of cardiac action potentials by a methanesulfonanilide class III antiarrhythmic agent. Specific block of rapidly activating delayed rectifier K^{+} current by dofetilide. **Circ Res** 72: 75–83, 1993. doi:10.1161/01.res.72.1.75.
228. Varró A, Baláti B, Jost N, Takács J, Virág L, Lathrop DA, Csaba L, Tálosi L, Papp JG. The role of the delayed rectifier component IKs in dog ventricular muscle and Purkinje fibre repolarization. **J Physiol** 523: 67–81, 2000. doi:10.1111/j.1469-7793.2000.00067.x.
229. Magyar J, Jost N, Körtvély A, Bányász T, Virág L, Szigligeti P, Varró A, Opincariu M, Szécsi J, Papp JG, Nánási PP. Effects of endothelin-1 on calcium and potassium currents in undiseased human ventricular myocytes. **Pflugers Arch** 441: 144–149, 2000. doi:10.1007/s004240000400.
230. Karle CA, Zitron E, Zhang W, Kathöfer S, Schoels W, Kiehn J. Rapid component IK_r of the guinea-pig cardiac delayed rectifier K^{+} current is inhibited by beta₂-adrenoreceptor activation, via cAMP/protein kinase A-dependent pathways. **Cardiovasc Res** 53: 355–362, 2002. doi:10.1016/s0008-6363(01)00509-0.
231. Wang S, Xu D, Wu TT, Guo Y, Chen YH, Zou JG. Beta1-adrenergic regulation of rapid component of delayed rectifier K^{+} currents in guinea-pig cardiac myocytes. **Mol Med Rep** 9: 1923–1928, 2014. doi:10.3892/mmr.2014.2035.
232. Wang S, Xu DJ, Cai JB, Huang YZ, Zou JG, Cao KJ. Rapid component IK_r of cardiac delayed rectifier potassium currents in guinea-pig is inhibited by alpha₁-adrenoreceptor activation via protein kinase A and protein kinase C-dependent pathways. **Eur J Pharmacol** 608: 1–6, 2009. doi:10.1016/j.ejphar.2009.02.017.
233. Christé G. Effects of low $[\text{K}^{+}]_o$ on the electrical activity of human cardiac ventricular and Purkinje cells. **Cardiovasc Res** 17: 243–250, 1983. doi:10.1093/cvr/17.4.243.
234. Firek L, Giles WR. Outward currents underlying repolarization in human atrial myocytes. **Cardiovasc Res** 30: 31–38, 1995.
235. Sanguinetti MC, Jurkiewicz NK. Role of external Ca^{2+} and K^{+} in gating of cardiac delayed rectifier K^{+} currents. **Pflugers Arch** 420: 180–186, 1992. doi:10.1007/BF00374988.
236. Yang T, Roden DM. Extracellular potassium modulation of drug block of IKr. Implications for torsade de pointes and reverse use-dependence. **Circulation** 93: 407–411, 1996. doi:10.1161/01.cir.93.3.407.
237. Bérubé J, Chahine M, Daleau P. Modulation of HERG potassium channel properties by external pH. **Pflugers Arch** 438: 419–422, 1999. doi:10.1007/s004240050930.
238. Vereecke J, Carmeliet E. The effect of external pH on the delayed rectifying K^{+} current in cardiac ventricular myocytes. **Pflugers Arch** 439: 739–751, 2000. doi:10.1007/s004249900243.

239. Du CY, El Harchi A, McPate MJ, Orchard CH, Hancox JC. Enhanced inhibitory effect of acidosis on hERG potassium channels that incorporate the hERG1b isoform. **Biochem Biophys Res Commun** 405: 222–227, 2011. doi:[10.1016/j.bbrc.2011.01.014](https://doi.org/10.1016/j.bbrc.2011.01.014).
240. Jiang M, Cabo C, Yao J, Boyden PA, Tseng G. Delayed rectifier K currents have reduced amplitudes and altered kinetics in myocytes from infarcted canine ventricle. **Cardiovasc Res** 48: 34–43, 2000. doi:[10.1016/s0008-6363\(00\)00159-0](https://doi.org/10.1016/s0008-6363(00)00159-0).
241. Janse MJ. Electrophysiological changes in heart failure and their relationship to arrhythmogenesis. **Cardiovasc Res** 61: 208–217, 2004. doi:[10.1016/j.cardiores.2003.11.018](https://doi.org/10.1016/j.cardiores.2003.11.018).
242. Froese A, Breher SS, Waldeyer C, Schindler RF, Nikolaev VO, Rinné S, Wischmeyer E, Schlueter J, Becher J, Simrick S, Vauti F, Kuhtz J, Meister P, Kreissl S, Torlopp A, Liebig SK, Laakmann S, Müller TD, Neumann J, Stieber J, Ludwig A, Maier SK, Decher N, Arnold HH, Kirchhof P, Fabritz L, Brand T. Popeye domain containing proteins are essential for stress-mediated modulation of cardiac pacemaking in mice. **J Clin Invest** 122: 1119–1130, 2012. doi:[10.1172/JCI59410](https://doi.org/10.1172/JCI59410).
243. Richard P, Charron P, Carrier L, Ledeuil C, Cheav T, Pichereau C, Benaiche A, Isnard R, Dubourg O, Burban M, Gueffet JP, Millaire A, Desnos M, Schwartz K, Hainque B, Komajda M; EUROGENE Heart Failure Project. Hypertrophic cardiomyopathy: distribution of disease genes, spectrum of mutations, and implications for a molecular diagnosis strategy. **Circulation** 107: 2227–2232, 2003. doi:[10.1161/01.CIR.0000066323.15244.54](https://doi.org/10.1161/01.CIR.0000066323.15244.54).
244. Campuzano O, Sarquella-Brugada G, Cesar S, Arbelo E, Brugada J, Brugada R. Recent advances in short QT syndrome. **Front Cardiovasc Med** 5: 149, 2018. doi:[10.3389/fcvm.2018.00149](https://doi.org/10.3389/fcvm.2018.00149).
245. Khera S, Jacobson JT. Short QT syndrome in current clinical practice. **Cardiol Rev** 24: 190–193, 2016. doi:[10.1097/CRD.0000000000000091](https://doi.org/10.1097/CRD.0000000000000091).
246. Schwartz PJ, Ackerman MJ, Antzelevitch C, Bezzina CR, Borggrefe M, Cuneo BF, Wilde AA. Inherited cardiac arrhythmias. **Nat Rev Dis Primers** 6: 58, 2020. doi:[10.1038/s41572-020-0188-7](https://doi.org/10.1038/s41572-020-0188-7).
247. Barhanin J, Lesage F, Guillemare E, Fink M, Lazdunski M, Romey G. K_vLQT1 and IsK (mink) proteins associate to form the I_{Ks} cardiac potassium current. **Nature** 384: 78–80, 1996. doi:[10.1038/384078a0](https://doi.org/10.1038/384078a0).
248. Sanguinetti MC, Curran ME, Zou A, Shen J, Spector PS, Atkinson DL, Keating MT. Coassembly of K_vLQT1 and mink (IsK) proteins to form cardiac I_{Ks} potassium channel. **Nature** 384: 80–83, 1996. doi:[10.1038/384080a0](https://doi.org/10.1038/384080a0).
249. Gögelein H, Brüggemann A, Gerlach U, Brendel J, Busch AE. Inhibition of I_{Ks} channels by HMR 1556. **Naunyn Schmiedeberg Arch Pharmacol** 362: 480–488, 2000. doi:[10.1007/s00210000284](https://doi.org/10.1007/s00210000284).
250. Lengyel C, Varró A, Tábori K, Papp JG, Baczkó I. Combined pharmacological block of I_{Kr} and I_{Ks} increases short-term QT interval variability and provokes torsades de pointes. **Br J Pharmacol** 151: 941–951, 2007. doi:[10.1038/sj.bjp.0707297](https://doi.org/10.1038/sj.bjp.0707297).
251. Salata JJ, Jurkiewicz NK, Jow B, Folander K, Guinasso PJ Jr, Raynor B, Swanson R, Fermini B. I_{K1} of rabbit ventricle is composed of two currents: evidence for I_{Ks} . **Am J Physiol Heart Circ Physiol** 271: H2477–H2489, 1996. doi:[10.1152/ajpheart.1996.271.6.H2477](https://doi.org/10.1152/ajpheart.1996.271.6.H2477).
252. Li GR, Feng J, Yue L, Carrier M, Nattel S. Evidence for two components of delayed rectifier K^+ current in human ventricular myocytes. **Circ Res** 78: 689–696, 1996. doi:[10.1161/01.RES.78.4.689](https://doi.org/10.1161/01.RES.78.4.689).
253. Virág L, Iost N, Opincariu M, Szolnoky J, Szécsi J, Bogáts G, Szenohradszky P, Varró A, Papp JG. The slow component of the delayed rectifier potassium current in undiseased human ventricular myocytes. **Cardiovasc Res** 49: 790–797, 2001. doi:[10.1016/s0008-6363\(00\)00306-0](https://doi.org/10.1016/s0008-6363(00)00306-0).
254. Jost N, Papp JG, Varró A. Slow delayed rectifier potassium current (I_{Ks}) and the repolarization reserve. **Ann Noninvasive Electrocardiol** 12: 64–78, 2007. doi:[10.1111/j.1542-474X.2007.00140.x](https://doi.org/10.1111/j.1542-474X.2007.00140.x).
255. Volders PG, Stengl M, van Opstal JM, Gerlach U, Spätjens RL, Beekman JD, Sipido KR, Vos MA. Probing the contribution of I_{Ks} to canine ventricular repolarization: key role for beta-adrenergic receptor stimulation. **Circulation** 107: 2753–2760, 2003. doi:[10.1161/01.CIR.0000068344.54010.B3](https://doi.org/10.1161/01.CIR.0000068344.54010.B3).
256. Han W, Wang Z, Nattel S. Slow delayed rectifier current and repolarization in canine cardiac Purkinje cells. **Am J Physiol Heart Circ Physiol** 280: H1075–H1080, 2001. doi:[10.1152/ajpheart.2001.280.3.H1075](https://doi.org/10.1152/ajpheart.2001.280.3.H1075).
257. Roden DM. Long QT syndrome: reduced repolarization reserve and the genetic link. **J Intern Med** 259: 59–69, 2006. doi:[10.1111/j.1365-2796.2005.01589.x](https://doi.org/10.1111/j.1365-2796.2005.01589.x).
258. Roden DM. Taking the “idio” out of “idiopathic”: predicting torsades de pointes. **Pacing Clin Electrophysiol** 21: 1029–1034, 1998. doi:[10.1111/j.1540-8159.1998.tb00148.x](https://doi.org/10.1111/j.1540-8159.1998.tb00148.x).
259. Varkevisser R, Wijers SC, van der Heyden MA, Beekman JD, Meine M, Vos MA. Beat-to-beat variability of repolarization as a new biomarker for proarrhythmia in vivo. **Heart Rhythm** 9: 1718–1726, 2012. doi:[10.1016/j.hrthm.2012.05.016](https://doi.org/10.1016/j.hrthm.2012.05.016).
260. Varro A, Baczkó I. Cardiac ventricular repolarization reserve: a principle for understanding drug-related proarrhythmic risk. **Br J Pharmacol** 164: 14–36, 2011. doi:[10.1111/j.1476-5381.2011.01367.x](https://doi.org/10.1111/j.1476-5381.2011.01367.x).
261. Bosch RF, Schneck AC, Csillag S, Eigenberger B, Gerlach U, Brendel J, Lang HJ, Mewis C, Gögelein H, Seipel L, Kühlkamp V. Effects of the chromanol HMR 1556 on potassium currents in atrial myocytes. **Naunyn Schmiedeberg Arch Pharmacol** 367: 281–288, 2003. doi:[10.1007/s00210-002-0672-5](https://doi.org/10.1007/s00210-002-0672-5).
262. Zankov DP, Salloum FN, Jiang M, Tseng GN. Chronic in vivo angiotensin II administration differentially modulates the slow delayed rectifier channels in atrial and ventricular myocytes. **Heart Rhythm** 16: 108–116, 2019. doi:[10.1016/j.hrthm.2018.07.036](https://doi.org/10.1016/j.hrthm.2018.07.036).
263. Fülöp L, Bányász T, Szabó G, Tóth IB, Bíró T, Lőrincz I, Balogh A, Pető K, Mikó I, Nánási PP. Effects of sex hormones on ECG parameters and expression of cardiac ion channels in dogs. **Acta Physiol (Oxf)** 188: 163–171, 2006. doi:[10.1111/j.1748-1716.2006.01618.x](https://doi.org/10.1111/j.1748-1716.2006.01618.x).
264. Li Y, Chen L, Kass RS, Dessauer CW. The A-kinase anchoring protein Yotiao facilitates complex formation between adenylyl cyclase type 9 and the I_{Ks} potassium channel in heart. **J Biol Chem** 287: 29815–29824, 2012. doi:[10.1074/jbc.M112.380568](https://doi.org/10.1074/jbc.M112.380568).
265. Odening KE, Koren G. How do sex hormones modify arrhythmogenesis in long QT syndrome? Sex hormone effects on arrhythmogenic substrate and triggered activity. **Heart Rhythm** 11: 2107–2115, 2014. doi:[10.1016/j.hrthm.2014.06.023](https://doi.org/10.1016/j.hrthm.2014.06.023).
266. Lo CF, Numann R. Independent and exclusive modulation of cardiac delayed rectifying K^+ current by protein kinase C and protein kinase A. **Circ Res** 83: 995–1002, 1998. doi:[10.1161/01.res.83.10.995](https://doi.org/10.1161/01.res.83.10.995).
267. Toda H, Ding WG, Yasuda Y, Toyoda F, Ito M, Matsuura H, Horie M. Stimulatory action of protein kinase C (ϵ) isoform on the slow component of delayed rectifier K^+ current in guinea-pig atrial

- myocytes. **Br J Pharmacol** 150: 1011–1021, 2007. doi:[10.1038/sj.bjp.0707191](https://doi.org/10.1038/sj.bjp.0707191).
268. Xiao GQ, Mochly-Rosen D, Boutjdir M. PKC isozyme selective regulation of cloned human cardiac delayed slow rectifier K current. **Biochem Biophys Res Commun** 306: 1019–1025, 2003. doi:[10.1016/s0006-291x\(03\)01095-7](https://doi.org/10.1016/s0006-291x(03)01095-7).
269. Salata JJ, Jurkiewicz NK, Wang J, Evans BE, Orme HT, Sanguinetti MC. A novel benzodiazepine that activates cardiac slow delayed rectifier K⁺ currents. **Mol Pharmacol** 54: 220–230, 1998. doi:[10.1124/mol.54.1.220](https://doi.org/10.1124/mol.54.1.220).
270. Bartos DC, Morotti S, Ginsburg KS, Grandi E, Bers DM. Quantitative analysis of the Ca²⁺-dependent regulation of delayed rectifier K⁺ current IKs in rabbit ventricular myocytes. **J Physiol** 595: 2253–2268, 2017. doi:[10.1113/JP273676](https://doi.org/10.1113/JP273676).
271. Lengyel C, Virág L, Biró T, Jost N, Magyar J, Biliczki P, Kocsis E, Skoumal R, Nánási PP, Tóth M, Kecskeméti V, Papp JG, Varró A. Diabetes mellitus attenuates the repolarization reserve in mammalian heart. **Cardiovasc Res** 73: 512–520, 2007. doi:[10.1016/j.cardiores.2006.11.010](https://doi.org/10.1016/j.cardiores.2006.11.010).
272. Stengl M, Ramakers C, Donker DW, Nabar A, Rybin AV, Spätjens RL, van der Nagel T, Wodzig WK, Sipido KR, Antoons G, Moorman AF, Vos MA, Volders PG. Temporal patterns of electrical remodeling in canine ventricular hypertrophy: focus on IKs downregulation and blunted beta-adrenergic activation. **Cardiovasc Res** 72: 90–100, 2006. doi:[10.1016/j.cardiores.2006.07.015](https://doi.org/10.1016/j.cardiores.2006.07.015).
273. Bartos DC, Anderson JB, Bastiaenen R, Johnson JN, Gollob MH, Tester DJ, Burgess DE, Homfray T, Behr ER, Ackerman MJ, Guicheney P, Delisle BP. A KCNQ1 mutation causes a high penetrance for familial atrial fibrillation. **J Cardiovasc Electrophysiol** 24: 562–569, 2013. doi:[10.1111/jce.12068](https://doi.org/10.1111/jce.12068).
274. Bartos DC, Duchatelet S, Burgess DE, Klug D, Denjoy I, Peat R, Lupoglazoff JM, Fressart V, Berthet M, Ackerman MJ, January CT, Guicheney P, Delisle BP. R231C mutation in KCNQ1 causes long QT syndrome type 1 and familial atrial fibrillation. **Heart Rhythm** 8: 48–55, 2011. doi:[10.1016/j.hrthm.2010.09.010](https://doi.org/10.1016/j.hrthm.2010.09.010).
275. Chen YH, Xu SJ, Bendahhou S, Wang XL, Wang Y, Xu WY, Jin HW, Sun H, Su XY, Zhuang QN, Yang YQ, Li YB, Liu Y, Xu HJ, Li XF, Ma N, Mou CP, Chen Z, Barhanin J, Huang W. KCNQ1 gain-of-function mutation in familial atrial fibrillation. **Science** 299: 251–254, 2003. doi:[10.1126/science.1077771](https://doi.org/10.1126/science.1077771).
276. Das S, Makino S, Melman YF, Shea MA, Goyal SB, Rosenzweig A, Macrae CA, Ellinor PT. Mutation in the S3 segment of KCNQ1 results in familial lone atrial fibrillation. **Heart Rhythm** 6: 1146–1153, 2009. doi:[10.1016/j.hrthm.2009.04.015](https://doi.org/10.1016/j.hrthm.2009.04.015).
277. Hong K, Piper DR, Diaz-Valdecantos A, Brugada J, Oliva A, Burashnikov E, Santos-de-Soto J, Gueso-Montero J, Diaz-Engante E, Brugada P, Sachse F, Sanguinetti MC, Brugada R. De novo KCNQ1 mutation responsible for atrial fibrillation and short QT syndrome in utero. **Cardiovasc Res** 68: 433–440, 2005. doi:[10.1016/j.cardiores.2005.06.023](https://doi.org/10.1016/j.cardiores.2005.06.023).
278. Ki CS, Jung CL, Kim HJ, Baek KH, Park SJ, On YK, Kim KS, Noh SJ, Youm JB, Kim JS, Cho H. A KCNQ1 mutation causes age-dependent bradycardia and persistent atrial fibrillation. **Pflugers Arch** 466: 529–540, 2014. doi:[10.1007/s00424-013-1337-6](https://doi.org/10.1007/s00424-013-1337-6).
279. Lundby A, Ravn LS, Svendsen JH, Olesen SP, Schmitt N. KCNQ1 mutation Q147R is associated with atrial fibrillation and prolonged QT interval. **Heart Rhythm** 4: 1532–1541, 2007. doi:[10.1016/j.hrthm.2007.07.022](https://doi.org/10.1016/j.hrthm.2007.07.022).
280. Moreno C, Oliveras A, de la Cruz A, Bartolucci C, Muñoz C, Salar E, Gimeno JR, Severi S, Comes N, Felipe A, González T, Lambiase P, Valenzuela C. A new KCNQ1 mutation at the S5 segment that impairs its association with KCNE1 is responsible for short QT syndrome. **Cardiovasc Res** 107: 613–623, 2015. doi:[10.1093/cvr/cvv196](https://doi.org/10.1093/cvr/cvv196).
281. Zhou X, Bueno-Orovio A, Schilling RJ, Kirkby C, Denning C, Rajamohan D, Burrage K, Tinker A, Rodríguez B, Harmer SC. Investigating the complex arrhythmic phenotype caused by the gain-of-function mutation KCNQ1-G229D. **Front Physiol** 10: 259, 2019. doi:[10.3389/fphys.2019.00259](https://doi.org/10.3389/fphys.2019.00259).
282. Gadsby DC, Cranefield PF. Electrogenic sodium extrusion in cardiac Purkinje fibers. **J Gen Physiol** 73: 819–837, 1979. doi:[10.1085/jgp.73.6.819](https://doi.org/10.1085/jgp.73.6.819).
283. Hirano Y, Hiraoka M. Changes in K⁺ currents induced by Ba²⁺ in guinea pig ventricular muscles. **Am J Physiol Heart Circ Physiol** 251: H24–H33, 1986. doi:[10.1152/ajpheart.1986.251.1.H24](https://doi.org/10.1152/ajpheart.1986.251.1.H24).
284. Martin R, Koumi S, Teneick R, Ten Eick RE. Comparison of the effects of internal [Mg²⁺] on IK1 in cat and guinea-pig cardiac ventricular myocytes. **J Mol Cell Cardiol** 27: 673–691, 1995. doi:[10.1016/S0022-2828\(08\)80059-4](https://doi.org/10.1016/S0022-2828(08)80059-4).
285. Matsuda H. Effects of external and internal K⁺ ions on magnesium block of inwardly rectifying K⁺ channels in guinea-pig heart cells. **J Physiol** 435: 83–99, 1991. doi:[10.1113/jphysiol.1991.sp018499](https://doi.org/10.1113/jphysiol.1991.sp018499).
286. Biermans G, Vereecke J, Carmeliet E. The mechanism of the inactivation of the inward-rectifying K current during hyperpolarizing steps in guinea-pig ventricular myocytes. **Pflugers Arch** 410: 604–613, 1987. doi:[10.1007/BF00581320](https://doi.org/10.1007/BF00581320).
287. Nagy N, Acsai K, Kormos A, Sebők Z, Farkas AS, Jost N, Nánási PP, Papp JG, Varró A, Tóth A. [Ca²⁺]_i-induced augmentation of the inward rectifier potassium current (IK1) in canine and human ventricular myocardium. **Pflugers Arch** 465: 1621–1635, 2013. doi:[10.1007/s00424-013-1309-x](https://doi.org/10.1007/s00424-013-1309-x).
288. Noble D, Tsien RW. Outward membrane currents activated in the plateau range of potentials in cardiac Purkinje fibres. **J Physiol** 200: 205–231, 1969. doi:[10.1113/jphysiol.1969.sp008689](https://doi.org/10.1113/jphysiol.1969.sp008689).
289. Fauconnier J, Lacampagne A, Rauzier JM, Vassort G, Richard S. Ca²⁺-dependent reduction of IK1 in rat ventricular cells: a novel paradigm for arrhythmia in heart failure? **Cardiovasc Res** 68: 204–212, 2005. doi:[10.1016/j.cardiores.2005.05.024](https://doi.org/10.1016/j.cardiores.2005.05.024).
290. Zaza A, Rocchetti M, Brioschi A, Cantadori A, Ferroni A. Dynamic Ca²⁺-induced inward rectification of K⁺ current during the ventricular action potential. **Circ Res** 82: 947–956, 1998. doi:[10.1161/01.res.82.9.947](https://doi.org/10.1161/01.res.82.9.947).
291. Dhamoon AS, Jalife J. The inward rectifier current (IK1) controls cardiac excitability and is involved in arrhythmogenesis. **Heart Rhythm** 2: 316–324, 2005. doi:[10.1016/j.hrthm.2004.11.012](https://doi.org/10.1016/j.hrthm.2004.11.012).
292. Lopatin AN, Nichols CG. [K⁺] dependence of polyamine-induced rectification in inward rectifier potassium channels (IRK1, Kir2.1). **J Gen Physiol** 108: 105–113, 1996. doi:[10.1085/jgp.108.2.105](https://doi.org/10.1085/jgp.108.2.105).
293. Nichols CG, Lopatin AN. Inward rectifier potassium channels. **Annu Rev Physiol** 59: 171–191, 1997. doi:[10.1146/annurev.physiol.59.1.171](https://doi.org/10.1146/annurev.physiol.59.1.171).
294. Weiss JN, Qu Z, Shivkumar K. Electrophysiology of hypokalemia and hyperkalemia. **Circ Arrhythm Electrophysiol** 10: e004667, 2017. doi:[10.1161/CIRCEP.116.004667](https://doi.org/10.1161/CIRCEP.116.004667).
295. Karle CA, Zitron E, Zhang W, Wendt-Nordahl G, Kathöfer S, Thomas D, Gut B, Scholz E, Vahl CF, Katus HA, Kiehn J. Human cardiac

- inwardly-rectifying K^+ channel Kir(2.1b) is inhibited by direct protein kinase C-dependent regulation in human isolated cardiomyocytes and in an expression system. **Circulation** 106: 1493–1499, 2002. doi:[10.1161/01.cir.0000029747.53262.5c](https://doi.org/10.1161/01.cir.0000029747.53262.5c).
296. Koumi S, Wasserstrom JA, Ten Eick RE. Beta-adrenergic and cholinergic modulation of inward rectifier K^+ channel function and phosphorylation in guinea-pig ventricle. **J Physiol** 486: 661–678, 1995. doi:[10.1113/jphysiol.1995.sp020842](https://doi.org/10.1113/jphysiol.1995.sp020842).
297. Veldkamp MW, Geuzebroek GS, Baartscheer A, Verkerk AO, Schumacher CA, Suarez GG, Berger WR, Casini S, van Amersfoort SC, Scholman KT, Driessen AH, Belterman CN, van Ginneken AC, de Groot JR, de Bakker JM, Remme CA, Boukens BJ, Coronel R. Neurokinin-3 receptor activation selectively prolongs atrial refractoriness by inhibition of a background K^+ channel. **Nat Commun** 9: 4357, 2018. doi:[10.1038/s41467-018-06530-5](https://doi.org/10.1038/s41467-018-06530-5).
298. Takanari H, Nalos L, Stary-Weinzinger A, de Git KC, Varkevisser R, Linder T, Houtman MJ, Peschar M, de Boer TP, Tidwell RR, Rook MB, Vos MA, van der Heyden MA. Efficient and specific cardiac IK_1 inhibition by a new pentamidine analogue. **Cardiovasc Res** 99: 203–214, 2013. doi:[10.1093/cvr/cvt103](https://doi.org/10.1093/cvr/cvt103).
299. Veerapandian A, Statland JM, Tawil R, Andersen-Tawil syndrome. In: **GeneReviews**, edited by Adam MP, Ardinger HH, Pagon RA, Wallace SE, Bean LJ, Stephens K, Amemiya A. Seattle, WA: Univ. of Washington, 1993.
300. Tsuboi M, Antzelevitch C. Cellular basis for electrocardiographic and arrhythmic manifestations of Andersen-Tawil syndrome (LQT7). **Heart Rhythm** 3: 328–335, 2006. doi:[10.1016/j.hrthm.2005.11.026](https://doi.org/10.1016/j.hrthm.2005.11.026).
301. Tamkun MM, Knoth KM, Walbridge JA, Kroemer H, Roden DM, Glover DM. Molecular cloning and characterization of two voltage-gated K^+ channel cDNAs from human ventricle. **FASEB J** 5: 331–337, 1991. doi:[10.1096/fasebj.5.3.2001794](https://doi.org/10.1096/fasebj.5.3.2001794).
302. Fedida D, Wible B, Wang Z, Fermini B, Faust F, Nattel S, Brown AM. Identity of a novel delayed rectifier current from human heart with a cloned K^+ channel current. **Circ Res** 73: 210–216, 1993. doi:[10.1161/01.res.73.1.210](https://doi.org/10.1161/01.res.73.1.210).
303. Amos GJ, Wettwer E, Metzger F, Li Q, Himmel HM, Ravens U. Differences between outward currents of human atrial and subepicardial ventricular myocytes. **J Physiol** 491: 31–50, 1996. doi:[10.1113/jphysiol.1996.sp021194](https://doi.org/10.1113/jphysiol.1996.sp021194).
304. Majumder K, De Biasi M, Wang Z, Wible BA. Molecular cloning and functional expression of a novel potassium channel beta-subunit from human atrium. **FEBS Lett** 361: 13–16, 1995. doi:[10.1016/0014-5793\(95\)00120-x](https://doi.org/10.1016/0014-5793(95)00120-x).
305. Nattel S. The molecular and ionic specificity of antiarrhythmic drug actions. **J Cardiovasc Electrophysiol** 10: 272–282, 1999. doi:[10.1111/j.1540-8167.1999.tb00673.x](https://doi.org/10.1111/j.1540-8167.1999.tb00673.x).
306. Yue L, Feng J, Li GR, Nattel S. Characterization of an ultrarapid delayed rectifier potassium channel involved in canine atrial repolarization. **J Physiol** 496: 647–662, 1996. doi:[10.1113/jphysiol.1996.sp021716](https://doi.org/10.1113/jphysiol.1996.sp021716).
307. Yue L, Feng J, Wang Z, Nattel S. Adrenergic control of the ultrarapid delayed rectifier current in canine atrial myocytes. **J Physiol** 516: 385–398, 1999. doi:[10.1111/j.1469-7793.1999.0385v.x](https://doi.org/10.1111/j.1469-7793.1999.0385v.x).
308. Sridhar A, da Cunha DN, Lacombe VA, Zhou Q, Fox JJ, Hamlin RL, Carnes CA. The plateau outward current in canine ventricle, sensitive to 4-aminopyridine, is a constitutive contributor to ventricular repolarization. **Br J Pharmacol** 152: 870–879, 2007. doi:[10.1038/sj.bjp.0707403](https://doi.org/10.1038/sj.bjp.0707403).
309. Wettwer E, Ha'la O, Christ T, Heubach JF, Dobrev D, Knaut M, Varro' A, Ravens U. Role of IK_{ur} in controlling action potential shape and contractility in the human atrium: influence of chronic atrial fibrillation. **Circulation** 110: 2299–2306, 2004. doi:[10.1161/01.CIR.0000145155.60288.71](https://doi.org/10.1161/01.CIR.0000145155.60288.71).
310. Ford J, Milnes J, Wettwer E, Christ T, Rogers M, Sutton K, Madge D, Virag L, Jost N, Horvath Z, Matschke K, Varro A, Ravens U. Human electrophysiological and pharmacological properties of XEN-D0101: a novel atrial-selective $Kv1.5/IK_{ur}$ inhibitor. **J Cardiovasc Pharmacol** 61: 408–415, 2013. doi:[10.1097/FJC.0b013e31828780eb](https://doi.org/10.1097/FJC.0b013e31828780eb).
311. Shunmugam SR, Sugihara C, Freemantle N, Round P, Furniss S, Sulke N. A double-blind, randomised, placebo-controlled, cross-over study assessing the use of XEN-D0103 in patients with paroxysmal atrial fibrillation and implanted pacemakers allowing continuous beat-to-beat monitoring of drug efficacy. **J Interv Card Electrophysiol** 51: 191–197, 2018. doi:[10.1007/s10840-018-0318-2](https://doi.org/10.1007/s10840-018-0318-2).
312. Eisner DA, Vaughan-Jones RD. Do calcium-activated potassium channels exist in the heart? **Cell Calcium** 4: 371–386, 1983. doi:[10.1016/0143-4160\(83\)90015-5](https://doi.org/10.1016/0143-4160(83)90015-5).
313. Xu Y, Tuteja D, Zhang Z, Xu D, Zhang Y, Rodriguez J, Nie L, Tuxson HR, Young JN, Glatzer KA, Vázquez AE, Yamoah EN, Chiamvimonvat N. Molecular identification and functional roles of a Ca^{2+} -activated K^+ channel in human and mouse hearts. **J Biol Chem** 278: 49085–49094, 2003. doi:[10.1074/jbc.M307508200](https://doi.org/10.1074/jbc.M307508200).
314. Skibsbjerg L, Poulet C, Diness JG, Bentzen BH, Yuan L, Kappert U, Matschke K, Wettwer E, Ravens U, Grunnet M, Christ T, Jespersen T. Small-conductance calcium-activated potassium (SK) channels contribute to action potential repolarization in human atria. **Cardiovasc Res** 103: 156–167, 2014. doi:[10.1093/cvr/cvu121](https://doi.org/10.1093/cvr/cvu121).
315. Chang PC, Turker I, Lopshire JC, Masroor S, Nguyen BL, Tao W, Rubart M, Chen PS, Chen Z, Ai T. Heterogeneous upregulation of apamin-sensitive potassium currents in failing human ventricles. **J Am Heart Assoc** 2: e004713, 2013. doi:[10.1161/JAHA.112.004713](https://doi.org/10.1161/JAHA.112.004713).
316. Kirchhoff JE, Diness JG, Sheykade M, Grunnet M, Jespersen T. Synergistic antiarrhythmic effect of combining inhibition of Ca^{2+} -activated K^+ (SK) channels and voltage-gated Na^+ channels in an isolated heart model of atrial fibrillation. **Heart Rhythm** 12: 409–418, 2015. doi:[10.1016/j.hrthm.2014.12.010](https://doi.org/10.1016/j.hrthm.2014.12.010).
317. Nattel S. Calcium-activated potassium current: a novel ion channel candidate in atrial fibrillation. **J Physiol** 587: 1385–1386, 2009. doi:[10.1113/jphysiol.2009.170621](https://doi.org/10.1113/jphysiol.2009.170621).
318. Hamilton S, Polina I, Terentyeva R, Bronk P, Kim TY, Roder K, Clements RT, Koren G, Choi BR, Terentyev D. PKA phosphorylation underlies functional recruitment of sarcolemmal SK2 channels in ventricular myocytes from hypertrophic hearts. **J Physiol** 598: 2847–2873, 2020. doi:[10.1113/JP277618](https://doi.org/10.1113/JP277618).
319. Fan X, Yu Y, Lan H, Ou X, Yang L, Li T, Cao J, Zeng X, Li M. Ca^{2+} /calmodulin-dependent protein kinase II (CaMKII) increases small-conductance Ca^{2+} -activated K^+ current in patients with chronic atrial fibrillation. **Med Sci Monit** 24: 3011–3023, 2018. doi:[10.12659/MSM.909684](https://doi.org/10.12659/MSM.909684).
320. Xia XM, Fakler B, Rivard A, Wayman G, Johnson-Pais T, Keen JE, Ishii T, Hirschberg B, Bond CT, Lutsenko S, Maylie J, Adelman JP. Mechanism of calcium gating in small-conductance calcium-activated potassium channels. **Nature** 395: 503–507, 1998. doi:[10.1038/26758](https://doi.org/10.1038/26758).
321. Nagy N, Szuts V, Horváth Z, Seprényi G, Farkas AS, Acsai K, Prorok J, Bitay M, Kun A, Pataricza J, Papp JG, Nánási PP, Varró A, Tóth A.

- Does small-conductance calcium-activated potassium channel contribute to cardiac repolarization? **J Mol Cell Cardiol** 47: 656–663, 2009. doi:10.1016/j.yjmcc.2009.07.019.
322. Nagy N, Márton Z, Kiss L, Varró A, Nánási PP, Tóth A. Role of Ca^{2+} -sensitive K^+ currents in controlling ventricular repolarization: possible implications for future antiarrhythmic drug therapy. **Curr Med Chem** 18: 3622–3639, 2011. doi:10.2174/092986711796642463.
323. Reher TA, Wang Z, Hsueh CH, Chang PC, Pan Z, Kumar M, Patel J, Tan J, Shen C, Chen Z, Fishbein MC, Rubart M, Boyden P, Chen PS. Small-conductance calcium-activated potassium current in normal rabbit cardiac Purkinje cells. **J Am Heart Assoc** 6: e005471, 2017. doi:10.1161/JAHA.117.005471.
324. Duan DY, Fermini B, Nattel S. Sustained outward current observed after I_{to1} inactivation in rabbit atrial myocytes is a novel Cl^- current. **Am J Physiol Heart Circ Physiol** 263: H1967–H1971, 1992. doi:10.1152/ajpheart.1992.263.6.H1967.
325. Noma A. ATP-regulated K^+ channels in cardiac muscle. **Nature** 305: 147–148, 1983. doi:10.1038/305147a0.
326. Inagaki N, Gonoi T, Clement JP, Namba N, Inazawa J, Gonzalez G, Aguilar-Bryan L, Seino S, Bryan J. Reconstitution of IK_{ATP} : an inward rectifier subunit plus the sulfonylurea receptor. **Science** 270: 1166–1170, 1995. doi:10.1126/science.270.5239.1166.
327. Chutkow WA, Simon MC, Le Beau MM, Burant CF. Cloning, tissue expression, and chromosomal localization of SUR2, the putative drug-binding subunit of cardiac, skeletal muscle, and vascular K_{ATP} channels. **Diabetes** 45: 1439–1445, 1996. doi:10.2337/diab.45.10.1439.
328. Deutsch N, Klitzner TS, Lamp ST, Weiss JN. Activation of cardiac ATP-sensitive K^+ current during hypoxia: correlation with tissue ATP levels. **Am J Physiol Heart Circ Physiol** 261: H671–H676, 1991. doi:10.1152/ajpheart.1991.261.3.H671.
329. Loussouarn G, Marton LJ, Nichols CG. Molecular basis of inward rectification: structural features of the blocker defined by extended polyamine analogs. **Mol Pharmacol** 68: 298–304, 2005. doi:10.1124/mol.105.012377.
330. Nichols CG. K_{ATP} channels as molecular sensors of cellular metabolism. **Nature** 440: 470–476, 2006. doi:10.1038/nature04711.
331. Shyng S, Ferrigni T, Nichols CG. Control of rectification and gating of cloned K_{ATP} channels by the Kir6.2 subunit. **J Gen Physiol** 110: 141–153, 1997. doi:10.1085/jgp.110.2.141.
332. Chi L, Uprichard AC, Lucchesi BR. Profibrillatory actions of pinacidil in a conscious canine model of sudden coronary death. **J Cardiovasc Pharmacol** 15: 452–464, 1990. doi:10.1097/00005344-199003000-00016.
333. Billman GE, Englert HC, Schölkens BA. HMR 1883, a novel cardioselective inhibitor of the ATP-sensitive potassium channel. Part II: effects on susceptibility to ventricular fibrillation induced by myocardial ischemia in conscious dogs. **J Pharmacol Exp Ther** 286: 1465–1473, 1998.
334. Englert HC, Heitsch H, Gerlach U, Knieps S. Blockers of the ATP-sensitive potassium channel SUR2A/Kir6.2: a new approach to prevent sudden cardiac death. **Curr Med Chem Cardiovasc Hematol Agents** 1: 253–271, 2003. doi:10.2174/1568016033477423.
335. Vajda S, Baczkó I, Leprán I. Selective cardiac plasma-membrane K_{ATP} channel inhibition is defibrillatory and improves survival during acute myocardial ischemia and reperfusion. **Eur J Pharmacol** 577: 115–123, 2007. doi:10.1016/j.ejphar.2007.08.016.
336. Chi LG, Tamura Y, Hoff PT, Macha M, Gallagher KP, Schork MA, Lucchesi BR. Effect of superoxide dismutase on myocardial infarct size in the canine heart after 6 hours of regional ischemia and reperfusion: a demonstration of myocardial salvage. **Circ Res** 64: 665–675, 1989. doi:10.1161/01.res.64.4.665.
337. del Valle HF, Lascano EC, Negroni JA, Crottogini AJ. Glibenclamide effects on reperfusion-induced malignant arrhythmias and left ventricular mechanical recovery from stunning in conscious sheep. **Cardiovasc Res** 50: 474–485, 2001. doi:10.1016/S0008-6363(01)00209-7.
338. Carlsson L, Abrahamsson C, Drews L, Duker G. Antiarrhythmic effects of potassium channel openers in rhythm abnormalities related to delayed repolarization. **Circulation** 85: 1491–1500, 1992. doi:10.1161/01.cir.85.4.1491.
339. Spinelli W, Sorota S, Siegal M, Hoffman BF. Antiarrhythmic actions of the ATP-regulated K^+ current activated by pinacidil. **Circ Res** 68: 1127–1137, 1991. doi:10.1161/01.res.68.4.1127.
340. Wolk R, Cobbe SM, Kane KA, Hicks MN. Relevance of inter- and intraventricular electrical dispersion to arrhythmogenesis in normal and ischaemic rabbit myocardium: a study with cromakalim, 5-hydroxydecanoate and glibenclamide. **J Cardiovasc Pharmacol** 33: 323–334, 1999. doi:10.1097/00005344-199902000-00022.
341. Bril A, Man RY. Effects of the potassium channel activator, BRL 34915, on the action potential characteristics of canine cardiac Purkinje fibers. **J Pharmacol Exp Ther** 253: 1090–1096, 1990.
342. Lathrop DA, Nánási PP, Varró A. In vitro cardiac models of dog Purkinje fibre triggered and spontaneous electrical activity: effects of nicorandil. **Br J Pharmacol** 99: 119–123, 1990. doi:10.1111/j.1476-5381.1990.tb14664.x.
343. Cole WC, McPherson CD, Sontag D. ATP-regulated K^+ channels protect the myocardium against ischemia/reperfusion damage. **Circ Res** 69: 571–581, 1991. doi:10.1161/01.res.69.3.571.
344. Maddaford TG, Dibrov E, Hurtado C, Pierce GN. Reduced expression of the $\text{Na}^+/\text{Ca}^{2+}$ exchanger in adult cardiomyocytes via adenovirally delivered shRNA results in resistance to simulated ischemic injury. **Am J Physiol Heart Circ Physiol** 298: H360–H366, 2010. doi:10.1152/ajpheart.00932.2009.
345. McPherson CD, Pierce GN, Cole WC. Ischemic cardioprotection by ATP-sensitive K^+ channels involves high-energy phosphate preservation. **Am J Physiol Heart Circ Physiol** 265: H1809–H1818, 1993. doi:10.1152/ajpheart.1993.265.5.H1809.
346. Baczkó I, Giles WR, Light PE. Pharmacological activation of plasma-membrane K_{ATP} channels reduces reoxygenation-induced Ca^{2+} overload in cardiac myocytes via modulation of the diastolic membrane potential. **Br J Pharmacol** 141: 1059–1067, 2004. doi:10.1038/sj.bjp.0705702.
347. Baczkó I, Giles WR, Light PE. Resting membrane potential regulates $\text{Na}^+/\text{Ca}^{2+}$ exchange-mediated Ca^{2+} overload during hypoxia-reoxygenation in rat ventricular myocytes. **J Physiol** 550: 889–898, 2003. doi:10.1113/jphysiol.2003.043372.
348. Inoue I, Nagase H, Kishi K, Higuti T. ATP-sensitive K^+ channel in the mitochondrial inner membrane. **Nature** 352: 244–247, 1991. doi:10.1038/352244a0.
349. Paucek P, Mironova G, Mahdi F, Beavis AD, Woldegiorgis G, Garlid KD. Reconstitution and partial purification of the glibenclamide-sensitive, ATP-dependent K^+ channel from rat liver and beef heart mitochondria. **J Biol Chem** 267: 26062–26069, 1992. doi:10.1016/S0021-9258(18)35717-X.

350. Light PE, Kanji HD, Fox JE, French RJ. Distinct myoprotective roles of cardiac sarcolemmal and mitochondrial KATP channels during metabolic inhibition and recovery. **FASEB J** 15: 2586–2594, 2001. doi:[10.1096/fj.01-0188com](https://doi.org/10.1096/fj.01-0188com).
351. Nakayama K, Suzuki Y, Hashimoto K. Sustained atrial fibrillation by acetylcholine infusion into the sinus node artery. **Tohoku J Exp Med** 96: 333–339, 1968. doi:[10.1620/tjem.96.333](https://doi.org/10.1620/tjem.96.333).
352. Corey S, Clapham DE. Identification of native atrial G-protein-regulated inwardly rectifying K⁺ (GIRK4) channel homomultimers. **J Biol Chem** 273: 27499–27504, 1998. doi:[10.1074/jbc.273.42.27499](https://doi.org/10.1074/jbc.273.42.27499).
353. Nobles M, Montaigne D, Sebastian S, Birnbaumer L, Tinker A. Differential effects of inhibitory G protein isoforms on G protein-gated inwardly rectifying K⁺ currents in adult murine atria. **Am J Physiol Cell Physiol** 314: C616–C626, 2018. doi:[10.1152/ajpcell.00271.2016](https://doi.org/10.1152/ajpcell.00271.2016).
354. Kurachi Y. G protein regulation of cardiac muscarinic potassium channel. **Am J Physiol Cell Physiol** 269: C821–C830, 1995. doi:[10.1152/ajpcell.1995.269.4.C821](https://doi.org/10.1152/ajpcell.1995.269.4.C821).
355. Moreno-Galindo EG, Alamilla J, Sanchez-Chapula JA, Tristani-Firouzi M, Navarro-Polanco RA. The agonist-specific voltage dependence of M2 muscarinic receptors modulates the deactivation of the acetylcholine-gated K⁺ current (I KACH). **Pflugers Arch** 468: 1207–1214, 2016. doi:[10.1007/s00424-016-1812-y](https://doi.org/10.1007/s00424-016-1812-y).
356. Navarro-Polanco RA, Aréchiga-Figueroa IA, Salazar-Fajardo PD, Benavides-Haro DE, Rodríguez-Eliás JC, Sachse FB, Tristani-Firouzi M, Sánchez-Chapula JA, Moreno-Galindo EG. Voltage sensitivity of M2 muscarinic receptors underlies the delayed rectifier-like activation of ACh-gated K⁺ current by choline in feline atrial myocytes. **J Physiol** 591: 4273–4286, 2013. doi:[10.1113/jphysiol.2013.255166](https://doi.org/10.1113/jphysiol.2013.255166).
357. Kaseda S, Zipes DP. Supersensitivity to acetylcholine of canine sinus and AV nodes after parasympathetic denervation. **Am J Physiol Heart Circ Physiol** 255: H534–H539, 1988. doi:[10.1152/ajpheart.1988.255.3.H534](https://doi.org/10.1152/ajpheart.1988.255.3.H534).
358. Dobrev D, Friedrich A, Voigt N, Jost N, Wettwer E, Christ T, Knaut M, Ravens U. The G protein-gated potassium current I_{KACH} is constitutively active in patients with chronic atrial fibrillation. **Circulation** 112: 3697–3706, 2005. doi:[10.1161/CIRCULATIONAHA.105.575332](https://doi.org/10.1161/CIRCULATIONAHA.105.575332).
359. Ravens U. Atrial-selective K⁺ channel blockers: potential antiarrhythmic drugs in atrial fibrillation? **Can J Physiol Pharmacol** 95: 1313–1318, 2017. doi:[10.1139/cjpp-2017-0024](https://doi.org/10.1139/cjpp-2017-0024).
360. Bukiya AN, Rosenhouse-Dantsker A. Synergistic activation of G protein-gated inwardly rectifying potassium channels by cholesterol and PI(4,5)P₂. **Biochim Biophys Acta Biomembr** 1859: 1233–1241, 2017. doi:[10.1016/j.bbamem.2017.03.023](https://doi.org/10.1016/j.bbamem.2017.03.023).
361. Pfaffinger PJ, Martin JM, Hunter DD, Nathanson NM, Hille B. GTP-binding proteins couple cardiac muscarinic receptors to a K channel. **Nature** 317: 536–538, 1985. doi:[10.1038/317536a0](https://doi.org/10.1038/317536a0).
362. Voigt N, Abu-Taha I, Heijman J, Dobrev D. Constitutive activity of the acetylcholine-activated potassium current I_{KACH} in cardiomyocytes. **Adv Pharmacol** 70: 393–409, 2014. doi:[10.1016/B978-0-12-417197-8.00013-4](https://doi.org/10.1016/B978-0-12-417197-8.00013-4).
363. Morishima M, Iwata E, Nakada C, Tsukamoto Y, Takanari H, Miyamoto S, Moriyama M, Ono K. Atrial fibrillation-mediated upregulation of miR-30d regulates myocardial electrical remodeling of the G-protein-gated K⁺ channel, I_{KACH}. **Circ J** 80: 1346–1355, 2016. doi:[10.1253/circj.CJ-15-1276](https://doi.org/10.1253/circj.CJ-15-1276).
364. Dascal N, Schreibmayer W, Lim NF, Wang W, Chavkin C, DiMugno L, Labarca C, Kieffer BL, Gaveriaux-Ruff C, Trollinger D. Atrial G protein-activated K⁺ channel: expression cloning and molecular properties. **Proc Natl Acad Sci USA** 90: 10235–10239, 1993. doi:[10.1073/pnas.90.21.10235](https://doi.org/10.1073/pnas.90.21.10235).
365. Holmes AP, Yu TY, Tull S, Syeda F, Kuhlmann SM, O'Brien SM, Patel P, Brain KL, Pavlovic D, Brown NA, Fabritz L, Kirchhof P. A regional reduction in I_{to} and I_{KACH} in the murine posterior left atrial myocardium is associated with action potential prolongation and increased ectopic activity. **PLoS One** 11: e0154077, 2016. doi:[10.1371/journal.pone.0154077](https://doi.org/10.1371/journal.pone.0154077).
366. Kuß J, Stallmeyer B, Goldstein M, Rinné S, Pees C, Zumhagen S, Seeböhm G, Decher N, Pott L, Kienitz MC, Schulze-Bahr E. Familial sinus node disease caused by a gain of GIRK (G-protein activated inwardly rectifying K⁺ channel) channel function. **Circ Genom Precis Med** 12: e002238, 2019. doi:[10.1161/CIRCGEN.118.002238](https://doi.org/10.1161/CIRCGEN.118.002238).
367. Hume JR, Harvey RD. Chloride conductance pathways in heart. **Am J Physiol Cell Physiol** 261: C399–C412, 1991. doi:[10.1152/ajpcell.1991.261.3.C399](https://doi.org/10.1152/ajpcell.1991.261.3.C399).
368. Hiraoka M, Kawano S, Hirano Y, Furukawa T. Role of cardiac chloride currents in changes in action potential characteristics and arrhythmias. **Cardiovasc Res** 40: 23–33, 1998. doi:[10.1016/s0008-6363\(98\)00173-4](https://doi.org/10.1016/s0008-6363(98)00173-4).
369. Duan D. Phenomics of cardiac chloride channels: the systematic study of chloride channel function in the heart. **J Physiol** 587: 2163–2177, 2009. doi:[10.1113/jphysiol.2008.165860](https://doi.org/10.1113/jphysiol.2008.165860).
370. Duan DD. Phenomics of cardiac chloride channels. **Compr Physiol** 3: 667–692, 2013. doi:[10.1002/cphy.c110014](https://doi.org/10.1002/cphy.c110014).
371. Baumgarten CM, Clemo HF. Swelling-activated chloride channels in cardiac physiology and pathophysiology. **Prog Biophys Mol Biol** 82: 25–42, 2003. doi:[10.1016/s0079-6107\(03\)00003-8](https://doi.org/10.1016/s0079-6107(03)00003-8).
372. Dudel J, Peper K, Rüdell R, Trautwein W. The dynamic chloride component of membrane current in Purkinje fibers. **Pflugers Arch Gesamte Physiol Menschen Tiere** 295: 197–212, 1967. doi:[10.1007/BF01844100](https://doi.org/10.1007/BF01844100).
373. Kenyon JL, Gibbons WR. Influence of chloride, potassium, and tetraethylammonium on the early outward current of sheep cardiac Purkinje fibers. **J Gen Physiol** 73: 117–138, 1979. doi:[10.1085/jgp.73.2.117](https://doi.org/10.1085/jgp.73.2.117).
374. Tseng GN, Hoffman BF. Two components of transient outward current in canine ventricular myocytes. **Circ Res** 64: 633–647, 1989. doi:[10.1161/01.res.64.4.633](https://doi.org/10.1161/01.res.64.4.633).
375. Zygmunt AC, Gibbons WR. Properties of the calcium-activated chloride current in heart. **J Gen Physiol** 99: 391–414, 1992. doi:[10.1085/jgp.99.3.391](https://doi.org/10.1085/jgp.99.3.391).
376. Fülöp L, Fiák E, Szentandrassy N, Magyar J, Nánási PP, Bányász T. The role of transmembrane chloride current in afterdepolarisations in canine ventricular cardiomyocytes. **Gen Physiol Biophys** 22: 341–353, 2003.
377. Horváth B, Vácz K, Hegyi B, Gönczi M, Dienes B, Kistámas K, Bányász T, Magyar J, Bacsko I, Varró A, Seprényi G, Csernoch L, Nánási PP, Szentandrassy N. Sarcolemmal Ca²⁺-entry through L-type Ca²⁺ channels controls the profile of Ca²⁺-activated Cl[−] current in canine ventricular myocytes. **J Mol Cell Cardiol** 97: 125–139, 2016. doi:[10.1016/j.yjmcc.2016.05.006](https://doi.org/10.1016/j.yjmcc.2016.05.006).
378. O'Driscoll KE, Hatton WJ, Burkin HR, Leblanc N, Britton FC. Expression, localization, and functional properties of Bestrophin 3

- channel isolated from mouse heart. **Am J Physiol Cell Physiol** 295: C1610–C1624, 2008. doi:10.1152/ajpcell.00461.2008.
379. O'Driscoll KE, Leblanc N, Hatton WJ, Britton FC. Functional properties of murine bestrophin 1 channel. **Biochem Biophys Res Commun** 384: 476–481, 2009. doi:10.1016/j.bbrc.2009.05.008.
380. Sun H, Tsunenari T, Yau KW, Nathans J. The vitelliform macular dystrophy protein defines a new family of chloride channels. **Proc Natl Acad Sci USA** 99: 4008–4013, 2002. doi:10.1073/pnas.052692999.
381. Caputo A, Caci E, Ferrera L, Pedemonte N, Barsanti C, Sondo E, Pfeiffer U, Ravazzolo R, Zegar-Moran O, Galletta LJ. TMEM16A, a membrane protein associated with calcium-dependent chloride channel activity. **Science** 322: 590–594, 2008. doi:10.1126/science.1163518.
382. Schroeder BC, Cheng T, Jan YN, Jan LY. Expression cloning of TMEM16A as a calcium-activated chloride channel subunit. **Cell** 134: 1019–1029, 2008. doi:10.1016/j.cell.2008.09.003.
383. Yang YD, Cho H, Koo JY, Tak MH, Cho Y, Shim WS, Park SP, Lee J, Lee B, Kim BM, Raouf R, Shin YK, Oh U. TMEM16A confers receptor-activated calcium-dependent chloride conductance. **Nature** 455: 1210–1215, 2008. doi:10.1038/nature07313.
384. Zygmunt AC. Intracellular calcium activates a chloride current in canine ventricular myocytes. **Am J Physiol Heart Circ Physiol** 267: H1984–H1995, 1994. doi:10.1152/ajpheart.1994.267.5.H1984.
385. Zygmunt AC, Gibbons WR. Calcium-activated chloride current in rabbit ventricular myocytes. **Circ Res** 68: 424–437, 1991. doi:10.1161/01.res.68.2.424.
386. Zygmunt AC, Goodrow RJ, Weigel CM. INaCa and ICl(Ca) contribute to isoproterenol-induced delayed after depolarizations in mid-myocardial cells. **Am J Physiol Heart Circ Physiol** 275: H1979–H1992, 1998. doi:10.1152/ajpheart.1998.275.6.H1979.
387. Wu MM, Lou J, Song BL, Gong YF, Li YC, Yu CJ, Wang QS, Ma TX, Ma K, Hartzell HC, Duan DD, Zhao D, Zhang ZR. Hypoxia augments the calcium-activated chloride current carried by anoctamin-1 in cardiac vascular endothelial cells of neonatal mice. **Br J Pharmacol** 171: 3680–3692, 2014. doi:10.1111/bph.12730.
388. Aggarwal R, Pu J, Boyden PA. Ca²⁺-dependent outward currents in myocytes from epicardial border zone of 5-day infarcted canine heart. **Am J Physiol Heart Circ Physiol** 273: H1386–H1394, 1997. doi:10.1152/ajpheart.1997.273.3.H1386.
389. Bahinski A, Nairn AC, Greengard P, Gadsby DC. Chloride conductance regulated by cyclic AMP-dependent protein kinase in cardiac myocytes. **Nature** 340: 718–721, 1989. doi:10.1038/340718a0.
390. Harvey RD, Hume JR. Autonomic regulation of a chloride current in heart. **Science** 244: 983–985, 1989. doi:10.1126/science.2543073.
391. Harvey RD, Jurevicius JA, Hume JR. Intracellular Na⁺ modulates the cAMP-dependent regulation of ion channels in the heart. **Proc Natl Acad Sci USA** 88: 6946–6950, 1991. doi:10.1073/pnas.88.16.6946.
392. Xiang SY, Ye LL, Duan LL, Liu LH, Ge ZD, Auchampach JA, Gross GJ, Duan DD. Characterization of a critical role for CFTR chloride channels in cardioprotection against ischemia/reperfusion injury. **Acta Pharmacol Sin** 32: 824–833, 2011. doi:10.1038/aps.2011.61.
393. Tseng GN. Cell swelling increases membrane conductance of canine cardiac cells: evidence for a volume-sensitive Cl channel. **Am J Physiol Cell Physiol** 262: C1056–C1068, 1992. doi:10.1152/ajpcell.1992.262.4.C1056.
394. Duan D, Ye L, Britton F, Horowitz B, Hume JR. UltraRapid communications: a novel anionic inward rectifier in native cardiac myocytes. **Circ Res** 86: 485, 2000.
395. Furukawa T, Ogura T, Katayama Y, Hiraoka M. Characteristics of rabbit ClC-2 current expressed in *Xenopus* oocytes and its contribution to volume regulation. **Am J Physiol Cell Physiol** 274: C500–C512, 1998. doi:10.1152/ajpcell.1998.274.2.C500.
396. Huang ZM, Prasad C, Britton FC, Ye LL, Hatton WJ, Duan D. Functional role of CLC-2 chloride inward rectifier channels in cardiac sinoatrial nodal pacemaker cells. **J Mol Cell Cardiol** 47: 121–132, 2009. doi:10.1016/j.yjmcc.2009.04.008.
397. Yamamoto S, Ehara T. Acidic extracellular pH-activated outwardly rectifying chloride current in mammalian cardiac myocytes. **Am J Physiol Heart Circ Physiol** 290: H1905–H1914, 2006. doi:10.1152/ajpheart.00965.2005.
398. Sadoshima J, Izumo S. The cellular and molecular response of cardiac myocytes to mechanical stress. **Annu Rev Physiol** 59: 551–571, 1997. doi:10.1146/annurev.physiol.59.1.551.
399. Sadoshima J, Qiu Z, Morgan JP, Izumo S. Tyrosine kinase activation is an immediate and essential step in hypotonic cell swelling-induced ERK activation and c-fos gene expression in cardiac myocytes. **EMBO J** 15: 5535–5546, 1996. doi:10.1002/j.1460-2075.1996.tb00938.x.
400. Clemp HF, Stambler BS, Baumgarten CM. Persistent activation of a swelling-activated cation current in ventricular myocytes from dogs with tachycardia-induced congestive heart failure. **Circ Res** 83: 147–157, 1998. doi:10.1161/01.res.83.2.147.
401. Clemp HF, Stambler BS, Baumgarten CM. Swelling-activated chloride current is persistently activated in ventricular myocytes from dogs with tachycardia-induced congestive heart failure. **Circ Res** 84: 157–165, 1999. doi:10.1161/01.res.84.2.157.
402. Zou Y, Akazawa H, Qin Y, Sano M, Takano H, Minamino T, Makita N, Iwanaga K, Zhu W, Kudoh S, Toko H, Tamura K, Kihara M, Nagai T, Fukamizu A, Umemura S, Iiri T, Fujita T, Komuro I. Mechanical stress activates angiotensin II type 1 receptor without the involvement of angiotensin II. **Nat Cell Biol** 6: 499–506, 2004. doi:10.1038/ncb1137.
403. Du XY, Sorota S. Cardiac swelling-induced chloride current depolarizes canine atrial myocytes. **Am J Physiol Heart Circ Physiol** 272: H1904–H1916, 1997. doi:10.1152/ajpheart.1997.272.4.H1904.
404. Hagiwara N, Masuda H, Shoda M, Irisawa H. Stretch-activated anion currents of rabbit cardiac myocytes. **J Physiol** 456: 285–302, 1992. doi:10.1113/jphysiol.1992.sp019337.
405. Duan DD. The ClC-3 chloride channels in cardiovascular disease. **Acta Pharmacol Sin** 32: 675–684, 2011. doi:10.1038/aps.2011.30.
406. Decher N, Maier M, Dittich W, Gassenhuber J, Brüggemann A, Busch AE, Steinmeyer K. Characterization of TASK-4, a novel member of the pH-sensitive, two-pore domain potassium channel family. **FEBS Lett** 492: 84–89, 2001. doi:10.1016/S0014-5793(01)02222-0.
407. Lesage F, Guillemare E, Fink M, Duprat F, Lazdunski M, Romey G, Barhanin J. TWIK-1, a ubiquitous human weakly inward rectifying K⁺ channel with a novel structure. **EMBO J** 15: 1004–1011, 1996.
408. O'Connell AD, Morton MJ, Hunter M. Two-pore domain K⁺ channels-molecular sensors. **Biochim Biophys Acta** 1566: 152–161, 2002. doi:10.1016/S0005-2736(02)00597-7.
409. Christensen AH, Chatelain FC, Huttner IG, Olesen MS, Soka M, Feliciangeli S, Horvat C, Santiago CF, Vandenberg JI, Schmitt N,

- Olesen SP, Lesage F, Fatkin D. The two-pore domain potassium channel, TWIK-1, has a role in the regulation of heart rate and atrial size. *J Mol Cell Cardiol* 97: 24–35, 2016. doi:10.1016/j.jmcc.2016.04.006.
410. Ma L, Zhang X, Zhou M, Chen H. Acid-sensitive TWIK and TASK two-pore domain potassium channels change ion selectivity and become permeable to sodium in extracellular acidification. *J Biol Chem* 287: 37145–37153, 2012. doi:10.1074/jbc.M112.398164.
411. Chen H, Chatelain FC, Lesage F. Altered and dynamic ion selectivity of K⁺ channels in cell development and excitability. *Trends Pharmacol Sci* 35: 461–469, 2014. doi:10.1016/j.tips.2014.06.002.
412. Limberg SH, Netter MF, Rolfes C, Rinné S, Schlichthörl G, Zuzarte M, Vassiliou T, Moosdorf R, Wulf H, Daut J, Sachse FB, Decher N. TASK-1 channels may modulate action potential duration of human atrial cardiomyocytes. *Cell Physiol Biochem* 28: 613–624, 2011. doi:10.1159/000335757.
413. Schmidt C, Wiedmann F, Voigt N, Zhou XB, Heijman J, Lang S, Albert V, Kallenberger S, Ruhparwar A, Szabó G, Kallenbach K, Karck M, Borggreffe M, Biliczki P, Ehrlich JR, Baczkó I, Lugenbiel P, Schweizer PA, Donner BC, Katus HA, Dobrev D, Thomas D. Upregulation of K_{2p}3.1 K⁺ current causes action potential shortening in patients with chronic atrial fibrillation. *Circulation* 132: 82–92, 2015. doi:10.1161/CIRCULATIONAHA.114.012657.
414. Schmidt C, Wiedmann F, Kallenberger SM, Ratte A, Schulte JS, Scholz B, Müller FU, Voigt N, Zafeiriou MP, Ehrlich JR, Tochtermann U, Veres G, Ruhparwar A, Karck M, Katus HA, Thomas D. Stretch-activated two-pore-domain (K2P) potassium channels in the heart: focus on atrial fibrillation and heart failure. *Prog Biophys Mol Biol* 130: 233–243, 2017. doi:10.1016/j.pbiomolbio.2017.05.004.
415. Wiedmann F, Schulte JS, Gomes B, Zafeiriou MP, Ratte A, Rathjens F, Fehrmann E, Scholz B, Voigt N, Müller FU, Thomas D, Katus HA, Schmidt C. Atrial fibrillation and heart failure-associated remodeling of two-pore-domain potassium (K2P) channels in murine disease models: focus on TASK-1. *Basic Res Cardiol* 113: 27, 2018. doi:10.1007/s00395-018-0687-9.
416. Rinné S, Kiper AK, Schlichthörl G, Dittmann S, Netter MF, Limberg SH, Silbernagel N, Zuzarte M, Moosdorf R, Wulf H, Schulze-Bahr E, Rolfes C, Decher N. TASK-1 and TASK-3 may form heterodimers in human atrial cardiomyocytes. *J Mol Cell Cardiol* 81: 71–80, 2015. doi:10.1016/j.jmcc.2015.01.017.
417. Rinné S, Kiper AK, Schmidt C, Ortiz-Bonnin B, Zwiener S, Seeböhm G, Decher N. Stress-kinase regulation of TASK-1 and TASK-3. *Cell Physiol Biochem* 44: 1024–1037, 2017. doi:10.1159/000485402.
418. Friedrich C, Rinné S, Zumhagen S, Kiper AK, Silbernagel N, Netter MF, Stallmeyer B, Schulze-Bahr E, Decher N. Gain-of-function mutation in TASK-4 channels and severe cardiac conduction disorder. *EMBO Mol Med* 6: 937–951, 2014. doi:10.15252/emmm.201303783.
419. Bodnár M, Schlichthörl G, Daut J. The potassium current carried by TREK-1 channels in rat cardiac ventricular muscle. *Pflügers Arch* 467: 1069–1079, 2015. doi:10.1007/s00424-014-1678-9.
420. Decher N, Kiper AK, Rinné S. Stretch-activated potassium currents in the heart: Focus on TREK-1 and arrhythmias. *Prog Biophys Mol Biol* 130: 223–232, 2017. doi:10.1016/j.pbiomolbio.2017.05.005.
421. Decher N, Ortiz-Bonnin B, Friedrich C, Schewe M, Kiper AK, Rinné S, Seemann G, Peyronnet R, Zumhagen S, Bustos D, Kockskämper J, Kohl P, Just S, González W, Baukrowitz T, Stallmeyer B, Schulze-Bahr E. Sodium permeable and “hypersensitive” TREK-1 channels cause ventricular tachycardia. *EMBO Mol Med* 9: 403–414, 2017. doi:10.15252/emmm.201606690.
422. Lugenbiel P, Wenz F, Syren P, Geschwill P, Govorov K, Seyler C, Frank D, Schweizer PA, Franke J, Weis T, Bruehl C, Schmack B, Ruhparwar A, Karck M, Frey N, Katus HA, Thomas D. TREK-1 (K2P2.1) K⁺ channels are suppressed in patients with atrial fibrillation and heart failure and provide therapeutic targets for rhythm control. *Basic Res Cardiol* 112: 8, 2017. doi:10.1007/s00395-016-0597-7.
423. Schmidt C, Wiedmann F, Schweizer PA, Katus HA, Thomas D. Inhibition of cardiac two-pore-domain K⁺ (K2P) channels—an emerging antiarrhythmic concept. *Eur J Pharmacol* 738: 250–255, 2014. doi:10.1016/j.ejphar.2014.05.056.
424. Schmidt C, Wiedmann F, Tristram F, Anand P, Wenzel W, Lugenbiel P, Schweizer PA, Katus HA, Thomas D. Cardiac expression and atrial fibrillation-associated remodeling of K_{2p}2.1 (TREK-1) K⁺ channels in a porcine model. *Life Sci* 97: 107–115, 2014. doi:10.1016/j.lfs.2013.12.006.
425. Schmidt C, Wiedmann F, Zhou XB, Heijman J, Voigt N, Ratte A, Lang S, Kallenberger SM, Campana C, Weymann A, De Simone R, Szabo G, Ruhparwar A, Kallenbach K, Karck M, Ehrlich JR, Baczkó I, Borggreffe M, Ravens U, Dobrev D, Katus HA, Thomas D. Inverse remodelling of K2P3.1 K⁺ channel expression and action potential duration in left ventricular dysfunction and atrial fibrillation: implications for patient-specific antiarrhythmic drug therapy. *Eur Heart J* 38: 1764–1774, 2017. doi:10.1093/eurheartj/ehw559.
426. Abraham DM, Lee TE, Watson LJ, Mao L, Chandok G, Wang HG, Frangakis S, Pitt GS, Shah SH, Wolf MJ, Rockman HA. The two-pore domain potassium channel TREK-1 mediates cardiac fibrosis and diastolic dysfunction. *J Clin Invest* 128: 4843–4855, 2018. doi:10.1172/JCI95945.
427. Goonetilleke L, Quayle J. TREK-1 K⁺ channels in the cardiovascular system: their significance and potential as a therapeutic target. *Cardiovasc Ther* 30: e23–e29, 2012. doi:10.1111/j.1755-5922.2010.00227.x.
428. Schindler RF, Poon KL, Simrick S, Brand T. The Popeye domain containing genes: essential elements in heart rate control. *Cardiovasc Diagn Ther* 2: 308–319, 2012. doi:10.3978/j.issn.2223-3652.2012.12.01.
429. Zuo D, Chen K, Zhou M, Liu Z, Chen H. Kir2.1 and K2P1 channels reconstitute two levels of resting membrane potential in cardiomyocytes. *J Physiol* 595: 5129–5142, 2017. doi:10.1113/JP274268.
430. Masuda M, de Magalhães Engel G, Barbosa Moreira A. Characterization of isolated ventricular myocytes: two levels of resting potential. *J Mol Cell Cardiol* 19: 831–839, 1987. doi:10.1016/S0022-2828(87)80612-0.
431. Wiggins JR, Cranefield PF. Two levels of resting potential in canine cardiac Purkinje fibers exposed to sodium-free solutions. *Circ Res* 39: 466–474, 1976. doi:10.1161/01.res.39.4.466.
432. Gadsby DC, Cranefield PF. Two levels of resting potential in cardiac Purkinje fibers. *J Gen Physiol* 70: 725–746, 1977. doi:10.1085/jgp.70.6.725.
433. McCullough JR, Chua WT, Rasmussen HH, Ten Eick RE, Singer DH. Two stable levels of diastolic potential at physiological K⁺ concentrations in human ventricular myocardial cells. *Circ Res* 66: 191–201, 1990. doi:10.1161/01.res.66.1.191.
434. Morotti S, McCulloch AD, Bers DM, Edwards AG, Grandi E. Atrial-selective targeting of arrhythmogenic phase-3 early after-

- depolarizations in human myocytes. **J Mol Cell Cardiol** 96: 63–71, 2016. doi:10.1016/j.yjmcc.2015.07.030.
435. Bueno-Orovio A, Sánchez C, Pueyo E, Rodríguez B. Na/K pump regulation of cardiac repolarization: insights from a systems biology approach. **Pflugers Arch** 466: 183–193, 2014. doi:10.1007/s00424-013-1293-1.
436. Britton OJ, Bueno-Orovio A, Virág L, Varró A, Rodríguez B. The electrogenic Na⁺/K⁺ pump is a key determinant of repolarization abnormality susceptibility in human ventricular cardiomyocytes: a population-based simulation study. **Front Physiol** 8: 278, 2017. doi:10.3389/fphys.2017.00278.
437. Bers DM, Despa S. Na/K-ATPase—an integral player in the adrenergic fight-or-flight response. **Trends Cardiovasc Med** 19: 111–118, 2009. doi:10.1016/j.tcm.2009.07.001.
438. Stein WD. Energetics and the design principles of the Na/K-ATPase. **J Theor Biol** 147: 145–159, 1990. doi:10.1016/s0022-5193(05)80049-9.
439. Lingrel J, Moseley A, Dostanic I, Coughon M, He S, James P, Woo A, O'Connor K, Neumann J. Functional roles of the alpha isoforms of the Na,K-ATPase. **Ann NY Acad Sci** 986: 354–359, 2003. doi:10.1111/j.1749-6632.2003.tb07214.x.
440. Shattock MJ, Ottolia M, Bers DM, Blaustein MP, Boguslavskyi A, Bossuyt J, Bridge JH, Chen-Izu Y, Clancy CE, Edwards A, Goldhaber J, Kaplan J, Lingrel JB, Pavlovic D, Philipson K, Sipido KR, Xie ZJ. Na⁺/Ca²⁺ exchange and Na⁺/K⁺-ATPase in the heart. **J Physiol** 593: 1361–1382, 2015. doi:10.1113/jphysiol.2014.282319.
441. Despa S, Bers DM. Functional analysis of Na⁺/K⁺-ATPase isoform distribution in rat ventricular myocytes. **Am J Physiol Cell Physiol** 293: C321–C327, 2007. doi:10.1152/ajpcell.00597.2006.
442. Despa S, Lingrel JB, Bers DM. Na⁺/K⁺-ATPase alpha2-isoform preferentially modulates Ca²⁺ transients and sarcoplasmic reticulum Ca²⁺ release in cardiac myocytes. **Cardiovasc Res** 95: 480–486, 2012. doi:10.1093/cvr/cvs213.
443. Yuen GK, Galice S, Bers DM. Subcellular localization of Na/K-ATPase isoforms in ventricular myocytes. **J Mol Cell Cardiol** 108: 158–169, 2017. doi:10.1016/j.yjmcc.2017.05.013.
444. Berry RG, Despa S, Fuller W, Bers DM, Shattock MJ. Differential distribution and regulation of mouse cardiac Na⁺/K⁺-ATPase alpha1 and alpha2 subunits in T-tubule and surface sarcolemmal membranes. **Cardiovasc Res** 73: 92–100, 2007. doi:10.1016/j.cardiores.2006.11.006.
445. Eisner DA, Lederer WJ, Vaughan-Jones RD. The electrogenic Na pump in mammalian cardiac muscle. **Soc Gen Physiol Ser** 38: 193–213, 1984.
446. Bossuyt J, Despa S, Han F, Hou Z, Robia SL, Lingrel JB, Bers DM. Isoform specificity of the Na/K-ATPase association and regulation by phospholemman. **J Biol Chem** 284: 26749–26757, 2009. doi:10.1074/jbc.M109.047357.
447. Glitsch HG, Krahn T, Pusch H, Suleymanian M. Effect of isoprenaline on active Na transport in sheep cardiac Purkinje fibres. **Pflugers Arch** 415: 88–94, 1989. doi:10.1007/BF00373145.
448. Shah A, Cohen IS, Rosen MR. Stimulation of cardiac alpha receptors increases Na/K pump current and decreases gK via a pertussis toxin-sensitive pathway. **Biophys J** 54: 219–225, 1988. doi:10.1016/S0006-3495(88)82950-3.
449. Hansen PS, Buhagiar KA, Gray DF, Rasmussen HH. Voltage-dependent stimulation of the Na⁺-K⁺ pump by insulin in rabbit cardiac myocytes. **Am J Physiol Cell Physiol** 278: C546–C553, 2000. doi:10.1152/ajpcell.2000.278.3.C546.
450. Geering K. Functional roles of Na,K-ATPase subunits. **Curr Opin Nephrol Hypertens** 17: 526–532, 2008. doi:10.1097/MNH.0b013e3283036cbf.
451. Pavlovic D, Fuller W, Shattock MJ. Novel regulation of cardiac Na pump via phospholemman. **J Mol Cell Cardiol** 61: 83–93, 2013. doi:10.1016/j.yjmcc.2013.05.002.
452. Schatzmann HJ. [Cardiac glycosides as inhibitors of active potassium and sodium transport by erythrocyte membrane]. **Helv Physiol Pharmacol Acta** 11: 346–354, 1953.
453. Glitsch HG. Electrophysiology of the sodium-potassium-ATPase in cardiac cells. **Physiol Rev** 81: 1791–1826, 2001. doi:10.1152/physrev.2001.81.4.1791.
454. Lytton J. Na⁺/Ca²⁺ exchangers: three mammalian gene families control Ca²⁺ transport. **Biochem J** 406: 365–382, 2007. doi:10.1042/BJ20070619.
455. Lee SL, Yu AS, Lytton J. Tissue-specific expression of Na⁺-Ca²⁺ exchanger isoforms. **J Biol Chem** 269: 14849–14852, 1994. doi:10.1016/S0021-9258(17)36540-7.
456. Nicoll DA, Longoni S, Philipson KD. Molecular cloning and functional expression of the cardiac sarcolemmal Na⁺-Ca²⁺ exchanger. **Science** 250: 562–565, 1990. doi:10.1126/science.1700476.
457. Nicoll DA, Quednau BD, Qui Z, Xia YR, Lusi AJ, Philipson KD. Cloning of a third mammalian Na⁺-Ca²⁺ exchanger, NCX3. **J Biol Chem** 271: 24914–24921, 1996. doi:10.1074/jbc.271.40.24914.
458. Quednau BD, Nicoll DA, Philipson KD. Tissue specificity and alternative splicing of the Na⁺/Ca²⁺ exchanger isoforms NCX1, NCX2, and NCX3 in rat. **Am J Physiol Cell Physiol** 272: C1250–C1261, 1997. doi:10.1152/ajpcell.1997.272.4.C1250.
459. Ren X, Philipson KD. The topology of the cardiac Na⁺/Ca²⁺ exchanger, NCX1. **J Mol Cell Cardiol** 57: 68–71, 2013. doi:10.1016/j.yjmcc.2013.01.010.
460. Khananshvil D. The SLC8 gene family of sodium-calcium exchangers (NCX)—structure, function, and regulation in health and disease. **Mol Aspects Med** 34: 220–235, 2013. doi:10.1016/j.mam.2012.07.003.
461. Matsuoka S, Nicoll DA, He Z, Philipson KD. Regulation of cardiac Na⁺-Ca²⁺ exchanger by the endogenous XIP region. **J Gen Physiol** 109: 273–286, 1997. doi:10.1085/jgp.109.2.273.
462. Szerencsei RT, Kinjo TG, Schnetkamp PP. The topology of the C-terminal sections of the NCX1 Na⁺/Ca²⁺ exchanger and the NCKX2 Na⁺/Ca²⁺-K⁺ exchanger. **Channels (Austin)** 7: 109–114, 2013. doi:10.4161/chan.23898.
463. Eisner DA, Caldwell JL, Kistamas K, Trafford AW. Calcium and excitation-contraction coupling in the heart. **Circ Res** 121: 181–195, 2017. doi:10.1161/CIRCRESAHA.117.310230.
464. Hurtado C, Prociuk M, Maddaford TG, Dibrov E, Mesaali N, Hryshko LV, Pierce GN. Cells expressing unique Na⁺/Ca²⁺ exchange (NCX1) splice variants exhibit different susceptibilities to Ca²⁺ overload. **Am J Physiol Heart Circ Physiol** 290: H2155–H2162, 2006. doi:10.1152/ajpheart.00958.2005.
465. Kraev A, Chumakov I, Carafoli E. Molecular biological studies of the cardiac sodium-calcium exchanger. **Ann NY Acad Sci** 779: 103–109, 1996. doi:10.1111/j.1749-6632.1996.tb44774.x.

466. Li GR, Nattel S. Demonstration of an inward Na^+ - Ca^{2+} exchange current in adult human atrial myocytes. *Ann NY Acad Sci* 779: 525–528, 1996. doi:[10.1111/j.1749-6632.1996.tb44827.x](https://doi.org/10.1111/j.1749-6632.1996.tb44827.x).
467. Sher AA, Noble PJ, Hinch R, Gavaghan DJ, Noble D. The role of the $\text{Na}^+/\text{Ca}^{2+}$ exchangers in Ca^{2+} dynamics in ventricular myocytes. *Prog Biophys Mol Biol* 96: 377–398, 2008. doi:[10.1016/j.pbiomolbio.2007.07.018](https://doi.org/10.1016/j.pbiomolbio.2007.07.018).
468. Bers DM, Weber CR. Na/Ca exchange function in intact ventricular myocytes. *Ann NY Acad Sci* 976: 500–512, 2002. doi:[10.1111/j.1749-6632.2002.tb04784.x](https://doi.org/10.1111/j.1749-6632.2002.tb04784.x).
469. Kohajda Z, Farkas-Morvay N, Jost N, Nagy N, Geramipour A, Horvath A, Varga RS, Hornyik T, Corici C, Acsai K, Horváth B, Prorok J, Ördög B, Déri S, Tóth D, Levijoki J, Pollesello P, Koskelainen T, Otsomaa L, Tóth A, Baczkó I, Leprán I, Nánási PP, Papp JG, Varró A, Virág L. The effect of a novel highly selective inhibitor of the sodium/calcium exchanger (NCX) on cardiac arrhythmias in in vitro and in vivo experiments. *PLoS One* 11: e0166041, 2016. doi:[10.1371/journal.pone.0166041](https://doi.org/10.1371/journal.pone.0166041).
470. Nagy N, Kormos A, Kohajda Z, Szebeni A, Szepesi J, Pollesello P, Levijoki J, Acsai K, Virág L, Nánási PP, Papp JG, Varró A, Tóth A. Selective $\text{Na}^+/\text{Ca}^{2+}$ exchanger inhibition prevents Ca^{2+} overload-induced triggered arrhythmias. *Br J Pharmacol* 171: 5665–5681, 2014. doi:[10.1111/bph.12867](https://doi.org/10.1111/bph.12867).
471. Christ T, Kovács PP, Acsai K, Knaut M, Eschenhagen T, Jost N, Varró A, Wettwer E, Ravens U. Block of $\text{Na}^+/\text{Ca}^{2+}$ exchanger by SEA0400 in human right atrial preparations from patients in sinus rhythm and in atrial fibrillation. *Eur J Pharmacol* 788: 286–293, 2016. doi:[10.1016/j.ejphar.2016.06.050](https://doi.org/10.1016/j.ejphar.2016.06.050).
472. Hurtado C, Ander BP, Maddaford TG, Lukas A, Hryshko LV, Pierce GN. Adenovirally delivered shRNA strongly inhibits $\text{Na}^+/\text{Ca}^{2+}$ exchanger expression but does not prevent contraction of neonatal cardiomyocytes. *J Mol Cell Cardiol* 38: 647–654, 2005. doi:[10.1016/j.yjmcc.2005.02.007](https://doi.org/10.1016/j.yjmcc.2005.02.007).
473. Puglisi JL, Bassani RA, Bassani JW, Amin JN, Bers DM. Temperature and relative contributions of Ca transport systems in cardiac myocyte relaxation. *Am J Physiol Heart Circ Physiol* 270: H1772–H1778, 1996. doi:[10.1152/ajpheart.1996.270.5.H1772](https://doi.org/10.1152/ajpheart.1996.270.5.H1772).
474. Jost N, Nagy N, Corici C, Kohajda Z, Horváth A, Acsai K, Biliczki P, Levijoki J, Pollesello P, Koskelainen T, Otsomaa L, Tóth A, Papp JG, Varró A, Virág L. ORM-10103, a novel specific inhibitor of the $\text{Na}^+/\text{Ca}^{2+}$ exchanger, decreases early and delayed afterdepolarizations in the canine heart. *Br J Pharmacol* 170: 768–778, 2013. doi:[10.1111/bph.12228](https://doi.org/10.1111/bph.12228).
475. Nagy ZA, Virág L, Tóth A, Biliczki P, Acsai K, Bányász T, Nánási P, Papp JG, Varró A. Selective inhibition of sodium-calcium exchanger by SEA-0400 decreases early and delayed after depolarization in canine heart. *Br J Pharmacol* 143: 827–831, 2004. doi:[10.1038/sj.bjp.0706026](https://doi.org/10.1038/sj.bjp.0706026).
476. Zhao Z, Wen H, Fefelova N, Allen C, Baba A, Matsuda T, Xie LH. Revisiting the ionic mechanisms of early afterdepolarizations in cardiomyocytes: predominant by Ca waves or Ca currents? *Am J Physiol Heart Circ Physiol* 302: H1636–H1644, 2012. doi:[10.1152/ajpheart.00742.2011](https://doi.org/10.1152/ajpheart.00742.2011).
477. Milberg P, Pott C, Fink M, Frommeyer G, Matsuda T, Baba A, Osada N, Breithardt G, Noble D, Eckardt L. Inhibition of the $\text{Na}^+/\text{Ca}^{2+}$ exchanger suppresses torsades de pointes in an intact heart model of long QT syndrome-2 and long QT syndrome-3. *Heart Rhythm* 5: 1444–1452, 2008. doi:[10.1016/j.hrthm.2008.06.017](https://doi.org/10.1016/j.hrthm.2008.06.017).
478. Bovo E, de Tombe PP, Zima AV. The role of dyadic organization in regulation of sarcoplasmic reticulum Ca^{2+} handling during rest in rabbit ventricular myocytes. *Biophys J* 106: 1902–1909, 2014. doi:[10.1016/j.bpj.2014.03.032](https://doi.org/10.1016/j.bpj.2014.03.032).
479. Garciarena CD, Youm JB, Swietach P, Vaughan-Jones RD. H^+ -activated Na^+ influx in the ventricular myocyte couples Ca^{2+} -signalling to intracellular pH. *J Mol Cell Cardiol* 61: 51–59, 2013. doi:[10.1016/j.yjmcc.2013.04.008](https://doi.org/10.1016/j.yjmcc.2013.04.008).
480. Sipido KR, Acsai K, Antoons G, Bito V, Macquaide N. T-tubule remodelling and ryanodine receptor organization modulate sodium-calcium exchange. *Adv Exp Med Biol* 961: 375–383, 2013. doi:[10.1007/978-1-4614-4756-6_32](https://doi.org/10.1007/978-1-4614-4756-6_32).
481. Scriven DR, Moore ED. Ca^{2+} channel and $\text{Na}^+/\text{Ca}^{2+}$ exchange localization in cardiac myocytes. *J Mol Cell Cardiol* 58: 22–31, 2013. doi:[10.1016/j.yjmcc.2012.11.022](https://doi.org/10.1016/j.yjmcc.2012.11.022).
482. Levesque PC, Leblanc N, Hume JR. Role of reverse-mode $\text{Na}^+/\text{Ca}^{2+}$ exchange in excitation-contraction coupling in the heart. *Ann NY Acad Sci* 639: 386–397, 1991. doi:[10.1111/j.1749-6632.1991.tb17327.x](https://doi.org/10.1111/j.1749-6632.1991.tb17327.x).
483. Acsai K, Antoons G, Livshitz L, Rudy Y, Sipido KR. Microdomain $[\text{Ca}^{2+}]$ near ryanodine receptors as reported by L-type Ca^{2+} and $\text{Na}^+/\text{Ca}^{2+}$ exchange currents. *J Physiol* 589: 2569–2583, 2011. doi:[10.1113/jphysiol.2010.202663](https://doi.org/10.1113/jphysiol.2010.202663).
484. Zamparelli C, Macquaide N, Colotti G, Verzili D, Seidler T, Smith GL, Chiancone E. Activation of the cardiac $\text{Na}^+/\text{Ca}^{2+}$ exchanger by sorcin via the interaction of the respective Ca^{2+} -binding domains. *J Mol Cell Cardiol* 49: 132–141, 2010. doi:[10.1016/j.yjmcc.2010.03.003](https://doi.org/10.1016/j.yjmcc.2010.03.003).
485. Villa-Abrille MC, Sidor A, O'Rourke B. Insulin effects on cardiac $\text{Na}^+/\text{Ca}^{2+}$ exchanger activity: role of the cytoplasmic regulatory loop. *J Biol Chem* 283: 16505–16513, 2008. doi:[10.1074/jbc.M801424200](https://doi.org/10.1074/jbc.M801424200).
486. Condrescu M, Reeves JP. Actin-dependent regulation of the cardiac $\text{Na}^+/\text{Ca}^{2+}$ exchanger. *Am J Physiol Cell Physiol* 290: C691–C701, 2006. doi:[10.1152/ajpcell.00232.2005](https://doi.org/10.1152/ajpcell.00232.2005).
487. Whitmer JT, Idell-Wenger JA, Rovetto MJ, Neely JR. Control of fatty acid metabolism in ischemic and hypoxic hearts. *J Biol Chem* 253: 4305–4309, 1978.
488. Finck BN, Han X, Courtois M, Aïmond F, Nerbonne JM, Kovacs A, Gross RW, Kelly DP. A critical role for PPAR α -mediated lipotoxicity in the pathogenesis of diabetic cardiomyopathy: modulation by dietary fat content. *Proc Natl Acad Sci USA* 100: 1226–1231, 2003. doi:[10.1073/pnas.0336724100](https://doi.org/10.1073/pnas.0336724100).
489. Sharma S, Adroque JV, Golfman L, Uray I, Lemm J, Youker K, Noon GP, Frazier OH, Taegtmeyer H. Intramyocardial lipid accumulation in the failing human heart resembles the lipotoxic rat heart. *FASEB J* 18: 1692–1700, 2004. doi:[10.1096/fj.04-2263com](https://doi.org/10.1096/fj.04-2263com).
490. Riedel MJ, Baczkó I, Searle GJ, Webster N, Fercho M, Jones L, Lang J, Lytton J, Dyck JR, Light PE. Metabolic regulation of sodium-calcium exchange by intracellular acyl CoAs. *EMBO J* 25: 4605–4614, 2006. doi:[10.1038/sj.emboj.7601321](https://doi.org/10.1038/sj.emboj.7601321).
491. Orchard CH, Cingolani HE. Acidosis and arrhythmias in cardiac muscle. *Cardiovasc Res* 28: 1312–1319, 1994. doi:[10.1093/cvr/28.9.1312](https://doi.org/10.1093/cvr/28.9.1312).
492. Scranton K, John S, Escobar A, Goldhaber J, Ottolia M. Modulation of the cardiac $\text{Na}^+/\text{Ca}^{2+}$ exchanger by cytoplasmic protons: molecular mechanisms and physiological implications. *Cell Calcium* 87: 102140, 2020. doi:[10.1016/j.ceca.2019.102140](https://doi.org/10.1016/j.ceca.2019.102140).

493. Langenbacher AD, Dong Y, Shu X, Choi J, Nicoll DA, Goldhaber JL, Philipson KD, Chen JN. Mutation in sodium-calcium exchanger 1 (NCX1) causes cardiac fibrillation in zebrafish. **Proc Natl Acad Sci USA** 102: 17699–17704, 2005. doi:10.1073/pnas.0502679102.
494. Murer H, Hopfer U, Kinne R. Sodium/proton antiport in brush-border-membrane vesicles isolated from rat small intestine and kidney. **Biochem J** 154: 597–604, 1976. doi:10.1042/bj1540597.
495. Orlowski J, Grinstein S. Na^+/H^+ exchangers of mammalian cells. **J Biol Chem** 272: 22373–22376, 1997. doi:10.1074/jbc.272.36.22373.
496. Wakabayashi S, Hisamitsu T, Nakamura TY. Regulation of the cardiac Na^+/H^+ exchanger in health and disease. **J Mol Cell Cardiol** 61: 68–76, 2013. doi:10.1016/j.yjmcc.2013.02.007.
497. Fliegel L, Dyck JR, Wang H, Fong C, Haworth RS. Cloning and analysis of the human myocardial Na^+/H^+ exchanger. **Mol Cell Biochem** 125: 137–143, 1993. doi:10.1007/BF00936442.
498. Aharonovitz O, Zaun HC, Balla T, York JD, Orlowski J, Grinstein S. Intracellular pH regulation by Na^+/H^+ exchange requires phosphatidylinositol 4,5-bisphosphate. **J Cell Biol** 150: 213–224, 2000. doi:10.1083/jcb.150.1.213.
499. Köster S, Pavkov-Keller T, Kühlbrandt W, Yildiz O. Structure of human Na^+/H^+ exchanger NHE1 regulatory region in complex with calmodulin and Ca^{2+} . **J Biol Chem** 286: 40954–40961, 2011. doi:10.1074/jbc.M111.286906.
500. Lee BL, Sykes BD, Fliegel L. Structural and functional insights into the cardiac Na^+/H^+ exchanger. **J Mol Cell Cardiol** 61: 60–67, 2013. doi:10.1016/j.yjmcc.2012.11.019.
501. Orlowski J, Kandasamy RA. Delineation of transmembrane domains of the Na^+/H^+ exchanger that confer sensitivity to pharmacological antagonists. **J Biol Chem** 271: 19922–19927, 1996. doi:10.1074/jbc.271.33.19922.
502. Pang T, Su X, Wakabayashi S, Shigekawa M. Calcineurin homologous protein as an essential cofactor for Na^+/H^+ exchangers. **J Biol Chem** 276: 17367–17372, 2001. doi:10.1074/jbc.M100296200.
503. Sardet C, Franchi A, Pouyssegur J. Molecular cloning, primary structure, and expression of the human growth factor-activatable Na^+/H^+ antiporter. **Cell** 56: 271–280, 1989. doi:10.1016/0092-8674(89)90901-x.
504. Wakabayashi S, Pang T, Su X, Shigekawa M. A novel topology model of the human Na^+/H^+ exchanger isoform 1. **J Biol Chem** 275: 7942–7949, 2000. doi:10.1074/jbc.275.11.7942.
505. Fafournoux P, Noël J, Pouyssegur J. Evidence that Na^+/H^+ exchanger isoforms NHE1 and NHE3 exist as stable dimers in membranes with a high degree of specificity for homodimers. **J Biol Chem** 269: 2589–2596, 1994.
506. Fuster D, Moe OW, Hilgemann DW. Steady-state function of the ubiquitous mammalian Na^+/H^+ exchanger (NHE1) in relation to dimer coupling models with $2\text{Na}^+/\text{H}^+$ stoichiometry. **J Gen Physiol** 132: 465–480, 2008. doi:10.1085/jgp.200810016.
507. Wakabayashi S, Shigekawa M, Pouyssegur J. Molecular physiology of vertebrate Na^+/H^+ exchangers. **Physiol Rev** 77: 51–74, 1997. doi:10.1152/physrev.1997.77.1.51.
508. Alexander RT, Grinstein S. Na^+/H^+ exchangers and the regulation of volume. **Acta Physiol (Oxf)** 187: 159–167, 2006. doi:10.1111/j.1748-1716.2006.01558.x.
509. Despa S. Myocyte $[\text{Na}^+]_i$ dysregulation in heart failure and diabetic cardiomyopathy. **Front Physiol** 9: 1303, 2018. doi:10.3389/fphys.2018.01303.
510. Frelin C, Vigne P, Lazdunski M. The role of the Na^+/H^+ exchange system in the regulation of the internal pH in cultured cardiac cells. **Eur J Biochem** 149: 1–4, 1985. doi:10.1111/j.1432-1033.1985.tb08884.x.
511. Baczkó I, Mraiche F, Light PE, Fliegel L. Diastolic calcium is elevated in metabolic recovery of cardiomyocytes expressing elevated levels of the Na^+/H^+ exchanger. **Can J Physiol Pharmacol** 86: 850–859, 2008. doi:10.1139/Y08-092.
512. Bkaily G, Chahine M, Al-Khoury J, Avedanian L, Beier N, Scholz W, Jacques D. Na^+/H^+ exchanger inhibitor prevents early death in hereditary cardiomyopathy. **Can J Physiol Pharmacol** 93: 923–934, 2015. doi:10.1139/cjpp-2015-0107.
513. Bkaily G, Jacques D. Na^+/H^+ exchanger and proton channel in heart failure associated with Becker and Duchenne muscular dystrophies. **Can J Physiol Pharmacol** 95: 1213–1223, 2017. doi:10.1139/cjpp-2017-0265.
514. Packer M. Activation and inhibition of sodium-hydrogen exchanger is a mechanism that links the pathophysiology and treatment of diabetes mellitus with that of heart failure. **Circulation** 136: 1548–1559, 2017. doi:10.1161/CIRCULATIONAHA.117.030418.
515. DiFrancesco D. The role of the funny current in pacemaker activity. **Circ Res** 106: 434–446, 2010. doi:10.1161/CIRCRESAHA.109.208041.
516. DiFrancesco D, Noble D. Rebuttal: “The funny current in the context of the coupled clock pacemaker cell system”. **Heart Rhythm** 9: 457–458, 2012. doi:10.1016/j.hrthm.2011.09.023.
517. Morad M, Zhang XH. Mechanisms of spontaneous pacing: sinoatrial nodal cells, neonatal cardiomyocytes, and human stem cell derived cardiomyocytes. **Can J Physiol Pharmacol** 95: 1100–1107, 2017. doi:10.1139/cjpp-2016-0743.
518. Verkerk AO, Wilders R, van Borren MM, Peters RJ, Broekhuis E, Lam K, Coronel R, de Bakker JM, Tan HL. Pacemaker current (I_h) in the human sinoatrial node. **Eur Heart J** 28: 2472–2478, 2007. doi:10.1093/eurheartj/ehm339.
519. Vinogradova TM, Tagirova Sirenko S, Lakatta EG. Unique Ca^{2+} -cycling protein abundance and regulation sustains local Ca^{2+} releases and spontaneous firing of rabbit sinoatrial node cells. **Int J Mol Sci** 19: 2173, 2018. doi:10.3390/ijms19082173.
520. Weidmann S. Effect of current flow on the membrane potential of cardiac muscle. **J Physiol** 115: 227–236, 1951. doi:10.1113/jphysiol.1951.sp004667.
521. Hauswirth O, Noble D, Tsien RW. Adrenaline: mechanism of action on the pacemaker potential in cardiac Purkinje fibers. **Science** 162: 916–917, 1968. doi:10.1126/science.162.3856.916.
522. Hauswirth O, Noble D, Tsien RW. Separation of the pace-maker and plateau components of delayed rectification in cardiac Purkinje fibres. **J Physiol** 225: 211–235, 1972. doi:10.1113/jphysiol.1972.sp009934.
523. Alings AM, Bouman LN. Electrophysiology of the ageing rabbit and cat sinoatrial node—a comparative study. **Eur Heart J** 14: 1278–1288, 1993. doi:10.1093/eurheartj/14.9.1278.
524. DiFrancesco D. A new interpretation of the pace-maker current in calf Purkinje fibres. **J Physiol** 314: 359–376, 1981. doi:10.1113/jphysiol.1981.sp013713.

525. Maylie J, Morad M. Ionic currents responsible for the generation of pace-maker current in the rabbit sino-atrial node. **J Physiol** 355: 215–235, 1984. doi:[10.1113/jphysiol.1984.sp015415](https://doi.org/10.1113/jphysiol.1984.sp015415).
526. Hagiwara N, Irisawa H, Kameyama M. Contribution of two types of calcium currents to the pacemaker potentials of rabbit sino-atrial node cells. **J Physiol** 395: 233–253, 1988. doi:[10.1113/jphysiol.1988.sp016916](https://doi.org/10.1113/jphysiol.1988.sp016916).
527. Li Y, Fu X, Zhang Z, Yu B. Knockdown of cardiac Kir3.1 gene with siRNA can improve bradycardia in an experimental sinus bradycardia rat model. **Mol Cell Biochem** 429: 103–111, 2017. doi:[10.1007/s11010-017-2939-7](https://doi.org/10.1007/s11010-017-2939-7).
528. Verkerk AO, van Borren MM, Wilders R. Calcium transient and sodium-calcium exchange current in human versus rabbit sinoatrial node pacemaker cells. **ScientificWorldJournal** 2013: 507872, 2013. doi:[10.1155/2013/507872](https://doi.org/10.1155/2013/507872).
529. Verkerk AO, Wilders R, van Borren MM, Tan HL. Is sodium current present in human sinoatrial node cells? **Int J Biol Sci** 5: 201–204, 2009. doi:[10.7150/ijbs.5.201](https://doi.org/10.7150/ijbs.5.201).
530. Noma A, Morad M, Irisawa H. Does the “pacemaker current” generate the diastolic depolarization in the rabbit SA node cells? **Pflugers Arch** 397: 190–194, 1983. doi:[10.1007/BF00584356](https://doi.org/10.1007/BF00584356).
531. Capel RA, Terrar DA. Cytosolic calcium ions exert a major influence on the firing rate and maintenance of pacemaker activity in guinea-pig sinus node. **Front Physiol** 6: 23, 2015. doi:[10.3389/fphys.2015.00023](https://doi.org/10.3389/fphys.2015.00023).
532. Capel RA, Terrar DA. The importance of Ca²⁺-dependent mechanisms for the initiation of the heartbeat. **Front Physiol** 6: 80, 2015. doi:[10.3389/fphys.2015.00080](https://doi.org/10.3389/fphys.2015.00080).
533. Hüser J, Blatter LA, Lipsius SL. Intracellular Ca²⁺ release contributes to automaticity in cat atrial pacemaker cells. **J Physiol** 524: 415–422, 2000. doi:[10.1111/j.1469-7793.2000.00415.x](https://doi.org/10.1111/j.1469-7793.2000.00415.x).
534. Lakatta EG, Maltsev VA, Bogdanov KY, Stern MD, Vinogradova TM. Cyclic variation of intracellular calcium: a critical factor for cardiac pacemaker cell dominance. **Circ Res** 92: e45–e50, 2003. doi:[10.1161/01.res.0000055920.64384.fb](https://doi.org/10.1161/01.res.0000055920.64384.fb).
535. Lakatta EG, DiFrancesco D. What keeps us ticking: a funny current, a calcium clock, or both? **J Mol Cell Cardiol** 47: 157–170, 2009. doi:[10.1016/j.yjmcc.2009.03.022](https://doi.org/10.1016/j.yjmcc.2009.03.022).
536. Boyett MR, Honjo H, Kodama I. The sinoatrial node, a heterogeneous pacemaker structure. **Cardiovasc Res** 47: 658–687, 2000. doi:[10.1016/s0008-6363\(00\)00135-8](https://doi.org/10.1016/s0008-6363(00)00135-8).
537. Aréchiga-Figueroa IA, Rodríguez-Martínez M, Sánchez-Chapula JA. Voltage-dependent potassium currents in feline sino-atrial node myocytes. **Pflugers Arch** 462: 385–396, 2011. doi:[10.1007/s00424-011-0984-8](https://doi.org/10.1007/s00424-011-0984-8).
538. Kohajda Z, Tóth N, Szlovák J, Loewe A, Bitay G, Gazdag P, Prorok J, Jost N, Levijoki J, Pollesello P, Papp JG, Varró A, Nagy N. Novel Na⁺/Ca²⁺ exchanger inhibitor ORM-10962 supports coupled function of funny-current and Na⁺/Ca²⁺ exchanger in pacemaking of rabbit sinus node tissue. **Front Pharmacol** 10: 1632, 2019. doi:[10.3389/fphar.2019.01632](https://doi.org/10.3389/fphar.2019.01632).
539. Lei M, Cooper PJ, Camelliti P, Kohl P. Role of the 293b-sensitive, slowly activating delayed rectifier potassium current, I_{Ks}, in pacemaker activity of rabbit isolated sino-atrial node cells. **Cardiovasc Res** 53: 68–79, 2002. doi:[10.1016/S0008-6363\(01\)00459-X](https://doi.org/10.1016/S0008-6363(01)00459-X).
540. Ono K, Shibata S, Iijima T. Properties of the delayed rectifier potassium current in porcine sino-atrial node cells. **J Physiol** 524: 51–62, 2000. doi:[10.1111/j.1469-7793.2000.00051.x](https://doi.org/10.1111/j.1469-7793.2000.00051.x).
541. DiFrancesco D. Funny channel gene mutations associated with arrhythmias. **J Physiol** 591: 4117–4124, 2013. doi:[10.1113/jphysiol.2013.253765](https://doi.org/10.1113/jphysiol.2013.253765).
542. DiFrancesco D, Mangoni M. Modulation of single hyperpolarization-activated channels (i_h) by cAMP in the rabbit sino-atrial node. **J Physiol** 474: 473–482, 1994. doi:[10.1113/jphysiol.1994.sp020038](https://doi.org/10.1113/jphysiol.1994.sp020038).
543. Mesirca P, Marger L, Toyoda F, Rizzetto R, Audoubert M, Dubel S, Torrente AG, DiFrancesco ML, Muller JC, Leoni AL, Couette B, Nargeot J, Clapham DE, Wickman K, Mangoni ME. The G-protein-gated K⁺ channel, IKACH, is required for regulation of pacemaker activity and recovery of resting heart rate after sympathetic stimulation. **J Gen Physiol** 142: 113–126, 2013. doi:[10.1085/jgp.201310996](https://doi.org/10.1085/jgp.201310996).
544. Mangoni ME, Couette B, Bourinet E, Platzer J, Reimer D, Striessnig J, Nargeot J. Functional role of L-type Cav1.3 Ca²⁺ channels in cardiac pacemaker activity. **Proc Natl Acad Sci USA** 100: 5543–5548, 2003. doi:[10.1073/pnas.0935295100](https://doi.org/10.1073/pnas.0935295100).
545. Mangoni ME, Nargeot J. Genesis and regulation of the heart automaticity. **Physiol Rev** 88: 919–982, 2008. doi:[10.1152/physrev.00018.2007](https://doi.org/10.1152/physrev.00018.2007).
546. Zaniboni M, Cacciani F, Lux RL. Beat-to-beat cycle length variability of spontaneously beating guinea pig sinoatrial cells: relative contributions of the membrane and calcium clocks. **PLoS One** 9: e100242, 2014. doi:[10.1371/journal.pone.0100242](https://doi.org/10.1371/journal.pone.0100242).
547. Baruscotti M, Bianco E, Bucchi A, DiFrancesco D. Current understanding of the pathophysiological mechanisms responsible for inappropriate sinus tachycardia: role of the If “funny” current. **J Interv Card Electrophysiol** 46: 19–28, 2016. doi:[10.1007/s10840-015-0097-y](https://doi.org/10.1007/s10840-015-0097-y).
548. Huang X, Yang P, Du Y, Zhang J, Ma A. Age-related down-regulation of HCN channels in rat sinoatrial node. **Basic Res Cardiol** 102: 429–435, 2007. doi:[10.1007/s00395-007-0660-5](https://doi.org/10.1007/s00395-007-0660-5).
549. Caballero R, de la Fuente MG, Gómez R, Barana A, Amorós I, Dolz-Gaitón P, Osuna L, Almendral J, Atienza F, Fernández-Avilés F, Pita A, Rodríguez-Roda J, Pinto A, Tamargo J, Delpón E. In humans, chronic atrial fibrillation decreases the transient outward current and ultrarapid component of the delayed rectifier current differentially on each atria and increases the slow component of the delayed rectifier current in both. **J Am Coll Cardiol** 55: 2346–2354, 2010. doi:[10.1016/j.jacc.2010.02.028](https://doi.org/10.1016/j.jacc.2010.02.028).
550. Sánchez C, Bueno-Orovio A, Wettwer E, Loose S, Simon J, Ravens U, Pueyo E, Rodríguez B. Inter-subject variability in human atrial action potential in sinus rhythm versus chronic atrial fibrillation. **PLoS One** 9: e105897, 2014. doi:[10.1371/journal.pone.0105897](https://doi.org/10.1371/journal.pone.0105897).
551. Xu ZX, Jin MW. Characterization of transient outward K⁺ current and ultra-rapid delayed rectifier K⁺ current in isolated human atrial myocytes from patients with congestive heart failure. **Acta Pharmacol Sin** 23: 110–116, 2002.
552. Ravens U, Poulet C, Wettwer E, Knaut M. Atrial selectivity of antiarrhythmic drugs. **J Physiol** 591: 4087–4097, 2013. doi:[10.1113/jphysiol.2013.256115](https://doi.org/10.1113/jphysiol.2013.256115).
553. Li GR, Feng J, Wang Z, Fermini B, Nattel S. Comparative mechanisms of 4-aminopyridine-resistant I_{to} in human and rabbit atrial myocytes. **Am J Physiol Heart Circ Physiol** 269: H463–H472, 1995. doi:[10.1152/ajpheart.1995.269.2.H463](https://doi.org/10.1152/ajpheart.1995.269.2.H463).

554. Li GR, Feng J, Wang Z, Nattel S. Transmembrane chloride currents in human atrial myocytes. **Am J Physiol Cell Physiol** 270: C500–C507, 1996. doi:10.1152/ajpcell.1996.270.2.C500.
555. Xiao GS, Zhang YH, Wang Y, Sun HY, Baumgarten CM, Li GR. Noradrenaline up-regulates volume-regulated chloride current by PKA-independent cAMP/exchange protein activated by cAMP pathway in human atrial myocytes. **Br J Pharmacol** 175: 3422–3432, 2018. doi:10.1111/bph.14392.
556. Casini S, Marchal GA, Kawasaki M, Nariswari FA, Portero V, van den Berg NW, Guan K, Driessen AH, Veldkamp MW, Mengarelli I, de Groot JR, Verkerk AO, Remme CA. Absence of functional Nav1.8 channels in non-diseased atrial and ventricular cardiomyocytes. **Cardiovasc Drugs Ther** 33: 649–660, 2019. doi:10.1007/s10557-019-06925-6.
557. Bénitah JP, Gómez AM, Fauconnier J, Kerfant BG, Perrier E, Vassort G, Richard S. Voltage-gated Ca^{2+} currents in the human pathophysiologic heart: a review. **Basic Res Cardiol** 97, Suppl 1: 111–118, 2002. doi:10.1007/s003950200023.
558. Juhász V, Hornyik T, Benák A, Nagy N, Husty Z, Pap R, Ságghy L, Virág L, Varró A, Baczkó I. Comparison of the effects of IK, ACh, IKr, and INa block in conscious dogs with atrial fibrillation and on action potentials in remodeled atrial trabeculae. **Can J Physiol Pharmacol** 96: 18–25, 2018. doi:10.1139/cjpp-2017-0342.
559. Oshikawa N, Watanabe I, Masaki R, Shindo A, Kojima T, Saito S, Ozawa Y, Kanmatsuse K. Frequency-dependent electrophysiological effect of ibutilide on human atrium and ventricle. **J Interv Card Electrophysiol** 5: 81–87, 2001. doi:10.1023/a:1009866126492.
560. Du XL, Lau CP, Chiu SW, Tse HF, Gerlach U, Li GR. Effects of chromanol 293B on transient outward and ultra-rapid delayed rectifier potassium currents in human atrial myocytes. **J Mol Cell Cardiol** 35: 293–300, 2003. doi:10.1016/S0022-2828(03)00007-5.
561. Peng G, Barro-Soria R, Sampson KJ, Larsson HP, Kass RS. Gating mechanisms underlying deactivation slowing by two KCNQ1 atrial fibrillation mutations. **Sci Rep** 7: 45911, 2017. doi:10.1038/srep45911.
562. Qi XY, Diness JG, Brundel BJ, Zhou XB, Naud P, Wu CT, Huang H, Harada M, Aflaki M, Dobrev D, Grunnet M, Nattel S. Role of small-conductance calcium-activated potassium channels in atrial electrophysiology and fibrillation in the dog. **Circulation** 129: 430–440, 2014. doi:10.1161/CIRCULATIONAHA.113.003019.
563. Davis LD. Effects of autonomic neurohumors on transmembrane potentials of atrial plateau fibers. **Am J Physiol** 229: 1351–1356, 1975. doi:10.1152/ajplegacy.1975.229.5.1351.
564. Li N, Csepe TA, Hansen BJ, Sul LV, Kalyanasundaram A, Zakharkin SO, Zhao J, Guha A, Van Wagoner DR, Kilic A, Mohler PJ, Janssen PM, Biesiadecki BJ, Hummel JD, Weiss R, Fedorov VV. Adenosine-induced atrial fibrillation: localized reentrant drivers in lateral right atria due to heterogeneous expression of adenosine A_1 receptors and GIRK4 subunits in the human heart. **Circulation** 134: 486–498, 2016. doi:10.1161/CIRCULATIONAHA.115.021165.
565. Workman AJ, Kane KA, Rankin AC. Ionic basis of a differential effect of adenosine on refractoriness in rabbit AV nodal and atrial isolated myocytes. **Cardiovasc Res** 43: 974–984, 1999. doi:10.1016/S0008-6363(99)00166-2.
566. Pau D, Workman AJ, Kane KA, Rankin AC. Electrophysiological and arrhythmogenic effects of 5-hydroxytryptamine on human atrial cells are reduced in atrial fibrillation. **J Mol Cell Cardiol** 42: 54–62, 2007. doi:10.1016/j.yjmcc.2006.08.007.
567. Brunton TL, Fayrer J. XXII. Note on independent pulsation of the pulmonary veins and vena cava. **Proc R Soc Lond** 25: 174–176, 1877. doi:10.1098/rsp.1876.0041.
568. Cheung DW. Electrical activity of the pulmonary vein and its interaction with the right atrium in the guinea-pig. **J Physiol** 314: 445–456, 1981. doi:10.1113/jphysiol.1981.sp013718.
569. Haïssaguerre M, Jaïs P, Shah DC, Takahashi A, Hocini M, Quiniou G, Garrigue S, Le Mouroux A, Le MP, Clémenty J. Spontaneous initiation of atrial fibrillation by ectopic beats originating in the pulmonary veins. **N Engl J Med** 339: 659–666, 1998. doi:10.1056/NEJM199809033391003.
570. Hocini M, Ho SY, Kawara T, Linnenbank AC, Potse M, Shah D, Jaïs P, Janse MJ, Haïssaguerre M, De Bakker JM. Electrical conduction in canine pulmonary veins: electrophysiological and anatomic correlation. **Circulation** 105: 2442–2448, 2002. doi:10.1161/01.cir.0000016062.80020.11.
571. Chen YJ, Chen SA. Electrophysiology of pulmonary veins. **J Cardiovasc Electrophysiol** 17: 220–224, 2006. doi:10.1111/j.1540-8167.2005.00317.x.
572. Roney CH, Bayer JD, Cochet H, Meo M, Dubois R, Jaïs P, Vigmond EJ. Variability in pulmonary vein electrophysiology and fibrosis determines arrhythmia susceptibility and dynamics. **PLoS Comput Biol** 14: e1006166, 2018. doi:10.1371/journal.pcbi.1006166.
573. Huang SY, Chen YC, Kao YH, Hsieh MH, Chen YA, Chen WP, Lin YK, Chen SA, Chen YJ. Renal failure induces atrial arrhythmogenesis from discrepant electrophysiological remodeling and calcium regulation in pulmonary veins, sinoatrial node, and atria. **Int J Cardiol** 202: 846–857, 2016. doi:10.1016/j.ijcard.2015.10.004.
574. Huang SY, Chen YC, Kao YH, Hsieh MH, Lin YK, Chung CC, Lee TI, Tsai WC, Chen SA, Chen YJ. Fibroblast growth factor 23 dysregulates late sodium current and calcium homeostasis with enhanced arrhythmogenesis in pulmonary vein cardiomyocytes. **Oncotarget** 7: 69231–69242, 2016. doi:10.18632/oncotarget.12470.
575. Chen YJ, Chen SA, Chen YC, Yeh HI, Chan P, Chang MS, Lin CI. Effects of rapid atrial pacing on the arrhythmogenic activity of single cardiomyocytes from pulmonary veins: implication in initiation of atrial fibrillation. **Circulation** 104: 2849–2854, 2001. doi:10.1161/hc4801.099736.
576. Ehrlich JR, Cha TJ, Zhang L, Chartier D, Melnyk P, Hohnloser SH, Nattel S. Cellular electrophysiology of canine pulmonary vein cardiomyocytes: action potential and ionic current properties. **J Physiol** 551: 801–813, 2003. doi:10.1113/jphysiol.2003.046417.
577. Hamaguchi S, Hikita K, Tanaka Y, Tsuneoka Y, Namekata I, Tanaka H. Enhancement of automaticity by mechanical stretch of the isolated guinea pig pulmonary vein myocardium. **Biol Pharm Bull** 39: 1216–1219, 2016. doi:10.1248/bpb.b15-01013.
578. Chen YJ, Chen SA, Chang MS, Lin CI. Arrhythmogenic activity of cardiac muscle in pulmonary veins of the dog: implication for the genesis of atrial fibrillation. **Cardiovasc Res** 48: 265–273, 2000. doi:10.1016/S0008-6363(00)00179-6.
579. Ehrlich JR, Cha TJ, Zhang L, Chartier D, Villeneuve L, Hébert TE, Nattel S. Characterization of a hyperpolarization-activated time-dependent potassium current in canine cardiomyocytes from pulmonary vein myocardial sleeves and left atrium. **J Physiol** 557: 583–597, 2004. doi:10.1113/jphysiol.2004.061119.
580. Chen YC, Chen SA, Chen YJ, Chang MS, Chan P, Lin CI. Effects of thyroid hormone on the arrhythmogenic activity of pulmonary vein cardiomyocytes. **J Am Coll Cardiol** 39: 366–372, 2002. doi:10.1016/S0735-1097(01)01731-4.

581. Tsuneoka Y, Irie M, Tanaka Y, Sugimoto T, Kobayashi Y, Kusakabe T, Kato K, Hamaguchi S, Namekata I, Tanaka H. Permissive role of reduced inwardly-rectifying potassium current density in the automaticity of the guinea pig pulmonary vein myocardium. **J Pharmacol Sci** 133: 195–202, 2017. doi:[10.1016/j.jphs.2016.12.006](https://doi.org/10.1016/j.jphs.2016.12.006).
582. Okamoto Y, Kawamura K, Nakamura Y, Ono K. Pathological impact of hyperpolarization-activated chloride current peculiar to rat pulmonary vein cardiomyocytes. **J Mol Cell Cardiol** 66: 53–62, 2014. doi:[10.1016/j.yjmcc.2013.11.002](https://doi.org/10.1016/j.yjmcc.2013.11.002).
583. Chan CS, Chen YC, Chang SL, Lin YK, Kao YH, Chen SA, Chen YJ. Heart failure differentially modulates the effects of ivabradine on the electrical activity of the sinoatrial node and pulmonary veins. **J Card Fail** 24: 763–772, 2018. doi:[10.1016/j.cardfail.2018.09.016](https://doi.org/10.1016/j.cardfail.2018.09.016).
584. Chang CJ, Cheng CC, Yang TF, Chen YC, Lin YK, Chen SA, Chen YJ. Selective and non-selective non-steroidal anti-inflammatory drugs differentially regulate pulmonary vein and atrial arrhythmogenesis. **Int J Cardiol** 184: 559–567, 2015. doi:[10.1016/j.ijcard.2015.03.066](https://doi.org/10.1016/j.ijcard.2015.03.066).
585. Lu YY, Lin YK, Wen ZH, Chen YC, Chen SA, Chen YJ. Latrunculin B modulates electrophysiological characteristics and arrhythmogenesis in pulmonary vein cardiomyocytes. **Clin Sci (Lond)** 130: 721–732, 2016. doi:[10.1042/CS20150593](https://doi.org/10.1042/CS20150593).
586. Sicouri S, Antzelevitch C. Pulmonary vein sleeves as a pharmacologic model for the study of atrial fibrillation. **Electroфизиол Arritm** 3: 108–113, 2010.
587. Sicouri S, Cordeiro JM, Talarico M, Antzelevitch C. Antiarrhythmic effects of losartan and enalapril in canine pulmonary vein sleeve preparations. **J Cardiovasc Electrophysiol** 22: 698–705, 2011. doi:[10.1111/j.1540-8167.2010.01972.x](https://doi.org/10.1111/j.1540-8167.2010.01972.x).
588. Chan CS, Lin YK, Kao YH, Chen YC, Chen SA, Chen YJ. Hydrogen sulphide increases pulmonary veins and atrial arrhythmogenesis with activation of protein kinase C. **J Cell Mol Med** 22: 3503–3513, 2018. doi:[10.1111/jcmm.13627](https://doi.org/10.1111/jcmm.13627).
589. Lin YK, Lai MS, Chen YC, Cheng CC, Huang JH, Chen SA, Chen YJ, Lin CI. Hypoxia and reoxygenation modulate the arrhythmogenic activity of the pulmonary vein and atrium. **Clin Sci (Lond)** 122: 121–132, 2012. doi:[10.1042/CS20101078](https://doi.org/10.1042/CS20101078).
590. Chang CJ, Cheng CC, Chen YC, Higa S, Huang JH, Chen SA, Chen YJ. Factor Xa inhibitors differently modulate electrical activities in pulmonary veins and the sinoatrial node. **Eur J Pharmacol** 833: 462–471, 2018. doi:[10.1016/j.ejphar.2018.07.003](https://doi.org/10.1016/j.ejphar.2018.07.003).
591. Lin WS, Tai CT, Hsieh MH, Tsai CF, Lin YK, Tsao HM, Huang JL, Yu WC, Yang SP, Ding YA, Chang MS, Chen SA. Catheter ablation of paroxysmal atrial fibrillation initiated by non-pulmonary vein ectopy. **Circulation** 107: 3176–3183, 2003. doi:[10.1161/01.CIR.0000074206.52056.2D](https://doi.org/10.1161/01.CIR.0000074206.52056.2D).
592. Miyazaki S, Kuwahara T, Kobori A, Takahashi Y, Takei A, Sato A, Isobe M, Takahashi A. Long-term clinical outcome of extensive pulmonary vein isolation-based catheter ablation therapy in patients with paroxysmal and persistent atrial fibrillation. **Heart** 97: 668–673, 2011. doi:[10.1136/hrt.2009.186874](https://doi.org/10.1136/hrt.2009.186874).
593. Liu J, Noble PJ, Xiao G, Abdelrahman M, Dobrzynski H, Boyett MR, Lei M, Noble D. Role of pacemaking current in cardiac nodes: insights from a comparative study of sinoatrial node and atrioventricular node. **Prog Biophys Mol Biol** 96: 294–304, 2008. doi:[10.1016/j.biombio.2007.07.009](https://doi.org/10.1016/j.biombio.2007.07.009).
594. Tomaselli GF, Rubart M, Zipes D. Mechanisms of cardiac arrhythmias. In: **Braunwald's Heart Disease A Textbook of Cardiovascular Medicine**, edited by Zipes DP, Libby P, Bonow RO. Amsterdam: Elsevier, 2019, p. 619–647.
595. Yuill KH, Hancox JC. Characteristics of single cells isolated from the atrioventricular node of the adult guinea-pig heart. **Pflugers Arch** 445: 311–320, 2002. doi:[10.1007/s00424-002-0932-8](https://doi.org/10.1007/s00424-002-0932-8).
596. Hancox JC, Levi AJ, Lee CO, Heap P. A method for isolating rabbit atrioventricular node myocytes which retain normal morphology and function. **Am J Physiol Heart Circ Physiol** 265: H755–H766, 1993. doi:[10.1152/ajpheart.1993.265.2.H755](https://doi.org/10.1152/ajpheart.1993.265.2.H755).
597. Hancox JC, Patel KC, Jones JV. Antiarrhythmics—from cell to clinic: past, present, and future. **Heart** 84: 14–24, 2000. doi:[10.1136/heart.84.1.14](https://doi.org/10.1136/heart.84.1.14).
598. Meijler FL, Janse MJ. Morphology and electrophysiology of the mammalian atrioventricular node. **Physiol Rev** 68: 608–647, 1988. doi:[10.1152/physrev.1988.68.2.608](https://doi.org/10.1152/physrev.1988.68.2.608).
599. Munk AA, Adjemian RA, Zhao J, Ogbaghebriel A, Shrier A. Electrophysiological properties of morphologically distinct cells isolated from the rabbit atrioventricular node. **J Physiol** 493: 801–818, 1996. doi:[10.1113/jphysiol.1996.sp021424](https://doi.org/10.1113/jphysiol.1996.sp021424).
600. Atkinson AJ, Logantha SJ, Hao G, Yanni J, Fedorenko O, Sinha A, Gilbert SH, Benson AP, Buckley DL, Anderson RH, Boyett MR, Dobrzynski H. Functional, anatomical, and molecular investigation of the cardiac conduction system and arrhythmogenic atrioventricular ring tissue in the rat heart. **J Am Heart Assoc** 2: e000246, 2013. doi:[10.1161/JAHA.113.000246](https://doi.org/10.1161/JAHA.113.000246).
601. Greener ID, Tellez JO, Dobrzynski H, Yamamoto M, Graham GM, Billeter R, Boyett MR. Ion channel transcript expression at the rabbit atrioventricular conduction axis. **Circ Arrhythm Electrophysiol** 2: 305–315, 2009. doi:[10.1161/CIRCEP.108.803569](https://doi.org/10.1161/CIRCEP.108.803569).
602. Hancox JC, Mitcheson JS. Ion channel and exchange currents in single myocytes isolated from the rabbit atrioventricular node. **Can J Cardiol** 13: 1175–1182, 1997.
603. Markowitz SM, Lerman BB. A contemporary view of atrioventricular nodal physiology. **J Interv Card Electrophysiol** 52: 271–279, 2018. doi:[10.1007/s10840-018-0392-5](https://doi.org/10.1007/s10840-018-0392-5).
604. Belardinelli L, Shryock JC, Song Y, Wang D, Srinivas M. Ionic basis of the electrophysiological actions of adenosine on cardiomyocytes. **FASEB J** 9: 359–365, 1995. doi:[10.1096/fasebj.9.5.7896004](https://doi.org/10.1096/fasebj.9.5.7896004).
605. Cheng H, Curtis AE, Fellingham C, Hancox JC. Multiple ion channel block by the cation channel inhibitor SKF-96365 in myocytes from the rabbit atrioventricular node. **Physiol Rep** 4: e12819, 2016. doi:[10.14814/phy2.12819](https://doi.org/10.14814/phy2.12819).
606. Martynuk AE, Kane KA, Cobbe SM, Rankin AC. Adenosine increases potassium conductance in isolated rabbit atrioventricular nodal myocytes. **Cardiovasc Res** 30: 668–675, 1995. doi:[10.1016/S0008-6363\(95\)00078-X](https://doi.org/10.1016/S0008-6363(95)00078-X).
607. Orito K, Satoh K, Taira N. Cardiovascular profile of Ro 40-5967, a new nondihydropyridine calcium antagonist, delineated in isolated, blood-perfused dog hearts. **J Cardiovasc Pharmacol** 22: 293–299, 1993. doi:[10.1097/00005344-199308000-00019](https://doi.org/10.1097/00005344-199308000-00019).
608. Wang D, Shryock JC, Belardinelli L. Cellular basis for the negative dromotropic effect of adenosine on rabbit single atrioventricular nodal cells. **Circ Res** 78: 697–706, 1996. doi:[10.1161/01.RES.78.4.697](https://doi.org/10.1161/01.RES.78.4.697).
609. Zhang Y. In vivo recording of Zhang's phenomenon (His electrogram alternans): a novel index of atrioventricular node dual

- pathway conduction. **J Interv Card Electrophysiol** 40: 99–103, 2014. doi:[10.1007/s10840-014-9905-z](https://doi.org/10.1007/s10840-014-9905-z).
610. Janse MJ, van Capelle FJ, Freud GE, Durrer D. Circus movement within the AV node as a basis for supraventricular tachycardia as shown by multiple microelectrode recording in the isolated rabbit heart. **Circ Res** 28: 403–414, 1971. doi:[10.1161/01.res.28.4.403](https://doi.org/10.1161/01.res.28.4.403).
 611. Freilich A, Tepper D. Adenosine and its cardiovascular effects. **Am Heart J** 123: 1324–1328, 1992. doi:[10.1016/0002-8703\(92\)91040-8](https://doi.org/10.1016/0002-8703(92)91040-8).
 612. Martynuk AE, Seubert CN, Zima A, Morey TE, Belardinelli L, Lin G, Cucchiara RF, Dennis DM. Contribution of $I_{K,ADO}$ to the negative dromotropic effect of adenosine. **Basic Res Cardiol** 97: 286–294, 2002. doi:[10.1007/s00395-002-0349-8](https://doi.org/10.1007/s00395-002-0349-8).
 613. Cheng H, Li J, James AF, Inada S, Choisy SC, Orchard CH, Zhang H, Boyett MR, Hancox JC. Characterization and influence of cardiac background sodium current in the atrioventricular node. **J Mol Cell Cardiol** 97: 114–124, 2016. doi:[10.1016/j.yjmcc.2016.04.014](https://doi.org/10.1016/j.yjmcc.2016.04.014).
 614. Hancox J, Levi A. The hyperpolarisation-activated current, I_f , is not required for pacemaking in single cells from the rabbit atrio-ventricular node. **Pflugers Arch** 427: 121–128, 1994. doi:[10.1007/BF00585950](https://doi.org/10.1007/BF00585950).
 615. Boyden PA. Purkinje physiology and pathophysiology. **J Interv Card Electrophysiol** 52: 255–262, 2018. doi:[10.1007/s10840-018-0414-3](https://doi.org/10.1007/s10840-018-0414-3).
 616. Dun W, Boyden PA. The Purkinje cell; 2008 style. **J Mol Cell Cardiol** 45: 617–624, 2008. doi:[10.1016/j.yjmcc.2008.08.001](https://doi.org/10.1016/j.yjmcc.2008.08.001).
 617. Adamantidis MM, Caron JF, Dupuis BA. Triggered activity induced by combined mild hypoxia and acidosis in guinea-pig Purkinje fibers. **J Mol Cell Cardiol** 18: 1287–1299, 1986. doi:[10.1016/s0022-2828\(86\)80432-1](https://doi.org/10.1016/s0022-2828(86)80432-1).
 618. Friedman PL, Stewart JR, Fenoglio JJ Jr, Wit AL. Survival of subendocardial Purkinje fibers after extensive myocardial infarction in dogs. **Circ Res** 33: 597–611, 1973. doi:[10.1161/01.res.33.5.597](https://doi.org/10.1161/01.res.33.5.597).
 619. Boyden PA, Barbaiya C, Lee T, ter Keurs HE. Nonuniform Ca^{2+} transients in arrhythmogenic Purkinje cells that survive in the infarcted canine heart. **Cardiovasc Res** 57: 681–693, 2003. doi:[10.1016/S0008-6363\(02\)00725-3](https://doi.org/10.1016/S0008-6363(02)00725-3).
 620. Rosen MR, Gelband H, Hoffman BF. Effects of phentolamine on electrophysiologic properties of isolated canine purkinje fibers. **J Pharmacol Exp Ther** 179: 586–593, 1971.
 621. Colatsky TJ. Voltage clamp measurements of sodium channel properties in rabbit cardiac Purkinje fibres. **J Physiol** 305: 215–234, 1980. doi:[10.1113/jphysiol.1980.sp013359](https://doi.org/10.1113/jphysiol.1980.sp013359).
 622. Papp Z, Sipido KR, Callewaert G, Carmeliet E. Two components of $[Ca^{2+}]_i$ -activated Cl^- current during large $[Ca^{2+}]_i$ transients in single rabbit heart Purkinje cells. **J Physiol** 483: 319–330, 1995. doi:[10.1113/jphysiol.1995.sp020588](https://doi.org/10.1113/jphysiol.1995.sp020588).
 623. McGillivray RM, Wald RW. Measurement of the maximum rate of rise of the cardiac action potential V_{max} . **Med Biol Eng Comput** 22: 275–276, 1984. doi:[10.1007/BF02442757](https://doi.org/10.1007/BF02442757).
 624. Haufe V, Chamberland C, Dumaine R. The promiscuous nature of the cardiac sodium current. **J Mol Cell Cardiol** 42: 469–477, 2007. doi:[10.1016/j.yjmcc.2006.12.005](https://doi.org/10.1016/j.yjmcc.2006.12.005).
 625. Haufe V, Cordeiro JM, Zimmer T, Wu YS, Schicitano S, Benndorf K, Dumaine R. Contribution of neuronal sodium channels to the cardiac fast sodium current I_{Na} is greater in dog heart Purkinje fibers than in ventricles. **Cardiovasc Res** 65: 117–127, 2005. doi:[10.1016/j.cardiores.2004.08.017](https://doi.org/10.1016/j.cardiores.2004.08.017).
 626. Jalife J, Sicouri S, Delmar M, Michaels DC. Electrical uncoupling and impulse propagation in isolated sheep Purkinje fibers. **Am J Physiol Heart Circ Physiol** 257: H179–H189, 1989. doi:[10.1152/ajpheart.1989.257.1.H179](https://doi.org/10.1152/ajpheart.1989.257.1.H179).
 627. Sheets MF, Hanck DA, Fozzard HA. Nonlinear relation between V_{max} and I_{Na} in canine cardiac Purkinje cells. **Circ Res** 63: 386–398, 1988. doi:[10.1161/01.res.63.2.386](https://doi.org/10.1161/01.res.63.2.386).
 628. Spach MS, Miller WT 3rd, Miller-Jones E, Warren RB, Barr RC. Extracellular potentials related to intracellular action potentials during impulse conduction in anisotropic canine cardiac muscle. **Circ Res** 45: 188–204, 1979. doi:[10.1161/01.res.45.2.188](https://doi.org/10.1161/01.res.45.2.188).
 629. Kanter HL, Laing JG, Beau SL, Beyer EC, Saffitz JE. Distinct patterns of connexin expression in canine Purkinje fibers and ventricular muscle. **Circ Res** 72: 1124–1131, 1993. doi:[10.1161/01.RES.72.5.1124](https://doi.org/10.1161/01.RES.72.5.1124).
 630. Han W, Bao W, Wang Z, Nattel S. Comparison of ion-channel subunit expression in canine cardiac Purkinje fibers and ventricular muscle. **Circ Res** 91: 790–797, 2002. doi:[10.1161/01.res.0000039534.18114.d9](https://doi.org/10.1161/01.res.0000039534.18114.d9).
 631. Szigeti G, Rusznák Z, Kovács L, Papp Z. Calcium-activated transient membrane currents are carried mainly by chloride ions in isolated atrial, ventricular and Purkinje cells of rabbit heart. **Exp Physiol** 83: 137–153, 1998. doi:[10.1113/expphysiol.1998.sp004097](https://doi.org/10.1113/expphysiol.1998.sp004097).
 632. Verkerk AO, Veldkamp MW, Bouman LN, van Ginneken AC. Calcium-activated Cl^- current contributes to delayed afterdepolarizations in single Purkinje and ventricular myocytes. **Circulation** 101: 2639–2644, 2000. doi:[10.1161/01.cir.101.22.2639](https://doi.org/10.1161/01.cir.101.22.2639).
 633. Rosati B, Dun W, Hirose M, Boyden PA, McKinnon D. Molecular basis of the T- and L-type Ca^{2+} currents in canine Purkinje fibres. **J Physiol** 579: 465–471, 2007. doi:[10.1113/jphysiol.2006.127480](https://doi.org/10.1113/jphysiol.2006.127480).
 634. DiFrancesco D. Characterization of the pace-maker current kinetics in calf Purkinje fibres. **J Physiol** 348: 341–367, 1984. doi:[10.1113/jphysiol.1984.sp015114](https://doi.org/10.1113/jphysiol.1984.sp015114).
 635. Cordeiro JM, Spitzer KW, Giles WR. Repolarizing K^+ currents in rabbit heart Purkinje cells. **J Physiol** 508: 811–823, 1998. doi:[10.1111/j.1469-7793.1998.811bp.x](https://doi.org/10.1111/j.1469-7793.1998.811bp.x).
 636. Dumaine R, Cordeiro JM. Comparison of K^+ currents in cardiac Purkinje cells isolated from rabbit and dog. **J Mol Cell Cardiol** 42: 378–389, 2007. doi:[10.1016/j.yjmcc.2006.10.019](https://doi.org/10.1016/j.yjmcc.2006.10.019).
 637. Gadsby DC, Wit AL, Cranefield PF. The effects of acetylcholine on the electrical activity of canine cardiac Purkinje fibers. **Circ Res** 43: 29–35, 1978. doi:[10.1161/01.res.43.1.29](https://doi.org/10.1161/01.res.43.1.29).
 638. Callewaert G, Carmeliet E, Vereecke J. Single cardiac Purkinje cells: general electrophysiology and voltage-clamp analysis of the pace-maker current. **J Physiol** 349: 643–661, 1984. doi:[10.1113/jphysiol.1984.sp015179](https://doi.org/10.1113/jphysiol.1984.sp015179).
 639. DiFrancesco D, Noble D. A model of cardiac electrical activity incorporating ionic pumps and concentration changes. **Philos Trans R Soc Lond B Biol Sci** 307: 353–398, 1985. doi:[10.1098/rstb.1985.0001](https://doi.org/10.1098/rstb.1985.0001).
 640. Vassalle M, Yu H, Cohen IS. The pacemaker current in cardiac Purkinje myocytes. **J Gen Physiol** 106: 559–578, 1995. doi:[10.1085/jgp.106.3.559](https://doi.org/10.1085/jgp.106.3.559).
 641. Boyden PA, Pu J, Pinto J, Keurs HE. Ca^{2+} transients and Ca^{2+} waves in purkinje cells: role in action potential initiation. **Circ Res** 86: 448–455, 2000. doi:[10.1161/01.res.86.4.448](https://doi.org/10.1161/01.res.86.4.448).

642. Tranum-Jensen J, Wilde AA, Vermeulen JT, Janse MJ. Morphology of electrophysiologically identified junctions between Purkinje fibers and ventricular muscle in rabbit and pig hearts. **Circ Res** 69: 429–437, 1991. doi:[10.1161/01.res.69.2.429](https://doi.org/10.1161/01.res.69.2.429).
643. Nattel S, Quantz MA. Pharmacological response of quinidine induced early afterdepolarisations in canine cardiac Purkinje fibres: insights into underlying ionic mechanisms. **Cardiovasc Res** 22: 808–817, 1988. doi:[10.1093/cvr/22.11.808](https://doi.org/10.1093/cvr/22.11.808).
644. Janse MJ, Kleber AG, Capucci A, Coronel R, Wilms-Schopman F. Electrophysiological basis for arrhythmias caused by acute ischemia. Role of the subendocardium. **J Mol Cell Cardiol** 18: 339–355, 1986. doi:[10.1016/s0022-2828\(86\)80898-7](https://doi.org/10.1016/s0022-2828(86)80898-7).
645. Cordeiro JM, Zeina T, Goodrow R, Kaplan AD, Thomas LM, Nesterenko VV, Treat JA, Hawel L 3rd, Byus C, Bett GC, Rasmusson RL, Panama BK. Regional variation of the inwardly rectifying potassium current in the canine heart and the contributions to differences in action potential repolarization. **J Mol Cell Cardiol** 84: 52–60, 2015. doi:[10.1016/j.yjmcc.2015.04.010](https://doi.org/10.1016/j.yjmcc.2015.04.010).
646. Liu DW, Gintant GA, Antzelevitch C. Ionic bases for electrophysiological distinctions among epicardial, midmyocardial, and endocardial myocytes from the free wall of the canine left ventricle. **Circ Res** 72: 671–687, 1993. doi:[10.1161/01.res.72.3.671](https://doi.org/10.1161/01.res.72.3.671).
647. Verduyn SC, Vos MA, van der Zande J, Kulcsár A, Wellens HJ. Further observations to elucidate the role of interventricular dispersion of repolarization and early afterdepolarizations in the genesis of acquired torsade de pointes arrhythmias: a comparison between almokalant and d-sotalol using the dog as its own control. **J Am Coll Cardiol** 30: 1575–1584, 1997. doi:[10.1016/S0735-1097\(97\)00333-1](https://doi.org/10.1016/S0735-1097(97)00333-1).
648. Volders PG, Sipido KR, Carmeliet E, Späthjens RL, Wellens HJ, Vos MA. Repolarizing K⁺ currents ITO1 and IKs are larger in right than left canine ventricular midmyocardium. **Circulation** 99: 206–210, 1999. doi:[10.1161/01.cir.99.2.206](https://doi.org/10.1161/01.cir.99.2.206).
649. Di Diego JM, Sun ZQ, Antzelevitch C. I_{to} and action potential notch are smaller in left vs. right canine ventricular epicardium. **Am J Physiol Heart Circ Physiol** 271: H548–H561, 1996. doi:[10.1152/ajpheart.1996.271.2.H548](https://doi.org/10.1152/ajpheart.1996.271.2.H548).
650. Calloe K, Aistrup GL, Di Diego JM, Goodrow RJ, Treat JA, Cordeiro JM. Interventricular differences in sodium current and its potential role in Brugada syndrome. **Physiol Rep** 6: e13787, 2018. doi:[10.14814/phy2.13787](https://doi.org/10.14814/phy2.13787).
651. Osadchii OE. Arrhythmogenic drugs can amplify spatial heterogeneities in the electrical restitution in perfused guinea-pig heart: an evidence from assessments of monophasic action potential durations and JT intervals. **PLoS One** 13: e0191514, 2018. doi:[10.1371/journal.pone.0191514](https://doi.org/10.1371/journal.pone.0191514).
652. Bueno-Orovio A, Hanson BM, Gill JS, Taggart P, Rodriguez B. In vivo human left-to-right ventricular differences in rate adaptation transiently increase pro-arrhythmic risk following rate acceleration. **PLoS One** 7: e52234, 2012. doi:[10.1371/journal.pone.0052234](https://doi.org/10.1371/journal.pone.0052234).
653. Sekiya S, Ichikawa S, Tsutsumi T, Harumi K. Nonuniform action potential durations at different sites in canine left ventricle. **Jpn Heart J** 24: 935–945, 1983. doi:[10.1536/ihj.24.935](https://doi.org/10.1536/ihj.24.935).
654. Sicouri S, Antzelevitch C. A subpopulation of cells with unique electrophysiological properties in the deep subepicardium of the canine ventricle. The M cell. **Circ Res** 68: 1729–1741, 1991. doi:[10.1161/01.res.68.6.1729](https://doi.org/10.1161/01.res.68.6.1729).
655. Szentadrassy N, Banyasz T, Biro T, Szabo G, Toth BI, Magyar J, Lazar J, Varro A, Kovacs L, Nanasi PP. Apico-basal inhomogeneity in distribution of ion channels in canine and human ventricular myocardium. **Cardiovasc Res** 65: 851–860, 2005. doi:[10.1016/j.cardiores.2004.11.022](https://doi.org/10.1016/j.cardiores.2004.11.022).
656. Antzelevitch C. Modulation of transmural repolarization. **Ann NY Acad Sci** 1047: 314–323, 2005. doi:[10.1196/annals.1341.028](https://doi.org/10.1196/annals.1341.028).
657. Litovsky SH, Antzelevitch C. Transient outward current prominent in canine ventricular epicardium but not endocardium. **Circ Res** 62: 116–126, 1988. doi:[10.1161/01.res.62.1.116](https://doi.org/10.1161/01.res.62.1.116).
658. Zygmunt AC, Eddlestone GT, Thomas GP, Nesterenko VV, Antzelevitch C. Larger late sodium conductance in M cells contributes to electrical heterogeneity in canine ventricle. **Am J Physiol Heart Circ Physiol** 281: H689–H697, 2001. doi:[10.1152/ajpheart.2001.281.2.H689](https://doi.org/10.1152/ajpheart.2001.281.2.H689).
659. Zygmunt AC, Goodrow RJ, Antzelevitch C. I_{NaCa} contributes to electrical heterogeneity within the canine ventricle. **Am J Physiol Heart Circ Physiol** 278: H1671–H1678, 2000. doi:[10.1152/ajpheart.2000.278.5.H1671](https://doi.org/10.1152/ajpheart.2000.278.5.H1671).
660. Liu DW, Antzelevitch C. Characteristics of the delayed rectifier current (IKr and IKs) in canine ventricular epicardial, midmyocardial, and endocardial myocytes. A weaker IKs contributes to the longer action potential of the M cell. **Circ Res** 76: 351–365, 1995. doi:[10.1161/01.res.76.3.351](https://doi.org/10.1161/01.res.76.3.351).
661. Anyukhovskiy EP, Sosunov EA, Rosen MR. Regional differences in electrophysiological properties of epicardium, midmyocardium, and endocardium. In vitro and in vivo correlations. **Circulation** 94: 1981–1988, 1996. doi:[10.1161/01.CIR.94.8.1981](https://doi.org/10.1161/01.CIR.94.8.1981).
662. Boukens BJ, Meijborg VM, Belterman CN, Opthof T, Janse MJ, Schuessler RB, Coronel R, Efimov IR. Local transmural action potential gradients are absent in the isolated, intact dog heart but present in the corresponding coronary-perfused wedge. **Physiol Rep** 5: e13251, 2017. doi:[10.14814/phy2.13251](https://doi.org/10.14814/phy2.13251).
663. Di Diego JM, Sicouri S, Myles RC, Burton FL, Smith GL, Antzelevitch C. Optical and electrical recordings from isolated coronary-perfused ventricular wedge preparations. **J Mol Cell Cardiol** 54: 53–64, 2013. doi:[10.1016/j.yjmcc.2012.10.017](https://doi.org/10.1016/j.yjmcc.2012.10.017).
664. Yan GX, Shimizu W, Antzelevitch C. Characteristics and distribution of M cells in arterially perfused canine left ventricular wedge preparations. **Circulation** 98: 1921–1927, 1998. doi:[10.1161/01.cir.98.18.1921](https://doi.org/10.1161/01.cir.98.18.1921).
665. Janse MJ, Coronel R, Opthof T, Sosunov EA, Anyukhovskiy EP, Rosen MR. Repolarization gradients in the intact heart: transmural or apico-basal? **Prog Biophys Mol Biol** 109: 6–15, 2012. doi:[10.1016/j.pbiomolbio.2012.03.001](https://doi.org/10.1016/j.pbiomolbio.2012.03.001).
666. Meijborg VM, Conrath CE, Opthof T, Belterman CN, de Bakker JM, Coronel R. Electrocardiographic T wave and its relation with ventricular repolarization along major anatomical axes. **Circ Arrhythm Electrophysiol** 7: 524–531, 2014. doi:[10.1161/CIRCEP.113.001622](https://doi.org/10.1161/CIRCEP.113.001622).
667. Anderson RD, Kumar S, Parameswaran R, Wong G, Voskoboinik A, Sugumar H, Watts T, Sparks PB, Morton JB, McLellan A, Kistler PM, Kalman J, Lee G. Differentiating right- and left-sided outflow tract ventricular arrhythmias: classical ECG signatures and prediction algorithms. **Circ Arrhythm Electrophysiol** 12: e007392, 2019. doi:[10.1161/CIRCEP.119.007392](https://doi.org/10.1161/CIRCEP.119.007392).
668. Ashino S, Watanabe I, Kofune M, Nagashima K, Ohkubo K, Okumura Y, Nakai T, Kasamaki Y, Hirayama A. Abnormal action potential duration restitution property in the right ventricular outflow tract in Brugada syndrome. **Circ J** 74: 664–670, 2010. doi:[10.1253/circj.CJ-09-0872](https://doi.org/10.1253/circj.CJ-09-0872).

669. Lu YY, Cheng CC, Tsai CF, Lin YK, Lee TI, Chen YC, Chen SA, Chen YJ. Discrepant effects of heart failure on electrophysiological property in right ventricular outflow tract and left ventricular outflow tract cardiomyocytes. **Clin Sci (Lond)** 131: 1317–1327, 2017. doi:[10.1042/CS20170121](https://doi.org/10.1042/CS20170121).
670. Morita H, Zipes DP, Morita ST, Wu J. Differences in arrhythmogenicity between the canine right ventricular outflow tract and anteroinferior right ventricle in a model of Brugada syndrome. **Heart Rhythm** 4: 66–74, 2007. doi:[10.1016/j.hrthm.2006.08.030](https://doi.org/10.1016/j.hrthm.2006.08.030).
671. Lu YY, Chung FP, Chen YC, Tsai CF, Kao YH, Chao TF, Huang JH, Chen SA, Chen YJ. Distinctive electrophysiological characteristics of right ventricular outflow tract cardiomyocytes. **J Cell Mol Med** 18: 1540–1548, 2014. doi:[10.1111/jcmm.12329](https://doi.org/10.1111/jcmm.12329).
672. Huang CL. Murine electrophysiological models of cardiac arrhythmogenesis. **Physiol Rev** 97: 283–409, 2017. doi:[10.1152/physrev.00007.2016](https://doi.org/10.1152/physrev.00007.2016).
673. Boukens BJ, Rivaud MR, Rentschler S, Coronel R. Misinterpretation of the mouse ECG: ‘musing the waves of *Mus musculus*’. **J Physiol** 592: 4613–4626, 2014. doi:[10.1113/jphysiol.2014.279380](https://doi.org/10.1113/jphysiol.2014.279380).
674. Nerbonne JM, Nichols CG, Schwarz TL, Escande D. Genetic manipulation of cardiac K⁺ channel function in mice: what have we learned, and where do we go from here? **Circ Res** 89: 944–956, 2001. doi:[10.1161/hh2301.100349](https://doi.org/10.1161/hh2301.100349).
675. Wang L, Feng ZP, Kondo CS, Sheldon RS, Duff HJ. Developmental changes in the delayed rectifier K⁺ channels in mouse heart. **Circ Res** 79: 79–85, 1996. doi:[10.1161/01.RES.79.1.79](https://doi.org/10.1161/01.RES.79.1.79).
676. Brunner M, Peng X, Liu GX, Ren XQ, Ziv O, Choi BR, Mathur R, Hajjiri M, Odening KE, Steinberg E, Folco EJ, Pringa E, Centracchio J, Macharzina RR, Donahay T, Schofield L, Rana N, Kirk M, Mitchell GF, Poppas A, Zehender M, Koren G. Mechanisms of cardiac arrhythmias and sudden death in transgenic rabbits with long QT syndrome. **J Clin Invest** 118: 2246–2259, 2008. doi:[10.1172/JCI33578](https://doi.org/10.1172/JCI33578).
677. Major P, Baczkó I, Hiripi L, Odening KE, Juhász V, Kohajda Z, Horváth A, Seprényi G, Kovács M, Virág L, Jost N, Prorok J, Ördög B, Doleschall Z, Nattel S, Varró A, Bószé Z. A novel transgenic rabbit model with reduced repolarization reserve: long QT syndrome caused by a dominant-negative mutation of the KCNE1 gene. **Br J Pharmacol** 173: 2046–2061, 2016. doi:[10.1111/bph.13500](https://doi.org/10.1111/bph.13500).
678. Odening KE, Bodi I, Franke G, Rieke R, Ryan de Medeiros A, Perez-Feliz S, Füniss H, Mettke L, Michaelides K, Lang CN, Steinfurt J, Pantulu ND, Ziupa D, Menza M, Zehender M, Bugger H, Peyronnet R, Behrends JC, Doleschall Z, Zur Hausen A, Bode C, Jolivet G, Brunner M. Transgenic short-QT syndrome 1 rabbits mimic the human disease phenotype with QT/action potential duration shortening in the atria and ventricles and increased ventricular tachycardia/ventricular fibrillation inducibility. **Eur Heart J** 40: 842–853, 2019. doi:[10.1093/eurheartj/ehy761](https://doi.org/10.1093/eurheartj/ehy761).
679. Martinez-Mateu L, Saiz J, Aromolaran AS. Differential modulation of IK and ICa,L channels in high-fat diet-induced obese guinea pig atria. **Front Physiol** 10: 1212, 2019. doi:[10.3389/fphys.2019.01212](https://doi.org/10.3389/fphys.2019.01212).
680. Pustovit KB, Potekhina VM, Ivanova AD, Petrov AM, Abramochkin DV, Kuzmin VS. Extracellular ATP and beta-NAD alter electrical properties and cholinergic effects in the rat heart in age-specific manner. **Purinergic Signal** 15: 107–117, 2019. doi:[10.1007/s11302-019-09645-6](https://doi.org/10.1007/s11302-019-09645-6).
681. Molina CE, Abu-Taha IH, Wang Q, Roselló-Díez E, Kamler M, Nattel S, Ravens U, Wehrens XH, Hove-Madsen L, Heijman J, Dobrev D. Profibrotic, electrical, and calcium-handling remodeling of the atria in heart failure patients with and without atrial fibrillation. **Front Physiol** 9: 1383, 2018. doi:[10.3389/fphys.2018.01383](https://doi.org/10.3389/fphys.2018.01383).
682. Carmeliet E. Repolarisation and frequency in cardiac cells. **J Physiol (Paris)** 73: 903–923, 1977.
683. Li GR, Du XL, Siow YL, O K, Tse HF, Lau CP. Calcium-activated transient outward chloride current and phase 1 repolarization of swine ventricular action potential. **Cardiovasc Res** 58: 89–98, 2003. doi:[10.1016/s0008-6363\(02\)00859-3](https://doi.org/10.1016/s0008-6363(02)00859-3).
684. Schultz JH, Volk T, Bassaláy P, Hennings JC, Hübner CA, Ehmke H. Molecular and functional characterization of Kv4.2 and KChIP2 expressed in the porcine left ventricle. **Pflügers Arch** 454: 195–207, 2007. doi:[10.1007/s00424-006-0203-1](https://doi.org/10.1007/s00424-006-0203-1).
685. Jost N, Virág L, Comtois P, Ördög B, Szuts V, Seprényi G, Bitay M, Kohajda Z, Koncz I, Nagy N, Szél T, Magyar J, Kovács M, Puskás LG, Lengyel C, Wettwer E, Ravens U, Nánási PP, Papp JG, Varró A, Nattel S. Ionic mechanisms limiting cardiac repolarization reserve in humans compared to dogs. **J Physiol** 591: 4189–4206, 2013. doi:[10.1113/jphysiol.2013.261198](https://doi.org/10.1113/jphysiol.2013.261198).
686. Kopljár I, Lu HR, Van Ammel K, Otava M, Tekle F, Teisman A, Gallacher DJ. Development of a human iPSC cardiomyocyte-based scoring system for cardiac hazard identification in early drug safety de-risking. **Stem Cell Rep** 11: 1365–1377, 2018. doi:[10.1016/j.stemcr.2018.11.007](https://doi.org/10.1016/j.stemcr.2018.11.007).
687. Mummery CL. Perspectives on the use of human induced pluripotent stem cell-derived cardiomyocytes in biomedical research. **Stem Cell Rep** 11: 1306–1311, 2018. doi:[10.1016/j.stemcr.2018.11.011](https://doi.org/10.1016/j.stemcr.2018.11.011).
688. Brodehl A, Ebbinghaus H, Deutsch MA, Gummert J, Gartner A, Ratnavadivel S, Milting H. Human induced pluripotent stem-cell-derived cardiomyocytes as models for genetic cardiomyopathies. **Int J Mol Sci** 20: 4381, 2019. doi:[10.3390/ijms20184381](https://doi.org/10.3390/ijms20184381).
689. Casini S, Verkerk AO, Remme CA. Human iPSC-derived cardiomyocytes for investigation of disease mechanisms and therapeutic strategies in inherited arrhythmia syndromes: strengths and limitations. **Cardiovasc Drugs Ther** 31: 325–344, 2017. doi:[10.1007/s10557-017-6735-0](https://doi.org/10.1007/s10557-017-6735-0).
690. Garg P, Garg V, Shrestha R, Sanguinetti MC, Kamp TJ, Wu JC. Human induced pluripotent stem cell-derived cardiomyocytes as models for cardiac channelopathies: a primer for non-electrophysiologists. **Circ Res** 123: 224–243, 2018. doi:[10.1161/CIRCRESAHA.118.311209](https://doi.org/10.1161/CIRCRESAHA.118.311209).
691. Karakikes I, Ameen M, Termglinchan V, Wu JC. Human induced pluripotent stem cell-derived cardiomyocytes: insights into molecular, cellular, and functional phenotypes. **Circ Res** 117: 80–88, 2015. doi:[10.1161/CIRCRESAHA.117.305365](https://doi.org/10.1161/CIRCRESAHA.117.305365).
692. Horváth A, Lemoine MD, Löser A, Mannhardt I, Flenner F, Uzun AU, Neuber C, Breckwoldt K, Hansen A, Girdauskas E, Reichenspurner H, Willems S, Jost N, Wettwer E, Eschenhagen T, Christ T. Low resting membrane potential and low inward rectifier potassium currents are not inherent features of hiPSC-derived cardiomyocytes. **Stem Cell Rep** 10: 822–833, 2018. doi:[10.1016/j.stemcr.2018.01.012](https://doi.org/10.1016/j.stemcr.2018.01.012).
693. Horváth B, Banyasz T, Jian Z, Hegyi B, Kistamas K, Nanasi PP, Izu LT, Chen-Izu Y. Dynamics of the late Na⁺ current during cardiac action potential and its contribution to afterdepolarizations. **J Mol Cell Cardiol** 64: 59–68, 2013. doi:[10.1016/j.yjmcc.2013.08.010](https://doi.org/10.1016/j.yjmcc.2013.08.010).
694. Verkerk AO, Remme CA. ‘Mature’ resting membrane potentials in human-induced pluripotent stem cell-derived cardiomyocytes: fact or artefact? **Europace** 21: 1928, 2019. doi:[10.1093/europace/euz243](https://doi.org/10.1093/europace/euz243).

695. Angsutararux P, Luanpitpong S, Chingsuwanrote P, Supraditaporn K, Waeteekul S, Terbto P, Lorthongpanich C, Laowtammathron C, U-Pratya Y, Issaragrisil S. Generation of human induced pluripotent stem cell line carrying SCN5A C2204>T Brugada mutation (MUSli009-A-1) introduced by CRISPR/Cas9-mediated genome editing. **Stem Cell Res** 41: 101618, 2019. doi:[10.1016/j.scr.2019.101618](https://doi.org/10.1016/j.scr.2019.101618).
696. Ben Jehuda R, Shemer Y, Binah O. Genome editing in induced pluripotent stem cells using CRISPR/Cas9. **Stem Cell Rev Rep** 14: 323–336, 2018. doi:[10.1007/s12015-018-9811-3](https://doi.org/10.1007/s12015-018-9811-3).
697. Mesquita FC, Arantes PC, Kasai-Brunswick TH, Araujo DS, Gubert F, Monnerat G, Silva Dos Santos D, Neiman G, Leitão IC, Barbosa RA, Coutinho JL, Vaz IM, Dos Santos MN, Borgonovo T, Cruz FE, Miriuka S, Medei EH, Campos de Carvalho AC, Carvalho AB. R534C mutation in hERG causes a trafficking defect in iPSC-derived cardiomyocytes from patients with type 2 long QT syndrome. **Sci Rep** 9: 19203, 2019. doi:[10.1038/s41598-019-55837-w](https://doi.org/10.1038/s41598-019-55837-w).
698. Mura M, Bastaroli F, Corli M, Ginevrino M, Calabrò F, Boni M, Crotti L, Valente EM, Schwartz PJ, Gneocchi M. Generation of the human induced pluripotent stem cell (hiPSC) line PSMi006-A from a patient affected by an autosomal recessive form of long QT syndrome type 1. **Stem Cell Res** 42: 101658, 2020. doi:[10.1016/j.scr.2019.101658](https://doi.org/10.1016/j.scr.2019.101658).
699. Krause J, Löser A, Lemoine MD, Christ T, Scherschel K, Meyer C, Blankenberg S, Zeller T, Eschenhagen T, Stenzig J. Rat atrial engineered heart tissue: a new in vitro model to study atrial biology. **Basic Res Cardiol** 113: 41, 2018. doi:[10.1007/s00395-018-0701-2](https://doi.org/10.1007/s00395-018-0701-2).
700. Park SJ, Zhang D, Qi Y, Li Y, Lee KY, Bezzerides VJ, Yang P, Xia S, Kim SL, Liu X, Lu F, Pasqualini FS, Campbell PH, Geva J, Roberts AE, Kleber AG, Abrams DJ, Pu WT, Parker KK. Insights into the pathogenesis of catecholaminergic polymorphic ventricular tachycardia from engineered human heart tissue. **Circulation** 140: 390–404, 2019. doi:[10.1161/CIRCULATIONAHA.119.039711](https://doi.org/10.1161/CIRCULATIONAHA.119.039711).
701. Prüller J, Mannhardt I, Eschenhagen T, Zammit PS, Figeac N. Satellite cells delivered in their niche efficiently generate functional myotubes in three-dimensional cell culture. **PLoS One** 13: e0202574, 2018. doi:[10.1371/journal.pone.0202574](https://doi.org/10.1371/journal.pone.0202574).
702. Noble D. Successes and failures in modeling heart cell electrophysiology. **Heart Rhythm** 8: 1798–1803, 2011. doi:[10.1016/j.hrthm.2011.06.014](https://doi.org/10.1016/j.hrthm.2011.06.014).
703. Noble D. A modification of the Hodgkin–Huxley equations applicable to Purkinje fibre action and pace-maker potentials. **J Physiol** 160: 317–352, 1962. doi:[10.1113/jphysiol.1962.sp006849](https://doi.org/10.1113/jphysiol.1962.sp006849).
704. Beeler GW, Reuter H. Reconstruction of the action potential of ventricular myocardial fibres. **J Physiol** 268: 177–210, 1977. doi:[10.1113/jphysiol.1977.sp011853](https://doi.org/10.1113/jphysiol.1977.sp011853).
705. Hodgkin AL, Huxley AF. A quantitative description of membrane current and its application to conduction and excitation in nerve. **J Physiol** 117: 500–544, 1952. doi:[10.1113/jphysiol.1952.sp004764](https://doi.org/10.1113/jphysiol.1952.sp004764).
706. Dutta S, Mincholé A, Zacur E, Quinn TA, Taggart P, Rodriguez B. Early afterdepolarizations promote transmural reentry in ischemic human ventricles with reduced repolarization reserve. **Prog Biophys Mol Biol** 120: 236–248, 2016. doi:[10.1016/j.pbiomolbio.2016.01.008](https://doi.org/10.1016/j.pbiomolbio.2016.01.008).
707. Luo CH, Rudy Y. A dynamic model of the cardiac ventricular action potential. I. Simulations of ionic currents and concentration changes. **Circ Res** 74: 1071–1096, 1994. doi:[10.1161/01.res.74.6.1071](https://doi.org/10.1161/01.res.74.6.1071).
708. Luo CH, Rudy Y. A dynamic model of the cardiac ventricular action potential. II. Afterdepolarizations, triggered activity, and potentiation. **Circ Res** 74: 1097–1113, 1994. doi:[10.1161/01.res.74.6.1097](https://doi.org/10.1161/01.res.74.6.1097).
709. Tomek J, Rodriguez B, Bub G, Heijman J. beta-Adrenergic receptor stimulation inhibits proarrhythmic alternans in postinfarction border zone cardiomyocytes: a computational analysis. **Am J Physiol Heart Circ Physiol** 313: H338–H353, 2017. doi:[10.1152/ajpheart.00094.2017](https://doi.org/10.1152/ajpheart.00094.2017).
710. Trayanova NA. Whole-heart modeling: applications to cardiac electrophysiology and electromechanics. **Circ Res** 108: 113–128, 2011. doi:[10.1161/CIRCRESAHA.110.223610](https://doi.org/10.1161/CIRCRESAHA.110.223610).
711. Vandersickel N, Van Nieuwenhuysse E, Seemann G, Panfilov AV. Spatial patterns of excitation at tissue and whole organ level due to early afterdepolarizations. **Front Physiol** 8: 404, 2017. doi:[10.3389/fphys.2017.00404](https://doi.org/10.3389/fphys.2017.00404).
712. Weiss JN, Karma A, Shiferaw Y, Chen PS, Garfinkel A, Qu Z. From pulsus to pulseless: the saga of cardiac alternans. **Circ Res** 98: 1244–1253, 2006. doi:[10.1161/01.RES.0000224540.97431.f0](https://doi.org/10.1161/01.RES.0000224540.97431.f0).
713. Dutta S, Chang KC, Beattie KA, Sheng J, Tran PN, Wu WW, Wu M, Strauss DG, Colatsky T, Li Z. Optimization of an in silico cardiac cell model for proarrhythmia risk assessment. **Front Physiol** 8: 616, 2017. doi:[10.3389/fphys.2017.00616](https://doi.org/10.3389/fphys.2017.00616).
714. Li Z, Dutta S, Sheng J, Tran PN, Wu W, Chang K, Mdluli T, Strauss DG, Colatsky T. Improving the in silico assessment of proarrhythmia risk by combining hERG (human Ether-a-go-go-Related gene) channel-drug binding kinetics and multichannel pharmacology. **Circ Arrhythm Electrophysiol** 10: e004628, 2017. doi:[10.1161/CIRCEP.116.004628](https://doi.org/10.1161/CIRCEP.116.004628).
715. Passini E, Britton OJ, Lu HR, Rohrbacher J, Hermans AN, Gallacher DJ, Greig RJ, Bueno-Orovio A, Rodriguez B. Human in silico drug trials demonstrate higher accuracy than animal models in predicting clinical pro-arrhythmic cardiotoxicity. **Front Physiol** 8: 668, 2017. doi:[10.3389/fphys.2017.00668](https://doi.org/10.3389/fphys.2017.00668).
716. Carusi A, Burrage K, Rodríguez B. Bridging experiments, models and simulations: an integrative approach to validation in computational cardiac electrophysiology. **Am J Physiol Heart Circ Physiol** 303: H144–H155, 2012. doi:[10.1152/ajpheart.01151.2011](https://doi.org/10.1152/ajpheart.01151.2011).
717. Tomek J, Bueno-Orovio A, Passini E, Zhou X, Mincholé A, Britton O, Bartolucci C, Severi S, Shrier A, Virag L, Varro A, Rodriguez B. Development, calibration, and validation of a novel human ventricular myocyte model in health, disease, and drug block. **Elife** 8: e48890, 2019. doi:[10.7554/eLife.48890](https://doi.org/10.7554/eLife.48890).
718. Beattie KA, Hill AP, Bardenet R, Cui Y, Vandenberg JI, Gavaghan DJ, de Boer TP, Mirams GR. Sinusoidal voltage protocols for rapid characterisation of ion channel kinetics. **J Physiol** 596: 1813–1828, 2018. doi:[10.1113/JP275733](https://doi.org/10.1113/JP275733).
719. Lu Y, Mahaut-Smith MP, Varghese A, Huang CL, Kemp PR, Vandenberg JI. Effects of premature stimulation on hERG K⁺ channels. **J Physiol** 537: 843–851, 2001. doi:[10.1111/j.1469-7793.2001.00843.x](https://doi.org/10.1111/j.1469-7793.2001.00843.x).
720. Clancy CE, Tateyama M, Kass RS. Insights into the molecular mechanisms of bradycardia-triggered arrhythmias in long QT-3 syndrome. **J Clin Invest** 110: 1251–1262, 2002. doi:[10.1172/JCI15928](https://doi.org/10.1172/JCI15928).
721. Mahajan A, Shiferaw Y, Sato D, Baher A, Olcese R, Xie LH, Yang MJ, Chen PS, Restrepo JG, Karma A, Garfinkel A, Qu Z, Weiss JN. A rabbit ventricular action potential model replicating cardiac dynamics at rapid heart rates. **Biophys J** 94: 392–410, 2008. doi:[10.1529/biophysj.106.98160](https://doi.org/10.1529/biophysj.106.98160).

722. Ramasubramanian S, Rudy Y. The structural basis of IKs ion-channel activation: mechanistic insights from molecular simulations. **Biophys J** 114: 2584–2594, 2018. doi:[10.1016/j.bpj.2018.04.023](https://doi.org/10.1016/j.bpj.2018.04.023).
723. Xu J, Rudy Y. Effects of beta-subunit on gating of a potassium ion channel: molecular simulations of cardiac IKs activation. **J Mol Cell Cardiol** 124: 35–44, 2018. doi:[10.1016/j.yjmcc.2018.10.003](https://doi.org/10.1016/j.yjmcc.2018.10.003).
724. Hund TJ, Rudy Y. Rate dependence and regulation of action potential and calcium transient in a canine cardiac ventricular cell model. **Circulation** 110: 3168–3174, 2004. doi:[10.1161/01.CIR.0000147231.69595.D3](https://doi.org/10.1161/01.CIR.0000147231.69595.D3).
725. Zeng J, Laurita KR, Rosenbaum DS, Rudy Y. Two components of the delayed rectifier K⁺ current in ventricular myocytes of the guinea pig type. Theoretical formulation and their role in repolarization. **Circ Res** 77: 140–152, 1995. doi:[10.1161/01.res.77.1.140](https://doi.org/10.1161/01.res.77.1.140).
726. Decker KF, Heijman J, Silva JR, Hund TJ, Rudy Y. Properties and ionic mechanisms of action potential adaptation, restitution, and accommodation in canine epicardium. **Am J Physiol Heart Circ Physiol** 296: H1017–H1026, 2009. doi:[10.1152/ajpheart.01216.2008](https://doi.org/10.1152/ajpheart.01216.2008).
727. Decker KF, Rudy Y. Ionic mechanisms of electrophysiological heterogeneity and conduction block in the infarct border zone. **Am J Physiol Heart Circ Physiol** 299: H1588–H1597, 2010. doi:[10.1152/ajpheart.00362.2010](https://doi.org/10.1152/ajpheart.00362.2010).
728. Heijman J, Volders PG, Westra RL, Rudy Y. Local control of beta-adrenergic stimulation: effects on ventricular myocyte electrophysiology and Ca²⁺-transient. **J Mol Cell Cardiol** 50: 863–871, 2011. doi:[10.1016/j.yjmcc.2011.02.007](https://doi.org/10.1016/j.yjmcc.2011.02.007).
729. Shannon TR, Wang F, Puglisi J, Weber C, Bers DM. A mathematical treatment of integrated Ca dynamics within the ventricular myocyte. **Biophys J** 87: 3351–3371, 2004. doi:[10.1529/biophysj.104.047449](https://doi.org/10.1529/biophysj.104.047449).
730. Bondarenko VE, Szigeti GP, Bett GC, Kim SJ, Rasmusson RL. Computer model of action potential of mouse ventricular myocytes. **Am J Physiol Heart Circ Physiol** 287: H1378–H1403, 2004. doi:[10.1152/ajpheart.00185.2003](https://doi.org/10.1152/ajpheart.00185.2003).
731. Morotti S, Edwards AG, McCulloch AD, Bers DM, Grandi E. A novel computational model of mouse myocyte electrophysiology to assess the synergy between Na⁺ loading and CaMKII. **J Physiol** 592: 1181–1197, 2014. doi:[10.1113/jphysiol.2013.266676](https://doi.org/10.1113/jphysiol.2013.266676).
732. ten Tusscher KH, Noble D, Noble PJ, Panfilov AV. A model for human ventricular tissue. **Am J Physiol Heart Circ Physiol** 286: H1573–H1589, 2004. doi:[10.1152/ajpheart.00794.2003](https://doi.org/10.1152/ajpheart.00794.2003).
733. ten Tusscher KH, Panfilov AV. Alternans and spiral breakup in a human ventricular tissue model. **Am J Physiol Heart Circ Physiol** 291: H1088–H1100, 2006. doi:[10.1152/ajpheart.00109.2006](https://doi.org/10.1152/ajpheart.00109.2006).
734. Grandi E, Pasqualini FS, Bers DM. A novel computational model of the human ventricular action potential and Ca transient. **J Mol Cell Cardiol** 48: 112–121, 2010. doi:[10.1016/j.yjmcc.2009.09.019](https://doi.org/10.1016/j.yjmcc.2009.09.019).
735. Carro J, Rodríguez JF, Laguna P, Pueyo E. A human ventricular cell model for investigation of cardiac arrhythmias under hyperkalaemic conditions. **Philos Trans A Math Phys Eng Sci** 369: 4205–4232, 2011. doi:[10.1098/rsta.2011.0127](https://doi.org/10.1098/rsta.2011.0127).
736. O'Hara T, Virág L, Varró A, Rudy Y. Simulation of the undiseased human cardiac ventricular action potential: model formulation and experimental validation. **PLoS Comput Biol** 7: e1002061, 2011. doi:[10.1371/journal.pcbi.1002061](https://doi.org/10.1371/journal.pcbi.1002061).
737. Strauss DG, Gintant G, Li Z, Wu W, Blinova K, Vicente J, Turner JR, Sager PT. Comprehensive in vitro proarrhythmia assay (CiPA) update from a Cardiac Safety Research Consortium/Health and Environmental Sciences Institute/FDA meeting. **Ther Innov Regul Sci** 53: 519–525, 2019. doi:[10.1177/2168479018795117](https://doi.org/10.1177/2168479018795117).
738. Courtemanche M, Ramirez RJ, Nattel S. Ionic mechanisms underlying human atrial action potential properties: insights from a mathematical model. **Am J Physiol Heart Circ Physiol** 275: H301–H321, 1998. doi:[10.1152/ajpheart.1998.275.1.H301](https://doi.org/10.1152/ajpheart.1998.275.1.H301).
739. Nygren A, Fiset C, Firek L, Clark JW, Lindblad DS, Clark RB, Giles WR. Mathematical model of an adult human atrial cell: the role of K⁺ currents in repolarization. **Circ Res** 82: 63–81, 1998. doi:[10.1161/01.res.82.1.63](https://doi.org/10.1161/01.res.82.1.63).
740. Lindblad DS, Murphey CR, Clark JW, Giles WR. A model of the action potential and underlying membrane currents in a rabbit atrial cell. **Am Physiol Heart Circ J Physiol** 271: H1666–H1696, 1996. doi:[10.1152/ajpheart.1996.271.4.H1666](https://doi.org/10.1152/ajpheart.1996.271.4.H1666).
741. Grandi E, Pandit SV, Voigt N, Workman AJ, Dobrev D, Jalife J, Bers DM. Human atrial action potential and Ca²⁺ model: sinus rhythm and chronic atrial fibrillation. **Circ Res** 109: 1055–1066, 2011. doi:[10.1161/CIRCRESAHA.111.253955](https://doi.org/10.1161/CIRCRESAHA.111.253955).
742. Koivumäki JT, Korhonen T, Tavi P. Impact of sarcoplasmic reticulum calcium release on calcium dynamics and action potential morphology in human atrial myocytes: a computational study. **PLoS Comput Biol** 7: e1001067, 2011. doi:[10.1371/journal.pcbi.1001067](https://doi.org/10.1371/journal.pcbi.1001067).
743. Maleckar MM, Greenstein JL, Trayanova NA, Giles WR. Mathematical simulations of ligand-gated and cell-type specific effects on the action potential of human atrium. **Prog Biophys Mol Biol** 98: 161–170, 2008. doi:[10.1016/j.pbiomolbio.2009.01.010](https://doi.org/10.1016/j.pbiomolbio.2009.01.010).
744. Grandi E, Maleckar MM. Anti-arrhythmic strategies for atrial fibrillation: the role of computational modeling in discovery, development, and optimization. **Pharmacol Ther** 168: 126–142, 2016. doi:[10.1016/j.pharmthera.2016.09.012](https://doi.org/10.1016/j.pharmthera.2016.09.012).
745. Vagos M, van Herck IG, Sundnes J, Arevalo HJ, Edwards AG, Koivumäki JT. Computational modeling of electrophysiology and pharmacotherapy of atrial fibrillation: recent advances and future challenges. **Front Physiol** 9: 1221, 2018. doi:[10.3389/fphys.2018.01221](https://doi.org/10.3389/fphys.2018.01221).
746. Wilhelms M, Hettmann H, Maleckar MM, Koivumäki JT, Dössel O, Seemann G. Benchmarking electrophysiological models of human atrial myocytes. **Front Physiol** 3: 487, 2012. doi:[10.3389/fphys.2012.00487](https://doi.org/10.3389/fphys.2012.00487).
747. Stewart P, Aslanidi OV, Noble D, Noble PJ, Boyett MR, Zhang H. Mathematical models of the electrical action potential of Purkinje fibre cells. **Philos Trans A Math Phys Eng Sci** 367: 2225–2255, 2009. doi:[10.1098/rsta.2008.0283](https://doi.org/10.1098/rsta.2008.0283).
748. Li J, Logantha SJ, Yanni J, Cai X, Zhang H, Dobrzynski H, Hart G, Boyett M. **Computer simulation of Purkinje fibres from a rabbit model of congestive heart failure**. *Computing in Cardiology 2013*. Zaragoza, Spain, 2013, p. 361–364.
749. Corrias A, Giles W, Rodríguez B. Ionic mechanisms of electrophysiological properties and repolarization abnormalities in rabbit Purkinje fibers. **Am J Physiol Heart Circ Physiol** 300: H1806–H1813, 2011. doi:[10.1152/ajpheart.01170.2010](https://doi.org/10.1152/ajpheart.01170.2010).
750. Behradfar E, Nygren A, Vigmond EJ. The role of Purkinje-myocardial coupling during ventricular arrhythmia: a modeling study. **PLoS One** 9: e88000, 2014. doi:[10.1371/journal.pone.0088000](https://doi.org/10.1371/journal.pone.0088000).
751. Sampson KJ, Iyer V, Marks AR, Kass RS. A computational model of Purkinje fibre single cell electrophysiology: implications for the

- long QT syndrome. **J Physiol** 588: 2643–2655, 2010. doi:[10.1113/jphysiol.2010.187328](https://doi.org/10.1113/jphysiol.2010.187328).
752. Trovato C, Passini E, Nagy N, Varró A, Abi-Gerges N, Severi S, Rodriguez B. Human Purkinje in silico model enables mechanistic investigations into automaticity and pro-arrhythmic abnormalities. **J Mol Cell Cardiol** 142: 24–38, 2020. doi:[10.1016/j.yjmcc.2020.04.001](https://doi.org/10.1016/j.yjmcc.2020.04.001).
753. Severi S, Fantini M, Charawi LA, DiFrancesco D. An updated computational model of rabbit sinoatrial action potential to investigate the mechanisms of heart rate modulation. **J Physiol** 590: 4483–4499, 2012. doi:[10.1113/jphysiol.2012.229435](https://doi.org/10.1113/jphysiol.2012.229435).
754. Zhang H, Holden AV, Kodama I, Honjo H, Lei M, Varghese T, Boyett MR. Mathematical models of action potentials in the periphery and center of the rabbit sinoatrial node. **Am J Physiol Heart Circ Physiol** 279: H397–H421, 2000. doi:[10.1152/ajpheart.2000.279.1.H397](https://doi.org/10.1152/ajpheart.2000.279.1.H397).
755. Fabbri A, Fantini M, Wilders R, Severi S. Computational analysis of the human sinus node action potential: model development and effects of mutations. **J Physiol** 595: 2365–2396, 2017. doi:[10.1113/JP273259](https://doi.org/10.1113/JP273259).
756. Yaniv Y, Lakatta EG, Maltsev VA. From two competing oscillators to one coupled-clock pacemaker cell system. **Front Physiol** 6: 28, 2015. doi:[10.3389/fphys.2015.00028](https://doi.org/10.3389/fphys.2015.00028).
757. Paci M, Hyttinen J, Aalto-Setälä K, Severi S. Computational models of ventricular- and atrial-like human induced pluripotent stem cell derived cardiomyocytes. **Ann Biomed Eng** 41: 2334–2348, 2013. doi:[10.1007/s10439-013-0833-3](https://doi.org/10.1007/s10439-013-0833-3).
758. Koivumäki JT, Naumenko N, Tuomainen T, Takalo J, Oksanen M, Puttonen KA, Lehtonen S, Kuusisto J, Laakso M, Koistinaho J, Tavi P. Structural immaturity of human iPSC-derived cardiomyocytes: in silico investigation of effects on function and disease modeling. **Front Physiol** 9: 80, 2018. doi:[10.3389/fphys.2018.00080](https://doi.org/10.3389/fphys.2018.00080).
759. Paci M, Pölönen RP, Cori D, Penttinen K, Aalto-Setälä K, Severi S, Hyttinen J. Automatic optimization of an in silico model of human iPSC derived cardiomyocytes recapitulating calcium handling abnormalities. **Front Physiol** 9: 709, 2018. doi:[10.3389/fphys.2018.00709](https://doi.org/10.3389/fphys.2018.00709).
760. Colman MA, Pinali C, Trafford AW, Zhang H, Kitmitto A. A computational model of spatio-temporal cardiac intracellular calcium handling with realistic structure and spatial flux distribution from sarcoplasmic reticulum and t-tubule reconstructions. **PLoS Comput Biol** 13: e1005714, 2017. doi:[10.1371/journal.pcbi.1005714](https://doi.org/10.1371/journal.pcbi.1005714).
761. Restrepo JG, Karma A. Spatiotemporal intracellular calcium dynamics during cardiac alternans. **Chaos** 19: 037115, 2009. doi:[10.1063/1.3207835](https://doi.org/10.1063/1.3207835).
762. Sato D, Bers DM, Shiferaw Y. Formation of spatially discordant alternans due to fluctuations and diffusion of calcium. **PLoS One** 8: e85365, 2013. doi:[10.1371/journal.pone.0085365](https://doi.org/10.1371/journal.pone.0085365).
763. Fenton F, Karma A. Vortex dynamics in three-dimensional continuous myocardium with fiber rotation: filament instability and fibrillation. **Chaos** 8: 20–47, 1998. doi:[10.1063/1.166311](https://doi.org/10.1063/1.166311).
764. Bueno-Orovio A, Cherry EM, Fenton FH. Minimal model for human ventricular action potentials in tissue. **J Theor Biol** 253: 544–560, 2008. doi:[10.1016/j.jtbi.2008.03.029](https://doi.org/10.1016/j.jtbi.2008.03.029).
765. Relan J, Chinchapatnam P, Sermesant M, Rhode K, Ginks M, Delingette H, Rinaldi CA, Razavi R, Ayache N. Coupled personalization of cardiac electrophysiology models for prediction of ischaemic ventricular tachycardia. **Interface Focus** 1: 396–407, 2011. doi:[10.1098/rsfs.2010.0041](https://doi.org/10.1098/rsfs.2010.0041).
766. Bueno-Orovio A, Kay D, Grau V, Rodriguez B, Burrage K. Fractional diffusion models of cardiac electrical propagation: role of structural heterogeneity in dispersion of repolarization. **J R Soc Interface** 11: 20140352, 2014. doi:[10.1098/rsif.2014.0352](https://doi.org/10.1098/rsif.2014.0352).
767. Patel RB, Ng J, Reddy V, Chokshi M, Parikh K, Subacius H, Alsheikh-Ali AA, Nguyen T, Link MS, Goldberger JJ, Ilkhanoff L, Kadish AH. Early repolarization associated with ventricular arrhythmias in patients with chronic coronary artery disease. **Circ Arrhythm Electrophysiol** 3: 489–495, 2010. doi:[10.1161/CIRCEP.109.921130](https://doi.org/10.1161/CIRCEP.109.921130).
768. Britton OJ, Bueno-Orovio A, Van Ammel K, Lu HR, Towart R, Gallacher DJ, Rodriguez B. Experimentally calibrated population of models predicts and explains intersubject variability in cardiac cellular electrophysiology. **Proc Natl Acad Sci USA** 110: E2098–E2105, 2013. doi:[10.1073/pnas.1304382110](https://doi.org/10.1073/pnas.1304382110).
769. Groenendaal W, Ortega FA, Kherlopian AR, Zygmunt AC, Krogh-Madsen T, Christini DJ. Cell-specific cardiac electrophysiology models. **PLoS Comput Biol** 11: e1004242, 2015. doi:[10.1371/journal.pcbi.1004242](https://doi.org/10.1371/journal.pcbi.1004242).
770. Johnstone RH, Chang ET, Bardenet R, de Boer TP, Gavaghan DJ, Pathmanathan P, Clayton RH, Mirams GR. Uncertainty and variability in models of the cardiac action potential: can we build trustworthy models? **J Mol Cell Cardiol** 96: 49–62, 2016. doi:[10.1016/j.yjmcc.2015.11.018](https://doi.org/10.1016/j.yjmcc.2015.11.018).
771. Ni H, Morotti S, Grandi E. A heart for diversity: simulating variability in cardiac arrhythmia research. **Front Physiol** 9: 958, 2018. doi:[10.3389/fphys.2018.00958](https://doi.org/10.3389/fphys.2018.00958).
772. Pueyo E, Dangerfield CE, Britton OJ, Virág L, Kistamás K, Szentandrassy N, Jost N, Varró A, Nánási PP, Burrage K, Rodríguez B. Experimentally-based computational investigation into beat-to-beat variability in ventricular repolarization and its response to ionic current inhibition. **PLoS One** 11: e0151461, 2016. doi:[10.1371/journal.pone.0151461](https://doi.org/10.1371/journal.pone.0151461).
773. Sarkar AX, Christini DJ, Sobie EA. Exploiting mathematical models to illuminate electrophysiological variability between individuals. **J Physiol** 590: 2555–2567, 2012. doi:[10.1113/jphysiol.2011.223313](https://doi.org/10.1113/jphysiol.2011.223313).
774. Muszkiewicz A, Britton OJ, Gemmell P, Passini E, Sánchez C, Zhou X, Carusi A, Quinn TA, Burrage K, Bueno-Orovio A, Rodriguez B. Variability in cardiac electrophysiology: using experimentally-calibrated populations of models to move beyond the single virtual physiological human paradigm. **Prog Biophys Mol Biol** 120: 115–127, 2016. doi:[10.1016/j.pbiomolbio.2015.12.002](https://doi.org/10.1016/j.pbiomolbio.2015.12.002).
775. Muszkiewicz A, Liu X, Bueno-Orovio A, Lawson BA, Burrage K, Casadei B, Rodriguez B. From ionic to cellular variability in human atrial myocytes: an integrative computational and experimental study. **Am J Physiol Heart Circ Physiol** 314: H895–H916, 2018. doi:[10.1152/ajpheart.00477.2017](https://doi.org/10.1152/ajpheart.00477.2017).
776. Passini E, Mincholé A, Coppini R, Cerbai E, Rodríguez B, Severi S, Bueno-Orovio A. Mechanisms of pro-arrhythmic abnormalities in ventricular repolarisation and anti-arrhythmic therapies in human hypertrophic cardiomyopathy. **J Mol Cell Cardiol** 96: 72–81, 2016. doi:[10.1016/j.yjmcc.2015.09.003](https://doi.org/10.1016/j.yjmcc.2015.09.003).
777. Reilly SN, Liu X, Carnicer R, Recalde A, Muszkiewicz A, Jayaram R, Carena MC, Wijesurendra R, Stefanini M, Surdo NC, Lomas O, Ratnatunga C, Sayeed R, Krasopoulos G, Rajakumar T, Bueno-Orovio A, Verheule S, Fulga TA, Rodriguez B, Schotten U, Casadei B. Up-regulation of miR-31 in human atrial fibrillation begets the

- arrhythmia by depleting dystrophin and neuronal nitric oxide synthase. **Sci Transl Med** 8: 340ra, 2016. doi:[10.1126/scitranslmed.aac4296](https://doi.org/10.1126/scitranslmed.aac4296).
778. Brugada J, Campuzano O, Arbelo E, Sarquella-Brugada G, Brugada R. present Status of Brugada syndrome: JACC State-of-the-Art Review. **J Am Coll Cardiol** 72: 1046–1059, 2018. doi:[10.1016/j.jacc.2018.06.037](https://doi.org/10.1016/j.jacc.2018.06.037).
 779. Li KH, Lee S, Yin C, Liu T, Ngarmukos T, Conte G, Yan GX, Sy RW, Letsas KP, Tse G. Brugada syndrome: a comprehensive review of pathophysiological mechanisms and risk stratification strategies. **Int J Cardiol Heart Vasc** 26: 100468, 2020. doi:[10.1016/j.ijcha.2020.100468](https://doi.org/10.1016/j.ijcha.2020.100468).
 780. Bueno-Orovio A, Cherry EM, Evans SJ, Fenton FH. Basis for the induction of tissue-level phase-2 reentry as a repolarization disorder in the Brugada syndrome. **Biomed Res Int** 2015: 197586, 2015. doi:[10.1155/2015/197586](https://doi.org/10.1155/2015/197586).
 781. Cascio WE, Johnson TA, Gettes LS. Electrophysiologic changes in ischemic ventricular myocardium: I. Influence of ionic, metabolic, and energetic changes. **J Cardiovasc Electrophysiol** 6: 1039–1062, 1995. doi:[10.1111/j.1540-8167.1995.tb00381.x](https://doi.org/10.1111/j.1540-8167.1995.tb00381.x).
 782. Janse MJ, D'Alnoncourt CN. Reflections on reentry and focal activity. **Am J Cardiol** 60: 21F–26F, 1987. doi:[10.1016/0002-9149\(87\)90716-8](https://doi.org/10.1016/0002-9149(87)90716-8).
 783. Kleber AG, Riegger CB, Janse MJ. Extracellular K^+ and H^+ shifts in early ischemia: mechanisms and relation to changes in impulse propagation. **J Mol Cell Cardiol** 19: 35–44, 1987. doi:[10.1016/S0022-2828\(87\)80608-9](https://doi.org/10.1016/S0022-2828(87)80608-9).
 784. Pinto JM, Boyden PA. Electrical remodeling in ischemia and infarction. **Cardiovasc Res** 42: 284–297, 1999. doi:[10.1016/s0008-6363\(99\)00013-9](https://doi.org/10.1016/s0008-6363(99)00013-9).
 785. Wit AL, Hoffman BF, Cranefield PF. Slow conduction, reentry, and the mechanism of ventricular arrhythmias in myocardial infarction. **Bull NY Acad Med** 47: 1233–1234, 1971.
 786. Ruskin JN. The cardiac arrhythmia suppression trial (CAST). **N Engl J Med** 321: 386–388, 1989. doi:[10.1056/NEJM198908103210608](https://doi.org/10.1056/NEJM198908103210608).
 787. Singh BN. Controlling cardiac arrhythmias: to delay conduction or to prolong refractoriness. **Cardiovasc Drugs Ther** 3: 671–674, 1989. doi:[10.1007/BF01857618](https://doi.org/10.1007/BF01857618).
 788. Cerbai E, Pino R, Porciatti F, Sani G, Toscano M, Maccherini M, Giunti G, Mugelli A. Characterization of the hyperpolarization-activated current, I_h , in ventricular myocytes from human failing heart. **Circulation** 95: 568–571, 1997. doi:[10.1161/01.cir.95.3.568](https://doi.org/10.1161/01.cir.95.3.568).
 789. Stillitano F, Lonardo G, Zicha S, Varro A, Cerbai E, Mugelli A, Nattel S. Molecular basis of funny current (I_f) in normal and failing human heart. **J Mol Cell Cardiol** 45: 289–299, 2008. doi:[10.1016/j.yjmcc.2008.04.013](https://doi.org/10.1016/j.yjmcc.2008.04.013).
 790. Stillitano F, Lonardo G, Giunti G, Del Lungo M, Coppini R, Spinelli V, Sartiani L, Poggesi C, Mugelli A, Cerbai E. Chronic atrial fibrillation alters the functional properties of I_f in the human atrium. **J Cardiovasc Electrophysiol** 24: 1391–1400, 2013. doi:[10.1111/jce.12212](https://doi.org/10.1111/jce.12212).
 791. Riesen SC, Schober KE, Bonagura JD, Carnes CA. Myocardial expression of hyperpolarization-activated, cyclic nucleotide-gated proteins in healthy cats and cats with hypertrophic cardiomyopathy. **Schweiz Arch Tierheilkd** 155: 143–147, 2013. doi:[10.1024/0036-7281/a000431](https://doi.org/10.1024/0036-7281/a000431).
 792. Wei-Qing H, Qing-Nuan K, Lin X, Cheng-Hao G, Qi-Yi Z. Expression of hyperpolarization-activated cyclic nucleotide-gated cation channel (HCN4) is increased in hypertrophic cardiomyopathy. **Cardiovasc Pathol** 20: 110–113, 2011. doi:[10.1016/j.carpath.2010.01.007](https://doi.org/10.1016/j.carpath.2010.01.007).
 793. Marban E, Robinson SW, Wier WG. Mechanisms of arrhythmogenic delayed and early afterdepolarizations in ferret ventricular muscle. **J Clin Invest** 78: 1185–1192, 1986. doi:[10.1172/JCI112701](https://doi.org/10.1172/JCI112701).
 794. Vandersickel N, de Boer TP, Vos MA, Panfilov AV. Perpetuation of torsade de pointes in heterogeneous hearts: competing foci or re-entry? **J Physiol** 594: 6865–6878, 2016. doi:[10.1113/JP271728](https://doi.org/10.1113/JP271728).
 795. Morotti S, Grandi E, Summa A, Ginsburg KS, Bers DM. Theoretical study of L-type Ca^{2+} current inactivation kinetics during action potential repolarization and early afterdepolarizations. **J Physiol** 590: 4465–4481, 2012. doi:[10.1113/jphysiol.2012.231886](https://doi.org/10.1113/jphysiol.2012.231886).
 796. Weiss JN, Garfinkel A, Karagueuzian HS, Chen PS, Qu Z. Early afterdepolarizations and cardiac arrhythmias. **Heart Rhythm** 7: 1891–1899, 2010. doi:[10.1016/j.hrthm.2010.09.017](https://doi.org/10.1016/j.hrthm.2010.09.017).
 797. Kurata Y, Tsumoto K, Hayashi K, Hisatome I, Tanida M, Kuda Y, Shibamoto T. Dynamical mechanisms of phase-2 early afterdepolarizations in human ventricular myocytes: insights from bifurcation analyses of two mathematical models. **Am J Physiol Heart Circ Physiol** 312: H106–H127, 2017. doi:[10.1152/ajpheart.00115.2016](https://doi.org/10.1152/ajpheart.00115.2016).
 798. Clancy CE, Tateyama M, Liu H, Wehrens XH, Kass RS. Non-equilibrium gating in cardiac Na^+ channels: an original mechanism of arrhythmia. **Circulation** 107: 2233–2237, 2003. doi:[10.1161/01.CIR.0000069273.51375.BD](https://doi.org/10.1161/01.CIR.0000069273.51375.BD).
 799. Dai L, Zang Y, Zheng D, Xia L, Gong Y. Role of CaMKII and PKA in early afterdepolarization of human ventricular myocardium cell: a computational model study. **Comput Math Methods Med** 2016: 4576313, 2016. doi:[10.1155/2016/4576313](https://doi.org/10.1155/2016/4576313).
 800. Uchinoumi H, Yang Y, Oda T, Li N, Alsina KM, Puglisi JL, Chen-Izu Y, Cornea RL, Wehrens XH, Bers DM. CaMKII-dependent phosphorylation of RyR2 promotes targetable pathological RyR2 conformational shift. **J Mol Cell Cardiol** 98: 62–72, 2016. doi:[10.1016/j.yjmcc.2016.06.007](https://doi.org/10.1016/j.yjmcc.2016.06.007).
 801. van Oort RJ, McCauley MD, Dixit SS, Pereira L, Yang Y, Respress JL, Wang Q, De Almeida AC, Skapura DG, Anderson ME, Bers DM, Wehrens XH. Ryanodine receptor phosphorylation by calcium/calmodulin-dependent protein kinase II promotes life-threatening ventricular arrhythmias in mice with heart failure. **Circulation** 122: 2669–2679, 2010. doi:[10.1161/CIRCULATIONAHA.110.982298](https://doi.org/10.1161/CIRCULATIONAHA.110.982298).
 802. Luo M, Anderson ME. Mechanisms of altered Ca^{2+} handling in heart failure. **Circ Res** 113: 690–708, 2013. doi:[10.1161/CIRCRESAHA.113.301651](https://doi.org/10.1161/CIRCRESAHA.113.301651).
 803. Voigt N, Li N, Wang Q, Wang W, Trafford AW, Abu-Taha I, Sun Q, Wieland T, Ravens U, Nattel S, Wehrens XH, Dobrev D. Enhanced sarcoplasmic reticulum Ca^{2+} leak and increased Na^+ - Ca^{2+} exchanger function underlie delayed afterdepolarizations in patients with chronic atrial fibrillation. **Circulation** 125: 2059–2070, 2012. doi:[10.1161/CIRCULATIONAHA.111.067306](https://doi.org/10.1161/CIRCULATIONAHA.111.067306).
 804. Gomis-Tena J, Saiz J. Role of Ca^{2+} -dependent Cl^- current on delayed afterdepolarizations. A simulation study. **Ann Biomed Eng** 36: 752–761, 2008. doi:[10.1007/s10439-008-9460-9](https://doi.org/10.1007/s10439-008-9460-9).
 805. Liu MB, Ko CY, Song Z, Garfinkel A, Weiss JN, Qu Z. A dynamical threshold for cardiac delayed afterdepolarization-mediated triggered activity. **Biophys J** 111: 2523–2533, 2016. doi:[10.1016/j.bpj.2016.10.009](https://doi.org/10.1016/j.bpj.2016.10.009).

806. Chang SH, Chen YC, Chiang SJ, Higa S, Cheng CC, Chen YJ, Chen SA. Increased Ca^{2+} sparks and sarcoplasmic reticulum Ca^{2+} stores potentially determine the spontaneous activity of pulmonary vein cardiomyocytes. **Life Sci** 83: 284–292, 2008. doi:[10.1016/j.lfs.2008.06.014](https://doi.org/10.1016/j.lfs.2008.06.014).
807. Cheng H, Lederer WJ. Calcium sparks. **Physiol Rev** 88: 1491–1545, 2008. doi:[10.1152/physrev.00030.2007](https://doi.org/10.1152/physrev.00030.2007).
808. Belevych AE, Ho HT, Bonilla IM, Terentyeva R, Schober KE, Terentyev D, Carnes CA, Györke S. The role of spatial organization of Ca^{2+} release sites in the generation of arrhythmogenic diastolic Ca^{2+} release in myocytes from failing hearts. **Basic Res Cardiol** 112: 44, 2017. doi:[10.1007/s00395-017-0633-2](https://doi.org/10.1007/s00395-017-0633-2).
809. Cheng H, Lederer MR, Lederer WJ, Cannell MB. Calcium sparks and $[\text{Ca}^{2+}]_i$ waves in cardiac myocytes. **Am J Physiol Cell Physiol** 270: C148–C159, 1996. doi:[10.1152/ajpcell.1996.270.1.C148](https://doi.org/10.1152/ajpcell.1996.270.1.C148).
810. Niggli E, Lederer WJ. Voltage-independent calcium release in heart muscle. **Science** 250: 565–568, 1990. doi:[10.1126/science.2173135](https://doi.org/10.1126/science.2173135).
811. Baader AP, Büchler L, Bircher-Lehmann L, Kléber AG. Real time, confocal imaging of Ca^{2+} waves in arterially perfused rat hearts. **Cardiovasc Res** 53: 105–115, 2002. doi:[10.1016/s0008-6363\(01\)00423-0](https://doi.org/10.1016/s0008-6363(01)00423-0).
812. Nivala M, de Lange E, Rovetti R, Qu Z. Computational modeling and numerical methods for spatiotemporal calcium cycling in ventricular myocytes. **Front Physiol** 3: 114, 2012. doi:[10.3389/fphys.2012.00114](https://doi.org/10.3389/fphys.2012.00114).
813. Nivala M, Ko CY, Nivala M, Weiss JN, Qu Z. The emergence of sub-cellular pacemaker sites for calcium waves and oscillations. **J Physiol** 591: 5305–5320, 2013. doi:[10.1113/jphysiol.2013.259960](https://doi.org/10.1113/jphysiol.2013.259960).
814. Song Z, Ko CY, Nivala M, Weiss JN, Qu Z. Calcium-voltage coupling in the genesis of early and delayed afterdepolarizations in cardiac myocytes. **Biophys J** 108: 1908–1921, 2015. doi:[10.1016/j.bpj.2015.03.011](https://doi.org/10.1016/j.bpj.2015.03.011).
815. Kléber AG, Riegger CB, Janse MJ. Electrical uncoupling and increase of extracellular resistance after induction of ischemia in isolated, arterially perfused rabbit papillary muscle. **Circ Res** 61: 271–279, 1987. doi:[10.1161/01.res.61.2.271](https://doi.org/10.1161/01.res.61.2.271).
816. Xie Y, Sato D, Garfinkel A, Qu Z, Weiss JN. So little source, so much sink: requirements for afterdepolarizations to propagate in tissue. **Biophys J** 99: 1408–1415, 2010. doi:[10.1016/j.bpj.2010.06.042](https://doi.org/10.1016/j.bpj.2010.06.042).
817. Rutherford SL, Trew ML, Sands GB, LeGrice IJ, Smail BH. High-resolution 3-dimensional reconstruction of the infarct border zone: impact of structural remodeling on electrical activation. **Circ Res** 111: 301–311, 2012. doi:[10.1161/CIRCRESAHA.111.260943](https://doi.org/10.1161/CIRCRESAHA.111.260943).
818. Wang Y, Joyner RW, Wagner MB, Cheng J, Lai D, Crawford BH. Stretch-activated channel activation promotes early afterdepolarizations in rat ventricular myocytes under oxidative stress. **Am J Physiol Heart Circ Physiol** 296: H1227–H1235, 2009. doi:[10.1152/ajpheart.00808.2008](https://doi.org/10.1152/ajpheart.00808.2008).
819. Höfer T, Politi A, Heinrich R. Intercellular Ca^{2+} wave propagation through gap-junctional Ca^{2+} diffusion: a theoretical study. **Biophys J** 80: 75–87, 2001. doi:[10.1016/S0006-3495\(01\)75996-6](https://doi.org/10.1016/S0006-3495(01)75996-6).
820. Bai J, Wang K, Liu Y, Li Y, Liang C, Luo G, Dong S, Yuan Y, Zhang H. Computational cardiac modeling reveals mechanisms of ventricular arrhythmogenesis in long QT syndrome type 8: CACNA1C R858H mutation linked to ventricular fibrillation. **Front Physiol** 8: 771, 2017. doi:[10.3389/fphys.2017.00771](https://doi.org/10.3389/fphys.2017.00771).
821. Roston TM, Haji-Ghassemi O, LaPage MJ, Batra AS, Bar-Cohen Y, Anderson C, Lau YR, Maginot K, Gebauer RA, Etheridge SP, Potts JE, Van Petegem F, Sanatani S. Catecholaminergic polymorphic ventricular tachycardia patients with multiple genetic variants in the PACES CPVT Registry. **PLoS One** 13: e0205925, 2018. doi:[10.1371/journal.pone.0205925](https://doi.org/10.1371/journal.pone.0205925).
822. Johnson DM, Heijman J, Bode EF, Greensmith DJ, van der Linde H, Abi-Gerges N, Eisner DA, Trafford AW, Volders PG. Diastolic spontaneous calcium release from the sarcoplasmic reticulum increases beat-to-beat variability of repolarization in canine ventricular myocytes after beta-adrenergic stimulation. **Circ Res** 112: 246–256, 2013. doi:[10.1161/CIRCRESAHA.112.275735](https://doi.org/10.1161/CIRCRESAHA.112.275735).
823. Marks AR, Priori S, Memmi M, Kontula K, Laitinen PJ. Involvement of the cardiac ryanodine receptor/calcium release channel in catecholaminergic polymorphic ventricular tachycardia. **J Cell Physiol** 190: 1–6, 2002. doi:[10.1002/jcp.10031](https://doi.org/10.1002/jcp.10031).
824. Landstrom AP, Dobrev D, Wehrens XH. Calcium signaling and cardiac arrhythmias. **Circ Res** 120: 1969–1993, 2017. doi:[10.1161/CIRCRESAHA.117.310083](https://doi.org/10.1161/CIRCRESAHA.117.310083).
825. Bányász T, Horváth B, Virág L, Bárándi L, Szentadrassy N, Harmati G, Magyar J, Marangoni S, Zaza A, Varró A, Nánási P. Reverse rate dependency is an intrinsic property of canine cardiac preparations. **Cardiovasc Res** 84: 237–244, 2009. doi:[10.1093/cvr/cvp213](https://doi.org/10.1093/cvr/cvp213).
826. Boyett MR, Jewell BR. A study of the factors responsible for rate-dependent shortening of the action potential in mammalian ventricular muscle. **J Physiol** 285: 359–380, 1978. doi:[10.1113/jphysiol.1978.sp012576](https://doi.org/10.1113/jphysiol.1978.sp012576).
827. Elharrar V, Surawicz B. Cycle length effect on restitution of action potential duration in dog cardiac fibers. **Am J Physiol Heart Circ Physiol** 244: H782–H792, 1983. doi:[10.1152/ajpheart.1983.244.6.H782](https://doi.org/10.1152/ajpheart.1983.244.6.H782).
828. Ito S, Surawicz B. Effect of tetraethylammonium chloride on action potential in cardiac Purkinje fibers. **Am J Physiol Heart Circ Physiol** 241: H139–H144, 1981. doi:[10.1152/ajpheart.1981.241.2.H139](https://doi.org/10.1152/ajpheart.1981.241.2.H139).
829. Virág L, Acsai K, Hála O, Zaza A, Bitay M, Bogáts G, Papp JG, Varró A. Self-augmentation of the lengthening of repolarization is related to the shape of the cardiac action potential: implications for reverse rate dependency. **Br J Pharmacol** 156: 1076–1084, 2009. doi:[10.1111/j.1476-5381.2009.00116.x](https://doi.org/10.1111/j.1476-5381.2009.00116.x).
830. Zaza A. Control of the cardiac action potential: the role of repolarization dynamics. **J Mol Cell Cardiol** 48: 106–111, 2010. doi:[10.1016/j.yjmcc.2009.07.027](https://doi.org/10.1016/j.yjmcc.2009.07.027).
831. Shattock MJ, Park KC, Yang HY, Lee AW, Niederer S, MacLeod KT, Winter J. Restitution slope is principally determined by steady-state action potential duration. **Cardiovasc Res** 113: 817–828, 2017. doi:[10.1093/cvr/cvx063](https://doi.org/10.1093/cvr/cvx063).
832. Nash MP, Bradley CP, Sutton PM, Clayton RH, Kallis P, Hayward MP, Paterson DJ, Taggart P. Whole heart action potential duration restitution properties in cardiac patients: a combined clinical and modelling study. **Exp Physiol** 91: 339–354, 2006. doi:[10.1113/expphysiol.2005.031070](https://doi.org/10.1113/expphysiol.2005.031070).
833. Pak HN, Hong SJ, Hwang GS, Lee HS, Park SW, Ahn JC, Moo Ro Y, Kim YH. Spatial dispersion of action potential duration restitution kinetics is associated with induction of ventricular tachycardia/fibrillation in humans. **J Cardiovasc Electrophysiol** 15: 1357–1363, 2004. doi:[10.1046/j.1540-8167.2004.03569.x](https://doi.org/10.1046/j.1540-8167.2004.03569.x).
834. Riccio ML, Koller ML, Gilmour RF Jr. Electrical restitution and spatio-temporal organization during ventricular fibrillation. **Circ Res** 84: 955–963, 1999. doi:[10.1161/01.RES.84.8.955](https://doi.org/10.1161/01.RES.84.8.955).

835. Robinson RB, Boyden PA, Hoffman BF, Hewett KW. Electrical restitution process in dispersed canine cardiac Purkinje and ventricular cells. **Am J Physiol Heart Circ Physiol** 253: H1018–H1025, 1987. doi:10.1152/ajpheart.1987.253.5.H1018.
836. Weiss JN, Garfinkel A, Karagueuzian HS, Nguyen TP, Olcese R, Chen PS, Qu Z. Perspective: a dynamics-based classification of ventricular arrhythmias. **J Mol Cell Cardiol** 82: 136–152, 2015. doi:10.1016/j.yjmcc.2015.02.017.
837. Garfinkel A, Kim YH, Voroshilovsky O, Qu Z, Kil JR, Lee MH, Karagueuzian HS, Weiss JN, Chen PS. Preventing ventricular fibrillation by flattening cardiac restitution. **Proc Natl Acad Sci USA** 97: 6061–6066, 2000. doi:10.1073/pnas.090492697.
838. Osadchii OE. Role of abnormal repolarization in the mechanism of cardiac arrhythmia. **Acta Physiol (Oxf)** 220, Suppl 712: 1–71, 2017. doi:10.1111/apha.12902.
839. Morgan JM, Cunningham D, Rowland E. Dispersion of monophasic action potential duration: demonstrable in humans after premature ventricular extrastimulation but not in steady state. **J Am Coll Cardiol** 19: 1244–1253, 1992. doi:10.1016/0735-1097(92)90331-g.
840. Wu TJ, Lin SF, Weiss JN, Ting CT, Chen PS. Two types of ventricular fibrillation in isolated rabbit hearts: importance of excitability and action potential duration restitution. **Circulation** 106: 1859–1866, 2002. doi:10.1161/01.cir.0000031334.49170.fb.
841. Ni H, Zhang H, Grandi E, Narayan SM, Giles WR. Transient outward K^+ current can strongly modulate action potential duration and initiate alternans in the human atrium. **Am J Physiol Heart Circ Physiol** 316: H527–H542, 2019. doi:10.1152/ajpheart.00251.2018.
842. Tolkacheva EG, Anumonwo JM, Jalife J. Action potential duration restitution portraits of mammalian ventricular myocytes: role of calcium current. **Biophys J** 91: 2735–2745, 2006. doi:10.1529/biophysj.106.083865.
843. Kline RP, Morad M. Potassium efflux in heart muscle during activity: extracellular accumulation and its implications. **J Physiol** 280: 537–558, 1978. doi:10.1113/jphysiol.1978.sp012400.
844. Weiss JN, Nivala M, Garfinkel A, Qu Z. Alternans and arrhythmias: from cell to heart. **Circ Res** 108: 98–112, 2011. doi:10.1161/CIRCRESAHA.110.223586.
845. Narayan SM, Franz MR, Clopton P, Pruvot EJ, Krummen DE. Repolarization alternans reveals vulnerability to human atrial fibrillation. **Circulation** 123: 2922–2930, 2011. doi:10.1161/CIRCULATIONAHA.110.977827.
846. Wilson LD, Jeyaraj D, Wan X, Hoeker GS, Said TH, Gittinger M, Laurita KR, Rosenbaum DS. Heart failure enhances susceptibility to arrhythmogenic cardiac alternans. **Heart Rhythm** 6: 251–259, 2009. doi:10.1016/j.hrthm.2008.11.008.
847. Tomek J, Hao G, Tomková M, Lewis A, Carr C, Paterson DJ, Rodríguez B, Bub G, Herring N. beta-Adrenergic receptor stimulation and alternans in the border zone of a healed infarct: an ex vivo study and computational investigation of arrhythmogenesis. **Front Physiol** 10: 350, 2019. doi:10.3389/fphys.2019.00350.
848. Wilson LD, Rosenbaum DS. Mechanisms of arrhythmogenic cardiac alternans. **Europace** 9 Suppl 6: vi77–82, 2007. doi:10.1093/europace/eum210.
849. Pastore JM, Girouard SD, Laurita KR, Akar FG, Rosenbaum DS. Mechanism linking T-wave alternans to the genesis of cardiac fibrillation. **Circulation** 99: 1385–1394, 1999. doi:10.1161/01.cir.99.10.1385.
850. Chudin E, Goldhaber J, Garfinkel A, Weiss J, Kogan B. Intracellular Ca^{2+} dynamics and the stability of ventricular tachycardia. **Biophys J** 77: 2930–2941, 1999. doi:10.1016/S0006-3495(99)77126-2.
851. Díaz ME, O'Neill SC, Eisner DA. Sarcoplasmic reticulum calcium content fluctuation is the key to cardiac alternans. **Circ Res** 94: 650–656, 2004. doi:10.1161/01.RES.0000119923.64774.72.
852. Nolasco JB, Dahlen RW. A graphic method for the study of alternation in cardiac action potentials. **J Appl Physiol** 25: 191–196, 1968. doi:10.1152/jappl.1968.25.2.191.
853. Pruvot EJ, Katta RP, Rosenbaum DS, Laurita KR. Role of calcium cycling versus restitution in the mechanism of repolarization alternans. **Circ Res** 94: 1083–1090, 2004. doi:10.1161/01.RES.0000125629.72053.95.
854. Eisner DA, Choi HS, Díaz ME, O'Neill SC, Trafford AW. Integrative analysis of calcium cycling in cardiac muscle. **Circ Res** 87: 1087–1094, 2000. doi:10.1161/01.res.87.12.1087.
855. Picht E, DeSantiago J, Blatter LA, Bers DM. Cardiac alternans do not rely on diastolic sarcoplasmic reticulum calcium content fluctuations. **Circ Res** 99: 740–748, 2006. doi:10.1161/01.RES.0000244002.88813.91.
856. Qu Z, Liu MB, Nivala M. A unified theory of calcium alternans in ventricular myocytes. **Sci Rep** 6: 35625, 2016. doi:10.1038/srep35625.
857. Livshitz LM, Rudy Y. Regulation of Ca^{2+} and electrical alternans in cardiac myocytes: role of CAMKII and repolarizing currents. **Am J Physiol Heart Circ Physiol** 292: H2854–H2866, 2007. doi:10.1152/ajpheart.01347.2006.
858. Tomek J, Tomková M, Zhou X, Bub G, Rodríguez B. Modulation of cardiac alternans by altered sarcoplasmic reticulum calcium release: a simulation study. **Front Physiol** 9: 1306, 2018. doi:10.3389/fphys.2018.01306.
859. Zhou X, Bueno-Orovio A, Orini M, Hanson B, Hayward M, Taggart P, Lambiase PD, Burrage K, Rodríguez B. In vivo and in silico investigation into mechanisms of frequency dependence of repolarization alternans in human ventricular cardiomyocytes. **Circ Res** 118: 266–278, 2016. doi:10.1161/CIRCRESAHA.115.307836.
860. Qu Z, Garfinkel A, Chen PS, Weiss JN. Mechanisms of discordant alternans and induction of reentry in simulated cardiac tissue. **Circulation** 102: 1664–1670, 2000. doi:10.1161/01.cir.102.14.1664.
861. Thomsen MB, Truin M, van Opstal JM, Beekman JD, Volders PG, Stengl M, Vos MA. Sudden cardiac death in dogs with remodeled hearts is associated with larger beat-to-beat variability of repolarization. **Basic Res Cardiol** 100: 279–287, 2005. doi:10.1007/s00395-005-0519-6.
862. Ufret-Vincenty CA, Baro DJ, Lederer WJ, Rockman HA, Quinones LE, Santana LF. Role of sodium channel deglycosylation in the genesis of cardiac arrhythmias in heart failure. **J Biol Chem** 276: 28197–28203, 2001. doi:10.1074/jbc.M102548200.
863. Shimoni Y, Emmett T, Schmidt R, Nygren A, Kargacin G. Sex-dependent impairment of cardiac action potential conduction in type 1 diabetic rats. **Am J Physiol Heart Circ Physiol** 296: H1442–H1450, 2009. doi:10.1152/ajpheart.01150.2008.
864. Yu P, Hu L, Xie J, Chen S, Huang L, Xu Z, Liu X, Zhou Q, Yuan P, Yan X, Jin J, Shen Y, Zhu W, Fu L, Chen Q, Yu J, Hu J, Cao Q, Wan R, Hong K. O-GlcNAcylation of cardiac Nav1.5 contributes to the development of arrhythmias in diabetic hearts. **Int J Cardiol** 260: 74–81, 2018. doi:10.1016/j.ijcard.2018.02.099.

865. Howarth FC, Qureshi MA, Hassan Z, Al Kury LT, Isaev D, Parekh K, Yammahi SR, Oz M, Adrian TE, Adeghate E. Changing pattern of gene expression is associated with ventricular myocyte dysfunction and altered mechanisms of Ca^{2+} signalling in young type 2 Zucker diabetic fatty rat heart. **Exp Physiol** 96: 325–337, 2011. doi:[10.1113/expphysiol.2010.055574](https://doi.org/10.1113/expphysiol.2010.055574).
866. Zicha S, Maltsev VA, Nattel S, Sabbah HN, Undrovinas AI. Post-transcriptional alterations in the expression of cardiac Na^+ channel subunits in chronic heart failure. **J Mol Cell Cardiol** 37: 91–100, 2004. doi:[10.1016/j.jmcc.2004.04.003](https://doi.org/10.1016/j.jmcc.2004.04.003).
867. Lengyel C, Virág L, Kovács PP, Kristóf A, Pacher P, Kocsis E, Koltay ZM, Nánási PP, Tóth M, Kecskeméti V, Papp JG, Varró A, Jost N. Role of slow delayed rectifier K^+ -current in QT prolongation in the alloxan-induced diabetic rabbit heart. **Acta Physiol (Oxf)** 192: 359–368, 2008. doi:[10.1111/j.1748-1716.2007.01753.x](https://doi.org/10.1111/j.1748-1716.2007.01753.x).
868. Shimoni Y, Ewart HS, Severson D. Type I and II models of diabetes produce different modifications of K^+ currents in rat heart: role of insulin. **J Physiol** 507: 485–496, 1998. doi:[10.1111/j.1469-7793.1998.485bt.x](https://doi.org/10.1111/j.1469-7793.1998.485bt.x).
869. Zhang Y, Xiao J, Wang H, Luo X, Wang J, Villeneuve LR, Zhang H, Bai Y, Yang B, Wang Z. Restoring depressed HERG K^+ channel function as a mechanism for insulin treatment of abnormal QT prolongation and associated arrhythmias in diabetic rabbits. **Am J Physiol Heart Circ Physiol** 291: H1446–H1455, 2006. doi:[10.1152/ajpheart.01356.2005](https://doi.org/10.1152/ajpheart.01356.2005).
870. Van Wagoner DR, Pond AL, McCarthy PM, Trimmer JS, Nerbonne JM. Outward K^+ current densities and Kv1.5 expression are reduced in chronic human atrial fibrillation. **Circ Res** 80: 772–781, 1997. doi:[10.1161/01.res.80.6.772](https://doi.org/10.1161/01.res.80.6.772).
871. Heijman J, Kirchner D, Kunze F, Chrétien EM, Michel-Reher MB, Voigt N, Knaut M, Michel MC, Ravens U, Dobrev D. Muscarinic type-1 receptors contribute to IK_{ACh} in human atrial cardiomyocytes and are upregulated in patients with chronic atrial fibrillation. **Int J Cardiol** 255: 61–68, 2018. doi:[10.1016/j.ijcard.2017.12.050](https://doi.org/10.1016/j.ijcard.2017.12.050).
872. Li N, Timofeyev V, Tuteja D, Xu D, Lu L, Zhang Q, Zhang Z, Singapuri A, Albert TR, Rajagopal AV, Bond CT, Periasamy M, Adelman J, Chiamvimonvat N. Ablation of a Ca^{2+} -activated K^+ channel (SK2 channel) results in action potential prolongation in atrial myocytes and atrial fibrillation. **J Physiol** 587: 1087–1100, 2009. doi:[10.1113/jphysiol.2008.167718](https://doi.org/10.1113/jphysiol.2008.167718).
873. Bonilla IM, Long VP 3rd, Vargas-Pinto P, Wright P, Belevych A, Lou Q, Mowrey K, Yoo J, Binkley PF, Fedorov VV, Györke S, Janssen PM, Kilic A, Mohler PJ, Carnes CA. Calcium-activated potassium current modulates ventricular repolarization in chronic heart failure. **PLoS One** 9: e108824, 2014. doi:[10.1371/journal.pone.0108824](https://doi.org/10.1371/journal.pone.0108824).
874. Yi F, Ling TY, Lu T, Wang XL, Li J, Claycomb WC, Shen WK, Lee HC. Down-regulation of the small conductance calcium-activated potassium channels in diabetic mouse atria. **J Biol Chem** 290: 7016–7026, 2015. doi:[10.1074/jbc.M114.607952](https://doi.org/10.1074/jbc.M114.607952).
875. Cerbai E, Sartiani L, DePaoli P, Pino R, Maccherini M, Bizzarri F, DiCiolla F, Davoli G, Sani G, Mugelli A. The properties of the pacemaker current I_{f} in human ventricular myocytes are modulated by cardiac disease. **J Mol Cell Cardiol** 33: 441–448, 2001. doi:[10.1006/jmcc.2000.1316](https://doi.org/10.1006/jmcc.2000.1316).
876. Hoppe UC, Jansen E, Südkamp M, Beuckelmann DJ. Hyperpolarization-activated inward current in ventricular myocytes from normal and failing human hearts. **Circulation** 97: 55–65, 1998. doi:[10.1161/01.cir.97.1.55](https://doi.org/10.1161/01.cir.97.1.55).
877. Ai X, Pogwizd SM. Connexin 43 downregulation and dephosphorylation in nonischemic heart failure is associated with enhanced colocalized protein phosphatase type 2A. **Circ Res** 96: 54–63, 2005. doi:[10.1161/01.RES.0000152325.07495.5a](https://doi.org/10.1161/01.RES.0000152325.07495.5a).
878. Boulaksil M, Bierhuizen MF, Engelen MA, Stein M, Kok BJ, van Amersfoort SC, Vos MA, van Rijen HV, de Bakker JM, van Veen TA. Spatial heterogeneity of Cx43 is an arrhythmogenic substrate of polymorphic ventricular tachycardias during compensated cardiac hypertrophy in rats. **Front Cardiovasc Med** 3: 5, 2016. doi:[10.3389/fcvm.2016.00005](https://doi.org/10.3389/fcvm.2016.00005).
879. Dupont E, Matsushita T, Kaba RA, Vozzi C, Coppens SR, Khan N, Kaprielian R, Yacoub MH, Severs NJ. Altered connexin expression in human congestive heart failure. **J Mol Cell Cardiol** 33: 359–371, 2001. doi:[10.1006/jmcc.2000.1308](https://doi.org/10.1006/jmcc.2000.1308).
880. Allesie M, Ausma J, Schotten U. Electrical, contractile and structural remodeling during atrial fibrillation. **Cardiovasc Res** 54: 230–246, 2002. doi:[10.1016/s0008-6363\(02\)00258-4](https://doi.org/10.1016/s0008-6363(02)00258-4).
881. Ma ZG, Yuan YP, Wu HM, Zhang X, Tang QZ. Cardiac fibrosis: new insights into the pathogenesis. **Int J Biol Sci** 14: 1645–1657, 2018. doi:[10.7150/ijbs.28103](https://doi.org/10.7150/ijbs.28103).
882. Vaidya K, Semsarian C, Chan KH. Atrial fibrillation in hypertrophic cardiomyopathy. **Heart Lung Circ** 26: 975–982, 2017. doi:[10.1016/j.hlc.2017.05.116](https://doi.org/10.1016/j.hlc.2017.05.116).
883. Macia E, Dolmatova E, Cabo C, Sosinsky AZ, Dun W, Coromilas J, Ciaccio EJ, Boyden PA, Wit AL, Duffy HS. Characterization of gap junction remodeling in epicardial border zone of healing canine infarcts and electrophysiological effects of partial reversal by rotigaptide. **Circ Arrhythm Electrophysiol** 4: 344–351, 2011. doi:[10.1161/CIRCEP.110.959312](https://doi.org/10.1161/CIRCEP.110.959312).
884. Martins RP, Kaur K, Hwang E, Ramirez RJ, Willis BC, Filgueiras-Rama D, Ennis SR, Takemoto Y, Ponce-Balbuena D, Zarzoso M, O'Connell RP, Musa H, Guerrero-Serna G, Avula UM, Swartz MF, Bhushal S, Deo M, Pandit SV, Berenfeld O, Jalife J. Dominant frequency increase rate predicts transition from paroxysmal to long-term persistent atrial fibrillation. **Circulation** 129: 1472–1482, 2014. doi:[10.1161/CIRCULATIONAHA.113.004742](https://doi.org/10.1161/CIRCULATIONAHA.113.004742).
885. Wu MS, Gabriels J, Khan M, Shaban N, D'Amato SA, Liu CF, Markowitz SM, Ip JE, Thomas G, Singh P, Lerman BB, Patel A, Cheung JW. Left atrial thrombus despite continuous direct oral anti-coagulant or warfarin therapy in patients with atrial fibrillation: insights into rates and timing of thrombus resolution. **J Interv Card Electrophysiol** 53: 159–167, 2018. doi:[10.1007/s10840-018-0432-1](https://doi.org/10.1007/s10840-018-0432-1).
886. Kannel WB, Abbott RD, Savage DD, McNamara PM. Epidemiologic features of chronic atrial fibrillation: the Framingham study. **N Engl J Med** 306: 1018–1022, 1982. doi:[10.1056/NEJM198204293061703](https://doi.org/10.1056/NEJM198204293061703).
887. Dobrev D. Atrial Ca^{2+} /calmodulin-dependent protein kinase II: a druggable master switch of atrial fibrillation-associated atrial remodeling? **Heart Rhythm** 16: 1089–1090, 2019. doi:[10.1016/j.hrthm.2019.02.002](https://doi.org/10.1016/j.hrthm.2019.02.002).
888. Schotten U, Dobrev D, Platonov PG, Kottkamp H, Hindricks G. Current controversies in determining the main mechanisms of atrial fibrillation. **J Intern Med** 279: 428–438, 2016. doi:[10.1111/joim.12492](https://doi.org/10.1111/joim.12492).
889. Wijffels MC, Kirchhof CJ, Dorland R, Allesie MA. Atrial fibrillation begets atrial fibrillation. A study in awake chronically instrumented goats. **Circulation** 92: 1954–1968, 1995. doi:[10.1161/01.cir.92.7.1954](https://doi.org/10.1161/01.cir.92.7.1954).
890. Lin YK, Chen YA, Lee TI, Chen YC, Chen SA, Chen YJ. Aging modulates the substrate and triggers remodeling in atrial fibrillation. **Circ J** 82: 1237–1244, 2018. doi:[10.1253/circj.CJ-17-0242](https://doi.org/10.1253/circj.CJ-17-0242).

891. Pandit SV, Workman AJ. Atrial electrophysiological remodeling and fibrillation in heart failure. **Clin Med Insights Cardiol** 10: 41–46, 2016. doi:10.4137/CMC.S39713.
892. Poulet C, Wettwer E, Grunnet M, Jespersen T, Fabritz L, Matschke K, Knaut M, Ravens U. Late sodium current in human atrial cardiomyocytes from patients in sinus rhythm and atrial fibrillation. **PLoS One** 10: e0131432, 2015. doi:10.1371/journal.pone.0131432.
893. Dobrev D, Wehrens XH. Calcium-mediated cellular triggered activity in atrial fibrillation. **J Physiol** 595: 4001–4008, 2017. doi:10.1113/JP273048.
894. Li D, Melnyk P, Feng J, Wang Z, Petrecca K, Shrier A, Nattel S. Effects of experimental heart failure on atrial cellular and ionic electrophysiology. **Circulation** 101: 2631–2638, 2000. doi:10.1161/01.CIR.101.22.2631.
895. Chen WT, Chen YC, Hsieh MH, Huang SY, Kao YH, Chen YA, Lin YK, Chen SA, Chen YJ. The uremic toxin indoxyl sulfate increases pulmonary vein and atrial arrhythmogenesis. **J Cardiovasc Electrophysiol** 26: 203–210, 2015. doi:10.1111/jce.12554.
896. Gutierrez A, Van Wagoner DR. Oxidant and inflammatory mechanisms and targeted therapy in atrial fibrillation: an update. **J Cardiovasc Pharmacol** 66: 523–529, 2015. doi:10.1097/FJC.0000000000000313.
897. Mihm MJ, Yu F, Carnes CA, Reiser PJ, McCarthy PM, Van Wagoner DR, Bauer JA. Impaired myofibrillar energetics and oxidative injury during human atrial fibrillation. **Circulation** 104: 174–180, 2001. doi:10.1161/01.CIR.104.2.174.
898. Anderson ME. Oxidant stress promotes disease by activating CaMKII. **J Mol Cell Cardiol** 89: 160–167, 2015. doi:10.1016/j.yjmcc.2015.10.014.
899. Liu Z, Finet JE, Wolfram JA, Anderson ME, Ai X, Donahue JK. Calcium/calmodulin-dependent protein kinase II causes atrial structural remodeling associated with atrial fibrillation and heart failure. **Heart Rhythm** 16: 1080–1088, 2019. doi:10.1016/j.hrthm.2019.01.013.
900. Kjekshus J. Arrhythmias and mortality in congestive heart failure. **Am J Cardiol** 65: 421–481, 1990. doi:10.1016/0002-9149(90)90125-k.
901. Akar FG, Spragg DD, Tunin RS, Kass DA, Tomaselli GF. Mechanisms underlying conduction slowing and arrhythmogenesis in nonischemic dilated cardiomyopathy. **Circ Res** 95: 717–725, 2004. doi:10.1161/01.RES.0000144125.61927.1c.
902. Chen Y, Wakili R, Xiao J, Wu CT, Luo X, Clauss S, Dawson K, Qi X, Naud P, Shi YF, Tardif JC, Käb S, Dobrev D, Nattel S. Detailed characterization of microRNA changes in a canine heart failure model: relationship to arrhythmogenic structural remodeling. **J Mol Cell Cardiol** 77: 113–124, 2014. doi:10.1016/j.yjmcc.2014.10.001.
903. Li GR, Lau CP, Ducharme A, Tardif JC, Nattel S. Transmural action potential and ionic current remodeling in ventricles of failing canine hearts. **Am J Physiol Heart Circ Physiol** 283: H1031–H1041, 2002. doi:10.1152/ajpheart.00105.2002.
904. Kodama M, Kato K, Hirono S, Okura Y, Hanawa H, Yoshida T, Hayashi M, Tachikawa H, Kashimura T, Watanabe K, Aizawa Y. Linkage between mechanical and electrical alternans in patients with chronic heart failure. **J Cardiovasc Electrophysiol** 15: 295–299, 2004. doi:10.1046/j.1540-8167.2004.03016.x.
905. Nivala M, Song Z, Weiss JN, Qu Z. T-tubule disruption promotes calcium alternans in failing ventricular myocytes: mechanistic insights from computational modeling. **J Mol Cell Cardiol** 79: 32–41, 2015. doi:10.1016/j.yjmcc.2014.10.018.
906. Wong KR, Trezise AE, Crozatier B, Vandenberg JI. Loss of the normal epicardial to endocardial gradient of cfr mRNA expression in the hypertrophied rabbit left ventricle. **Biochem Biophys Res Commun** 278: 144–149, 2000. doi:10.1006/bbrc.2000.3754.
907. Hobai IA, O'Rourke B. Enhanced Ca^{2+} -activated Na^{+} - Ca^{2+} exchange activity in canine pacing-induced heart failure. **Circ Res** 87: 690–698, 2000. doi:10.1161/01.res.87.8.690.
908. Gorski PA, Ceholski DK, Hajjar RJ. Altered myocardial calcium cycling and energetics in heart failure—a rational approach for disease treatment. **Cell Metab** 21: 183–194, 2015. doi:10.1016/j.cmet.2015.01.005.
909. Chang SL, Chen YC, Yeh YH, Lai YJ, Yeh HI, Lin CI, Lin YK, Lin YJ, Wu TJ, Huang YK, Chen SA, Chen YJ. Heart failure enhances arrhythmogenesis in pulmonary veins. **Clin Exp Pharmacol Physiol** 38: 666–674, 2011. doi:10.1111/j.1440-1681.2011.05553.x.
910. Priebe L, Beuckelmann DJ. Simulation study of cellular electric properties in heart failure. **Circ Res** 82: 1206–1223, 1998. doi:10.1161/01.res.82.11.1206.
911. Luo X, Lin H, Pan Z, Xiao J, Zhang Y, Lu Y, Yang B, Wang Z. Down-regulation of miR-1/miR-133 contributes to re-expression of pacemaker channel genes HCN2 and HCN4 in hypertrophic heart. **J Biol Chem** 283: 20045–20052, 2008. doi:10.1074/jbc.M801035200.
912. Zicha S, Fernández-Velasco M, Lonardo G, L'Heureux N, Nattel S. Sinus node dysfunction and hyperpolarization-activated (HCN) channel subunit remodeling in a canine heart failure model. **Cardiovasc Res** 66: 472–481, 2005. doi:10.1016/j.cardiores.2005.02.011.
913. Verkerk AO, Wilders R, Coronel R, Ravensloot JH, Verheijck EE. Ionic remodeling of sinoatrial node cells by heart failure. **Circulation** 108: 760–766, 2003. doi:10.1161/01.CIR.0000083719.51661.B9.
914. Verkerk AO, Veldkamp MW, Baartscheer A, Schumacher CA, Klöpping C, van Ginneken AC, Ravensloot JH. Ionic mechanism of delayed afterdepolarizations in ventricular cells isolated from human end-stage failing hearts. **Circulation** 104: 2728–2733, 2001. doi:10.1161/hc4701.099577.
915. Yeh YH, Wakili R, Qi XY, Chartier D, Boknik P, Käb S, Ravens U, Couto P, Dobrev D, Nattel S. Calcium-handling abnormalities underlying atrial arrhythmogenesis and contractile dysfunction in dogs with congestive heart failure. **Circ Arrhythm Electrophysiol** 1: 93–102, 2008. doi:10.1161/CIRCEP.107.754788.
916. Teare D. Asymmetrical hypertrophy of the heart in young adults. **Br Heart J** 20: 1–8, 1958. doi:10.1136/hrt.20.1.1.
917. Maron BJ, Gardin JM, Flack JM, Gidding SS, Kurosaki TT, Bild DE. Prevalence of hypertrophic cardiomyopathy in a general population of young adults. Echocardiographic analysis of 4111 subjects in the CARDIA Study. Coronary Artery Risk Development in (Young) Adults. **Circulation** 92: 785–789, 1995. doi:10.1161/01.cir.92.4.785.
918. Gersh BJ, Maron BJ, Bonow RO, Dearani JA, Fifer MA, Link MS, Naidu SS, Nishimura RA, Ommen SR, Rakowski H, Seidman CE, Towbin JA, Udelson JE, Yancy CW; American College of Cardiology Foundation/American Heart Association Task Force on Practice Guidelines. American College of Cardiology Foundation/American Heart Association Task Force on Practice Guidelines. 2011 ACCF/AHA Guideline for the Diagnosis and Treatment of Hypertrophic Cardiomyopathy: a report of the American College of

- Cardiology Foundation/American Heart Association Task Force on Practice Guidelines. **J Am Coll Cardiol** 58: e212–e260, 2011. doi:10.1016/j.jacc.2011.06.011.
919. Maron BJ. Hypertrophic cardiomyopathy and other causes of sudden cardiac death in young competitive athletes, with considerations for preparticipation screening and criteria for disqualification. **Cardiol Clin** 25: 399–414, 2007. doi:10.1016/j.ccl.2007.07.006.
920. Wigle ED, Rakowski H, Kimball BP, Williams WG. Hypertrophic cardiomyopathy. Clinical spectrum and treatment. **Circulation** 92: 1680–1692, 1995. doi:10.1161/01.cir.92.7.1680.
921. Decker JA, Rossano JW, Smith EO, Cannon B, Clunie SK, Gates C, Jefferies JL, Kim JJ, Price JF, Dreyer WJ, Towbin JA, Denfield SW. Risk factors and mode of death in isolated hypertrophic cardiomyopathy in children. **J Am Coll Cardiol** 54: 250–254, 2009. doi:10.1016/j.jacc.2009.03.051.
922. Kessler EL, Boulaksil M, van Rijen HV, Vos MA, van Veen TA. Passive ventricular remodeling in cardiac disease: focus on heterogeneity. **Front Physiol** 5: 482, 2014. doi:10.3389/fphys.2014.00482.
923. Maron BJ, Anan TJ, Roberts WC. Quantitative analysis of the distribution of cardiac muscle cell disorganization in the left ventricular wall of patients with hypertrophic cardiomyopathy. **Circulation** 63: 882–894, 1981. doi:10.1161/01.cir.63.4.882.
924. Sotgia B, Sciarra R, Olivetto I, Casolo G, Rega L, Betti I, Pupi A, Camici PG, Cecchi F. Spatial relationship between coronary microvascular dysfunction and delayed contrast enhancement in patients with hypertrophic cardiomyopathy. **J Nucl Med** 49: 1090–1096, 2008. doi:10.2967/jnumed.107.050138.
925. Galati G, Leone O, Pasquale F, Olivetto I, Biagini E, Grigioni F, Pilato E, Lorenzini M, Corti B, Foà A, Agostini V, Cecchi F, Rapezzi C. Histological and histometric characterization of myocardial fibrosis in end-stage hypertrophic cardiomyopathy: a clinical-pathological study of 30 explanted hearts. **Circ Heart Fail** 9: e003090, 2016. doi:10.1161/CIRCHEARTFAILURE.116.003090.
926. Hurtado-de-Mendoza D, Corona-Villalobos CP, Pozios I, Gonzales J, Soleimanifard Y, Sivalokanathan S, Montoya-Cerrillo D, Vakrou S, Kamel I, Mormontoy-Laurel W, Dolores-Cerna K, Suarez J, Perez-Melo S, Bluemke DA, Abraham TP, Zimmerman SL, Abraham MR. Diffuse interstitial fibrosis assessed by cardiac magnetic resonance is associated with dispersion of ventricular repolarization in patients with hypertrophic cardiomyopathy. **J Arrhythm** 33: 201–207, 2017. doi:10.1016/j.joa.2016.10.005.
927. Cannon RO 3rd, Schenke WH, Bonow RO, Leon MB, Rosing DR. Left ventricular pulsus alternans in patients with hypertrophic cardiomyopathy and severe obstruction to left ventricular outflow. **Circulation** 73: 276–285, 1986. doi:10.1161/01.cir.73.2.276.
928. Maurizi N, Passantino S, Spaziani G, Girolami F, Arretini A, Targetti M, Pollini I, Tomberli A, Pradella S, Calabri GB, Vinattieri V, Bertaccini B, Leone O, De Simone L, Rapezzi C, Marchionni N, Cecchi F, Favilli S, Olivetto I. Long-term outcomes of pediatric-onset hypertrophic cardiomyopathy and age-specific risk factors for lethal arrhythmic events. **JAMA Cardiol** 3: 520–525, 2018. doi:10.1001/jamacardio.2018.0789.
929. Adabag AS, Casey SA, Kuskowski MA, Zenovich AG, Maron BJ. Spectrum and prognostic significance of arrhythmias on ambulatory Holter electrocardiogram in hypertrophic cardiomyopathy. **J Am Coll Cardiol** 45: 697–704, 2005. doi:10.1016/j.jacc.2004.11.043.
930. Ulus T, Kudaiberdieva G, Gorenek B. The onset mechanisms of ventricular tachycardia. **Int J Cardiol** 167: 619–623, 2013. doi:10.1016/j.ijcard.2012.09.034.
931. Ferrantini C, Pioner JM, Mazzoni L, Gentile F, Tosi B, Rossi A, Belardinelli L, Tesi C, Palandri C, Matucci R, Cerbai E, Olivetto I, Poggesi C, Mugelli A, Coppini R. Late sodium current inhibitors to treat exercise-induced obstruction in hypertrophic cardiomyopathy: an in vitro study in human myocardium. **Br J Pharmacol** 175: 2635–2652, 2018. doi:10.1111/bph.14223.
932. Maron BJ, Pelliccia A. The heart of trained athletes: cardiac remodeling and the risks of sports, including sudden death. **Circulation** 114: 1633–1644, 2006. doi:10.1161/CIRCULATIONAHA.106.613562.
933. D'Souza A, Bucchi A, Johnsen AB, Logantha SJ, Monfredi O, Yanni J, Prehar S, Hart G, Cartwright E, Wisloff U, Dobrynski H, DiFrancesco D, Morris GM, Boyett MR. Exercise training reduces resting heart rate via downregulation of the funny channel HCN4. **Nat Commun** 5: 3775, 2014. doi:10.1038/ncomms4775.
934. Atchley AE Jr, Douglas PS. Left ventricular hypertrophy in athletes: morphologic features and clinical correlates. **Cardiol Clin** 25: 371–382, 2007. doi:10.1016/j.ccl.2007.06.009.
935. Corrado D, Michieli P, Basso C, Schiavon M, Thiene G. How to screen athletes for cardiovascular diseases. **Cardiol Clin** 25: 391–397, 2007. doi:10.1016/j.ccl.2007.07.008.
936. Lengyel C, Orosz A, Hegyi P, Komka Z, Udvardy A, Bosnyák E, Trájer E, Pavlik G, Tóth M, Wittmann T, Papp JG, Varró A, Baczkó I. Increased short-term variability of the QT interval in professional soccer players: possible implications for arrhythmia prediction. **PLoS One** 6: e18751, 2011. doi:10.1371/journal.pone.0018751.
937. Rowland T. Is the 'athlete's heart' arrhythmogenic? Implications for sudden cardiac death. **Sports Med** 41: 401–411, 2011. doi:10.2165/11583940-000000000-00000.
938. Tse G, Lai ET, Tse V, Yeo JM. Molecular and electrophysiological mechanisms underlying cardiac arrhythmogenesis in diabetes mellitus. **J Diabetes Res** 2016: 2848759, 2016. doi:10.1155/2016/2848759.
939. Zhang Y, Xiao J, Lin H, Luo X, Wang H, Bai Y, Wang J, Zhang H, Yang B, Wang Z. Ionic mechanisms underlying abnormal QT prolongation and the associated arrhythmias in diabetic rabbits: a role of rapid delayed rectifier K⁺ current. **Cell Physiol Biochem** 19: 225–238, 2007. doi:10.1159/000100642.
940. Fu X, Pan Y, Cao Q, Li B, Wang S, Du H, Duan N, Li X. Metformin restores electrophysiology of small conductance calcium-activated potassium channels in the atrium of GK diabetic rats. **BMC Cardiovasc Disord** 18: 63, 2018. doi:10.1186/s12872-018-0805-5.
941. D'Souza A, Howarth FC, Yanni J, Dobrynski H, Boyett MR, Adeghate E, Bidasee KR, Singh J. Left ventricle structural remodeling in the prediabetic Goto-Kakizaki rat. **Exp Physiol** 96: 875–888, 2011. doi:10.1113/expphysiol.2011.058271.
942. Lin YC, Huang J, Kan H, Castranova V, Frisbee JC, Yu HG. Defective calcium inactivation causes long QT in obese insulin-resistant rat. **Am J Physiol Heart Circ Physiol** 302: H1013–H1022, 2012. doi:10.1152/ajpheart.00837.2011.
943. Nygren A, Olson ML, Chen KY, Emmett T, Kargacin G, Shimoni Y. Propagation of the cardiac impulse in the diabetic rat heart: reduced conduction reserve. **J Physiol** 580: 543–560, 2007. doi:10.1113/jphysiol.2006.123729.
944. Fowlkes V, Clark J, Fix C, Law BA, Morales MO, Qiao X, Ako-Asare K, Goldsmith JG, Carver W, Murray DB, Goldsmith EC. Type II diabetes promotes a myofibroblast phenotype in cardiac fibroblasts. **Life Sci** 92: 669–676, 2013. doi:10.1016/j.lfs.2013.01.003.

945. Ghaly HA, Boyle PM, Vigmond EJ, Shimoni Y, Nygren A. Simulations of reduced conduction reserve in the diabetic rat heart: response to uncoupling and reduced excitability. **Ann Biomed Eng** 38: 1415–1425, 2010. doi:[10.1007/s10439-009-9855-2](https://doi.org/10.1007/s10439-009-9855-2).
946. Shao CH, Rozanski GJ, Patel KP, Bidasee KR. Dyssynchronous (non-uniform) Ca^{2+} release in myocytes from streptozotocin-induced diabetic rats. **J Mol Cell Cardiol** 42: 234–246, 2007. doi:[10.1016/j.yjmcc.2006.08.018](https://doi.org/10.1016/j.yjmcc.2006.08.018).
947. Shao CH, Tian C, Ouyang S, Moore CJ, Alomar F, Nemet I, D'Souza A, Nagai R, Kutty S, Rozanski GJ, Ramanadham S, Singh J, Bidasee KR. Carbonylation induces heterogeneity in cardiac ryanodine receptor function in diabetes mellitus. **Mol Pharmacol** 82: 383–399, 2012. doi:[10.1124/mol.112.078352](https://doi.org/10.1124/mol.112.078352).
948. Yaras N, Ugur M, Ozdemir S, Gurdal H, Purali N, Lacampagne A, Vassort G, Turan B. Effects of diabetes on ryanodine receptor Ca release channel (RyR2) and Ca^{2+} homeostasis in rat heart. **Diabetes** 54: 3082–3088, 2005. doi:[10.2337/diabetes.54.11.3082](https://doi.org/10.2337/diabetes.54.11.3082).
949. Neticadan T, Temsah RM, Kent A, Elimban V, Dhalla NS. Depressed levels of Ca^{2+} -cycling proteins may underlie sarcoplasmic reticulum dysfunction in the diabetic heart. **Diabetes** 50: 2133–2138, 2001. doi:[10.2337/diabetes.50.9.2133](https://doi.org/10.2337/diabetes.50.9.2133).
950. Tuncay E, Okatan EN, Toy A, Turan B. Enhancement of cellular antioxidant-defence preserves diastolic dysfunction via regulation of both diastolic Zn^{2+} and Ca^{2+} and prevention of RyR2-leak in hyperglycemic cardiomyocytes. **Oxid Med Cell Longev** 2014: 290381, 2014. doi:[10.1155/2014/290381](https://doi.org/10.1155/2014/290381).
951. Hamilton S, Terentyev D. Proarrhythmic remodeling of calcium homeostasis in cardiac disease; implications for diabetes and obesity. **Front Physiol** 9: 1517, 2018. doi:[10.3389/fphys.2018.01517](https://doi.org/10.3389/fphys.2018.01517).
952. Okatan EN, Durak AT, Turan B. Electrophysiological basis of metabolic-syndrome-induced cardiac dysfunction. **Can J Physiol Pharmacol** 94: 1064–1073, 2016. doi:[10.1139/cjpp-2015-0531](https://doi.org/10.1139/cjpp-2015-0531).
953. Nikolic G, Bishop RL, Singh JB. Sudden death recorded during Holter monitoring. **Circulation** 66: 218–225, 1982. doi:[10.1161/01.cir.66.1.218](https://doi.org/10.1161/01.cir.66.1.218).
954. Pantridge JF, Webb SW, Adgey AA. Arrhythmias in the first hours of acute myocardial infarction. **Prog Cardiovasc Dis** 23: 265–278, 1981. doi:[10.1016/0033-0620\(81\)90016-5](https://doi.org/10.1016/0033-0620(81)90016-5).
955. Manning AS, Hearse DJ. Reperfusion-induced arrhythmias: mechanisms and prevention. **J Mol Cell Cardiol** 16: 497–518, 1984. doi:[10.1016/s0022-2828\(84\)80638-0](https://doi.org/10.1016/s0022-2828(84)80638-0).
956. Tzivoni D, Keren A, Granot H, Gottlieb S, Benhorin J, Stern S. Ventricular fibrillation caused by myocardial reperfusion in Prinzmetal's angina. **Am Heart J** 105: 323–325, 1983. doi:[10.1016/0002-8703\(83\)90534-3](https://doi.org/10.1016/0002-8703(83)90534-3).
957. Maseri A, Severi S, Marzullo P. Role of coronary arterial spasm in sudden coronary ischemic death. **Ann NY Acad Sci** 382: 204–217, 1982. doi:[10.1111/j.1749-6632.1982.tb55218.x](https://doi.org/10.1111/j.1749-6632.1982.tb55218.x).
958. Clark BB, Cummings JR. Arrhythmias following experimental coronary occlusion and their response to drugs. **Ann NY Acad Sci** 64: 543–551, 1956. doi:[10.1111/j.1749-6632.1956.tb36828.x](https://doi.org/10.1111/j.1749-6632.1956.tb36828.x).
959. Kabell G, Scherlag BJ, Hope RR, Lazzara R. Regional myocardial blood flow and ventricular arrhythmias following one-stage and two-stage coronary artery occlusion in anesthetized dogs. **Am Heart J** 104: 537–544, 1982. doi:[10.1016/0002-8703\(82\)90224-1](https://doi.org/10.1016/0002-8703(82)90224-1).
960. Downar E, Janse MJ, Durrer D. The effect of acute coronary artery occlusion on subepicardial transmembrane potentials in the intact porcine heart. **Circulation** 56: 217–224, 1977. doi:[10.1161/01.cir.56.2.217](https://doi.org/10.1161/01.cir.56.2.217).
961. Kléber AG. Resting membrane potential, extracellular potassium activity, and intracellular sodium activity during acute global ischemia in isolated perfused guinea pig hearts. **Circ Res** 52: 442–450, 1983. doi:[10.1161/01.RES.52.4.442](https://doi.org/10.1161/01.RES.52.4.442).
962. Ferrero JM Jr, Sa'iz J, Ferrero JM, Thakor NV. Simulation of action potentials from metabolically impaired cardiac myocytes. Role of ATP-sensitive K^{+} current. **Circ Res** 79: 208–221, 1996. doi:[10.1161/01.RES.79.2.208](https://doi.org/10.1161/01.RES.79.2.208).
963. Beardslee MA, Lerner DL, Tadros PN, Laing JG, Beyer EC, Yamada KA, Kléber AG, Schuessler RB, Saffitz JE. Dephosphorylation and intracellular redistribution of ventricular connexin43 during electrical uncoupling induced by ischemia. **Circ Res** 87: 656–662, 2000. doi:[10.1161/01.res.87.8.656](https://doi.org/10.1161/01.res.87.8.656).
964. Janse MJ, Kléber AG. Electrophysiological changes and ventricular arrhythmias in the early phase of regional myocardial ischemia. **Circ Res** 49: 1069–1081, 1981. doi:[10.1161/01.res.49.5.1069](https://doi.org/10.1161/01.res.49.5.1069).
965. McCallister LP, Trapukdi S, Neely JR. Morphometric observations on the effects of ischemia in the isolated perfused rat heart. **J Mol Cell Cardiol** 11: 619–630, 1979. doi:[10.1016/0022-2828\(79\)90376-6](https://doi.org/10.1016/0022-2828(79)90376-6).
966. Kléber AG, Janse MJ, Wilms-Schopmann FJ, Wilde AA, Coronel R. Changes in conduction velocity during acute ischemia in ventricular myocardium of the isolated porcine heart. **Circulation** 73: 189–198, 1986. doi:[10.1161/01.cir.73.1.189](https://doi.org/10.1161/01.cir.73.1.189).
967. Baczkó I, Husti Z, Lang V, Leprán I, Light PE. Sarcolemmal KATP channel modulators and cardiac arrhythmias. **Curr Med Chem** 18: 3640–3661, 2011. doi:[10.2174/092986711796642472](https://doi.org/10.2174/092986711796642472).
968. Kaplinsky E, Ogawa S, Balke CW, Dreifus LS. Two periods of early ventricular arrhythmia in the canine acute myocardial infarction model. **Circulation** 60: 397–403, 1979. doi:[10.1161/01.cir.60.2.397](https://doi.org/10.1161/01.cir.60.2.397).
969. Martinez-Navarro H, Mincholé A, Bueno-Orovio A, Rodriguez B. High arrhythmic risk in antero-septal acute myocardial ischemia is explained by increased transmural reentry occurrence. **Sci Rep** 9: 16803, 2019. doi:[10.1038/s41598-019-53221-2](https://doi.org/10.1038/s41598-019-53221-2).
970. Schömig A, Dart AM, Dietz R, Mayer E, Kübler W. Release of endogenous catecholamines in the ischemic myocardium of the rat. Part A: Locally mediated release. **Circ Res** 55: 689–701, 1984. doi:[10.1161/01.res.55.5.689](https://doi.org/10.1161/01.res.55.5.689).
971. Arnsdorf MF, Sawicki GJ. The effects of lysophosphatidylcholine, a toxic metabolite of ischemia, on the components of cardiac excitability in sheep Purkinje fibers. **Circ Res** 49: 16–30, 1981. doi:[10.1161/01.res.49.1.16](https://doi.org/10.1161/01.res.49.1.16).
972. Coronel R, Wilms-Schopman FJ, Opthof T, van Capelle FJ, Janse MJ. Injury current and gradients of diastolic stimulation threshold, TQ potential, and extracellular potassium concentration during acute regional ischemia in the isolated perfused pig heart. **Circ Res** 68: 1241–1249, 1991. doi:[10.1161/01.res.68.5.1241](https://doi.org/10.1161/01.res.68.5.1241).
973. Janse MJ, van Capelle FJ. Electrotonic interactions across an inexcitable region as a cause of ectopic activity in acute regional myocardial ischemia. A study in intact porcine and canine hearts and computer models. **Circ Res** 50: 527–537, 1982. doi:[10.1161/01.res.50.4.527](https://doi.org/10.1161/01.res.50.4.527).
974. Katzung BG, Hondeghem LM, Grant AO. Letter: Cardiac ventricular automaticity induced by current of injury. **Pflugers Arch** 360: 193–197, 1975. doi:[10.1007/BF00580542](https://doi.org/10.1007/BF00580542).

975. Qin D, Zhang ZH, Caref EB, Boutjdir M, Jain P, el-Sherif N. Cellular and ionic basis of arrhythmias in postinfarction remodeled ventricular myocardium. **Circ Res** 79: 461–473, 1996. doi:[10.1161/01.res.79.3.461](https://doi.org/10.1161/01.res.79.3.461).
976. Friedman PL, Fenoglio JJ, Wit AL. Time course for reversal of electrophysiological and ultrastructural abnormalities in subendocardial Purkinje fibers surviving extensive myocardial infarction in dogs. **Circ Res** 36: 127–144, 1975. doi:[10.1161/01.res.36.1.127](https://doi.org/10.1161/01.res.36.1.127).
977. Lue WM, Boyden PA. Abnormal electrical properties of myocytes from chronically infarcted canine heart. Alterations in V_{max} and the transient outward current. **Circulation** 85: 1175–1188, 1992. doi:[10.1161/01.cir.85.3.1175](https://doi.org/10.1161/01.cir.85.3.1175).
978. Pinto JM, Boyden PA. Reduced inward rectifying and increased E-4031-sensitive K^+ current density in arrhythmogenic subendocardial Purkinje myocytes from the infarcted heart. **J Cardiovasc Electrophysiol** 9: 299–311, 1998. doi:[10.1111/j.1540-8167.1998.tb00915.x](https://doi.org/10.1111/j.1540-8167.1998.tb00915.x).
979. Boyden PA, Pinto JM. Reduced calcium currents in subendocardial Purkinje myocytes that survive in the 24- and 48-hour infarcted heart. **Circulation** 89: 2747–2759, 1994. doi:[10.1161/01.cir.89.6.2747](https://doi.org/10.1161/01.cir.89.6.2747).
980. Jeck C, Pinto J, Boyden P. Transient outward currents in subendocardial Purkinje myocytes surviving in the infarcted heart. **Circulation** 92: 465–473, 1995. doi:[10.1161/01.CIR.92.3.465](https://doi.org/10.1161/01.CIR.92.3.465).
981. Cabo C, Boyden PA. Electrical remodeling of the epicardial border zone in the canine infarcted heart: a computational analysis. **Am J Physiol Heart Circ Physiol** 284: H372–H384, 2003. doi:[10.1152/ajpheart.00512.2002](https://doi.org/10.1152/ajpheart.00512.2002).
982. Pu J, Boyden PA. Alterations of Na^+ currents in myocytes from epicardial border zone of the infarcted heart. A possible ionic mechanism for reduced excitability and postrepolarization refractoriness. **Circ Res** 81: 110–119, 1997. doi:[10.1161/01.RES.81.1.110](https://doi.org/10.1161/01.RES.81.1.110).
983. Peters NS, Coromilas J, Severs NJ, Wit AL. Disturbed connexin43 gap junction distribution correlates with the location of reentrant circuits in the epicardial border zone of healing canine infarcts that cause ventricular tachycardia. **Circulation** 95: 988–996, 1997. doi:[10.1161/01.CIR.95.4.988](https://doi.org/10.1161/01.CIR.95.4.988).
984. Dillon SM, Allesie MA, Ursell PC, Wit AL. Influences of anisotropic tissue structure on reentrant circuits in the epicardial border zone of subacute canine infarcts. **Circ Res** 63: 182–206, 1988. doi:[10.1161/01.res.63.1.182](https://doi.org/10.1161/01.res.63.1.182).
985. Gardner PI, Ursell PC, Fenoglio JJ Jr, Wit AL. Electrophysiologic and anatomic basis for fractionated electrograms recorded from healed myocardial infarcts. **Circulation** 72: 596–611, 1985. doi:[10.1161/01.cir.72.3.596](https://doi.org/10.1161/01.cir.72.3.596).
986. Ursell PC, Gardner PI, Albala A, Fenoglio JJ Jr, Wit AL. Structural and electrophysiological changes in the epicardial border zone of canine myocardial infarcts during infarct healing. **Circ Res** 56: 436–451, 1985. doi:[10.1161/01.res.56.3.436](https://doi.org/10.1161/01.res.56.3.436).
987. Aggarwal R, Boyden PA. Diminished Ca^{2+} and Ba^{2+} currents in myocytes surviving in the epicardial border zone of the 5-day infarcted canine heart. **Circ Res** 77: 1180–1191, 1995. doi:[10.1161/01.res.77.6.1180](https://doi.org/10.1161/01.res.77.6.1180).
988. Tomek J, Bub G. Hypertension-induced remodeling: on the interactions of cardiac risk factors. **J Physiol** 595: 4027–4036, 2017. doi:[10.1111/JP273043](https://doi.org/10.1111/JP273043).
989. Ho KK, Pinsky JL, Kannel WB, Levy D. The epidemiology of heart failure: the Framingham Study. **J Am Coll Cardiol** 22: 6A–13A, 1993. doi:[10.1016/0735-1097\(93\)90455-a](https://doi.org/10.1016/0735-1097(93)90455-a).
990. Benjamin EJ, Virani SS, Callaway CW, Chamberlain AM, Chang AR, Cheng S, et al. Heart Disease and Stroke Statistics-2018 Update: A Report From the American Heart Association. **Circulation** 137: e67–e492, 2018. doi:[10.1161/CIR.0000000000000558](https://doi.org/10.1161/CIR.0000000000000558).
991. Fishman GI, Chugh SS, Dimarco JP, Albert CM, Anderson ME, Bonow RO, Buxton AE, Chen PS, Estes M, Jouven X, Kwong R, Lathrop DA, Mascette AM, Nerbonne JM, O'Rourke B, Page RL, Roden DM, Rosenbaum DS, Sotoodehnia N, Trayanova NA, Zheng ZJ. Sudden cardiac death prediction and prevention: report from a National Heart, Lung, and Blood Institute and Heart Rhythm Society Workshop. **Circulation** 122: 2335–2348, 2010. doi:[10.1161/CIRCULATIONAHA.110.976092](https://doi.org/10.1161/CIRCULATIONAHA.110.976092).
992. Mirza M, Strunets A, Shen WK, Jahangir A. Mechanisms of arrhythmias and conduction disorders in older adults. **Clin Geriatr Med** 28: 555–573, 2012. doi:[10.1016/j.cger.2012.08.005](https://doi.org/10.1016/j.cger.2012.08.005).
993. Davies CH, Ferrara N, Harding SE. Beta-adrenoceptor function changes with age of subject in myocytes from non-failing human ventricle. **Cardiovasc Res** 31: 152–156, 1996. doi:[10.1016/S0008-6363\(95\)00187-5](https://doi.org/10.1016/S0008-6363(95)00187-5).
994. Gazoti Debessa CR, Mesiano Maifrino LB, Rodrigues de Souza R. Age related changes of the collagen network of the human heart. **Mech Ageing Dev** 122: 1049–1058, 2001. doi:[10.1016/s0047-6374\(01\)00238-x](https://doi.org/10.1016/s0047-6374(01)00238-x).
995. Lakatta EG, Levy D. Arterial and cardiac aging: major shareholders in cardiovascular disease enterprises: Part II: the aging heart in health: links to heart disease. **Circulation** 107: 346–354, 2003. doi:[10.1161/01.cir.0000048893.62841.7](https://doi.org/10.1161/01.cir.0000048893.62841.7).
996. Lakatta EG. Cardiovascular regulatory mechanisms in advanced age. **Physiol Rev** 73: 413–467, 1993. doi:[10.1152/physrev.1993.73.2.413](https://doi.org/10.1152/physrev.1993.73.2.413).
997. Larson ED, St Clair JR, Sumner WA, Bannister RA, Proenza C. Depressed pacemaker activity of sinoatrial node myocytes contributes to the age-dependent decline in maximum heart rate. **Proc Natl Acad Sci USA** 110: 18011–18016, 2013. doi:[10.1073/pnas.1308477110](https://doi.org/10.1073/pnas.1308477110).
998. Tellez JO, McZewski M, Yanni J, Sutayagin P, Mackiewicz U, Atkinson A, Inada S, Beresewicz A, Billeter R, Dobrzynski H, Boyett MR. Ageing-dependent remodelling of ion channel and Ca^{2+} clock genes underlying sino-atrial node pacemaking. **Exp Physiol** 96: 1163–1178, 2011. doi:[10.1113/expphysiol.2011.057752](https://doi.org/10.1113/expphysiol.2011.057752).
999. Schmidlin O, Bharati S, Lev M, Schwartz JB. Effects of physiological aging on cardiac electrophysiology in perfused Fischer 344 rat hearts. **Am J Physiol Heart Circ Physiol** 262: H97–H105, 1992. doi:[10.1152/ajpheart.1992.262.1.H97](https://doi.org/10.1152/ajpheart.1992.262.1.H97).
1000. Monfredi O, Boyett MR. Sick sinus syndrome and atrial fibrillation in older persons—a view from the sinoatrial nodal myocyte. **J Mol Cell Cardiol** 83: 88–100, 2015. doi:[10.1016/j.jymcc.2015.02.003](https://doi.org/10.1016/j.jymcc.2015.02.003).
1001. Bonda TA, Szynaka B, Sokołowska M, Dziemidowicz M, Winnicka MM, Chydzewski L, Kamiński KA. Remodeling of the intercalated disc related to aging in the mouse heart. **J Cardiol** 68: 261–268, 2016. doi:[10.1016/j.jcc.2015.10.001](https://doi.org/10.1016/j.jcc.2015.10.001).
1002. Jones SA. Ageing to arrhythmias: conundrums of connections in the ageing heart. **J Pharm Pharmacol** 58: 1571–1576, 2006. doi:[10.1211/jpp.58.12.0002](https://doi.org/10.1211/jpp.58.12.0002).

1003. Lie JT, Hammond PL. Pathology of the senescent heart: anatomic observations on 237 autopsy studies of patients 90 to 105 years old. *Mayo Clin Proc* 63: 552–564, 1988. doi:[10.1016/s0025-6196\(12\)64885-x](https://doi.org/10.1016/s0025-6196(12)64885-x).
1004. Anversa P, Palackal T, Sonnenblick EH, Olivetti G, Meggs LG, Capasso JM. Myocyte cell loss and myocyte cellular hyperplasia in the hypertrophied aging rat heart. *Circ Res* 67: 871–885, 1990. doi:[10.1161/01.res.67.4.871](https://doi.org/10.1161/01.res.67.4.871).
1005. Gottwald M, Gottwald E, Dhein S. Age-related electrophysiological and histological changes in rabbit hearts: age-related changes in electrophysiology. *Int J Cardiol* 62: 97–106, 1997. doi:[10.1016/s0167-5273\(97\)00183-6](https://doi.org/10.1016/s0167-5273(97)00183-6).
1006. Olivetti G, Melissari M, Capasso JM, Anversa P. Cardiomyopathy of the aging human heart. Myocyte loss and reactive cellular hypertrophy. *Circ Res* 68: 1560–1568, 1991. doi:[10.1161/01.res.68.6.1560](https://doi.org/10.1161/01.res.68.6.1560).
1007. Dibb KM, Rueckschloss U, Eisner DA, Isenberg G, Trafford AW. Mechanisms underlying enhanced cardiac excitation contraction coupling observed in the senescent sheep myocardium. *J Mol Cell Cardiol* 37: 1171–1181, 2004. doi:[10.1016/j.yjmcc.2004.09.005](https://doi.org/10.1016/j.yjmcc.2004.09.005).
1008. Sorrentino A, Signore S, Qanud K, Borghetti G, Meo M, Cannata A, Zhou Y, Wybieralska E, Luciani M, Kannappan R, Zhang E, Matsuda A, Webster A, Cimini M, Kertowidjojo E, D'Alessandro DA, Wunimenghe O, Michler RE, Royer C, Goichberg P, Leri A, Barrett EG, Anversa P, Hintze TH, Rota M. Myocyte repolarization modulates myocardial function in aging dogs. *Am J Physiol Heart Circ Physiol* 310: H873–H890, 2016. doi:[10.1152/ajpheart.00682.2015](https://doi.org/10.1152/ajpheart.00682.2015).
1009. Josephson IR, Guida A, Stern MD, Lakatta EG. Alterations in properties of L-type Ca channels in aging rat heart. *J Mol Cell Cardiol* 34: 297–308, 2002. doi:[10.1006/jmcc.2001.1512](https://doi.org/10.1006/jmcc.2001.1512).
1010. Signore S, Sorrentino A, Borghetti G, Cannata A, Meo M, Zhou Y, Kannappan R, Pasqualini F, O'Malley H, Sundman M, Tsigkas N, Zhang E, Arranto C, Mangiaracina C, Isobe K, Sena BF, Kim J, Goichberg P, Nahrendorf M, Isom LL, Leri A, Anversa P, Rota M. Late Na⁺ current and protracted electrical recovery are critical determinants of the aging myopathy. *Nat Commun* 6: 8803, 2015. doi:[10.1038/ncomms9803](https://doi.org/10.1038/ncomms9803).
1011. Koban MU, Moorman AF, Holtz J, Yacoub MH, Boheler KR. Expression analysis of the cardiac Na-Ca exchanger in rat development and senescence. *Cardiovasc Res* 37: 405–423, 1998. doi:[10.1016/S0008-6363\(97\)00276-9](https://doi.org/10.1016/S0008-6363(97)00276-9).
1012. Lompré AM, Lambert F, Lakatta EG, Schwartz K. Expression of sarcoplasmic reticulum Ca²⁺-ATPase and calsequestrin genes in rat heart during ontogenetic development and aging. *Circ Res* 69: 1380–1388, 1991. doi:[10.1161/01.res.69.5.1380](https://doi.org/10.1161/01.res.69.5.1380).
1013. Taffet GE, Tate CA. CaATPase content is lower in cardiac sarcoplasmic reticulum isolated from old rats. *Am J Physiol Heart Circ Physiol* 264: H1609–H1614, 1993. doi:[10.1152/ajpheart.1993.264.5.H1609](https://doi.org/10.1152/ajpheart.1993.264.5.H1609).
1014. Xu A, Narayanan N. Effects of aging on sarcoplasmic reticulum Ca²⁺-cycling proteins and their phosphorylation in rat myocardium. *Am J Physiol Heart Circ Physiol* 275: H2087–H2094, 1998. doi:[10.1152/ajpheart.1998.275.6.H2087](https://doi.org/10.1152/ajpheart.1998.275.6.H2087).
1015. Zhou YY, Lakatta EG, Xiao RP. Age-associated alterations in calcium current and its modulation in cardiac myocytes. *Drugs Aging* 13: 159–171, 1998. doi:[10.2165/00002512-199813020-00007](https://doi.org/10.2165/00002512-199813020-00007).
1016. Stratton JR, Levy WC, Caldwell JH, Jacobson A, May J, Matsuoka D, Madden K. Effects of aging on cardiovascular responses to para-sympathetic withdrawal. *J Am Coll Cardiol* 41: 2077–2083, 2003. doi:[10.1016/S0735-1097\(03\)00418-2](https://doi.org/10.1016/S0735-1097(03)00418-2).
1017. Ferrara N, Komici K, Corbi G, Pagano G, Furgi G, Rengo C, Femminella GD, Leosco D, Bonaduce D. Beta-adrenergic receptor responsiveness in aging heart and clinical implications. *Front Physiol* 4: 396, 2014. doi:[10.3389/fphys.2013.00396](https://doi.org/10.3389/fphys.2013.00396).
1018. Xiao RP, Tomhave ED, Wang DJ, Ji X, Boluyt MO, Cheng H, Lakatta EG, Koch WJ. Age-associated reductions in cardiac beta1- and beta2-adrenergic responses without changes in inhibitory G proteins or receptor kinases. *J Clin Invest* 101: 1273–1282, 1998. doi:[10.1172/JCI1335](https://doi.org/10.1172/JCI1335).
1019. Terrenoire C, Clancy CE, Cormier JW, Sampson KJ, Kass RS. Autonomic control of cardiac action potentials: role of potassium channel kinetics in response to sympathetic stimulation. *Circ Res* 96: e25–e34, 2005. doi:[10.1161/01.RES.0000160555.58046.9a](https://doi.org/10.1161/01.RES.0000160555.58046.9a).
1020. Hartzell HC, Méry PF, Fischmeister R, Szabo G. Sympathetic regulation of cardiac calcium current is due exclusively to cAMP-dependent phosphorylation. *Nature* 351: 573–576, 1991. doi:[10.1038/351573a0](https://doi.org/10.1038/351573a0).
1021. Korkushko OV, Shatilo VB, Plachinda Yu I, Shatilo TV. Autonomic control of cardiac chronotropic function in man as a function of age: assessment by power spectral analysis of heart rate variability. *J Auton Nerv Syst* 32: 191–198, 1991. doi:[10.1016/0165-1838\(91\)90113-H](https://doi.org/10.1016/0165-1838(91)90113-H).
1022. Poller U, Nedelka G, Radke J, Pöncke K, Brodde OE. Age-dependent changes in cardiac muscarinic receptor function in healthy volunteers. *J Am Coll Cardiol* 29: 187–193, 1997. doi:[10.1016/S0735-1097\(96\)00437-8](https://doi.org/10.1016/S0735-1097(96)00437-8).
1023. Kalla M, Herring N, Paterson DJ. Cardiac sympatho-vagal balance and ventricular arrhythmia. *Auton Neurosci* 199: 29–37, 2016. doi:[10.1016/j.autneu.2016.08.016](https://doi.org/10.1016/j.autneu.2016.08.016).
1024. Sesti F, Abbott GW, Wei J, Murray KT, Saksena S, Schwartz PJ, Priori SG, Roden DM, George AL Jr, Goldstein SA. A common polymorphism associated with antibiotic-induced cardiac arrhythmia. *Proc Natl Acad Sci USA* 97: 10613–10618, 2000. doi:[10.1073/pnas.180223197](https://doi.org/10.1073/pnas.180223197).
1025. Baruscotti M, Bucchi A, Milanese R, Paina M, Barbuti A, Gnecci-Ruscone T, Bianco E, Vitali-Serdoz L, Cappato R, DiFrancesco D. A gain-of-function mutation in the cardiac pacemaker HCN4 channel increasing cAMP sensitivity is associated with familial inappropriate Sinus Tachycardia. *Eur Heart J* 38: 280–288, 2017. doi:[10.1093/eurheartj/ehv582](https://doi.org/10.1093/eurheartj/ehv582).
1026. Jenewein T, Neumann T, Erkapic D, Kuniss M, Verhoff MA, Thiel G, Kaufertstein S. Influence of genetic modifiers on sudden cardiac death cases. *Int J Legal Med* 132: 379–385, 2018. doi:[10.1007/s00414-017-1739-7](https://doi.org/10.1007/s00414-017-1739-7).
1027. Rudy Y. Mathematical modeling of complex biological systems: from genes and molecules to organs and organisms: heart. In: *Comprehensive Biophysics. Simulation and Modeling*, edited by Weinstein H. Oxford: Academic Press, 2012.
1028. Vaidyanathan R, Reilly L, Eckhardt LL. Caveolin-3 microdomain: arrhythmia implications for potassium inward rectifier and cardiac sodium channel. *Front Physiol* 9: 1548, 2018. doi:[10.3389/fphys.2018.01548](https://doi.org/10.3389/fphys.2018.01548).
1029. Zhang Q, Chen J, Qin Y, Wang J, Zhou L. Mutations in voltage-gated L-type calcium channel: implications in cardiac arrhythmia. *Channels (Austin)* 12: 201–218, 2018. doi:[10.1080/19336950.2018.1499368](https://doi.org/10.1080/19336950.2018.1499368).
1030. Olesen MS, Bentzen BH, Nielsen JB, Steffensen AB, David JP, Jabbari J, Jensen HK, Haunsø S, Svendsen JH, Schmitt N. Mutations in the potassium channel subunit KCNE1 are associated

- with early-onset familial atrial fibrillation. **BMC Med Genet** 13: 24, 2012. doi:[10.1186/1471-2350-13-24](https://doi.org/10.1186/1471-2350-13-24).]
1031. Restier L, Cheng L, Sanguinetti MC. Mechanisms by which atrial fibrillation-associated mutations in the S1 domain of KCNQ1 slow deactivation of IKs channels. **J Physiol** 586: 4179–4191, 2008. doi:[10.1113/jphysiol.2008.157511](https://doi.org/10.1113/jphysiol.2008.157511).
1032. Steffensen AB, Refsgaard L, Andersen MN, Vallet C, Mujezinovic A, Haunsø S, Svendsen JH, Olesen SP, Olesen MS, Schmitt N. IKs gain- and loss-of-function in early-onset lone atrial fibrillation. **J Cardiovasc Electrophysiol** 26: 715–723, 2015. doi:[10.1111/jce.12666](https://doi.org/10.1111/jce.12666).
1033. Delaney JT, Muhammad R, Blair MA, Kor K, Fish FA, Roden DM, Darbar D. A KCNJ8 mutation associated with early repolarization and atrial fibrillation. **Europace** 14: 1428–1432, 2012. doi:[10.1093/eurpace/eus150](https://doi.org/10.1093/eurpace/eus150).
1034. Ishikawa T, Ohno S, Murakami T, Yoshida K, Mishima H, Fukuoka T, Kimoto H, Sakamoto R, Ohkusa T, Aiba T, Nogami A, Sumitomo N, Shimizu W, Yoshiura KI, Horigome H, Horie M, Makita N. Sick sinus syndrome with HCN4 mutations shows early onset and frequent association with atrial fibrillation and left ventricular noncompaction. **Heart Rhythm** 14: 717–724, 2017. doi:[10.1016/j.hrthm.2017.01.020](https://doi.org/10.1016/j.hrthm.2017.01.020).
1035. Kohn AD, Healey JS, Chauhan V, Birnie DH, Simpson CS, Champagne J, Gardner M, Sanatani S, Exner DV, Klein GJ, Yee R, Skanes AC, Gula LJ, Gollob MH. Systematic assessment of patients with unexplained cardiac arrest: Cardiac Arrest Survivors With Preserved Ejection Fraction Registry (CASPER). **Circulation** 120: 278–285, 2009. doi:[10.1161/CIRCULATIONAHA.109.853143](https://doi.org/10.1161/CIRCULATIONAHA.109.853143).
1036. Curran ME, Splawski I, Timothy KW, Vincent GM, Green ED, Keating MT. A molecular basis for cardiac arrhythmia: HERG mutations cause long QT syndrome. **Cell** 80: 795–803, 1995. doi:[10.1016/0092-8674\(95\)90358-5](https://doi.org/10.1016/0092-8674(95)90358-5).
1037. Wang Q, Curran ME, Splawski I, Burn TC, Millholland JM, VanRaay TJ, Shen J, Timothy KW, Vincent GM, de Jager T, Schwartz PJ, Toubin JA, Moss AJ, Atkinson DL, Landes GM, Connors TD, Keating MT. Positional cloning of a novel potassium channel gene: KVLQT1 mutations cause cardiac arrhythmias. **Nat Genet** 12: 17–23, 1996. doi:[10.1038/ng0196-17](https://doi.org/10.1038/ng0196-17).
1038. Antzelevitch C, Shimizu W. Cellular mechanisms underlying the long QT syndrome. **Curr Opin Cardiol** 17: 43–51, 2002. doi:[10.1097/00001573-200201000-00007](https://doi.org/10.1097/00001573-200201000-00007).
1039. Sicouri S, Glass A, Ferreiro M, Antzelevitch C. Transseptal dispersion of repolarization and its role in the development of torsade de pointes arrhythmias. **J Cardiovasc Electrophysiol** 21: 441–447, 2010. doi:[10.1111/j.1540-8167.2009.01641.x](https://doi.org/10.1111/j.1540-8167.2009.01641.x).
1040. Roden DM, Abraham RL. Refining repolarization reserve. **Heart Rhythm** 8: 1756–1757, 2011. doi:[10.1016/j.hrthm.2011.06.024](https://doi.org/10.1016/j.hrthm.2011.06.024).
1041. Roden DM, Yang T. Protecting the heart against arrhythmias: potassium current physiology and repolarization reserve. **Circulation** 112: 1376–1378, 2005. doi:[10.1161/CIRCULATIONAHA.105.562777](https://doi.org/10.1161/CIRCULATIONAHA.105.562777).
1042. Antzelevitch C. Cardiac repolarization. The long and short of it. **Europace** 7, Suppl 2: 3–9, 2005. doi:[10.1016/j.eupc.2005.05.010](https://doi.org/10.1016/j.eupc.2005.05.010).
1043. Gussak I, Brugada P, Brugada J, Wright RS, Kopecky SL, Chaitman BR, Bjerregaard P. Idiopathic short QT interval: a new clinical syndrome? **Cardiology** 94: 99–102, 2000. doi:[10.1159/000047299](https://doi.org/10.1159/000047299).
1044. Priori SG, Wilde AA, Horie M, Cho Y, Behr ER, Berul C, et al. Executive summary: HRS/EHRA/APHRS expert consensus statement on the diagnosis and management of patients with inherited primary arrhythmia syndromes. **Europace** 15: 1389–1406, 2013. doi:[10.1093/eurpace/eut272](https://doi.org/10.1093/eurpace/eut272).
1045. Giustetto C, Schimpf R, Mazzanti A, Scrocco C, Maury P, Anttonen O, Probst V, Blanc JJ, Sbragia P, Dalmasso P, Borggrefe M, Gaita F. Long-term follow-up of patients with short QT syndrome. **J Am Coll Cardiol** 58: 587–595, 2011. doi:[10.1016/j.jacc.2011.03.038](https://doi.org/10.1016/j.jacc.2011.03.038).
1046. Bellocq C, van Ginneken AC, Bezzina CR, Alders M, Escande D, Mannens MM, Baró I, Wilde AA. Mutation in the KCNQ1 gene leading to the short QT-interval syndrome. **Circulation** 109: 2394–2397, 2004. doi:[10.1161/01.CIR.0000130409.72142.FE](https://doi.org/10.1161/01.CIR.0000130409.72142.FE).
1047. Brugada R, Hong K, Dumaine R, Cordeiro J, Gaita F, Borggrefe M, Menendez TM, Brugada J, Pollevick GD, Wolpert C, Burashnikov E, Matsuo K, Wu YS, Guerchicoff A, Bianchi F, Giustetto C, Schimpf R, Brugada P, Antzelevitch C. Sudden death associated with short-QT syndrome linked to mutations in HERG. **Circulation** 109: 30–35, 2004. doi:[10.1161/01.CIR.0000109482.92774.3A](https://doi.org/10.1161/01.CIR.0000109482.92774.3A).
1048. Priori SG, Pandit SV, Rivolta I, Berenfeld O, Ronchetti E, Dhamoon A, Napolitano C, Anumonwo J, di Barletta MR, Gudapakkam S, Bosi G, Stramba-Badiale M, Jalife J. A novel form of short QT syndrome (SQT3) is caused by a mutation in the KCNJ2 gene. **Circ Res** 96: 800–807, 2005. doi:[10.1161/01.RES.0000162101.76263.8c](https://doi.org/10.1161/01.RES.0000162101.76263.8c).
1049. Templin C, Ghadri JR, Rougier JS, Baumer A, Kaplan V, Albesa M, Sticht H, Rauch A, Puleo C, Hu D, Barajas-Martinez H, Antzelevitch C, Lüscher TF, Abriel H, Duru F. Identification of a novel loss-of-function calcium channel gene mutation in short QT syndrome (SQT5). **Eur Heart J** 32: 1077–1088, 2011. doi:[10.1093/eurheartj/ehr076](https://doi.org/10.1093/eurheartj/ehr076).
1050. Antzelevitch C, Pollevick GD, Cordeiro JM, Casis O, Sanguinetti MC, Aizawa Y, Guerchicoff A, Pfeiffer R, Oliva A, Wollnik B, Gelber P, Bonaros EP Jr, Burashnikov E, Wu Y, Sargent JD, Schickel S, Oberheiden R, Bhatia A, Hsu LF, Haissaguerre M, Schimpf R, Borggrefe M, Wolpert C. Loss-of-function mutations in the cardiac calcium channel underlie a new clinical entity characterized by ST-segment elevation, short QT intervals, and sudden cardiac death. **Circulation** 115: 442–449, 2007. doi:[10.1161/CIRCULATIONAHA.106.668392](https://doi.org/10.1161/CIRCULATIONAHA.106.668392).
1051. Roussel J, Labarthe F, Thireau J, Ferro F, Farah C, Roy J, Horiuchi M, Tardieu M, Lefort B, Benoist J, Lacampagne A, Richard S, Fauconnier J, Babuty D, Le Guennec JY. Carnitine deficiency induces a short QT syndrome. **Heart Rhythm** 13: 165–174, 2016. doi:[10.1016/j.hrthm.2015.07.027](https://doi.org/10.1016/j.hrthm.2015.07.027).
1052. Ferro F, Ouillé A, Tran TA, Fontanaud P, Bois P, Babuty D, Labarthe F, Le Guennec JY. Long-chain acylcarnitines regulate the hERG channel. **PLoS One** 7: e41686, 2012. doi:[10.1371/journal.pone.0041686](https://doi.org/10.1371/journal.pone.0041686).
1053. Thorsen K, Dam VS, Kjaer-Sorensen K, Pedersen LN, Skeberdis VA, Jurevicius J, Treinys R, Petersen IM, Nielsen MS, Oxvig C, Morth JP, Matchkov VV, Aalkjaer C, Bundgaard H, Jensen HK. Loss-of-activity-mutation in the cardiac chloride-bicarbonate exchanger AE3 causes short QT syndrome. **Nat Commun** 8: 1696, 2017. doi:[10.1038/s41467-017-01630-0](https://doi.org/10.1038/s41467-017-01630-0).
1054. Nof E, Burashnikov A, Antzelevitch C. Cellular basis for atrial fibrillation in an experimental model of short QT1: implications for a pharmacological approach to therapy. **Heart Rhythm** 7: 251–257, 2010. doi:[10.1016/j.hrthm.2009.10.017](https://doi.org/10.1016/j.hrthm.2009.10.017).
1055. Shinnawi R, Shaheen N, Huber I, Shiti A, Arbel G, Gepstein A, Ballan N, Setter N, Tijssen AJ, Borggrefe M, Gepstein L. Modeling reentry in the short QT syndrome with human-induced pluripotent stem cell-derived cardiac cell sheets. **J Am Coll Cardiol** 73: 2310–2324, 2019. doi:[10.1016/j.jacc.2019.02.055](https://doi.org/10.1016/j.jacc.2019.02.055).

1056. Brugada P, Brugada J. Right bundle branch block, persistent ST segment elevation and sudden cardiac death: a distinct clinical and electrocardiographic syndrome. A multicenter report. **J Am Coll Cardiol** 20: 1391–1396, 1992. doi:[10.1016/0735-1097\(92\)90253-j](https://doi.org/10.1016/0735-1097(92)90253-j).
1057. Marcus FI, Fontaine GH, Guiraudon G, Frank R, Laurenceau JL, Malergue C, Grosgeat Y. Right ventricular dysplasia: a report of 24 adult cases. **Circulation** 65: 384–398, 1982. doi:[10.1161/01.cir.65.2.384](https://doi.org/10.1161/01.cir.65.2.384).
1058. Kapplinger JD, Tester DJ, Alders M, Benito B, Berthet M, Brugada J, Brugada P, Fressart V, Guericoff A, Harris-Kerr C, Kamakura S, Kyndt F, Koopmann TT, Miyamoto Y, Pfeiffer R, Pollevick GD, Probst V, Zumhagen S, Vatta M, Towbin JA, Shimizu W, Schulze-Bahr E, Antzelevitch C, Salisbury BA, Guicheney P, Wilde AA, Brugada R, Schott JJ, Ackerman MJ. An international compendium of mutations in the SCN5A-encoded cardiac sodium channel in patients referred for Brugada syndrome genetic testing. **Heart Rhythm** 7: 33–46, 2010. doi:[10.1016/j.hrthm.2009.09.069](https://doi.org/10.1016/j.hrthm.2009.09.069).
1059. Meregalli PG, Tan HL, Probst V, Koopmann TT, Tanck MW, Bhuiyan ZA, Sacher F, Kyndt F, Schott JJ, Albuissou J, Mabo P, Bezzina CR, Le Marec H, Wilde AA. Type of SCN5A mutation determines clinical severity and degree of conduction slowing in loss-of-function sodium channelopathies. **Heart Rhythm** 6: 341–348, 2009. doi:[10.1016/j.hrthm.2008.11.009](https://doi.org/10.1016/j.hrthm.2008.11.009).
1060. Tukkie R, Sogaard P, Vleugels J, de Groot IK, Wilde AA, Tan HL. Delay in right ventricular activation contributes to Brugada syndrome. **Circulation** 109: 1272–1277, 2004. doi:[10.1161/01.CIR.0000118467.53182.D1](https://doi.org/10.1161/01.CIR.0000118467.53182.D1).
1061. Antzelevitch C. The Brugada syndrome: diagnostic criteria and cellular mechanisms. **Eur Heart J** 22: 356–363, 2001. doi:[10.1053/eurhj.2000.2461](https://doi.org/10.1053/eurhj.2000.2461).
1062. Antzelevitch C, Patocskai B. Brugada syndrome: clinical, genetic, molecular, cellular, and ionic aspects. **Curr Probl Cardiol** 41: 7–57, 2016. doi:[10.1016/j.cpcardiol.2015.06.002](https://doi.org/10.1016/j.cpcardiol.2015.06.002).
1063. Verkerk AO, Remme CA, Schumacher CA, Scicluna BP, Wolswinkel R, de Jonge B, Bezzina CR, Veldkamp MW. Functional Nav1.8 channels in intracardiac neurons: the link between SCN10A and cardiac electrophysiology. **Circ Res** 111: 333–343, 2012. doi:[10.1161/CIRCRESAHA.112.274035](https://doi.org/10.1161/CIRCRESAHA.112.274035).
1064. Chambers JC, Zhao J, Terracciano CM, Bezzina CR, Zhang W, Kaba R, Navaratnarajah M, Lotlikar A, Sehmi JS, Kooner MK, Deng G, Siedlecka U, Parasramka S, El-Hamamsy I, Wass MN, Dekker LR, de Jong JS, Sternberg MJ, McKenna W, Severs NJ, de Silva R, Wilde AA, Anand P, Yacoub M, Scott J, Elliott P, Wood JN, Kooner JS. Genetic variation in SCN10A influences cardiac conduction. **Nat Genet** 42: 149–152, 2010. doi:[10.1038/ng.516](https://doi.org/10.1038/ng.516).
1065. Bezzina CR, Barc J, Mizusawa Y, Remme CA, Gourraud JB, Simonet F, et al. Common variants at SCN5A-SCN10A and HEY2 are associated with Brugada syndrome, a rare disease with high risk of sudden cardiac death. **Nat Genet** 45: 1044–1049, 2013. doi:[10.1038/ng.2712](https://doi.org/10.1038/ng.2712).
1066. Gaborit N, Wichter T, Varro A, Szuts V, Lamirault G, Eckardt L, Paul M, Breithardt G, Schulze-Bahr E, Escande D, Nattel S, Demolombe S. Transcriptional profiling of ion channel genes in Brugada syndrome and other right ventricular arrhythmogenic diseases. **Eur Heart J** 30: 487–496, 2009. doi:[10.1093/eurheartj/ehn520](https://doi.org/10.1093/eurheartj/ehn520).
1067. Awad MM, Calkins H, Judge DP. Mechanisms of disease: molecular genetics of arrhythmogenic right ventricular dysplasia/cardiomyopathy. **Nat Clin Pract Cardiovasc Med** 5: 258–267, 2008. doi:[10.1038/ncpcardio1182](https://doi.org/10.1038/ncpcardio1182).
1068. Gandjbakhch E, Redheuil A, Pousset F, Charron P, Frank R. Clinical diagnosis, imaging, and genetics of arrhythmogenic right ventricular cardiomyopathy/dysplasia: JACC State-of-the-Art Review. **J Am Coll Cardiol** 72: 784–804, 2018. doi:[10.1016/j.jacc.2018.05.065](https://doi.org/10.1016/j.jacc.2018.05.065).
1069. Que D, Yang P, Song X, Liu L. Traditional vs. genetic pathogenesis of arrhythmogenic right ventricular cardiomyopathy. **Europace** 17: 1770–1776, 2015. doi:[10.1093/europace/euv042](https://doi.org/10.1093/europace/euv042).
1070. Sen-Chowdhry S, Syrris P, McKenna WJ. Genetics of right ventricular cardiomyopathy. **J Cardiovasc Electrophysiol** 16: 927–935, 2005. doi:[10.1111/j.1540-8167.2005.40842.x](https://doi.org/10.1111/j.1540-8167.2005.40842.x).
1071. Sen-Chowdhry S, Lowe MD, Sporton SC, McKenna WJ. Arrhythmogenic right ventricular cardiomyopathy: clinical presentation, diagnosis, and management. **Am J Med** 117: 685–695, 2004. doi:[10.1016/j.amjmed.2004.04.028](https://doi.org/10.1016/j.amjmed.2004.04.028).
1072. Corrado D, Basso C, Thiene G, McKenna WJ, Davies MJ, Fontaliran F, Nava A, Silvestri F, Blomstrom-Lundqvist C, Wlodarska EK, Fontaine G, Camerini F. Spectrum of clinicopathologic manifestations of arrhythmogenic right ventricular cardiomyopathy/dysplasia: a multicenter study. **J Am Coll Cardiol** 30: 1512–1520, 1997. doi:[10.1016/s0735-1097\(97\)00332-x](https://doi.org/10.1016/s0735-1097(97)00332-x).
1073. Maron BJ, Shirani J, Poliac LC, Mathenge R, Roberts WC, Mueller FO. Sudden death in young competitive athletes. Clinical, demographic, and pathological profiles. **JAMA** 276: 199–204, 1996.
1074. Corrado D, Basso C, Leoni L, Tokajuk B, Bauce B, Frigo G, Tarantini G, Napodano M, Turrini P, Ramondo A, Daliento L, Nava A, Buja G, Iliceto S, Thiene G. Three-dimensional electroanatomic voltage mapping increases accuracy of diagnosing arrhythmogenic right ventricular cardiomyopathy/dysplasia. **Circulation** 111: 3042–3050, 2005. doi:[10.1161/CIRCULATIONAHA.104.486977](https://doi.org/10.1161/CIRCULATIONAHA.104.486977).
1075. Wijnmaalen AP, Schalij MJ, Bootsma M, Kies P, DE Roos A, Putter H, Bax JJ, Zeppenfeld K. Patients with scar-related right ventricular tachycardia: determinants of long-term outcome. **J Cardiovasc Electrophysiol** 20: 1119–1127, 2009. doi:[10.1111/j.1540-8167.2009.01516.x](https://doi.org/10.1111/j.1540-8167.2009.01516.x).
1076. Coumel P, Fidelle J, Lucet V, Attuel PY. Catecholamine induced severe ventricular arrhythmias with Adams-Stokes syndrome in children: report of four cases. **Br Heart J** : 28–37, 1978.
1077. Liu N, Rizzi N, Boveri L, Priori SG. Ryanodine receptor and calsequestrin in arrhythmogenesis: what we have learnt from genetic diseases and transgenic mice. **J Mol Cell Cardiol** 46: 149–159, 2009. doi:[10.1016/j.jymcc.2008.10.012](https://doi.org/10.1016/j.jymcc.2008.10.012).
1078. Iyer V, Hajjar RJ, Armoundas AA. Mechanisms of abnormal calcium homeostasis in mutations responsible for catecholaminergic polymorphic ventricular tachycardia. **Circ Res** 100: e22–e31, 2007. doi:[10.1161/01.RES.0000258468.31815.42](https://doi.org/10.1161/01.RES.0000258468.31815.42).
1079. Chiang DY, Kim JJ, Valdes SO, de la Uz C, Fan Y, Orcutt J, Domino M, Smith M, Wehrens XH, Miyake CY. Loss-of-function SCN5A mutations associated with sinus node dysfunction, atrial arrhythmias, and poor pacemaker capture. **Circ Arrhythm Electrophysiol** 8: 1105–1112, 2015. doi:[10.1161/CIRCEP.115.003098](https://doi.org/10.1161/CIRCEP.115.003098).
1080. Fatkin D, Otway R, Vandenberg JL. Genes and atrial fibrillation: a new look at an old problem. **Circulation** 116: 782–792, 2007. doi:[10.1161/CIRCULATIONAHA.106.688889](https://doi.org/10.1161/CIRCULATIONAHA.106.688889).
1081. Ehdiaie A, Cingolani E, Shehata M, Wang X, Curtis AB, Chugh SS. Sex differences in cardiac arrhythmias: clinical and research implications. **Circ Arrhythm Electrophysiol** 11: e005680, 2018. doi:[10.1161/CIRCEP.117.005680](https://doi.org/10.1161/CIRCEP.117.005680).

1082. Abi-Gerges N, Philp K, Pollard C, Wakefield I, Hammond TG, Valentin JP. Sex differences in ventricular repolarization: from cardiac electrophysiology to Torsades de Pointes. **Fundam Clin Pharmacol** 18: 139–151, 2004. doi:[10.1111/j.1472-8206.2004.00230.x](https://doi.org/10.1111/j.1472-8206.2004.00230.x).
1083. Makkar RR, Fromm BS, Steinman RT, Meissner MD, Lehmann MH. Female gender as a risk factor for torsades de pointes associated with cardiovascular drugs. **JAMA** 270: 2590–2597, 1993. doi:[10.1001/jama.1993.03510210076031](https://doi.org/10.1001/jama.1993.03510210076031).
1084. Merri M, Benhorin J, Alberti M, Locati E, Moss AJ. Electrocardiographic quantitation of ventricular repolarization. **Circulation** 80: 1301–1308, 1989. doi:[10.1161/01.cir.80.5.1301](https://doi.org/10.1161/01.cir.80.5.1301).
1085. Wolbrette DL. Risk of proarrhythmia with class III antiarrhythmic agents: sex-based differences and other issues. **Am J Cardiol** 91: 39D–44D, 2003. doi:[10.1016/s0002-9149\(02\)03378-7](https://doi.org/10.1016/s0002-9149(02)03378-7).
1086. Kundu P, Ciobotaru A, Foroughi S, Toro L, Stefani E, Eghbali M. Hormonal regulation of cardiac KCNE2 gene expression. **Mol Cell Endocrinol** 292: 50–62, 2008. doi:[10.1016/j.mce.2008.06.003](https://doi.org/10.1016/j.mce.2008.06.003).
1087. Mangelsdorf DJ, Thummel C, Beato M, Herrlich P, Schütz G, Umesono K, Blumberg B, Kastner P, Mark M, Chambon P, Evans RM. The nuclear receptor superfamily: the second decade. **Cell** 83: 835–839, 1995. doi:[10.1016/0092-8674\(95\)90199-x](https://doi.org/10.1016/0092-8674(95)90199-x).
1088. Furukawa T, Kurokawa J. Regulation of cardiac ion channels via non-genomic action of sex steroid hormones: implication for the gender difference in cardiac arrhythmias. **Pharmacol Ther** 115: 106–115, 2007. doi:[10.1016/j.pharmthera.2007.04.008](https://doi.org/10.1016/j.pharmthera.2007.04.008).
1089. Taneja T, Mahnert BW, Passman R, Goldberger J, Kadish A. Effects of sex and age on electrocardiographic and cardiac electrophysiological properties in adults. **Pacing Clin Electrophysiol** 24: 16–21, 2001. doi:[10.1046/j.1460-9592.2001.00016.x](https://doi.org/10.1046/j.1460-9592.2001.00016.x).
1090. El Khoury N, Mathieu S, Marger L, Ross J, El Gebeily G, Ethier N, Fiset C. Upregulation of the hyperpolarization-activated current increases pacemaker activity of the sinoatrial node and heart rate during pregnancy in mice. **Circulation** 127: 2009–2020, 2013. doi:[10.1161/CIRCULATIONAHA.113.001689](https://doi.org/10.1161/CIRCULATIONAHA.113.001689).
1091. Tsai WC, Chen YC, Kao YH, Lu YY, Chen SA, Chen YJ. Distinctive sodium and calcium regulation associated with sex differences in atrial electrophysiology of rabbits. **Int J Cardiol** 168: 4658–4666, 2013. doi:[10.1016/j.ijcard.2013.07.183](https://doi.org/10.1016/j.ijcard.2013.07.183).
1092. Tsai WC, Chen YC, Lin YK, Chen SA, Chen YJ. Sex differences in the electrophysiological characteristics of pulmonary veins and left atrium and their clinical implication in atrial fibrillation. **Circ Arrhythm Electrophysiol** 4: 550–559, 2011. doi:[10.1161/CIRCEP.111.961995](https://doi.org/10.1161/CIRCEP.111.961995).
1093. Song Y, Shryock JC, Belardinelli L. An increase of late sodium current induces delayed afterdepolarizations and sustained triggered activity in atrial myocytes. **Am J Physiol Heart Circ Physiol** 294: H2031–H2039, 2008. doi:[10.1152/ajpheart.01357.2007](https://doi.org/10.1152/ajpheart.01357.2007).
1094. Bai CX, Kurokawa J, Tamagawa M, Nakaya H, Furukawa T. Nontranscriptional regulation of cardiac repolarization currents by testosterone. **Circulation** 112: 1701–1710, 2005. doi:[10.1161/CIRCULATIONAHA.104.523217](https://doi.org/10.1161/CIRCULATIONAHA.104.523217).
1095. James AF, Arberry LA, Hancox JC. Gender-related differences in ventricular myocyte repolarization in the guinea pig. **Basic Res Cardiol** 99: 183–192, 2004. doi:[10.1007/s00395-003-0451-6](https://doi.org/10.1007/s00395-003-0451-6).
1096. Liu XK, Katchman A, Drici MD, Ebert SN, Ducic I, Morad M, Woosley RL. Gender difference in the cycle length-dependent QT and potassium currents in rabbits. **J Pharmacol Exp Ther** 285: 672–679, 1998.
1097. Kurokawa J, Tamagawa M, Harada N, Honda S, Bai CX, Nakaya H, Furukawa T. Acute effects of oestrogen on the guinea pig and human IKr channels and drug-induced prolongation of cardiac repolarization. **J Physiol** 586: 2961–2973, 2008. doi:[10.1113/jphysiol.2007.150367](https://doi.org/10.1113/jphysiol.2007.150367).
1098. Liu XK, Katchman A, Whitfield BH, Wan G, Janowski EM, Woosley RL, Ebert SN. In vivo androgen treatment shortens the QT interval and increases the densities of inward and delayed rectifier potassium currents in orchietomized male rabbits. **Cardiovasc Res** 57: 28–36, 2003. doi:[10.1016/S0008-6363\(02\)00673-9](https://doi.org/10.1016/S0008-6363(02)00673-9).
1099. Nakamura H, Kurokawa J, Bai CX, Asada K, Xu J, Oren RV, Zhu ZI, Clancy CE, Isobe M, Furukawa T. Progesterone regulates cardiac repolarization through a nongenomic pathway: an in vitro patch-clamp and computational modeling study. **Circulation** 116: 2913–2922, 2007. doi:[10.1161/CIRCULATIONAHA.107.702407](https://doi.org/10.1161/CIRCULATIONAHA.107.702407).
1100. Odening KE, Koren G, Kirk M. Normalization of QT interval duration in a long QT syndrome patient during pregnancy and the postpartum period due to sex hormone effects on cardiac repolarization. **Heart Rhythm Case Rep** 2: 223–227, 2016. doi:[10.1016/j.hrcr.2015.12.012](https://doi.org/10.1016/j.hrcr.2015.12.012).
1101. Xiao L, Zhang L, Han W, Wang Z, Nattel S. Sex-based transmural differences in cardiac repolarization and ionic-current properties in canine left ventricles. **Am J Physiol Heart Circ Physiol** 291: H570–H580, 2006. doi:[10.1152/ajpheart.01288.2005](https://doi.org/10.1152/ajpheart.01288.2005).
1102. Abi-Gerges N, Small BG, Lawrence CL, Hammond TG, Valentin JP, Pollard CE. Gender differences in the slow delayed (IKs) but not in inward (IK1) rectifier K⁺ currents of canine Purkinje fibre cardiac action potential: key roles for IKs, beta-adrenoceptor stimulation, pacing rate and gender. **Br J Pharmacol** 147: 653–660, 2006. doi:[10.1038/sj.bjp.0706491](https://doi.org/10.1038/sj.bjp.0706491).
1103. Lindenfeld J, Cleveland JC Jr, Kao DP, White M, Wichman S, Bristow JC, Peterson V, Rodegheri-Brito J, Korst A, Blain-Nelson P, Sederberg J, Hunt SA, Gilbert EM, Ambardekar AV, Minobe W, Port JD, Bristow MR. Sex-related differences in age-associated down-regulation of human ventricular myocardial beta1-adrenergic receptors. **J Heart Lung Transplant** 35: 352–361, 2016. doi:[10.1016/j.healun.2015.10.021](https://doi.org/10.1016/j.healun.2015.10.021).
1104. Barajas-Martinez H, Haufe V, Chamberland C, Roy MJ, Fecteau MH, Cordeiro JM, Dumaine R. Larger dispersion of INa in female dog ventricle as a mechanism for gender-specific incidence of cardiac arrhythmias. **Cardiovasc Res** 81: 82–89, 2009. doi:[10.1093/cvr/cvn255](https://doi.org/10.1093/cvr/cvn255).
1105. Yang X, Chen G, Papp R, Defranco DB, Zeng F, Salama G. Oestrogen upregulates L-type Ca²⁺ channels via oestrogen-receptor- by a regional genomic mechanism in female rabbit hearts. **J Physiol** 590: 493–508, 2012. doi:[10.1113/jphysiol.2011.219501](https://doi.org/10.1113/jphysiol.2011.219501).
1106. Odening KE, Choi BR, Liu GX, Hartmann K, Ziv O, Chaves L, Schofield L, Centracchio J, Zehender M, Peng X, Brunner M, Koren G. Estradiol promotes sudden cardiac death in transgenic long QT type 2 rabbits while progesterone is protective. **Heart Rhythm** 9: 823–832, 2012. doi:[10.1016/j.hrthm.2012.01.009](https://doi.org/10.1016/j.hrthm.2012.01.009).
1107. Er F, Michels G, Brandt MC, Khan I, Haase H, Eicks M, Lindner M, Hoppe UC. Impact of testosterone on cardiac L-type calcium channels and Ca²⁺ sparks: acute actions antagonize chronic effects. **Cell Calcium** 41: 467–477, 2007. doi:[10.1016/j.ceca.2006.09.003](https://doi.org/10.1016/j.ceca.2006.09.003).
1108. Chen G, Yang X, Alber S, Shusterman V, Salama G. Regional genomic regulation of cardiac sodium-calcium exchanger by

- oestrogen. **J Physiol** 589: 1061–1080, 2011. doi:[10.1113/jphysiol.2010.203398](https://doi.org/10.1113/jphysiol.2010.203398).
1109. Tsang S, Wong SS, Wu S, Kravtsov GM, Wong TM. Testosterone-augmented contractile responses to α 1- and β 1-adrenoceptor stimulation are associated with increased activities of RyR, SERCA, and NCX in the heart. **Am J Physiol Cell Physiol** 296: C766–C782, 2009. doi:[10.1152/ajpcell.00193.2008](https://doi.org/10.1152/ajpcell.00193.2008).
1110. Yan S, Chen Y, Dong M, Song W, Belcher SM, Wang HS. Bisphenol A and 17 β -estradiol promote arrhythmia in the female heart via alteration of calcium handling. **PLoS One** 6: e25455, 2011. doi:[10.1371/journal.pone.0025455](https://doi.org/10.1371/journal.pone.0025455).
1111. Lu YY, Cheng CC, Chen YC, Lin YK, Chen SA, Chen YJ. Electrolyte disturbances differentially regulate sinoatrial node and pulmonary vein electrical activity: A contribution to hypokalemia- or hyponatremia-induced atrial fibrillation. **Heart Rhythm** 13: 781–788, 2016. doi:[10.1016/j.hrthm.2015.12.005](https://doi.org/10.1016/j.hrthm.2015.12.005).
1112. Osadchii OE, Larsen AP, Olesen SP. Predictive value of electrical restitution in hypokalemia-induced ventricular arrhythmogenicity. **Am J Physiol Heart Circ Physiol** 298: H210–H220, 2010. doi:[10.1152/ajpheart.00695.2009](https://doi.org/10.1152/ajpheart.00695.2009).
1113. Tazmini K, Frisk M, Lewalle A, Laasmaa M, Morotti S, Lipsett DB, Manfra O, Skogested J, Aronsen JM, Sejersted OM, Sjaastad I, Edwards AG, Grandi E, Niederer SA, Øie E, Louch WE. Hypokalemia promotes arrhythmia by distinct mechanisms in atrial and ventricular myocytes. **Circ Res** 126: 889–906, 2020. doi:[10.1161/CIRCRESAHA.119.315641](https://doi.org/10.1161/CIRCRESAHA.119.315641).
1114. Shimoni Y, Clark RB, Giles WR. Role of an inwardly rectifying potassium current in rabbit ventricular action potential. **J Physiol** 448: 709–727, 1992. doi:[10.1113/jphysiol.1992.sp019066](https://doi.org/10.1113/jphysiol.1992.sp019066).
1115. Scamps F, Carmeliet E. Delayed K^+ current and external K^+ in single cardiac Purkinje cells. **Am J Physiol Cell Physiol** 257: C1086–C1092, 1989. doi:[10.1152/ajpcell.1989.257.6.C1086](https://doi.org/10.1152/ajpcell.1989.257.6.C1086).
1116. Eisner DA, Lederer WJ. The role of the sodium pump in the effects of potassium-depleted solutions on mammalian cardiac muscle. **J Physiol** 294: 279–301, 1979. doi:[10.1113/jphysiol.1979.sp012930](https://doi.org/10.1113/jphysiol.1979.sp012930).
1117. Osadchii OE. Mechanisms of hypokalemia-induced ventricular arrhythmogenicity. **Fundam Clin Pharmacol** 24: 547–559, 2010. doi:[10.1111/j.1472-8206.2010.00835.x](https://doi.org/10.1111/j.1472-8206.2010.00835.x).
1118. Bailie DS, Inoue H, Kaseda S, Ben-David J, Zipes DP. Magnesium suppression of early afterdepolarizations and ventricular tachyarrhythmias induced by cesium in dogs. **Circulation** 77: 1395–1402, 1988. doi:[10.1161/01.cir.77.6.1395](https://doi.org/10.1161/01.cir.77.6.1395).
1119. Nagasawa S, Saitoh H, Kasahara S, Chiba F, Torimitsu S, Abe H, Yajima D, Iwase H. Relationship between KCNQ1 (LQT1) and KCNH2 (LQT2) gene mutations and sudden death during illegal drug use. **Sci Rep** 8: 8443, 2018. doi:[10.1038/s41598-018-26723-8](https://doi.org/10.1038/s41598-018-26723-8).
1120. Kaumann AJ. Adrenaline and noradrenaline increase contractile force of human ventricle through both β 1- and β 2-adrenoceptors. **Biomed Biochim Acta** 46: S411–S416, 1987.
1121. Silver PJ, Harris AL, Canniff PC, Lepore RE, Bentley RG, Hamel LT, Evans DB. Phosphodiesterase isozyme inhibition, activation of the cAMP system, and positive inotropy mediated by milrinone in isolated guinea pig cardiac muscle. **J Cardiovasc Pharmacol** 13: 530–540, 1989.
1122. Corponi F, Fabbri C, Boriani G, Diemberger I, Albani D, Forloni G, Serretti A. Corrected QT interval prolongation in psychopharmacological treatment and its modulation by genetic variation. **Neuropsychobiology** 77: 67–72, 2019. doi:[10.1159/000493400](https://doi.org/10.1159/000493400).
1123. Sicouri S, Antzelevitch C. Mechanisms underlying the actions of antidepressant and antipsychotic drugs that cause sudden cardiac arrest. **Arrhythm Electrophysiol Rev** 7: 199–209, 2018. doi:[10.15420/aer.2018.29.2](https://doi.org/10.15420/aer.2018.29.2).
1124. Cardiac Arrhythmia Suppression Trial (CAST) Investigators. Preliminary report: effect of encainide and flecainide on mortality in a randomized trial of arrhythmia suppression after myocardial infarction. **N Engl J Med** 321: 406–412, 1989. doi:[10.1056/NEJM198908103210629](https://doi.org/10.1056/NEJM198908103210629).
1125. Siebels J, Kuck KH. Implantable cardioverter defibrillator compared with antiarrhythmic drug treatment in cardiac arrest survivors (the Cardiac Arrest Study Hamburg). **Am Heart J** 127: 1139–1144, 1994. doi:[10.1016/0002-8703\(94\)90101-5](https://doi.org/10.1016/0002-8703(94)90101-5).
1126. Waldo AL, Camm AJ, deRuyter H, Friedman PL, MacNeil DJ, Pauls JF, Pitt B, Pratt CM, Schwartz PJ, Veltri EP. Effect of d-sotalol on mortality in patients with left ventricular dysfunction after recent and remote myocardial infarction. The SWORD Investigators. Survival With Oral d-Sotalol. **Lancet** 348: 7–12, 1996. doi:[10.1016/S0140-6736\(96\)02149-6](https://doi.org/10.1016/S0140-6736(96)02149-6).
1127. Frommeyer G, Eckardt L. Drug-induced proarrhythmia: risk factors and electrophysiological mechanisms. **Nat Rev Cardiol** 13: 36–47, 2016. doi:[10.1038/nrcardio.2015.110](https://doi.org/10.1038/nrcardio.2015.110).
1128. Food and Drug Administration. International Conference on Harmonisation; guidance on S7B Nonclinical Evaluation of the Potential for Delayed Ventricular Repolarization (QT Interval Prolongation) by Human Pharmaceuticals; availability. Notice. **Fed Regist** 70: 61133–61134, 2005.
1129. Nattel S, Yue L, Wang Z. Cardiac ultrarapid delayed rectifiers: a novel potassium current family of functional similarity and molecular diversity. **Cell Physiol Biochem** 9: 217–226, 1999. doi:[10.1159/000016318](https://doi.org/10.1159/000016318).
1130. Ravens U, Wettwer E, Hálá O. Pharmacological modulation of ion channels and transporters. **Cell Calcium** 35: 575–582, 2004. doi:[10.1016/j.ceca.2004.01.011](https://doi.org/10.1016/j.ceca.2004.01.011).
1131. Spellmann I, Reinhard MA, Veverka D, Zill P, Obermeier M, Dehning S, Schennach R, Müller N, Möller HJ, Riedel M, Musil R. QTc prolongation in short-term treatment of schizophrenia patients: effects of different antipsychotics and genetic factors. **Eur Arch Psychiatry Clin Neurosci** 268: 383–390, 2018. doi:[10.1007/s00406-018-0880-8](https://doi.org/10.1007/s00406-018-0880-8).
1132. Woosley RL, Roden DM. Pharmacologic causes of arrhythmogenic actions of antiarrhythmic drugs. **Am J Cardiol** 59: 19e–25e, 1987. doi:[10.1016/0002-9149\(87\)90197-4](https://doi.org/10.1016/0002-9149(87)90197-4).
1133. Hilgemann DW, Ball R. Regulation of cardiac Na^+ , Ca^{2+} exchange and KATP potassium channels by PIP2. **Science** 273: 956–959, 1996. doi:[10.1126/science.273.5277.956](https://doi.org/10.1126/science.273.5277.956).
1134. He Z, Feng S, Tong Q, Hilgemann DW, Philipson KD. Interaction of PIP2 with the XIP region of the cardiac Na/Ca exchanger. **Am J Physiol Cell Physiol** 278: C661–C666, 2000. doi:[10.1152/ajpcell.2000.278.4.C661](https://doi.org/10.1152/ajpcell.2000.278.4.C661).
1135. Cha TJ, Ehrlich JR, Zhang L, Nattel S, Wong TM. Atrial ionic remodeling induced by atrial tachycardia in the presence of congestive heart failure. **Circulation** 110: 1520–1526, 2004. doi:[10.1161/01.CIR.0000142052.03565.87](https://doi.org/10.1161/01.CIR.0000142052.03565.87).